Editorials

Molecular biology and the diagnosis and treatment of liver diseases

Howard J. Worman, Feng Lin, Naoto Mamiya and Paul J. Mustacchia

Subject headings liver disease; molecular biology; viral hepatitis; metabolic diseases; recombinant DNA; rational drug design; gene therapy

Molecular biology has made a tremendous impact on the diagnosis and treatment of liver diseases[1]. This review will provide several recent examples. Emphasis will be placed on how molecular biology has influenced the diagnosis of viral hepatitis, autoimmune and metabolic liver diseases. The use of recombinant DNA technology for drug development and the possibility of gene therapy as a treatment modality will then be discussed.

DIAGNOSIS OF VIRAL HEPATITIS

Hepatitis B

Approximately 350 000 000 individuals are chronically infected with the hepatitis B virus (HBV) worldwide and the disease is endemic in eastern Asia including China[2]. As viral protein antigens can be readily detected in serum, chronic HBV infection can usually be diagnosed by serological assays for the presence of hepatitis B surface antigen (HBsAg). HBsAg is detectable in virtually all infected individuals and the hepatitis B e antigen (HBeAg) is detected in most individuals with high levels of viral replication. Serological assays, usually enzyme linked immunosorbant assays (ELISAs), can utilize either proteins purified from serum or recombinant proteins expressed in yeast or tissue culture cells. ELISAs for detection of antigens can utilize monoclonal antibodies.

Because HBV infection can usually be diagnosed by serological assays, molecular biological methods to measure or detect nucleic acids are usually not necessary in routine clinical diagnosis. In some instances, however, measurement of viral nucleic acids from serum may be helpful in the assessment of patients with chronic hepatitis B. Viral nucleic acid concentrations in serum can be assessed by hybridization to complementary DNA sequences and by a branched chain DNA (bDNA) assay[3]. Such assays can be quantitated to provide estimates of the concentration of viral DNA in serum. As serum viral DNA concentrations may be predictive of prognosis or of response to treatment and prognosis, estimation of viral loads may be useful clinically.

Polymerase chain reaction (PCR) amplification[4,5] of HBV DNA is also relatively easy as HBV is a double stranded DNA virus whose genome is fairly stable in blood and tissue. Sequencing of amplified DNA can be performed to identify mutant viruses of clinical significance. Truncating mutations in the HBV precore gene have been identified that prevent secretion of the e antigen but allow the continued assembly of infectious virus[6,7]. Such mutant strains may be actively replicating even though HBeAg is not detectable using serological assays.

Hepatitis C

In Western countries, molecular biology has arguably had its greatest clinical impact with regards to liver diseases in the diagnosis of viral hepatitis C. Although the virus that causes hepatitis C cannot be propagated in cell culture, molecular biological methods have enabled the identification of this virus and determination of the sequence of its entire genome. This has revolutionized the practice of hepatology.

The hepatitis C virus (HCV) was identified in 1989 by investigators at Chiron Corporation[8]. HCV was identified by antibody screening of cDNA expression libraries made from DNA and RNA from the plasma of chimpanzees infected with serum from humans with what was then called non-A, non-B hepatitis. The expression library was screened with serum antibodies from patients with non-A, non-B hepatitis. This work led to the isolation of cDNA clones that were derived from portions of the HCV genome and encoded fragments of viral polypeptides. The authors also showed that HCV was a positive stranded RNA virus[8] and that the vast majority of individuals with chronic non-A, non-B hepatitis had antibodies against this virus[9].

Departments of Medicine an d of Anatomy and Cell Biology, College of Physicians and Surgeons, Columbia University, 630 West 168th Street, New York, NY 10032, USA

Correspondence to: Dr. Worman J Howard, Department of Medicine, College of Physicians and Surgeons, Columbia University, 630 West 168th Street, New York, NY 10032, USA

Telephone: 212 • 305 • 8156, Fax. 212 • 305 • 6443

Email:hjw14@columbia.edu

Received: 1998-5-25

Following the identification of fragments of the HCV genome, the entire genome was cloned and sequenced in several laboratories[10-13]. This work showed the HCV genome to be a positive stranded RNA of approximately 10 000 nucleotides with a single open reading frame encoding a polyprotein of 3010 to 3033 depending upon the strain (Figure 1) . The polyprotein is processed by host cell and virally encoded proteases into several structural and non-structural polypeptides (Figure 1) . The structural proteins are the core and two envelope polypeptides. The several non structural proteins have various different enzymatic functions.

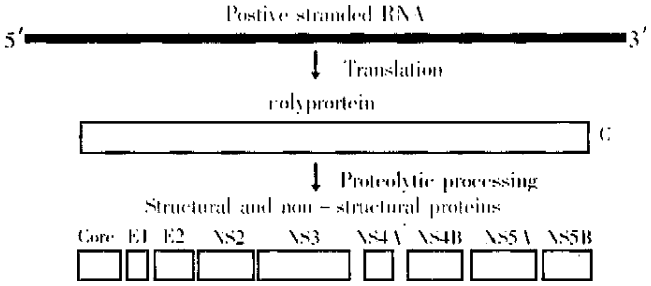

Figure 1 Schematic diagram of the HCV genome and proteins. The positive stranded RNA of about 10000 nucleotides is translated into a polyprotein of approximately 3 000 amino acids. This polyprotein is proteolytically cleaved into several smaller proteins. Core, E1 and E2 are structural polypeptides. Core protein is the virus nucleocapsid and E1 and E2 are viral envelope proteins. A small polypeptide known as P7 (not shown) is also produced by additional cleavage between E2 and NS2. The major non-structural proteins are NS2, NS3, NS4 and NS5. NS4 is further processed into NS4A and NS4B and NS5 into NS5A and NS5B. NS2 and part of NS3 are proteases that process the viral polyprotein. NS3 also has RNA helicase activity. NS4A is a cofactor for the NS3 protease and NS5B is an RNA-dependent, RNA polymerase. The functions of NS4B and NS5A are less well understood but NS5A is thought to play a role in determining sensitivity to interferon.

ELISAs utilizing recombinant HCV polypeptides have been available since the discovery of the virus to detect antibodies against HCV. In individuals with risk factors, the presence of anti-HCV antibodies and an elevated serum alanine aminotransferase activity is highly sensitive for the diagnosis of infection. However, false positive antibody tests are not uncommon and some individuals with HCV in fection develop antibodies at low titers that may not be detected.

In the past few years, assays have become routinely available for the detection of HCV RNA in serum. In the bDNA assay, viral RNA is captured by virus-specific nucleotide probes followed by hybridization to branched DNA molecules which are detected by a chemiluminescent substrate system[3,14]. The bDNA assay can be quantitated and is relatively easy to perform in the routine clinical laboratory. However, bDNA is of lower sensitivity than PCR that is now available to detect HCV RNA is serum and tissue. Since the HCV genome is RNA, reverse transcription must be performed before HCV complementary DNA sequences can be amplified by PCR. The amplified cDNA products are separated by agarose gel electrophoresis and detected by a variety of methods such as ethidium bromide staining or Southern hybridization. Care must be taken in the clinical laboratory to avoid contamination when using reverse transcription-PCR to detect HCV RNA, however, the standardization of this method in excellent clinical laboratories has made it the gold-standard for the detection of HCV infection. PCR has even been made semi-quantitative by using competitive inhibitors or highly standardized assay procedures.

The ability to readily reverse transcribe, amplify and sequence HCV RNA has led to the identification of several HCV genotypes[15]. By using different PCR primers and probes to amplify and detect different sequences from various isolates, routine HCV genotype analysis is possible in the clinical laboratory[16,17]. Different genotypes may differ in the severity of disease they cause and the response to treatment[18].

Hepatitis G

Sensitive molecular biological techniques led to the identification of a new virus in 1995 and 1996 in individuals with hepatitis[19,20]. This virus, termed both hepatitis G virus (HGV) and GB-C virus, is a novel Flavivirus with approximately 25% sequence identity to HCV. The initial identification of this virus was originally met with considerable enthusiasm as it was proposed to be a relatively common cause of non-A, non-B, non-C acute and chronic hepatitis. However, subsequent studies[21,22] have questioned the etiological role of HGV/GB-C as a cause of serious liver disease. Most investigators now feel that HGV/GB-C infection is quite common but that it does not cause clinically significant liver disease.

AUTOIMMUNE LIVER DISEASES

Autoimmune liver diseases such as primary biliary cirrhosis, autoimmune hepatitis and sclerosing cholangitis are associated with the presence of various autoantibodies. Although the pathophysiological significance of these autoantibodies are generally unclear, their detection is central to diagnosis. Basic molecular biological methods have made possible the identification and

cDNA cloning of some of the intracellular protein antigens and the predominant epitopes recognized by disease-specific autoantibodies. This work has led to the development of assays for their detection that can be used in the clinical laboratory.

Illustrative examples on the identification of intracellular antigens recognized by autoantibodies in a liver disease come from work on primary biliary cirrhosis (PBC). Almost all individuals with this disease have autoantibodies directed against the E2 subunits of mitochondrial oxo-acid dehydrogenases[23-25] and about 25% of patients have autoantibodies against gp210, an integral membrane protein of the nuclear pore complex[26,27]. Autoantibodies of these specificities are virtually 100% specific for primary biliary cirrhosis.

Screening of bacteriophage lambda cDNA expression libraries with autoantibodies from patients with PBC was used to identify the E2 subunits of the pyruvate dehydrogenase complex, the branched chain 2-oxo-acid dehydrogenase complex and the 2-oxo-glutarate dehydrogenase complex as the mitochondrial autoantigens in this disease[24,25,28-30]. ELISAs utilizing expressed recombinant proteins have been devised that are sensitive and specific for the detection of antibodies against these proteins[23,31,32]. Determination of the immunodominant epitopes the E2 subunits of all three oxo acid dehydrogenases has allowed for the construction a designer hybrid clone that contains the major epitope of each£ÛŰ32£Ý. An immunoassay utilizing a polypeptide expressed from this hybrid clone is highly sensitive and specific for the diagnosis of PBC[32].

In 1990, nuclear pore membrane glycoprotein gp210 was identified as an autoantigen recognized by approximately 25% of individuals with PBC[33]. Using overlapping cDNA for gp210, its immunodominant epitope which was mapped to a stretch of 15 amino acids in this protein of over 1880 amino acids[34]. Based on this information, two ELISAs have been developed for the detection of autoantibodies, one which utilizes a recombinant HJfusion protein expressed in bacteria[35] and the other which uses a synthetic polypeptide[36].

As PBC is a relative uncommon diseases, assays to detect autoantibodies again oxo-acid dehydorgenase subunits and gp210 have not received much commercial attention. These examples nonetheless demonstrate how molecular biology can impact on the diagnosis of a relatively rare disease.

GENE DISCOVERY AND METABOLIC LIVER DISEASES

Advances in positional cloning and genomics have led to the identification of the genes responsible for some of the major metabolic diseases that affect the liver. In the past decade, genes mutated in Wilson disease, hereditary hemochromatosis, congenital hyperbilirubinemias and inherited cholestatic disorders have been discovered (Table 1) . These discoveries will permit the use of molecular diagnostic methods to diagnose these disorders. An understanding of the defective genes will also lead to new treatment options. This section reviews some of the major discoveries of genes responsible for metabolic liver diseases in the 1990s. The entry number for On line Mendelian Inheritance in Man (OMIM; http://www3.ncbi.nlm.nih.gov/Omim/) is given for each diseased that is discussed.

Table 1 Some inherited diseases that affect the liver and the genes that were indentified in the 1990s by molecular biological and genetic methods.

Disease	Gene
Wilson disease	Cu-transporting ATPase
Hereditary hemochromatosis	HFE
Crigler-Najjar syndrome	UDP-glucuronosyltransferase
Dubin-Johnson syndrome	cMOAT
Benign Recurrent Intrahepatic Cholestasis	P-type ATPase
Progressive familial Intrahepatic Cholestasis Type 1	P-type ATPase

Wilson disease (OMIM # 277900)

Wilson disease is an autosomally inherited disorder that causes changes in the basal ganglia and liver that respectively lead to neuropsychiatric disease, hepatitis and cirrhosis. Abnormalities in serum ceruloplasmin, urinary copper excretion and copper accumulation in the liver have for many years suggested a primary defect in copper metabolism as the cause. In 1985, the Wilson disease gene was shown to be linked to the esterase D locus on chromosome 13[37]. Over the next eight years, the Wilson disease locus was more precisely localized by genetic analysis of various families and individuals and was placed at the junction of band q14.3 and q21.1 on chromosome 13 in 1993 by using fluorescence in situ hybridization studies of chromosomal aberrations[38]. Finally, in 1993, several yeast artificial chromosomes spanning this region were molecularly cloned and a gene encoding a P-type ATPase that was mutated in individuals with Wilson disease was identified[39-41]. This ATPase was highly similar to the ATPase previously shown to be responsible for Menke disease, another disorder of copper metabolism, and is thought to be a copper-translocating ATPase. At least 70 different mutations have since been described in this copper-ATPase gene in individuals with Wilson disease[42].

Hereditary hemochromatosis (OMIM #235200)

Hereditary hemochromatosis is the most common inherited disease in individuals of European

descent[43]. Homozygous individuals suffer from the complications of excess iron deposition in the liver, heart, joints and some endocrine organs. Excessive hepatocyte iron causes hepatitis and cirrhosis. The disease often goes undiagnosed which is especially unfortunate because phlebotomy is effective treatment.

In the 1970's, hereditary hemochromatosis was linked to the HLA-A locus on chromosome[44-46]. In 1996, investigators at Mercator Genetics[47] used linkage disequilibrium and full haplotype analysis to identify a candidate gene for hemochromatosis on chromosome 6. They termed this gene HLA-H because of its homology to other MHC class I family members; the current accepted designation of this gene is HFE . A guanine to adenine transition at coding nucleotide 845 of this gene resulted in a cysteine to tyrosine substitution at amino acid residue 282 in the protein in 85% of 178 patients they examined. Several other studies subsequently confirmed the mutations identified by the group at Mercator Genetics£Û48-50£Ý and the cysteine to tyrosine substitution in HFE is now felt to be present in between 70% and 100% of individuals with hered itary hemochromatosis[51]. Another mutation in HFE that converts histidine 63 to aspartate also increases the relative risk of for the development of hemochromatosis in individuals who are heterozygous for the cysteine to tyrosine substitution at amino acid 282[47,52].

When the HFE gene was discovered, it was unclear how a protein with homology to MHC class I proteins could be involved in the regulation of iron metabolism. Recently, however, it has been shown that the protein encoded by HFE associates with the transferrin receptor and decreases the affinity of transferrin receptor for iron bound transferrin[53-55]. The cysteine to tyrosine mutant protein does not interact with transferrin receptor and hence does not decrease its affinity for iron-bound transferrin, while the histidine to aspartate mutant protein associates with transferrin receptor but does not decrease its affinity for iron bound transferrin as much as the wild type protein[54]. These findings can explain how mutations in the HFE gene product cause iron overload.

Crigler-Najjar syndrome type 1 (OMIM #218800)

Individuals with Crigler-Najjar syndrome type 1 have a complete absence of activity of the UDP-glucuronosyltransferase isoform that catalyzes the conjugation of bilirubin to mono and di-glucuronides[56,57]. Affected individuals present with severe childhood disease manifested by jaundice, kernicterus, resultant abnormal neurologic development and early death. Patients with Crigler-Najjar syndrome type 2 have a partial deficiency of this enzyme activity and generally survive through adulthood without significant problems[57]. A single gene of chromosome 2 called UGT1 encodes bilirubin, phenol, and other UDP glucuronosyltransferase isozymes with identical carboxyl termini[58]. Several different mutations in UGT1 have since been described in individuals with Crigler Najjar syndrome type 1[58-61].

Dubin-Johnson syndrome (OMIM #237500)

Dubin-Johnson syndrome results form the inability of conjugated bilirubin to be secreted from hepatocytes. A cDNA for a rat multispecific organic anion transporter (cMOAT), a protein homologous to the multidrug resistance proteins that is located in the canalicular membrane of hepatocytes, was characterized in 1996£Û62£Ý. In 1997, the human orthologue of rat cMOAT was mapped to chromosome 10q24[63]. The human cMOAT cDNA was cloned and sequenced in 1997[64] and mutations in this gene have been identified in individuals with Dubin Johnson syndrome[64,65].

Benign recurrent intrahepatic cholestasis (OMIM #243300) and progressive familial intrahepatic cholestasis type 1 (OMIM # 211600)

Benign recurrent cholestasis type 1 or Summerskill syndrome is characterized by intermittent episodes of cholestasis without extrahepatic bile duct obstruction. The symptoms usually spontaneously resolve after periods of weeks to months and patients generally have a good prognosis. In 1994, a candidate gene was localized by linkage disequilibrium to chromosome 18[66], and in 1997, the localization was further refined to chromosome 18q21[67]. Progressive intrahepatic cholestasis or Byler disease was first described in the OLd Order Amish. This condition is severe and usually leads to death within the first decade of life. Because both benign recurrent intrahepatic cholestasis type 1 and progressive familial intrahepatic cholestasis have similar symptoms, albeit different prognoses, it was suspected that they may be caused by different mutations in the same gene. In 1995, the gene for progressive familial intrahepatic cholestasis was mapped to chromosome 18q21-22, the benign recurrent intrahepatic cholestasis region, in an extended Amish kindred[68]. In 1998, a gene at this locus that encodes a P-type ATPase was identified[69]. Different mutations in the gene encoding this P-type ATPase were identified in individuals with benign recurrent intrahepatic cholestasis and progressive familial intrahepatic cholestasis type 1. The P-type ATPases responsible for these two diseases likely actively transports bile

salts across cell membranes. Depending upon the specific mutation in this P-type ATPase, a cholestatic disorder with a relatively benign or very severe phenotype can result.

MOLECULAR BIOLOGY AND DRUG DEVELOPMENT

Recombinant vaccines to prevent viral hepatitis

Molecular biology has had an impact on the development of safe vaccines to prevent viral hepatitis. The greatest impact has been in the development of vaccines against HBV. Highly effective HBV vaccines have been produced by recombinant DNA technology[70,71]. For these preparations, HBV surface antigen is generally produced as a recombinant protein in yeast. In a landmark study published in 1997, it was demonstrated that universal hepatitis B vaccination reduced the incidence of hepatocellular carcinoma in children in Taiwan[72]. Universal vaccination with relatively inexpensive preparations produced by recombinant DNA technology could lead to the eradication of this disease. The use of recombinant proteins for vaccination against hepatitis viruses other than HBV has lagged. Preliminary results in monkeys suggest that vaccination with a recombinant protein containing part of the viral capsid antigen may be protective against hepatitis E[73].

Recombinant interferons for viral hepatitis

Interferon alpha is used in the treatment of chronic hepatitis B and C[74]. Cloning of the cDNA for interferon alpha has made it possible to produce it using recombinant DNA technology. Several slightly different recombinant preparations with various amino acid substitions are available. Although much leaves to be desired regarding long-term cure rates of treated individuals, recombinant interferons currently provide a partially effective first line treatment option for individuals with hepatitis B and C.

Rational drug design

Determination of the three-dimensional structures of target molecules facilitates the design of compounds that inhibit or possibly enhance the functions of the target. For example, inhibitors of an enzyme can be rationally designed if the three-dimensional structure of the active site is known. Structure based design can be combined with high throughput combinatorial methods to rapidly identify compounds that are effective against a target.

The ability to express portions of proteins from recombinant cDNA clones has tremendously simplified the ability to purify starting materials for structural studies. Improvements in methods for X-ray crystallography and nuclear magnetic resonance spectroscopy have also reduced the amount of time and starting material required for accurate structure determination. These advances have recently had an impact in the rational design of drugs to treat liver diseases as exemplified by the structure determinations of several non structural proteins of HCV (Table 2) . The NS3 polypeptides has two functional domains, one with protease activity that cleaves the viral polyprotein at several sites and the other with RNA helicase activity that unwinds viral RNA. Both of these activities are necessary for viral replication. Expression of recombinant polypeptides of the protease and helicase domains of NS3, as well as the protease domain complexed with its co-factor NS4A, has permitted their three dimensional structures to be determined[75-78]. Based on this knowledge, pharmaceutical and biotechnology companies are in the process of rationally designing inhibitors of these essential viral enzymatic functions.

Table 2 HCV non-structural proteins with three-dimensional structures determined and published in the literature

Polypeptide	Function	Reference
NS3 protease domain	Protease that cleaves HCV polyprotein at several locations	75,76
NS4A (complexed to NS3)	Cofactor for NS3 protease	76
NS3 RNA helicase domain	Unwinds viral RNA	77, 78

Novel processes have also recently been used to determine the structures of hepatitis viral proteins. Despite many efforts, the core protein of HBV has eluded crystallization. However, high resolution cryoelectron microscopy has recently been used to establish the three-dimensional structure of complexes of this protein[79,80]. This knowledge can also provide a rational foundation to develop inhibitors of HBV particle assembly.

With regards to liver diseases, rational drug design is not limited to hepatitis virus. For example, the domain of the hemochromatosis protein HFE that binds to transferrin receptor has been expressed as a recombinant protein and its three-dimensional structure determined by X-ray crystallography[55]. This knowledge can lead to the potential design of drugs that bind to transferrin receptor in a similar fashion to inhibit cellular iron uptake that may be increased in hereditary hemochromatosis because of defective HFE binding.

Gene therapy

Gene therapy for gastrointestinal and liver diseases have been reviewed in detail elsewhere[81,82]. A detailed discussion of hepatic gene therapy is beyond

the scope of this paper and only some of the major areas are touched upon here. Hepatic gene therapy will probably have the greatest initial impact in the treatment of inherited metabolic diseases but variations on classical techniques may also find utility in the treatment of viral diseases, cancer and in the production of vaccines.

In ex vivo hepatic gene therapy, hepatocytes are removed from the patient, cultured in vitro and the desired expression vector is introduced into the cultured hepatocytes. The transduced or transfected hepatocytes are then introduced into the portal vein and lodge in the patient's liver. Hepatocyte directed ex vivo gene therapy has already been performed in human subjects with familial hypercholesterolemia using the low density lipoprotein (LDL) receptor gene[83]. Several treated patients had persistent and significant reductions in serum cholesterol and LDL concentrations.

In *vivo* gene therapy is also an option for the treatment of liver diseases. In in vivo gene therapy, gene transfer vectors are introduced directly into the patient and taken up by the liver. Vectors for hepatic in vivo gene therapy include DNA complexed with proteins, DNA in liposomes, naked DNA and hepatotropic viral vectors such as those based on adenovirus.

Besides the transfer of human genes, other nucleic acid based therapies may be useful in the treatment of liver diseases. Antisense oligonucleotides[84] can be used to inhibit the expression of genes such as those essential for the replication of hepatitis viruses. Ribozymes are catalytic RNA molecules that can also be used for similar purposes[85]. Direct injection of DNA vectors into human cells may also be used for the production of vaccines against viral hepatitis[86]. All of these techniques are in their infancy, however, clinical trials will likely be common in the next decade.

CONCLUSIONS

Molecular biology will continue to have a tremendous impact on the diagnosis and treatment of liver diseases. The basic research conducted in the past three decades will revolutionize the way hepatology, and all of medicine, is practiced. As a result, common conditions such as viral hepatitis B and C and inherited metabolic diseases affecting the liver such as hemochromatosis will hopefully vanish from the world.

REFERENCES

1 Worman HJ. Molecular biological methods in the diagnosis and treatment of liver diseases. *Clin Chem,* 1997;43:1476-1486
2 Mamiya N, Worman, HJ. Epidemiology, prevention, clinical features and therapy of hepatitis B, C, and G. *Curr Opin Infect Dis,* 1997;10:390-397
3 Urdea MS. Synthesis and characterization of branch DNA for the direct and quantitative detection of CMV, HBV, HCV and HIV. *Clin Chem* 1993; 39:725-726
4 Saiki RK, Scharf S, Faloona F, Mullis KB, Horn GT, Erlich HA *et al*. Enzymatic amplification of beta globin genomic sequences and restriction site analysis for diagnosis of sickle cell anemia. *Science,* 1985;230:1350-1354
5 Mullis KB, Faloona FA. Specific synthesis of DNA in vitro via a polymerase-catalyzed chain reaction. *Methods Enzymol,*1987;155:335-350
6 Carman WF, Jacyna MR, Hadziyannis S, Karayiannis P, McGarvey MJ, Makris A *et al*. Mutation preventing formation of hepatitis B e antigen in patients with chronic hepatitis B infection. *Lancet,* 1989;2:588-591
7 Ulrich PP, Bhat RA, Kelly I, Brunetto MR, Bonino F, Vyas GN. A precore-defective mutant of hepatitis B virus associated with eantigen-negative chronic liver disease. *J Med Virol,* 1990;32:109-118
8 Choo QL, Kuo G, Weiner AJ, Overby LR, Bradley DW, Houghton M. Isolation of a cDNA clone derived from a blood-borne non-A, non-B viral hepatitis genome. *Science,* 1989;244:359-362
9 Kuo G, Choo QL, Alter HJ, Gitnick GL, Redeker AG, Purcell RH *et al*. An assay for circulating antibodies to a major etiologic virus of human non-A, non-B hepatitis. *Science,*1989;244:362-364
10 Kato N, Hijikata M, Ootsuyama Y, Nakagawa M, Ohkoshi S, Sugimura T et al. Molecular cloning of the human hepatitis C virus genome from Japanese patients with non-A, non-B hepatitis. *Proc Natl Acad Sci USA,* 1990; 87:9524-9528
11 Choo, QL, Richman KH, Han JH, Berger K, Lee C, Dong C *et al*. Genetic organization and diversity of the hepatitis C virus. Proc Natl Acad Sci USA, 1991; 88:2451-2455
12 Okamoto H, Okada S, Sugiyama Y, Kurai K, Iizuka H, Machida A *et al*. Nucleotide sequence of the genomic RNA hepatitis C virus isolated from a human carrier: comparison with reported isolates from conserved and divergent regions. *J Gen Virol,* 1991;72:2697-2704
13 Takamizawa A, Mori C, Fuke I, Manabe S, Murakami S, Fujita J *et al*. Structure and organization of the hepatitis C genome isolated from human carriers. *J Virol,* 1991;65:1105-1113
14 Urdea MS. Branched DNA signal amplification. *Biotechnology,* 1994;12:926-928
15 Simmonds P, Smith DB, McOmish F, Yap PL, Kolberg J, Urdea MS *et al*. Identification of genotypes of hepatitis C virus by sequence comparisons in the core, E1 and NS5 regions. *J Gen Virol,* 1994;75:1053-1061
16 Lau JY, Mizokami M, Kolberg JA, Davis GL, Prescott LE, Ohno T *et al*. Application of six hepatitis C virus genotyping systems to sera from chronic hepatitis C patients in the United States. *J Infect Dis,* 1994;171:281-289
17 Lau JY, Davis GL, Prescott LE, Maertens G, Lindsay KL, Qian K *et al*. Distribution of hepatitis C virus genotypes determined by line probe assay in patients with chronic hepatitis C seen at tertiary referral centers in the United States. *Ann Intern Med,* 1996;124:868-876
18 Zein NN, Rakela J, Krawitt EL, Reddy KR, Tominaga T, Persing DH *et al*. Hepatitis C virus genotype in the United States: epidemiology, pathogenicity, and response to interferon therapy. *Ann Intern Med,*1996;125:634-639
19 Simons JN, Leary TP, Dawson GJ, Pilot-Matias TJ, Muerhoff AS, Schlauder GG *et al*. Isolation of novel virus like sequences associated with human hepatitis. *Nature Med,* 1995;1:564-569
20 Linnen J, Wages J Jr, Zhang Keck ZY, Fry KE, Krawczynski KZ, Alter H *et al*. Molecular cloning and disease association of hepatitis G virus: a transfusiontransmissible agent. *Science,* 1996;271:505-508
21 Alter MJ, Gallagher M, Morris T, Moyer LA, Meeks EL., Krawczynski K *et al*. Acute Non-A-E hepatitis in the United States and the role of hepatitis G virus infection. *N Engl J Med,* 1997;336:741-746
22 Alter HJ, Nakatsuji Y, Melpolder J, Wages J, Wesley R, Shih WK *et al*. The incidence of transfusion-associated hepatitis G virus infection and its relation to liver disease. *N Engl J Med,* 1997;336:747-754
23 Van de Water J, Cooper A, Surh CD, Coppel R, Danner D, Ansari A *et al*. Detection of autoantibodies to recombinant mitochondrial proteins in patients with primary biliary cirrhosis. *N Engl J Med,* 1989;320:1377-1380
24 Gershwin ME, Coppel RL, Mackay IR. Primary biliary cirrhosis and mitochondrial autoantigens insights from molecular biology. *Hepatology,* 1988; 8:147-151
25 Gershwin ME, Mackay IR. Primary biliary cirrhosis: paradigm or paradox for autoimmunity. *Gastroenterology,* 1991;100:822-833
26 Worman HJ, Courvalin JC. Autoantibodies against nuclear envelope proteins in liver disease. *Hepatology,* 1991;14:1269-1279
27 Courvalin JC, Worman HJ. Nuclear envelope protein autoantibodies in primary biliary cirrhosis. *Semin Liver Dis,*1997;17:79-90
28 Coppel RL, McNeilage LJ, Surh CD, Van de Water J, Spithill TW, Whittingham S *et al*. Primary structure of the human M2 mitochondria autoantigen of primary biliary cirrhosis: dihydrolipoamide acetyltransferase. *Proc Natl Acad Sci USA,* 1988;85:7317-7321
29 Fussey SPM, Guest JR, James OFW, Bassendine MF, Yeaman SJ. Identification of the major M2 autoantigens in primary biliary cirrhosis. *Proc Natl Acad Sci USA,* 1988;85:8654-8658
30 Surh CD, Danner DJ, Ahmed A, Coppel RL, Mackay IR, Dickson ER *et al*. Reactivity of primary biliary cirrhosis sera with a human fetal liver cDNA line of branched chain alpha keto acid dehydrogenase dihydrolipoamide acetyltransferase, the 52 kD mitochondrial antigen. *Hepatology,* 1989;9:63-68
31 Leung PSC, Iwayama T, Prindiville T, Chuang DT, Ansari AA, Wynn RM *et al*. Use of designer recombinant mitochondrial antigens in the diagnosis of primary biliary cirrhosis. *Hepatology,* 1992;15:367-372
32 Moteki S, Leung PS, Coppel RL, Dickson ER, Kaplan MM, Munoz S *et al*. Use of a designer triple expression hybrid clone for three different lipoyl domain for the detection of antimitochondrial autoantibodies. *Hepatology,* 1996;24:97-103
33 Courvalin JC, Lassoued K, Bartnik E, Blobel G, Wozniak RW. The 210 kilodalton nuclear envelope polypeptide recognized by human autoantibodies in primary biliary cirrhosis is the major glycoprotein of the nuclear pore. *J Clin Invest,* 1990;86:279-285
34 Nickowitz RE, Worman HJ. Autoantibodies from patients with primary biliary cirrhosis recognize a restricted region within the cytoplasmic tail of nuclear pore membrane glycoprotein gp210. *J Exp Med,* 1993;178:2237-2242

35 Tartakovsky F, Worman HJ. Detection of gp210 autoantibodies in primary biliary cirrhosis using a recombinant fusion protein containing the predominant autoepitope. *Hepatology*, 1995;21:495-500

36 Bandin O, Courvalin JC, Poupon R, Dubel L, Homberg JC, Johanet C. Specificity and sensitivity of gp210 autoantibodies detected using an enzyme-linked immunosorbent assay and a synthetic polypeptide in the diagnosis of primary biliary cirrhosis. *Hepatology*, 1996;23:1020-1024

37 Frydman M, Bonne-Tamir B, Farrer LA, Conneally PM, Magazanik A, Ashbel S *et al.* Assignment of the gene for Wilson disease to chromosome 13: linkage to the esterase D locus. *Proc Natl Acad Sci USA*, 1985;82:1819-1821

38 Kooy RF, Van der Veen AY, Verlind E, Houwen RHJ, Scheffer H, Buys CHCM. Physical localisation of the chromosomal marker D13S31 places the Wilson disease locus at the junction of bands q14.3 and q21.1 of chromosome 13. *Hum Genet*, 1993;91:504-506

39 Bull PC, Thomas GR, Rommens JM, Forbes JR, Cox DW. The Wilson disease gene is a putative copper transporting P-type ATPase similar to the Menkes gene. *Nature Genet*, 1993;5:327-337

40 Petrukhin K, Fischer SG, Pirastu M, Tanzi RE, Chernov I, Devoto M *et al*. Mapping, cloning and genetic characterization of the region containing the Wilson disease gene. *Nature Genet*, 1993;5:338-343

41 Tanzi RE, Petrukhin K, Chernov I Pellequer JL, Wasco W, Ross B *et al*.The Wilson disease gene is a copper transporting ATPase with homology to the menkes disease gene. *Nature Genet*,1993;5:344-350

42 Thomas GR, Forbes JR, Roberts EA, Walshe JM, Cox DW. The Wilson disease gene: spectrum of mutations and their consequences. *Nature Genet*, 1995;9: 210-217

43 Edwards CQ, Griffen LM, Goldgar D, Drummond C, Skolnick MH, Kushner JP. Prevalence of hemochromatosis among 11065 presumably healthy blood donors. *N Engl J Med*, 1988;318:1355-1362

44 Simon M, Bourel M, Fauchet R, Genetet B. Association of HLA-A3 and HLA-B14 antigens with idiopathic haemochromatosis. *Gut*, 1976;17:332-334

45 Stevens FM, Walters JM, Watt DW, McCarthy CF. Inheritance of idiopathic haemochromatosis. *Lancet*, 1977;1:1107

46 Cartwright GE, Skolnick M, Amos DB, Edwards CQ, Kravitz K, Johnson A. Inheritance of hemochromatosis: linkage to HLA. *Trans Assoc Am Phys*, 1978; 91:273-281

47 Feder JN, Gnirke A, Thomas W, Tsuchihashi Z, Ruddy DA, Basava A *et al*. A novel MHC class I-like gene is mutated in patients with hereditary haemochromatosis. *Nature Genet*, 1996;13:399-408

48 Beutler E, Gelbart T, West C, Lee P, Adams M, Blackstone R *et al*. Mutation analysis in hereditary hemochromatosis. *Blood Cells Molec Dis*, 1996;22: 187-194

49 Jazwinska EC, Cullen LM, Busfield F, Pyper WR, Webb SI, Powell LW *et al*. Haemochromatosis and HLA H. *Nature Genet*, 1996;14:249-251

50 Jouanolle AM, Gandon G, Jezequel P, Blayau M, Campion ML, Yaouanq J *et al*. Haemochromatosis and HLA H. *Nature Genet*, 1996;14:251-252

51 Cuthbert JA. Iron, HFE, and hemochromatosis update. *J Invest Med*, 1997;45: 518-529

52 Beutler E. The significance of the 187G (H63D) mutation in hemochromatosis. *Am J Hum Genet*, 1997;61:762-764

53 Parkkila S, Waheed A, Britton RS, Bacon BR, Zhou XY, Tomatsu S *et al*. Association of the transferrin receptor in human placenta with HFE, the protein defective in hereditary hemochromatosis. *Proc Natl Acad Sci USA*, 1997;94: 13198-13202

54 Feder JN, Penny DM, Irrinke A, Lee VK, Lebr^n JA, Watson N *et al*. The hemochromatosis gene product complexes with the transferrin receptor and lowers its affinity for ligand binding. *Proc Natl Acad Sci USA*, 1998; 95:1472-1477

55 Lebr^n JA, Bennett MJ, Vaughn DE, Chirino AJ, Snow PM, Mintier GA *et al*. Crystal structure of the hemochromatosis protein HFE and characterization of its interaction with transferrin receptor. *Cell*, 1998;93:111-123

56 Crigler JF JR, Najjar VA. Congenital familial nonhemolytic jaundice with kernicterus. *Pediatrics*, 1952;10:169-179

57 Arias IM, Gartner LM, Cohen M, Ben-Ezzer J, Levi AJ. Chronic nonhemolytic unconjugated hyperbilirubinemia with glucuronyl transferase deficiency: clinical, biochemical, pharmacologic and genetic evidence for heterogeneity. *Am J Med*, 1969;47:395-409

58 Ritter JK, Chen F, Sheen YY, Tran HM, Kimura S, Yeatman MT *et al.* A novel complex locus UGT1 encodes human bilirubin, phenol, and other UDP-glucuronosyltransferase isozymes with identical carboxyl termini. *J Biol Chem*, 1992;267:3257-3261

59 Bosma PJ, Roy Chowdhury J, Huang TJ, Lahiri P, Oude Elferink RPJ, Van Es, HHG *et al*. Mechanisms of inherited deficiencies of multiple UDP-glucuronosyltransferase isoforms in two patients with Crigler-Najjar syndrome, type I. *FASEB J*, 1992;6:2859-2863

60 Ritter JK, Yeatman MT, Kaiser C, Gridelli B, Owens IS. A phenylalanine codon deletion at the UGT1 gene complex locus of a Crigler-Najjar type I patient generates a pH-sensitive billrubin UDP-glucuronosyltransferase. *J Biol Chem*, 1993;268:23573-23579

61 Aono S, Yamada Y, Keino H, Sasaoka Y, Nakagawa T, Onishi S *et al.* A new type of defect in the gene for bilirubin uridine 5-prime-diphosphate-glucuronosy ltransferase in a patient with Crigler-Najjar syndrome type I. *Ped Res*, 1994;35:629-632

62 Paulusma CC, Bosma PJ, Zaman GJR, Bakker CTM, Otter M, Scheffer GL *et al*. Congenital jaundice in rats with a mutation in a multidrug resistance-associated protein gene. *Science*,1996;271:1126-1128

63 van Kuijck MA, Kool M, Merkx GFM, Geurts van Kessel A, Bindels RJM, Deen PMT *et al.* Assignment of the canalicular multispecific organic anion transporter gene (CMOAT) to human chromosome 10q24 and mouse chromosome 19D2 by fluorescent in situ hybridization. *Cytogenet Cell Genet*, 1997;77:285-287

64 Paulusma CC, Kool M, Bosma PJ, Scheffer GL, Borg FT, Scheper RJ *et al*. A mutation in the human canalicular multispecific organic anion transporter gene causes the Dubin Johnson syndrome. *Hepatology*, 1997;25:1539-1542

65 Wada M, Toh S, Taniguchi K, Nakamura T, Uchiumi T, Kohno K *et al.* Mutations in the canalicular multispecific organic anion transporter (cMOAT) gene, a novel ABC transporter, in patients with hyperbilirubinemia II / Dubin-Johnson syndrome. *Hum Molec Genet*, 1998;7:203-207

66 Houwen RHJ, Baharloo S, Blankenship K, Raeymaekers P, Juyn J, Sandkuiji *et al*. Genome screening by searching for shared segments: mapping a gene for benign recurrent intrahepatic cholestasis. *Nature Genet*, 1994;8:380-386

67 Sinke RJ, Carlton VEH, Juijn JA, Delhaas T, Bull L, van Berge Henegouwen GP *et al*. Benign recurrent intrahepatic cholestasis (BRIC): evidence of genetic heterogeneity and delimitation of the BRIC locus to a 7-cM interval between D18S69 and D18S64. *Hum Genet*, 1997;100:382-387

68 Carlton VEH, Knisely AS, Freimer NB. Mapping of a locus for progressive familial intrahepatic cholestasis (Byler disease) to 18q21-q22, the benign recurrent intrahepatic cholestasis region. *Hum Molec Genet*, 1995;4: 1049-1053

69 Bull LN, van Eijk MJT, Pawlikowska L, DeYoung JA, Juijn JA, Liao M *et al*. A gene encoding a P-type ATPase mutated in two forms of hereditary cholestasis. *Nature Genet*, 1998;18:219-224

70 McAleer WJ, Buynak EB, Maigetter RZ, Wampler DE, Millr WJ, Hilleman MR. Human hepatitis B vaccine from recombinant yeast. *Nature*, 1984;307: 178-180

71 Lemon SM, Thomas DL. Vaccines to prevent viral hepatitis. *N Engl J Med*, 1997;336:196-204

72 Chang MH, Chen CJ, Lai MS, Hsu HM, Wu TC, Kong MS *et al*. Universal hepatitis B vaccination in Taiwan and the incidence of hepatocellular carcinoma in children. *N Engl J Med*, 1997;336:1855-1859

73 Tsarev SA, Tsareva TS, Emerson SU, Govindarajan S, Shapiro M, Gerin JL *et al*. Successful passive and active immunization of cynomolgus monkeys against hepatitis E. *Proc Natl Acad Sci USA*, 1994;91:10198-10202

74 Hoofnagle JH, Di Bisceglie AM. The treatment of chronic viral hepatitis. *N Engl J Med*, 336:347-356

75 Love RA, Parge HE, Wickersham JA, Hostomsky Z, Habuka N, Moomaw EW *et al*. The crystal stucture of hepatitis C virus NS3 proteinase reveals a trypsin-like fold and a structural zinc binding site. *Cell*, 1996;87:331-342

76 Kim JL, Morgenstern KA, Lin C, Fox T, Dwyer MD, Landro JA *et al.* Crystal structure of the hepatitis C virus NS3 protease domain complexed with a synthetic NS4A cofactor peptide. *Cell*,1996;87:343-355

77 Yao N, Hesson T, Cable M, Hong Z, Kwong AD, Le HV *et al.* Structure of the hepatitis C virus RNA helicase domain. *Nature Struct Biol*, 1997;4:463-467

78 Kim JL, Morgenstern KA, Griffith JP, Dwyer MD, Thomson JA, Murcko MA *et al*. Hepatitis C virus NS3 RNA helicase domain with a bound oligonucleotide: the crystal structure provides insights into the mode of unwinding. *Structure*, 1998;6:89-100

79 Bottcher B, Wynne SA, Crowther RA. Determination of the fold of the core protein of hepatitis B virus by electron cryomicroscopy. *Nature*, 1997;386: 89-91

80 Conway JF, Cheng N, Zlotnick A, Wingfield PT, Stahl SJ, Steven AC. Visualization of the 4 helix bundle in the hepatitis B virus capsid by cryoelectron microscopy. *Nature*, 1997;386:91-94

81 Wilson JM, Askari FK. Hepatic and gastrointestinal gene therapy. In: Yamada T, ed.Textbook of Gastroenterology (Yamada T, ed. Gastroenterology Updates, Vol. 1) Philadelphia: J.B. Lippincott Co. 1996:1-20

82 Xu CT, Pan BR. Current status of gene therapy in gastroenterology. *World J Gastroenterol*, 4:85-89

83 Grossman M, Raper SE, Kozarsky K, Stein EA, Engelhardt JF, Muller D *et al.* Successful ex vivo gene therapy directed to liver in a patient with familial hypercholesterolaemia. *Nature Genet*, 1994;6:335-441

84 Askari FK, McDonnell WM. Antisense oligonucleotide therapy. *N Engl J Med*, 1996;334:316-318

85 Christoffersen RE, Marr JJ. Ribozymes as human therapeutic agents. *J Med Chem*,1995;38:2023-2037

86 McDonnell WM, Askari FK. DNA vaccines. *N Engl J Med*, 1996;334:42-45

 ISSN 1007-9327 CN 14-1219/R WJG, 1998;4(3):192-196

Regulation of hepatic function by brain neuropeptides

Masashi Yoneda

Subject headings liver/physiology; thyrotropin releasing hormone; corticotropin releasing factor; neuropeptide Y; central nervous system; bombesin; β-endorphin; D-Ala-Met enkepalinamide

Since the central nervous system was first demonstrated to be involved in regulation of gastric function by Pavlov[1], and Selye[2] established the stress theory that physicopsychiatric stress altered physiological functions[3], electrical stimulation or lesion of specific brain nuclei identified specific sites in the hypothalamus, limbic system, and medulla that influence gastrointestinal functions. A plethora of peptides have been characterized in the brain by immunohistochemical and molecular biological techniques[4]. The development of retrograde tracing techniques combined with immunohistochemistry reveals that these peptides are localized in the nerve fibers or cell bodies of the hypothalamus and medulla which are important sites for autonomic nervous outflow to the gastrointestinal tract[5,6]. Based on these studies, Taché first reported the effect of central neuropeptides in regulation of gastric functions[7,8]. Since then, more than 40 peptides have been examined and it is well established that many neuropeptides, such as thyrotropin releasing hormone (TRH), corticotropin releasing factor (CRF), neuropeptide Y (NPY), bombesin and somatostatin, mediate a central nervous system induced stimulation or inhibition of gastrointestinal function[9,10]. On the other hand, the liver is also richly innervated[11,12] and retrograde tracing technique has revealed hepatic innervation through the vagus originating in the medulla[13], where abundant neuropeptides exist. This review introduces the current knowledge of central nervous system regulation of hepatic functions by various neuropeptides.

Department of Medicine, International University of Health and Welfare Second Department of Medicine, Asahikawa Medical College .
Dr. Masashi Yoneda, born in Tokyo, Japan on April 24, 1957. Graduated from School of Medicine, Hirosaki University, Japan in March 1983, and received Ph.D in March 1987 from the Postgraduate School, Hirosaki University, Japan. Visiting researcher, University of California, Los Angeles, 1989-1992; assistant professor, Second Department of Medicine, Asahikawa Medical College, Japan 1994-1998; and now associate professor, Department of Medicine, International University of Health and Welfare, Japan. A councilor of the Japanese Society of Gastroenterology. Recipient of Young Investigator Award in The 10th World Congress of Gastroenterology 1994. Recipient of Young Investigator Award in the 10th World Congress of Gastroenterology 1994.
Correspondence to: Masashi Yoneda, MD, Second Department of Medicine, Asahikawa Medical College Nishikagura 4-5-3, Asahikawa 078, Japan
Tel. +81·166·68·2454, Fax. +81·166·65·1182
E-mail: myoneda@asahikawa-med. ac.jp
Received 1998-04-29

THYROTROPIN RELEASING HORMONE (TRH)

TRH exists in the central nervous system and abundant TRH immunoreactive nerve terminals and TRH receptors are localized in the dorsal vagal complex including the vagal motor nucleus and the nucleus of the solitary truct[14,15]. Neuropharmachological studies demonstrated that TRH displayed a vast array of central nervous system-mediated actions unrelated to its physiological roel in the regulation of the pituitary thyroid axis[16]. TRH injected into the cerebrospinal fluid or into specific brain nuclei exerted a variety of behavioral effects. Accumulated evidence also demonstrated that TRH had potent central nervous system mediated stimulatory effects on gastrointestinal secretion, motility and transit, as well as on the development of gastric ulceration in rats and other animals[7,8,17,18] Mapping studies using microinjection of TRH or TRH analogs into selective nuclei have identified brain sites important for stimulation of gastric secretion and motility. The gastric secretory response has been elicited by microinjection of TRH into the lateral and the ventromedial hypothalamus[19]. More sensitive sites have been identified in the brainstem including the dorsal vagal complex, the nucleus ambiguus and the raphe pallidus[20-22].

Hepatic blood flow is composed of hepatic arterial and hepatic portal blood supplies. In rats portal blood flow constitutes 80% of hepatic circulation. Portal blood flow was altered by electrical stimulation of autonomic nerves and specific brain nuclei which are important sites for autonomic nervous regulation[23]. Stimulation of sympathetic nerves caused constriction of hepatic arterial and portal vessels, resulting in a decrease of liver blood volume and flow in hepatic artery, and an increase in portal pressure[24].Electrical stimulation of the hypothalamus produced changes in intestinal blood flow and, consequently, in portal vein and in intrahepatic arterial and portal beds[25]. Moreover, stimulation of the medial and posterior hypothalamus has been reported to increase hepatic arterial resistance and decrease portal blood flow

through sympathetic nerves[26]. On the other hand, using an in vivo microscopic technique in rats, dilatation of the liver sinusoid following electrical vagal stimulation and acetylcholine application has been observed[27,28].

We studied the effect of central TRH analog on hepatic microcirculation in anesthetized rats[29]. We used the stable TRH analog, RX 77368, which has the same receptor affinity and about the times the potency of natural TRH. In rats under urethan anesthesia, hepatic microcirculation was assessed by the hydrogengas clearance method. Intracisternal injection (the injection into the cisternal magna of the brain) of TRH analog induced stimulation of hepatic blood flow by 17%-74% in a dose dependent manner ranging from 5ng to 100ng. This stimulatory response of hepatic blood flow to central TRH analog occurred during the first 15-minute observation period, reached a plateau at 30 minutes and returned to basal value at 60 minutes. On the other hand, intravenous injection of the TRH analog did not modify hepatic blood flow, confirming the central but not peripheral action of the TRH analog. Although this increased hepatic blood flow by central TRH analog was not modified by spinal cord transection, it was reversed by atropine, vagotomy, and N-G-nitro-L-arginine methyl ester, an inhibitor of nitric oxide and indomethacin, indicating that TRH acted in the brain to stimulate hepatic blood flow through vagal, muscarinic, prostaglandin and nitric oxide pathways. Mapping studies by microinjection of TRH analog into the medullary nuclei revealed that the left but not right dorsal vagal complex was a responsive site for TRH on modulation of hepatic blood flow[30]. This finding agreed well with anatomical evidence that hepatic vagal nerve is originated in the left, but not right, dorsal vagal complex[13].

Although in adult animals the liver is normally in a state of growth arrest, once the liver is damaged or impaired because of hepatic injury or liver resection, hepatic regeneration or proliferation is immediately started. Seventy percent partial hepatectomy[31] performed in rats initiated a very striking response in the liver remnant through hypertrophy and hyperplasia, and returned to its original size in 7-10 days[31]. Hepatocytes in the non stimulated liver were essentially arrested in the G_0 state. After partial hepatectomy, growth related events started almost instantly as the cells underwent the transition from G_0 to G_1 state(prereplicative phase), which lasted about 12 hours, at which point DNA synthesis (S state) began and peaked at about 24 hours. Mitosis a similar course 6-8 hours later[32]. Many factors, such as hormones, peptides and cytokines, were thought to be involved and may interact synergistically to initiate and maintain hepatic proliferation. The autonomic nervous system was also suggested to play a role in the liver regeneration and regulation of hormones and growth factors related to hepatic proliferation. Partial hepatectomy suppressed the sympathetic nerve activity[33] and plasma adrenaline and noradrenaline increased immediately after partial hepatectomy and α-blockade reversed DNA synthesis induced by hepatectomy[34,35], indicating the involvement of an adrenergic effect on hepatic regeneration. The parasympathetic nervous system was also suggested to play an important role in hepatic proliferation. Subdiaphragmatic vagotomy more strongly suppressed DNA synthesis after partial hepatectomyas compared with the splanchnicectomy[36], and selective hepatic branch vagotomy suppressed or delayed liver regeneration in partially hepatectomized rats[37]. Moreover, lesion of the ventromedial hypothalamus has recently induced hepatic DNA synthesis through the vagal nerve[38].

The effect of central administration of TRH analog, RX 77368, on hepatic proliferation has recently been studied in conscious adult rats[39], because central TRH was known to activate vagal efferent fibers[40,41]. Rats was injected with TRH analog intracisternally and hepatic DNA synthesis was assessed by thymidine incorporation into the hepatic DNA fraction and BrdU accumulation 6-72 hours later. Hepatic proliferation was stimulated by intracisternal TRH analog (10ng) with a peak response at 48 hours after peptide injection and returned to basal at 72 hours. This stimulatory effect by central TRH on hepatic proliferation was dose related, ranging from 5ng to 100ng assessed at 24 hours. Intravenous TRH analog did not influence hepatic proliferation, confirming a central but not peripheral action of TRH. Stimulation of hepatic proliferation by central TRH was abolished by hepatic branch vagotomy, atropine and indomethacin, suggesting that TRH acts in the brain to stimulate hepatic proliferation through vagal, muscarinic and prostaglandin pathways. However, N-G-nitro-L-arginine methyl ester did not reverse central TRH induced stimulation of hepatic proliferation as it did central TRH induced hepatic circulation, indicating that stimulation of hepatic proliferation is not secondary to the change in hepatic circulation. These data suggest that TRH in the central nervous system may be involved in the vagal regulation of hepatic proliferation.

These findings led us to speculate that central TRH might also protect against experimental liver damage, so effect of central injection of TRH on CCl_4 induced liver injury has been investigated[£Û42£Ý]. Rats were coadministered CCl_4 (2ml/kg, ip) with TRH analog injected intracisternally and liver damage was assessed by serum alanine aminotransferase (ALT) levels. Intracisternal, bnt not intravenous, injection of TRH analog dose-

dependently protected against CCl_4 induced liver damage and this protective effect of central TRH was also block by hepatic vagotomy.

CORTICOTROPIN RELEASING FACTOR (CRF)

CRF is one of the brain neuropeptides, and effect of central CRF on physiological, pharmacological, and pathophysiological regulations of the gastrointestinal tract have been reported. Injection of CRF into the cerebrospinal fluid or the brain nuclei, such as paraventricular nucleus or loecus ceruleus inhibited gastric motility and secretion[43-46], and enhanced colonic motility through the autonomic nervous system[47,48]. Since CRF is known to act in the hypothalamus and stimulate the sympathetic nervous outflow, the opposite effect to TRH on hepatic function was expected when injected in the central nervous system.

We studied the effect of central CRF on hepatic microcirculation in anesthetized rats[49]. In rats under urethan anesthesia, hepatic microcirculation was assessed by the hydrogen gas clearance method and laser Doppler. Intracisternal injection of CRF induced inhibition of hepatic blood flow by 18%-36% in a dose dependent manner, ranging from 1μg to 5μg . This inhibitory response of hepatic blood flow to central CRF was noted during the first 15 minute observation period, reached a plateau at 30-60 minutes and maintained for more than 120 minutes. On the other hand, intravenous injection of the CRF did not modify hepatic blood flow, confirming the central but not peripheral action of the TRH analog. Although this deceased hepatic blood flow by central CRF was not modified by atropine and vagotomy, it was reversed by hepatic sympathectomy and 6-hydroxydopamine, which depleted noradrenergic fibers, indicating that CRF acted in the brain to inhibit hepatic blood flow through sympathetic and noradrenergic pathways. The effect of central injection of CRF on CCl_4 induced liver injury has also been investigated[50]. Rats were injected with CCl_4 (2ml/kg, sc) and CRF was injected just before and 6 hours after CCl_4 administration. Liver damage was assessed by serum ALT levels. Intracisternal, injection of CRF dose dependently aggravated CCl_4 induced liver damage and this aggravating effect of central CRF was block by 6-hydroxydopamine and chemical sympathectomy.

NEUROPEPTIDE Y (NPY)

NPY, a 36 amino acid peptide of the pancreatic polypeptide family, was first isolated from porcine brain[51,52]. NPY was localized mainly in the peripheral nervous system[53], where it contributed to the innervation of the digestive organs, including the biliary tree[54]. In the brain, NPY nerve fibers and terminals, and NPY receptors were localized in the paraventricular nucleus of the hypothalamus and the dorsal vagal complex[55-57] which are important sites for the autonomic nervous system[58]. Central administration of NPY affected feeding behavior and visceral function[57]. The bile duct was richly innervated by autonomic nerves[59] and electrical stimulation of sympathetic and parasympathetic nerves and stimulation or lesion of certain hypothalamic regions[60] altered bile secretion[61,62]. With respect to the gastrointestinal tract, injection of NPY into the cerebrospinal fluid stimulates gastric acid and pepsin secretion, and pancreatic exocrine and endocrine secretion in rats and dogs[63-65]. Farouk *et al*[66] and we[67] have found an effect of central NPY on bile secretion in dogs and rats. The effect of intracisternal injection of NPY on bile secretion in urethan anesthetized rats was investigated[67]. Rats were anesthetized with urethan (1.5g/kg , ip) and the common bile duct was cannulated to collect bile samples. Sodium taurocholic acid (30μmol·kg·h) was infused intravenously to compensate for bile acid loss due to biliary drainage. Intracisternal NPY (0.02nmol-0.12nmol)dose-dependently stimulated bile secretion by 9%-20%. The secretory response occurred within the first 20-40 minutes after injection and lasted 120 minutes. On the other hand, intravenous injection of NPY (0.12nmol) did not modify bile secretion, confirming that NPY did not leak from the cerebrospinal fluid to the peripheral circulation. Thus, central NPY stimulated bile secretion in a bile acid independent and bicarbonate dependent bile flow because central NPY increased only biliary bicarbonate secretion but not biliary bile acid, phospholipid or cholesterol secretion. In other words, central NPY stimulated ductal bile secretion. Although cervical cord transection, bilateral adrenalectomy or pretreatment with N-G-nitro-L-arginine methyl ester did not alter intracisternal NPY induced stimulation of bile secretion, atropine and bilateral cervical vagotomy completely abolished the stimulatory effect of intracisternal NPY on bile secretion, indicating that NPY acted in the brain to stimulate bile acid independent bile secretion through vagal and muscarinic pathways. Mapping studies by microinjection of NPY into the medullary nuclei have shown that the left dorsal vagal complex is a responsive site, like TRH on hepatic circulation, for NPY on stimulation of bile secretion[68].

OTHER NEUROPEPTIDES

Besides TRH, CRF and NPY, a few peptides were suggested to act in the central nervous system to modulate hepatobiliary function. β-endorphin has produced 70% inhibition in liver DNA synthesis in six day old rats[69]. Intracerebroventricular injection of bombesin with a dose of 10μg induces bicarbonate dependent inhibition of bile secretion in rats[70]. Moreover, intracisternal injection of opioid peptide, DAla-Met enkephalinamide decreased bile secretion in urethan anesthetized rats[71].

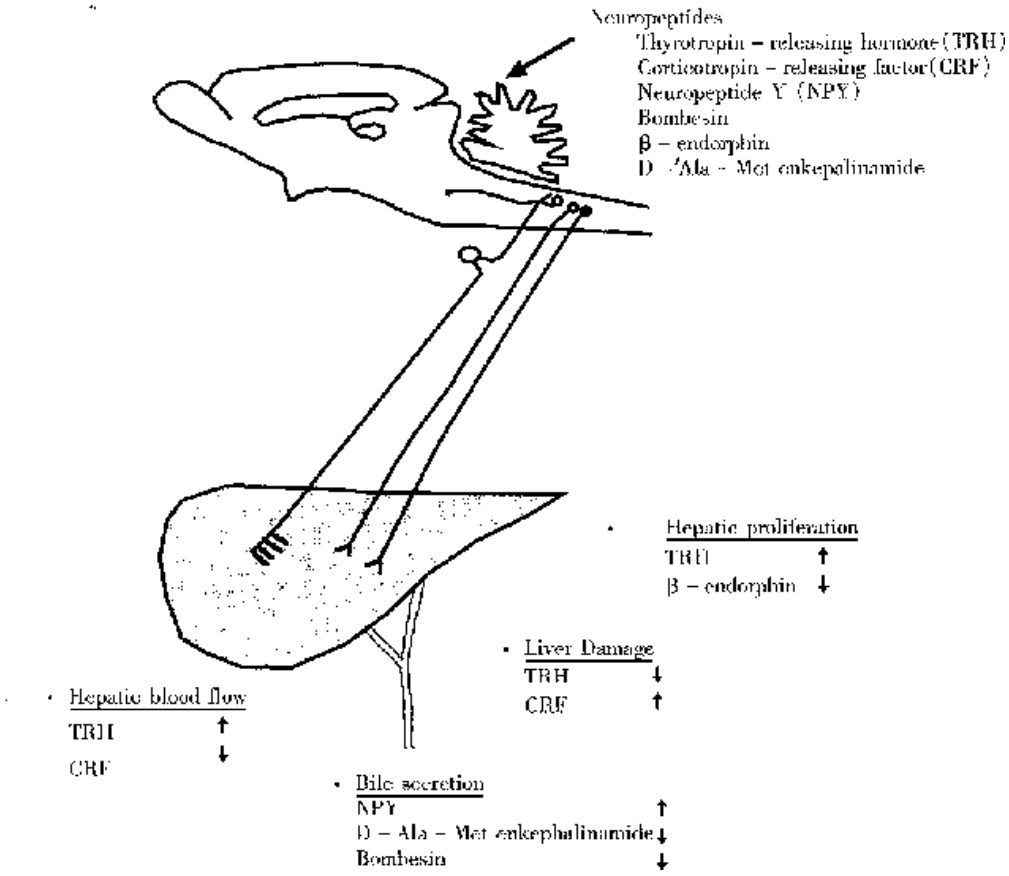

Figure 1 Schematic illustration of interaction bween neuropeptides in the central nervous system and hepatobiliary function.

SUMMARY AND CONCLUSIONS

Several peptides have been established to act in the brain to influence hepatic function (Figure 1) . Bile secretion is modified by central administration of bombesin, opioid peptide and NPY, hepatic blood flow is altered by central CRF and TRH, hepatic proliferation is regulated by central β-endorphin and TRH, and central CRF and TRH interfere experimental liver injury. Among these peptides central TRH is the strongest candidate for playing an important role in hepatic physiological function. Through their use, new knowledge on central and peripheral mechanisms underlying brain regulation of hepatic function will be revealed. Further studies in regard to the physiological relevance of the central action of neuropeptides on specific brain sites should be performed for unraveling the underlying pathways mediating brain liver interaction.

Acknowledgement This work was supported by Japan Research Foundation for Clinical Pharmacology, the Akiyama Foundation, Kanae Memorial Foundation and the Ministry of Education, Culture and Science of Japan (No. 0767554, No. 09670503).

REFERENCES

1 Pavlov I. The work of the digestive glands. (English translation. London: C. *Griffin & Co,* 1910
2 Selye H. Syndrome produced by diverse nocuos agents. *Nature,* 1932;138:32
3 Brooks FP. Central neural control of acid secretion. In: C.F. Code, eds. Handbook of physiology.Washington, D.C.: *American Physiological Society,*1967: 805
4 Krieger DT. Brain peptides: what, where and why? *Science,* 1983;222: 975-985
5 Leslie RA. Neuroactive substances in the dorsal vagal complex of the medulla oblongata: Nucleus of the tractus solitarius, area postrema, and dorsal motor nucleus of the vagus. *Neurochem Int,* 1985;7:191-211
6 Swanson LW, Sawchenko PE. Hypothalamic integration: Organization of the paraventricular and supraoptic nuclei.*Ann Rev Neurosci,*1983;6: 269-324
7 Tache Y, Vale W, Rivier J, Brown M. Brain regulation of gastric secretion: influence of neuropeptides. *Proc Nat Acad Sci USA,* 1980;77:5515-5519
8 Tache Y, Vale W, Brown M. Thyrotropin-releasing hormone-CNS action to stimulate gastric acid secretion. *Nature,* 1980;287:149-151
9 Lenz HJ, Klapdor R, Hester SE, Webb VJ, Galyean RF, Rivier JE, Brown MR. Inhibition of gastric acid secretion by brain peptides in the dog. Role of the autonomic nervous system and gastrin. *Gastroenterology,* 1986;91:905-912
10 Tache Y. Central regulation of gastric acid secretion. In: L.R. Johnson, J. Christensen, E.D. Jacobson and J.H. Walsh, eds. Physiology of the gastrointestinal tract.New York: *Raven Press,*1987:911-930
11 Skaaring P, Bierring F. On the intrinsic innervation of normal rat liver. Histochemical and scanning electron micro scopicalstudies. *Cell Tiss Res,* 1976; 171(2):141-155
12 Sutherland SD. An eveluation of cholinesterase techniques in the study of the intrinsic innervation of the liver. *J Anat,* 1964;98:321-326
13 Kohno T, Mori S, Mito M. Cells of origin innervating the liver and their axonal projections with synaptic terminals into the liver parenchyma in rats. *Hokkaido J Med Sci,* 1987;62:933-946
14 Manaker S, Rizio G. Autoradiographic localization of thyrotropin-releasing hormone and substance P receptors in the rat dorsal vagal complex. *J Comp Neurol,* 1989;290:516-526
15 Rinaman L, Miselis RR. Thyrotropin-releasing hormone-immunoreactive nerve terminals synapse on the dentrites of gastric vagal motoneurons in the rat. *J Comp Neurol,* 1990;294:235-251
16 Tache Y, Stephens RL, Ishikawa T. Central nervous system action of TRH to influence gastrointestinal function and ulceration. *Ann NY Acad Sci,* 1989; 553:269-285
17 Garrick T, Buack S, Veiseh A, Tache Y. Thyrotropin-releasing hormone (TRH)

acts centrally to stimulate gastric contractility in rats. *Life Sci*, 1987;40: 649-657
18 Goto Y, Tache Y. Gastric erosions induced by intracisternal thyrotropin releasing hormone (TRH) in rats. *Peptides*, 1985;6:153-156
19 Maeda-Hagiwara M, Watanabe H. Inhibitory effects of intrahypothalamic injection of calcitonin on TRH stimulated gastric acid secretion in rats. *Jpn J Pharmacol*, 1985;39:173-178
20 Ishikawa T, Yang H, Tache Y. Medullary sites of action of the TRH analogue, RX 77368, for stimulation of gastric acid secretion in the rat. *Gastroenterology*, 1988;95:1470-1476
21 Stephens RL, Ishikawa T, Weiner H, Novin D, Tache Y. TRH analogue, RX 77368, injected into dorsal vagal complex stimulates gastric secretion in rats. *Am J Physiol*, 1988;254:G639-G643
22 Yang H, Ishikawa T, Tache Y. Microinjection of TRH analogs into the raphe pallidus stimulates gastric acid secretion in the rat. *Brain Res*, 1990;531: 280-285
23 Carniero JJ, Donald DE. Change in liver blood flow and blood content in dogs during direct and reflex alteration of hepatic sympathetic nerve activity. *Circ Res*, 1977;40:150-158
24 Lautt WW. Hepatic nerves: a review of their functions and effects. *Can J Pharmacol Physiol*, 1980;58:105-123
25 Folkow B, Rubinstein E. Behavioral and autonomic patterns evoked by stimulation of the lateral hypothalamic area in the cat. *Acta Physiol Scand*, 1965; 65:292-299
26 Tsybenko VA, Yanchuk PI. Central nervous control of hepatic circulation. *J Auton Nerv Syst*, 1991;33:255-266
27 Koo A, Liang I. Microvascular filling pattern in rat liver sinusoids during vagal stimulation. *J Physiol (Lond)*, 1979;295:191-199
28 Koo A, Liang I. Stimulation and blockade of cholinergic receptors in terminal liver microcirculation in rats. *Am J Physiol*, 1979;236:E728-E732
29 Tamori K, Yoneda M, Nakamura K, I.M. Effect of intracisternal thyrotropin-releasing hormone on hepatic blood flow in rats. *Am J Physiol*, 1998;274: G277-G282
30 Yoneda M, Tamori K, Nakade Y, Takamoto S, Yokohama S, Aso K, Sato Y *et al*. Thyrotropin-releasing hormone (TRH) in the left dorsal vagal complex (DVC) increasea the hepatic blood flow in rats (abst). Gastroenterology (in press)
31 Higgins GM, R.M.A. Experimental pathology of the liver-I. Restration of the liver of the white rat following partial surgical removal. *Arch Path*, 1931;12: 186-202
32 Bucher NLR. Liver regeneration: an overview. *J Gastroenterol Hepatol*, 1991; 6:615-624
33 Iwai M, Shimazu T. Alteration in sympathetic nerve activity during liver regeneration in rats after partial hepatectomy. *J Auton Nerv Syst*, 1992;41: 209-214
34 MacManus JP, Braceland BM, Youdale T, Whitfield JF. Adrenergic antagonists, and a possible link between the increase in cyclic adenosine 3' ,5'-monophosphate and DNA synthesis during liver regeneration. *J Cell Physiol*, 1973;82:157-164
35 Cruise JL, Knechtle SJ, Bollinger RR, Kuhn C, Michalopoulas G. á-1 adrenergic effects and liver regeneration. Hepatology, 1987;7:1189-1194
36 Kato H, Shimazu T. Effect of autonomic denervation on DNA synthesis during liver regeneration after partial hepatectomy. *Eur J Biochem*, 1983; 190:473-478
37 Ohtake M, Sakaguchi T, Yoshida K, Muto T. Hepatic branch vagotomy cansuppress liver regeneration in partially hepatectomized rats. *HPB Surgery*, 1993;6:277-286
38 Kiba T, Tanaka K, Endo O, Inoue S. Role of vagus nerve in increased DNA synthesis after hypothalamic ventromedial lesion in rat liver. *Am J Physiol*, 1992;262:G483-G487
39 Yoneda M, Tamori K, Sato Y, Yokohama S, Nakamura K, Makino I. Central thyrotropin-releasing hormone stimulates hepatic DNA synthesis in rats. *Hepatology*, 1997;26:1203-1208
40 McCann MJ, Hermann GE, Rogers RC. Thyrotropin releasing hormone: effect on identified neurons of the dorsal vagal complex. *J AutonNerve Syst*, 1989;26:107-112
41 Somiya H, Tonoue T. Neuropeptides as central integrators of autonomic nerve activity: effect of TRH, SRIF, VIP and bombesin on gastric and adrenal nerves. *Regul Pept*, 1984; 9: 47-52
42 Sato Y, Yoneda M, Yokohama S, Tamori K, Nakamura K, Makino I. Protective effect of central thyrotropin releasing hormone (TRH) on CCl4-induced liver damage in rats (abst). *Gastroenterology*, 1996;110:A1312
43 Tache Y, Goto Y, Gunion MW, Vale W, River J, Brown M. Inhibition of gastric acid secretion in rats by intracerebral injection of corticotropin-releasing factor.Science,1983;222:935-937
44 Lenz HJ, Raedler A, Greten H, Vale WW, Rivier JE. Stress-induced gastrointestinal secretory and motor responses in rats are mediated by endogenous corticotropin releasing factor. *Gastroenterology*, 1988;95:1510-1517
45 Gunion MW and Tache Y. Intrahypothalamic microinfusion of corticotropin-releasing factor inhibits gastric acid secretion but increases secretion volume in rats. *Brain Res*, 1987;411:156-161
46 Lenz HJ, Burlage M, Raedler A, Greten H. Central nervous system effects of corticotropin-releasing factor on gastrointestinal transit in the rat. *Gastroenterology*, 1988;94:598-602
47 Monnikes H, Raybould HE, Schmidt B, Tache Y. CRF in the paraventricular nucleus of the hypothalamus stimulates colonic motor activity in fasted rats. *Peptides*, 1993;14:743-747
48 Monnikes H, Schmidt BG, Tebbe J, Bauer C, Tache Y. Microinfusion of corticotropin releasing factor into the locus coeruleus / subcoeruleus nuclei stimulates colonic motor function in rats. *Brain Research*, 1994; 644:101-108
49 Nakade Y, Yoneda M, Takamoto S, Yokohama S, Tamori K, Aso K, Sato Y *et al*. Central corticotropin releasing factor (CRF) decreases the hepatic blood flow in rats (abst). Gastroenterology (in press)
50 Yokohama S, Yoneda M, Tamori K, Sato Y, Hasegawa T, Nakamura K, Makino I. Effect of central corticotropin releasing factor (CRF) on carbon tetrachloride (CCl4)induced acute liver injury in rat (abst). *Gastroenterology*, 1997;112:A1201
51 Tatemoto K. Neuropeptide Y: Complete amino acid sequence of brain peptide. *Proc Nat Acad Sci USA*, 1982;79:2585-2589
52 Tatemoto K, Carlquist M, Mutt V. Neuropeptide Y-a novel brain peptide with structural similarities to peptide YY and pancreatic polypeptide. *Nature*, 1982;269:659-660
53 Lundberg JM, Terenius L, Hokfelt T, Goldstein M. High levels of neuropeptide Y in peripheral noradrenergic neurons in various mammals including man. *Neurosci Lett*, 1983;42:167-172
54 Allen JM, Gu J, Adrian TE, Polak JM, Bloom SR. Neuropeptide Y in the guinea-pig biliary tract. *Experientia*, 1984;40:765-767
55 De Quidt ME, Emson PC. Distribution of neuropeptide Y-like immunoreactivity in the rat central nervous system-2. Immunohistochemical analysis. *Neuroscience*, 1986;18:545-618
56 Hokelt T, Lundgerg JM, Tatemoto K, Mutt V, Terenius L, Polak J, Bloom S *et al*. Neuropeptide Y (NPY) and FMRFamide neuropeptide-like immunoreactivities in catecholamine neurons of the rat medulla oblongata. *Acta Physiol Scand*, 1983;117:315-318
57 Yamazoe M, Shiosaka S, Emson PC and Tohyama M. Distribution of neuropeptide Y in the lower brainstem: an immunohistochemical analysis. *Brain Res*, 1985;335:109-120
58 Gillis RA, Quest JA, Pagani FD, Norman WP. Central centers in the central nervous system for regulating gastrointestinal motility. In: J.D. Wood, eds. Handbook of Physiology. 6, The gastrointestinal system Bethesda: *American Physiological Society*, 1989:621-683
59 Reilly FD, McCuskey AP, R.S. M. Intrahepatic distribution of nerves in the rat. *Anat Rec*, 1978;191:55-67
60 Bogach PG, Lyashchenko PS. Changes in bile secretion during hypothalamic stimulation in dogs. In: eds. Problems of physiology of the hypothalamus. *Moscow: Kiev*, 1974:56-64
61 Cucchiaro G, Yamaguchi Y, Mills E, Kuhn CM, Branum GD, Meyers WC. Evaluation of selective liver denervation methods. *Am J Physiol*, 1990;259: G781-785
62 Fritz ME, Brooks FP. Control of bile flow in the cholecystectomized dog. *Am J Physiol*, 1963;204:825-828
63 Moltz JH, McDonald JK. Neuropeptide Y: direct and indirect action on insulin secretion in the rat. *Peptides*, 1985;6:1155-1159
64 Matsuda M, Aono M, Moriga M, Okuma M. Centrally administered NPY stimulated gastric acid and pepsin secretion by a vagally mediated mechanism. *Regul Pept*, 1991;35:31-41
65 Geoghegan JG, Lawson DC Cheng CA, Opara E, Taylor IL, Pappas TN. Intracerebroventricular neuropeptide Y increases gastric and pancreatic secretion in the dog. *Gastroenterology*, 1993;105:1069-1077
66 Farouk M, Geoghegan JG, Pruthi RS, Thomson HJ, Pappas TN, Meyers WC. Intracerebroventricular neuropeptide Y stimulates bile secretion via a vagal mechanism. *Gut*, 1992;33:1562-1565
67 Yoneda M, Tamasawa N, Takebe K, Tamori K, Yokohama S, Sato Y, Nakamura K *et al*. Central neuropeptide Y enhances bile secretion through vagal and muscarinic but not nitric oxide pathways in rats. *Peptides*, 1995; 16:727-732
68 Yoneda M, Yokohama S, Tamori K, Sato Y, Nakamura K, Makino I. Neuropeptide Y in the dorsal vagal complex stimulates bicarbonate-dependent bile secretion in rats. *Gastroenterology*, 1997;112:1673-1680
69 Bartolome JV, Bartolome MB, Lorber BA, Dileo SJ, Scanberg SM. Effect of central administration of beta-endorphin on brain and liver DNA synthesis in preweanling rats. *Neuroscince*, 1991;40:289-294
70 Yao CZ, MacLellan DG, Thompson JC. Intracerebroventricular administration of bombesin inhibits biliary and gastric secretion in the rat. *J Neurosci Res*, 1989;22:461-463
71 Berbasa NV, Zhou J, Ravi J. Intracisternal (ic) administration of the opioid peptide analogue D-ala-met-enkephalinamide (D-Ala-Met-Enk) modulate bile flow by an opioid receptor-mediated mechanism in the brain (abst). *Gastroenterology*, 1997;112:A1225

Evolution of gastrointestinal double contrast radiography in China: researches, application and popularization

SHANG Ke-Zhong

Subject headings Gastrointestinal diseases/radiotherapy; barium/diagnostic use;contrast media

Gastrointestinal double constrast radiography (DC) is a major procedure for gastrointestinal (GI) diagnoses, even for small and early structural lesions. Based on experiences reported at home and abroad, GI radiologists in China have studied DC in many aspects in the past few decades: including mechanisms of imaging, physical factors influencing appearance of images, better preparation of images barium surfate (contrast media), substructure of area gastrica, measurement of image density, significance of some phenomena and signs, etc. Great efforts have been dedicated to its clinical application and popularization throughout the country and noticeable achievements have made.

MECHANICS OF IMAGING[1-9]

Barium suspension (BS) and gas are contrast media for DC. Both are fluids. Being influenced by principles of fluid mechanics, most DC images often appeared pleomorphic andchangeable.

Wetting It is defined as a phenomenon occurring upon the contact of the liquid (e.g. BS) with solid (e. g. GI mucosa). Adoption of a kind of BS which has appropriate wetting as wellas high concentration andlow viscosity, is an important prerequiste for DC. Chinese radiologists have made significant improvement in the DC quality of home-made barium preparations[5-9].

Barium collection in recesses More BS is retained in the concave recesses of theangles formed by any protruding or depressing part of the mural surface. This is induced by the cohesive force of thefluid and the surface phenomenon and has considerable significance in differentiating protrusion (blurred in outer side) from depression (blurred in inner side) in nature of lesions. (Figure 1).

Ad-gravitational wall (Ad wall) and Ab-gravitational wall (Ab wall) The flow, spreading, distribution and stagnation of BS in the air filled sac (such as GI lumen) is much influenced by the effect of gravity. The wall of the enclosed sac may be divided into 3 catagories: Ad wall, Ab wall and lateral wall, just like the floor, ceiling and lateral wall of a room. These denominations of the walls are relative and interchangeable, which depends on the body position adopted at the time of examination. For example, the anterior wall of stomach is Ab wall in supine position, but will be changed to Ad wall in prone position. One notable point is that the lesion (e.g. polyp or ulcer) may give similar or entirely different manifestations when it is located on the Ad wall or Ab wall. Cretian phenomena (e.g. hanging droplet) can occur only on Ab wall whereas others (e.g. barium pool) are limited to the Ad wall These condotions and terms in DC imaging are very helpful in understanding and describing the shape and position of lesions (Figure 2).

SUB-STRUCTURE OF AREA GASTRICA[10-13]

Using a flexible specimen holder and magnifying technique, experimental DC was made on 10 human gastric specimens to investigate the differences in appearance of area gastric (AG,2mm-3mm in size) by the authors. The following new finer distinctions were discovered: silkworm-like and petal-like AG occurring in 25%-74%; sub[a2]groove and sub-area of AG; the "tep-over lines" are helpful in discrimination AG of the overlapping Ad wall or Ab wall. The diagnostic significance of such detailed AG study in early gastric carcinoma has been evaluated. (Figures 3-8).

NEASURMENT OF IMAGE DENSITY[1,3,4]

The image density (E) the figure obtained from a densitometer, i.e., the logarithm of the degree of light attenuation ("blackening") of the part of the film, was examined by our group. E is an important quantification standard for more subtle differentiation between various parts of DC. We

Department of Radiology, Shanghai Sixth People's Hospital Shanghai 200233, China

Dr. SHANG Ke Zhong, Professor of Radiology, Shanghai Second Medical University, Member of the Academic Committee of the Chinese Gastrointestinal Radiologist Association.

Correspondence to: SHANG Ke Zhong, Department of Radiology, Shanghai Sixth People's Hospital, 600 Yishan Rd, Shanghai 200233, China

Tel. +86 • 21 • 64850985

Received 1998-02-08

measured the E value of different phases in 97 DC cases. It is the first reported series of measurement of E value in DC.

PHENOMENA AND SIGNS[14-34]

Some DC phenomena and signs have been investigated. The results showed that several of them are extremely valuable for determining the shape, site and nature of? lesions (Table 1).

Vertical plate phenomenon It is the appearance of BS coating surface which lies in a direction tangential to the X-ray beam. It is similar to the change in transparency of a glass plate when its position is turned from transverse to vertical. The depth of BS in the site of vertical plate is much thicker than other parts. They, therefore, occur as single or multiple dense white lines. The majority of anatomical and pathological structures can be better revealed by this phenomena.

Overlapping white line The term is used to denote partially visible white line seen through a relatively shallow barium pool of the ad-gravitational wall. The overlapping white line is produced by linear image of the vertical plate that projects within the field of the Ab wall. We can always trace the existence and nature of such lesions and to determine its Ab wall origin (Figure 6).

Tide and rock phenomenon A protrusion (rock) within the shadow of barium pool(water tide) is rather similar to the relation between the ebb and tide of water and a rock in it. A low and small protrusion could only be demonstrated at "shallow water tide" phase (Figure 9).

Eye-like sign It is a characteristic feature of polyp (Figures 10-11).

Foggy droplets sign This is the characteristic feature of carcinoma located at Ab wall (Figure 12-19).

Foggy droplets sign This is the characteristic appearance of lateral wall carcinoma involving the Ab wall and often accompanied by thefoggy droplets sign (Figures 12-19).

APPLICATION AND POPULARIZTION[4,34]

GI radiologists in China have been giving increasing emphasis on the application and popularization of DC. Seminars have been held each year in Shanghai and other regions since the 80s. Among the radiological techniques to be popularized, DC may be a prominent one in terms of duration and scale of its nation-wide recommendation throughout these years.

In many regions of China, DC has been accepted as a routine technique for GI barium examination; and is one of the standard of assessment in testing the specialty level of radiological practice.

Preliminary data of inquiry from 315 radiology departments showed that among up to 90 000 DC cases, the detectability of GI structural lesions in DE was about 8% higher than when traditional barium studies were employed. The number of early GI cancer found by DC has been increased markedly.

According to a general survey in China, up to 41% of radiological departments have not yet employed DC; and in more than 20%, DC technology has not attained to a qualified standard. Besides, up to 31% DC cases were misdiagnosed because of unfamiliarity with DC appearances, or were not properly interpreted. This status suggests that more strenuous education of DC should be continued.

Table 1 Features and frequencies (%) occurring in 200 different lesions of Ab wall[19]

	Lesions (*n*=200)	Involving lateral wall	Foggy droplets	Multiple mural lines	Overlapping white line	Eye-like	Ring
Anterior gastric wall	150	-46					
		+104					
Carcinoma		-33	30(91)	0	16(48)	0	0
		+72	70(97)	70(97)	10(14)	0	0
Polyp	19	-12	0	0	0	3	12(90)
		+7	0	0	0	0	0
Ulcer	26	-6	0	0	0	0	3(50)
		+20	0	0	0	0	0
Localized colon wall							
Carcinoma	39		38(97)	35(87)	37(95)	0	5(13)
Polyp	8		0	0	5(56)		8(100)
Diverlieulum	3		0	0	0		3(100)

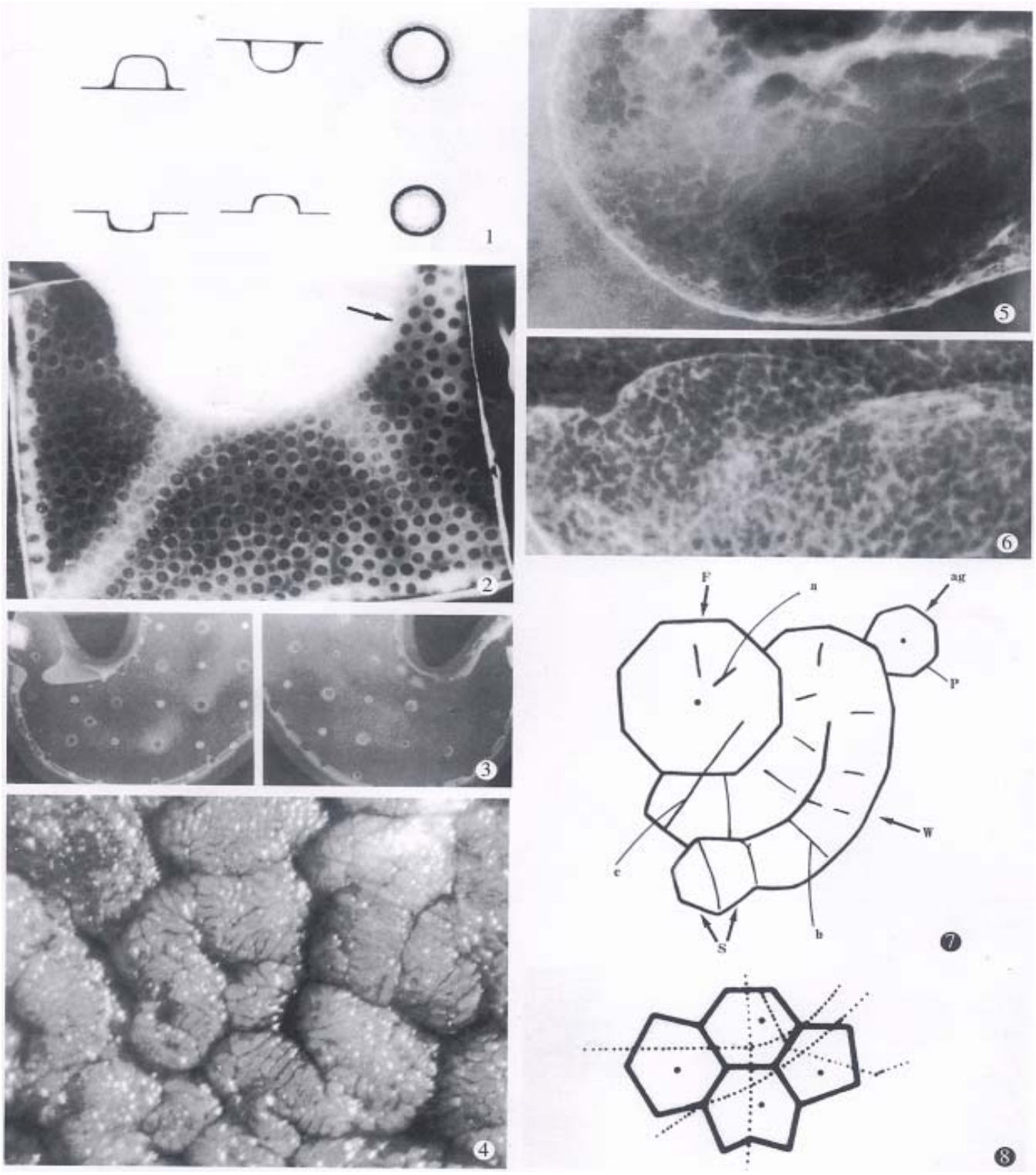

Figure 1 Diagramatic drawing shows the different menifestations in protrusion (blurring in outer side) and in depression (blurring in inner side) caused by barium collection in recesses.

Figure 2 Model DC. The larger round images are protrusions and the smaller ones are depressions. They are all located on Ad wall in A and in Ab wall in B. Note the difference in protrusion (blurring in outer) and in depression (blurring in inner); and the difference of the same lesion in Ad wall (A) or in Ab wall in B.

Figure 3 Gastric specimen magnified (×10) with a biomicroscopy shows the substructures of AG.

Figure 4 Area gastrica in clinical DC shows silkworm-like AG, petal-like AG and the step-over lines of two overlapping walls.

Figure 5 DC of human gastric specimen shows the subtle difference of AG in two overlapping walls (upper 1/3 part) and single unoverlapping wall (lower 2/3 part).

Figure 6 Diagramatic representation of AG. W, silkworm-like AG; SA, sub-AG; SV, subgrooves.

Figure 7 Diagram depicts the step-over lines of AG in two overlapping walls seen in DC film.

Figure 8 Gastric specimen with barium coated and radiographed by soft X-ray showing the ulcer crater and the grooves of AG surounding it.

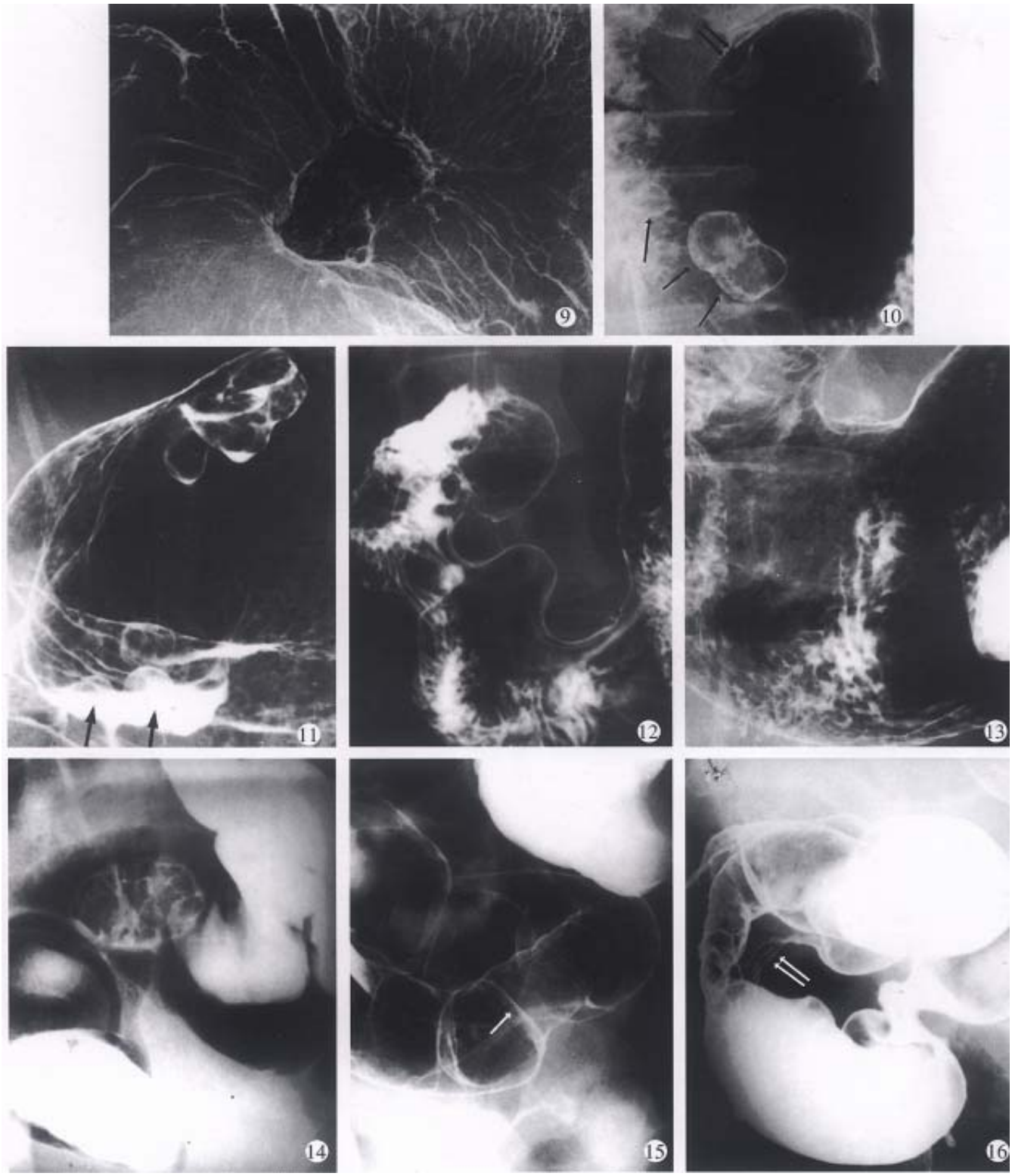

Figure 9 The same sized small round protruions located in Ads wall. Note the different appearance in various phase of "tide and rock". Those are most distinctable in "low water tide" (arrow).

Figure 10-11 A patient with 6 polyps in gastric antrum. In Fig 10, 3 polyps in Ab wall (anterior wall) appeared as eye-like sign (single arrow), one in lateral wall apeared as bowler hat sign (double arrows). In Figure 11, the 3 polyps in Ab wall and 3 in Ad wall (single arrow) all can be seen in horizontal projection.

Figure 12-13 Two patients with gastric carcinoma located in lessor curvature involving Ab wall. Both cases in DC appeared as multiple mural lines sign and foggy droplets sign.

Figure 14 Sigmoid colon carcinoma appeared as foggy droplets sign.

Figure 15-16 Localized carcinoma of sigmoid colon, two projections in the same case, showing the multiple mural lines sign (double arrows) and the foggy droplets sign (single arrow). Figure 16 the multiple mural lines sign (double arrows) and overlapping white lines (single arrow).

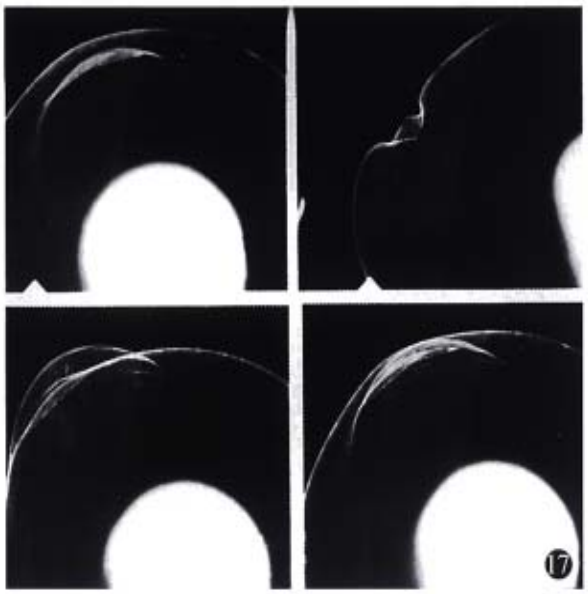

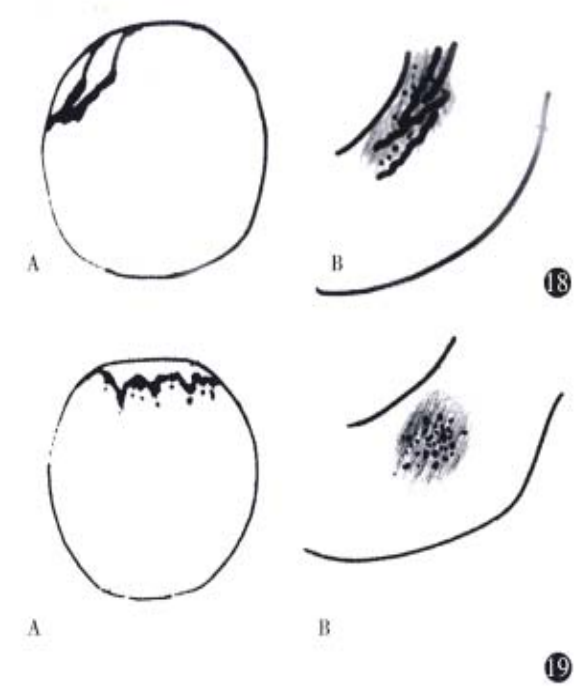

Figure 17 Model DC, demonstrating the mechanism of multiple mural lines sign. The "infiltration" of the lat-eral upper wall of the sac made the part of the wall less expansion (right upper picture, horizontal projection) and appeared as multiple lines of rigidifying, roughing and "whiter" in image density in other 3 pictures taken in perpendicular projection.

Figure 18 Diagramatic drawing demonstrates the mechanism of multiple mural lines sign on horizontal projection (A) and its appearance on perpendicular projection (B).

Figure 19 Diagram of foggy droplets sign. More BS have been stagnated on the irregular surface of Ab wall carcinoma (A) and "foggy doplets" appearance was formed (B).

A, Horizontal projection; B, perpendicular projection.

REFERENCES

1 Shang KZ, Yu X, Guo MJ. An experimental study on the mechanism of gastrointestinol double contrast image formation and its clinical application. *Chin J Radiol,* 1985;19(4):197-200
2 Shang KZ, Zou Z, Chang TQ *et al.* Physical interpretation and clinical significance of gastrointestinal double contrastradiography. *Shanghai Med J,*1982; 5(3):154-157
3 Shang KZ, Zou Z, and Yu X. Image formation in double contrast roentgennography of the GI tract: experimental and theoretical observation and practicle implications. *Chin Med J,* 1985;98(6):391-400
4 Shang KZ, Chen JR (ed). Principle amd diagnosis of gastrointestinal radiography. Shanghai: *Shanghai Scientific and Technical Publisher,* 1995: 23-88
5 Shang KZ, Gou MJ. Experimental investigation and evaluation of several home made barium surfate preparations for double contrast radiography. *Chin J Radiol,* 1984;18(2):95-98
6 Shang KZ. Property, function and application trend of DC barium surfate preparation. *Chin J Radiol,* 1996;30(11):795-798
7 Fan J, Chen XR, Shen TZ *et al.* Experimental reserches on flocculation and antiflocculation of double contrast barium surfate preparation. *J Clin Radiol,* 1984;3(3):125-127
8 Chen XR, Mei H, Shen TZ *et al.* Studies on heterogeneity in size and shape of barium sulfate particles for gastric double contrast radiography. *Acta Acdemiae Medicinae Shanghai,* 1984;11(2):112-116
9 Chen XR, Shang KZ. Current status of research studies in barium surfate preparation for double contrast radiography. *Foreign Med Scien-Clin Radiol,* 1984;7(2):65-68
10 Shang KZ, Guo MJ, Ji BQ *et al.* Evaluation on the anatomical and physical basis and the clinical significance of area gastrica. *Chin J Radiol,* 1990;24(3): 182-185
11 Li FS, Chang TL, Hu MH *et al.* Roentgenologic investigation of area gastrica. *Chin J Radiol,* 1984;18(1):6-8
12 Fan J, Chen XR, Shen TZ *et al.* X-ay appearences of areae gastricae in normal and chronic gastritis. *Chin J Radiol,* 1984;18(1):1-3
13 Shang KZ. The anatomy and radiology of the areae gastricae. 1989;23(Suppl): 33-35
14 Gao YO, Gao YG (ed). Double contrast radiography of gastrointestinal tract. *Beijing, People's Medical Publishing House,* 1984:32-53
15 Liu GN, Xie JX, Fan JD. Hypotonic duodenography. *Chin J Radiol,* 1980;14(3): 135-137
16 Chang TL, Li FS. Double contrast enteroclysis of small bowel. *Chin J Radiol;* 17(2):90-92
17 Xu JB, Shen MJ,Zhu YT *et al.* Duodenum and jejunum intubation for barium enama of small bower. *J Clin Radiol,* 1986;5(2):72-74
18 Shang KZ, Guo MJ, Ji BQ, Zuo Z. Investigation on characteristic appearence in double contrast radiography of gastric lesion involving anterior wall. *Chin J Dig,* 1990;10(5):271-273
19 Shang KZ, Ji BQ, Jio TD *et al.* "Foggy droplets" and "multiple mural lines": two valuble signs in double contrast radiography (DC) of gastric and colonic carcinoma. *J Pract Radiol,* 1994;10(9):514-518
20 Chen XR, Fan J, Shen TZ *et al.* Double contrast radiography of stomach. *J Clin Radiol,* 1982;1(2):115-117
21 Chen KM, Chen XR, Shen TZ *et al.* Double contrast radiography of colon after colonofiberscopy. *Chin J Radiol,* 1989;23(6):370-372
22 Chen KM, Chen XR. Comparison of colonic double conrast radiography and colonoendoscopy in patient with intestinal hemorrhage. *Acta Acdem Med Shanghai,* 1991;18(6):409-411
23 Chen JR. Single and double contrast gastric barium studies. *J Clin Radiol,* 1989;8(7);253-255
24 Chen JR. Mass survey of gastric carcinoma by X-ay screening. *J Clin Radiol,* 1984;24(Suppl):1-3
25 Chang TQ, Yang CR. Double contrast barium meal for small intestine by retrogred gas insufflation. *J Clin Radiol,* 1990;9(3):132-133
26 Chen KM, Chen XR, Shen TZ *et al.* X-ray diagnosis of ulcerative coitis. *Shanghai Med J,* 1988;11(3):178-180
27 Xie JX, Liu GN, Fan JD *et al.* Normal patterns of cardiac region in double contrast radiography. *Chin J Radiol,* 1985;19(4):235-238
28 Shi ML. X-ray diagnosis of malignant lynphoma in stomach (73 cases analysis). *J Clin Radiol,* 1984;3(1):57-59
29 Jiong H, Tang OR. Early gastric carcinoma diagnosed in gastrointestinal barium studies (64 cases report). *Chin J Dig,* 1992;12(3):177-199
30 Li SN, Gao YJ. Radiological and pathological investigation of carcinoid in gastrointestinal tract. *Chin J Radiol,* 1981;15(1):8-10
31 Chang JR, Chang XP. Double contrast radiographic findings in early gastric carcinoma (depresion type) and the relating technicality. *Chin J Radiol,* 1986; 20(Suppl):20-23
32 Cheng YD. Clinical application of duodenal double contrast radiography. *J Clin Radiol,* 1987;6(3):136-138
33 Shang KZ, Chen JR, Jio TD *et al.* Investigation on characteristic appearences of lesions located in ab-gravitational wall (AW) of stomach and colon in double contrast barium examination. *Chin J Radiol,* 1993;27(7):462-466
34 Shang KZ. Interpretation and differentiation of double contrast gastrointestinal studies. *Chin J Radiol,* 1994;28(3):201-203

 ISSN 1007-9327 CN 14-1219/R WJG, 1998;4(3):202-205

Original Articles

Expression of intercellular adhesive molecule-1 in liver cancer tissues andliver cancer metastasis

SUN Jing-Jing, Zhou Xin-Da, Zhou Ge, Liu Yin-Kun

Subject headings liver cancer; tumor metastasis; intercellular adhesion molecula-1

Abstract

AIM To study the relationship between intercellular adhesive molecule-1 (ICAM-1) and liver cancer metastasis and to search for factors to predict metastasis of liver cancer.

METHODS ICAM-1 expression in fresh tissues of normal liver and hepatocellular cancer (HCC) was examined by immunoperoxidase staining. The expression of ICAM-1 in human hepatoma, tumor surrounding tissues and normal livers were semiquantitatively analyzed by Dot immuno blot. Tissue ICAM-1 expression at mRNA level was detected by Northern blot.

RESULTS All 6 cases of normal liver samples were negative in anti-ICAM-1 immunohistochemical staining, 80.0% (36/45) of HCC presented various ICAM-1 expression. The number of positive cells was a little higher in large tumors, tumors with intact capsule and metastasis, but there was no significant difference. Two cases with cancer embolus also had high ICAM-1 expression. ICAM-1 concentration in HCC (13.43±0.09) was higher than that in tumor surrounding tissues (5. 89±0.17, $P<0.01$) and normal livers (4.27±0.21, $P<0.01$). It was also higher in metastasis group (20. 24±0.30) than in nonmetastasis group (10.23±0.12, $P<0.05$). Northern blot analysis revealed that ICAM-1 expression at mRNA level was also higher in HCC and cancer embolus than that in tumor surrounding tissues and normal livers.

CONCLUSION Tissue ICAM-1 could indicate the growth and metastasis of HCC, and may be an index that can predict liver cancer metastasis.

Liver Cancer Institute, Zhongshan Hospital, Shanghai Medical University, Shanghai 200032, China

SUN Jing Jing, female, born on 1966-01-08 in Hegang, Helongjiang Province, Han nationality, graduated from Harbin Medical University in 1986, worked in the First Hospital of Harbin Medical University as attending doctor of general surgery, now is studying in Shanghai Medical University as a Ph.D. student, majoring liver surgery, having 14 papers published.

***Supported with Grant for Leading Specialty by the Shanghai Health Bureau, National Natural Science Foundation No.396707 and China. Medical Board No.93-583**

Correspondence to: Prof. ZHOU Xin Da, Liver Cancer Institute, Zhongshan Hospital, Shanghai Medical University, Shanghai 200032, China
Tel. +86 • 21 • 64041990 est 2736, Fax. +86 • 21 • 64037181

Received 1998-01-20

INTRODUCTION

Tumor metastasis is one of the main causes of poor prognosis of hepatocellular carcinoma (HCC)[1]. The processe of metastasis includes dissociation of tumor cells from primary location; arrest, adhesion and extravasation of metastatic tumor cells. Adhesive molecules on endotheliocyte suchas selectin cause circulating tumor cells to roll along the surface. Other molecules on tumor cells including intercellular adhesive molecule-1 (ICAM-1), vascular cellular adhesive molecule-1 (VCAM-1) and so on, subsequently stop the cells completely, then extravasated through the blood vessels into selective target tissues. During the metastatic cascade, tumor cells interact with various host cells (endothelial cells, platelets or lymphocyte), and/or extracellular matrix and basement membrane components, the homotypic and heterotypic cell clumps form a multicellular embolus, which can enhance the survival, arrest and invasiveness of tumor cells[2]. The metastatic potential of cancer cells is related to the activity of their surface adhesive molecule[3]. Recently, it was noticed that ICAM-1 plays an important role in this processe. In this study, we investigated the relationship between ICAM-1 expression and the metastasis of HCC.

MATERIALS AND METHODS

Patients

The tissues of HCC used for immunohistochemical study were collected from 45 patients (39 males and 6 females, aged 10-82 years with a median of 51.1) who had undergone hepatectomy for HCC. All the cases were diagnosed pathologically. Eighteen of the patients were in early stage (without symptoms and signs of HCC), and 27 in moderate stage (having symptoms and signs of HCC, but no ascites, jaundice and long distance metastasis). Thirty patients had positive AFP ($\geqslant$30 μg/L) and 15 had negative AFP. The median diameter of the resected tumor was 6. 7cm (1.5-18), 30 had large tumors (>5cm) and 15 were had small tumors ($\leqslant$5cm). Patients with embolus in portal vein and its main branch or with intrahepatic and ultrahepatic metastasis nodules belonged to the metastasis group, the other patients were to nonmetastasis group. Six normal livers were from the surrounding noncirrhotic liver tissues of

pathologically proved benign tumors (4 hemangioma, 1 adenoma and 1 cyst).

The tissues used for detection of ICAM-1 were collected from 40 patients with HCC, 20 of them had large tumors and 22 encapsulated: 9 patients were in early stage and 31 in moderate stage. Positive AFP was found in 30 cases. There were 16 patients in the metastasis group, and 24 in nonmetastasis group. The 8 normal liver tissues were collected form thesurrounding noncirrhotic tissues of pathologically proved benign liver tumors (5 hemangioma, 1 adenoma and 2 cyst).

Reagents

Monoclonal antibody of ICAM-1(1g/L) was purchased from R-G Company, Britain; AKP goat anti mouse IgG andbiotinylated rabbit anti-mouse IgG were from Sino-Amercain Company, China; TRIzol™ total isolation reagent from Gibro Company, USA; and megaprime™ DNA labeling systems from Amersham Company,UK.

Methods

Indirect immunoperoxidase staining The fresh specimens embedded by O.C.T were frozen in liquid nitrogen, and then stored at -70℃. Serial frozen sections (6μm) of liver specimens were fixed with acetone. After preincubated with human serum to reduce background, the sides were incubated with the primary antibody (1:50) at 4℃ overnight, biotinylated rabbit anti mouse immunoglobulin (1:200) was used at 37℃ for 1 h, added with avidin biotin HRP mixture (1:100v/v), and counterstained with hematoxylin.

Dot immuno blot Three hundred mg tissue was homogenized in 1.5 ml suspended buffer solution (0.1mol/L NaCl,0.01mol/L Tris. Cl, pH 7.6, 0. 001mol/L EDTA pH 8.9, 1% Triton-X-100), the protein concentration was determined by Hatree method[4]. The supernatant (30μl) was spotted onto nitrocellulose membrane in a dot blot format. After non-specific blocking with 5% lipid free milk, the blots were incubated with ICAM-1 antibody (1:500) at room temperature for 2 h, and then incubated with AKP conjugated goat anti-mouse IgG (1:200) for 2 h at room temperature, then stained with NBT/ BCIP (2:1 v/v). The integrated optical density (IOD) of the blot was measured by MIAS 300 automatic image analyzer. Tissue ICAM 1=(sample IOD background IOD)×sample area/(μg protein concentration ×1000).

Northern blot Total RNA was extractedby TRIzol™ reagent according to the manufacturer's instruction (Gibco Life Technologies Cat No.15596. 026). Total RNA of 20 μg was denatured in formaldehyde, electrophoresed, and transferred to nitrocellulose membrane. The plasmid containing ICAM-1 probe sequence was kindly provided by Dr. Christian Stratowa (Ernst Boehringer Institute, Vienna, Austria). Northern transfer membranes were prehybridized for 4 h at 42℃ with 5×SSPE/5×SSPE/5× Denhardt's solution/1% SDS/100 mg/L Samon sperm DNA. The 1.8 kb cDNA was labeled with 32Pisotope by random primer method (Megaprime™ DNA Labeling Systems, Amersham). Nothern blot analysis was performed under stringent washing conditions, 1×SSC 0.1% SDS, 30 min at room temperture and 1×SSC 0.1% SDS, 1 h at 50℃. Autoradiography was carried out at -70℃ for 7 days.

Data analysis Significance was assessed by Student's *t* test. The results were expressed as $\chi \pm s$.

RESULTS

Immunohistoch emical observation of ICAM-1 in human HCC

By using anti ICAM-1 monoclone antibody, no ICAM-1 was foundin normal liver tissues (Figure 1). ICAM-1 was positive in fresh HCC (Figure 2), mainly on cell membrane, with a rate of 80% (36/ 45). In this group, 42.6% showed strong positive (++[aa], 30%-70% positive cells), others were weak positive (+, 0-30% positive cells). ICAM 1 was also positive in 2 cases with tumor embolus in portal vein (Figure 3).

Semi-quantitative analysis of human tissue ICAM-1

Dot immuno-blot was employed in semi-quantive analysis of tissue ICAM-1 (Figure 4). Table 1 demonstrats that ICAM-1 content in HCC was about two-fold higher than that in the tumor surrounding liver tissues and normal controls ($P<0.01$), no significant difference was found between the latter two.

Table 1 ICAM-1 expression in different liver tissues [($\chi \pm s$)/1000]

Groups	Cases	ICAM-1
HCC	40	13.43±0.09
Tumor surrounding liver tissues	40	5.89±0.17
bNormal liver	8	4.27±0.21

P<0.01, compared with HCC group

The expression of tissue ICAM 1 was also compared with tumor biological characters (Table 2), ICAM-1 in cancer tissues was only related to tumor metastasis, and there was no relationship with tumor size and capsule formation.

Table 2 The relationship of ICAM 1 content with some tumor biocharacters ($\chi \pm s$)

Groups	Cases	ICAM-1	*P*- value
Metastasis	16	20.24±0.30	<0.05
Nonmetastasis	24	10.23±0.12	
Metastasis tumor surrounding liver	16	6.80±0.08	>0.05
Nonmetastasis tumor surrounding liver	21	4.78±0.04	
Intact capsule	22	13.55±0.20	>0.05
Nonintact capsule	15	12.93±0.32	
Large HCC	20	14.45±0.26	>0.05
Small HCC	14	10.96±0.47	

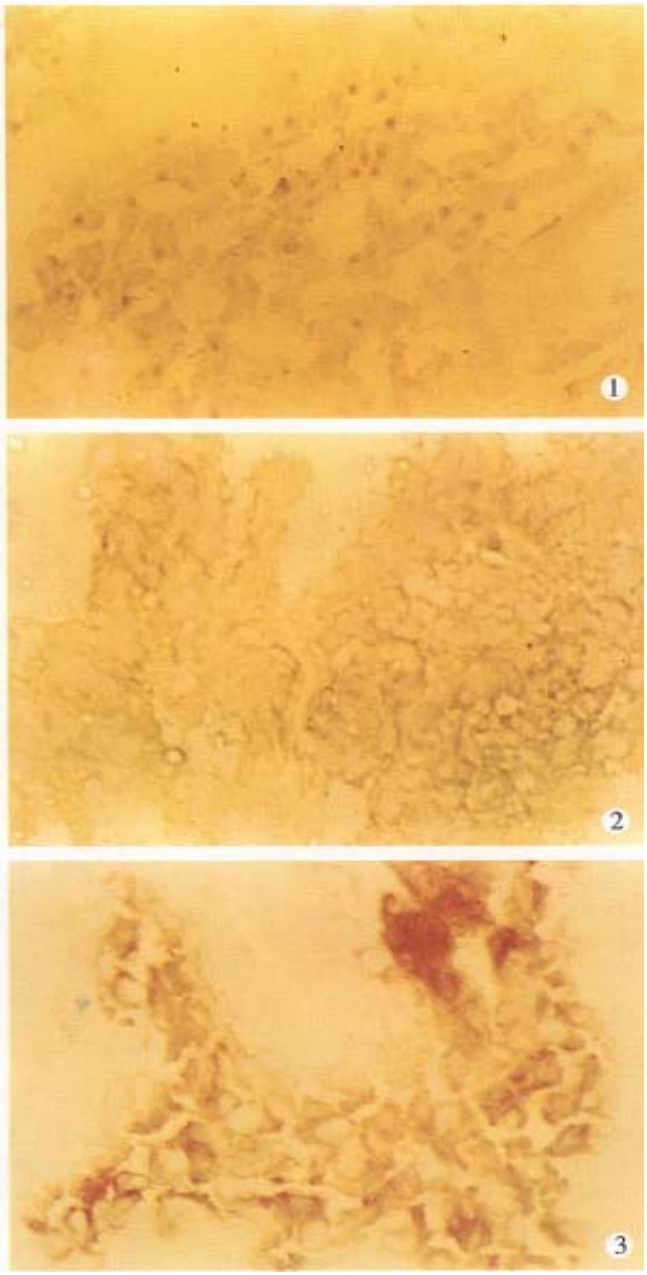

Figure 1 ICAM-1 expression in normal liver tissues by immunohistochemical staining.
Figure 2 ICAM-1 expression in liver cancer tissues by immunohistochemical staining.
Figure 3 CAM-1 expression in tumor embolus by immunohistochemical staining.

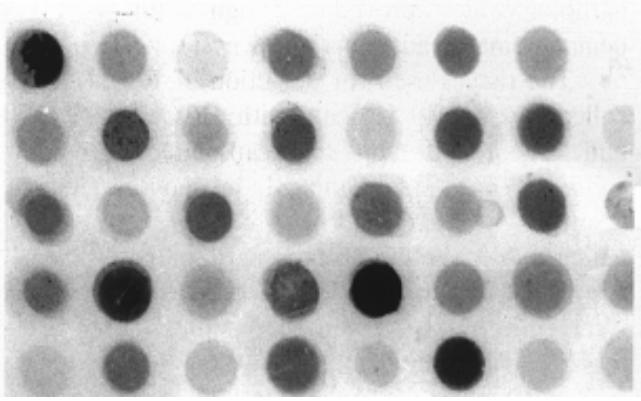

Figure 4 Tissue ICAM-1 expression by Dot immunoblot.

ICAM-1 expression at transcriptional level

In this study, special DNA probe was used in Northern blot for detecting ICAM-1 mRNA, two transcripts with 3.3 kb and 2.4 kb in length was defined. β-actin was acted as internal standard. The data obtained from image analysis indicated that ICAM-1 mRNA expression in tumors was higher than that in tumor surrounding liver tissues and normal controls as well as cancer embolus (Figure 5).

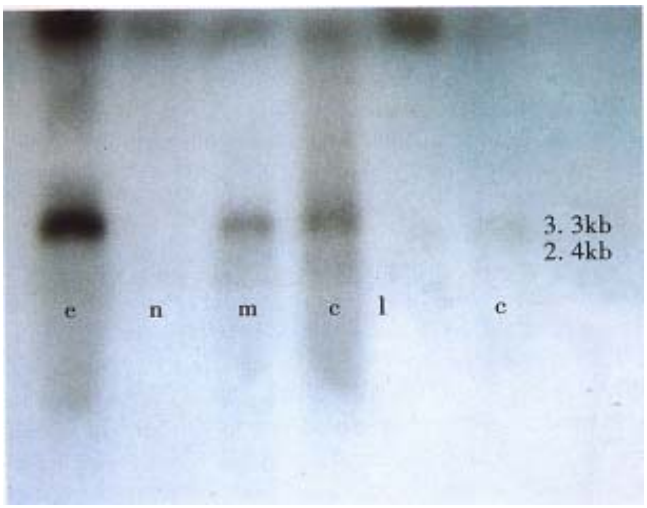

Figure 5 Detection of ICAM-1 mRNA by Northern blot. E: emblous; N; tumor surrounding liver; C: liver cancer; nurmal liver

DISCUSSION

Intercellular adhesive molecule-1 (ICAM-1, CD54), a transmembrane glucoprotein, is a member of the immunoglobulin superfamily and functions as counterreceptor for leukocyte function associated antigen-1 (LFA-1, CD11a/CD18) and complement receptor type 3 (MAC-1, CD11b/CD18)[5]. It mediates homotypic and heterotypic cell interaction, not only plays an important role in the tumor genesis, but also can reflect tumor curative

effect[6], and may be a critical factor in the process of bloodborne metastasis of cancer[7]. Recently it wasfound that ICAM-1 plays an important role in tumor recurrence and metastasis. Hung[8] *et al* found that anti-ICAM-1Ab can prevent the growth of APH-77 tumors in SCID mice by altering the homing and growth of tumor cells in certain anatomical sites. Most of normal tissues do not express ICAM-1, but ICAM-1 expression has been observed in many tumors, such as renal cancer, uterine cancer, lung cancer, gastric cancer, bladder cancer, etc. Santarosa[9] *et al* demontrated that renal cancer recurrence after operation was related to ICAM-1 expression in cancer tissues and patients with <50% of ICAM-1 positive cells in cancer tissues had prolonged disease-free survival after a median follow-up of 60 months.

In this study, all 6 cases of normal liver sample were negative in anti ICAM-1 immunohistochemical staining, 36/45 HCC presented various ICAM-1 expression. The rate of positive cell was a little higher in large tumors, tumors with intact capsule and tumors with metastasis, but there was no significant difference. It has been noticed that 2 cases with enbolus also had high ICAM-1 expression. As indicated in semiquantitative analysis of tissue ICAM-1, ICAM-1 concentration in liver cancer was higher than in tumor surrounding liver tissues and normal livers. Tissue ICAM-1 was higher in metastasis group than that in nonmetastasis group. Northern blot analysis revealed that ICAM-1 expression at mRNA level was also higher in HCC and cancer embolus than in tumor surrounding liver tissues and normal controls. So it was suggested that ICAM-1 might be one of the characters of liver cancer, and could be a diagnostic indicator for metastatic status of liver cancer.

The deduced ICAM-1 amino acid sequence analysis revealed the presence of C_3/C_4 binding protein consensus sequence between residues 341 and 404, so ICAM-1 may be involved in C_{3b} binding. Since C_{3b} binding protein generally acts to accelerate the dissociation of active complement complexes, ICAM-1 may help the tumor escape immune destruction, providing an important property needed for successful metastasis. Functioning as a ligand of LFA-1, ICAM-1 can establish the heterotypic adhesion of tumor cells with migratory and invasive leukocytes present in the tumor cells, enabling individual cell to dissociate from primary tumor and go into circulation[10]. There is soluble ICAM-1 (sICAM-1) in serum, which comes from proteolytic cleavage of membrane associate ICAM-1. Since LFA-1 could also be blocked with soluble ICAM-1, sICAM-1 may also block the attachment of cytotoxic T cell and/or NK cells to cancer cells. This could be one of the mechanisms of cancer cells escaping from the immunosurveillance system of the host, and can inhibit lymphocyte mediated cytotoxicity, therefore a favorable environment for tumor cell proliferation would be created[11]. Spontaneous regression of human liver tumor was quite rare and the tumors were unusually resistant to various immumotherapy, probably due to the high content of sICAM-lin those patients.

In our experiment, we also found that there was no statistically significant difference in ICAM-1 expression between tumor surrounding liver tissues and normal livers, and between tumor metastasis group and nonmetastasis group. So we think that ICAM-1 reflects the metastatic ability of cancer cells but not the cancer environment.

In conclusion, tissue ICAM-1 could reflect the growth and metastatic status of HCC and may be a factor to predict liver cancer metastasis.

REFERENCES

1 Zhou XD, Tang ZY, Yu YQ, Yang BH, Lu JZ, Lin ZY *et al*. Recurrence after resection of α-fetoprotein-positive hepatocellular carcinoma. *J Cancer Res Clin Oncol*, 1994;120(6):369-373

2 Yasoshima T, Denne R, Kawaguchi S, Sato N, Okada Y, Ura H *et al*.Establishment andcharacterization of human gastric carcinoma lines with high metastatic potential in the ability to metastasize in the liver of nude mice. *Jpn J Cancer Res*, 1996;87(2):153-160

3 Nasu K, Narahara H, Etoh Y, Kawano Y, Hirota Y, Miyakawa I. Serum levels of soluble intercellular adhesion molecule-1 (ICAM-1) and the expression of ICAM-1 mRNA in uterine cancer. *Gyneco Oncol*, 1997;65(2):304-308

4 Hartree EF. Determination of protein: A modification of Lowry method that give a linear photometrio response. *Ann Biochem*, 1972;48(3):422-427

5 Budnik A, Grewe M, Gyufko K, Krutmann J. Analysis of the production of solube ICAM-1 molecules by human cell. *Experi Hematol*, 1996;24(2):352-359

6 Yukihiro S, Masami M, Takashi T, Kashii Y, Miyamoto M, Nishimori H *et al*. Serum concentration of intercellular adhesion molecule-1 in patients with hepatocellilar cancinoma is a marker of the disease progression and prognosis. *epatology*, 1995;22(2):525-531

7 Regimbald H, Pilarski LM, Longernecker BM, Reddish MA, Zimmermann G, Hugh JC. The breast mucin as a novel adhesion ligand for endothelial intercellular adhesion molecule 1 in breast cancer. *Cancer Res*, 1996;56(8):4244-4229

8 Huang YW, Richardson JA, Vitctta ES. Anti-CD54(ICAM-1) has antitumor activity in SCID mice with human. *Cancer Res*, 1995;55(3):610-616

9 Santarose M, Fanaro D, Quaia M, Spada A, Sacco C, Talamini *et al*.Expression and release of intercellular adhesion molecule-1 in renal-cancer patients. *Int J Cancer*, 1995;62(3):271-275

10 Johnson P, Stade G, Holzmann B, Schwable W, Riethnuller G. De novo expression of intercellular adhesion molecuoe- in melanoma correlates with increased risk of metastasis. *Proc Natl Acad Sci USA*, 1989;86(2):641-644

11 Pirisi M, Falleti E, Fabris C, Soardo G, Toniutto P, Vitulli D *et al*. Circulating intercellular adhesion molecule-1 (cICAM-1) concentration in liver disease Relationship with cholestasis and functioning hepatic mass. *Clin Chen*, 1994; 102(5):600-604

 ISSN 1007-9327 CN 14-1219/R WJG, 1998;4(3):206-209

Study of heteroserum-induced rat liver fibrosis model and its mechanism

HUANG Zhi-Gang, ZHAI Wei-Rong, ZHANG Yue-E and ZHANG Xiu-Rong

Subject headings liver cirrhosis; heteroserum; disease models, animal; liver/pathology; mast cell; IgG; complement C3; rats

Abstract

AIM To investigate the morphological changes in the process of heteroserum induced rat liver fibrosis and the mechanism of fibrogenesis of this model.

METHODS A model of heteroserum-induced rat liver fibrosis was established by intraperitoneal injection of porcine serum. In addition to the observation of the morphological changes of this model, the infiltration of eosinophils and mast cells were measured quantitatively and the deposition of IgG and complement C3 was detected by immunofluorescence.

RESULTS The rat liver fibrosis was induced successfully at the end of the 8th week after the injection of heteroserum. Besides the increase of hepatic stellate cells (HSC) during the process of liver fibrosis, proliferation and activation of primary mesenchyma cells (PMCs) were also found. In the early stage, the infiltration of eosinophils and mast cells was significantly increased and the deposition of IgG and complement C3 was positive in the portal tracts and septa, while gradually reduced after the injection was stopped.

CONCLUSIONS This model is suitable for the research on liver fibrogenesis; the pathogenesis of this model may be related with the allergen-induced late phasereaction (LPR) caused by the injection of heteroserum, and the HSCs and the PMCs are important sources of ECM-producing cells.

Department of Pathology, School of Basic Medical Sciences, Shanghai Medical University, Shanghai 200032, China

Dr. HUANG Zhi Gang, male, born on 1968-05-09 in Xiangfan City, Hubei Province, graduated from Shanghai Medical University as a postgraduate in 1996, now an attending physician of gastroenterology, working in the Department of Internal Medicine, Baoshan Central Hospital, Shanghai 201900, China, having 2 papers published.

***Supported by the National Natural Science Fundation of China, 39330140 and Major Subject Fund of Shanghai Educational Committee.**

Correspondence to: Professor ZHAI Wei-Rong, Department of Pathology, School of Basic Medical Sciences, Shanghai Medical University, Shanghai 200032, China

Tel. +86¡¤21¡¤56601100-294

Received 1998-02-18

INTRODUCTION

There are several kinds of animal model of liver fibrosis in the literature, among which CCl4-induced model initiated with marked damage of liver tissues was extensively investigated and applied. There have been a few reports about immune liver fibrosis model without severe injury of hepatocytes because of the complexity of its making and the higher mortality of the animals. In this paper, a kind of immune liver fibrosis model established by intraperitoneal injection of heteroserum was reported in this paper, and the morphological characteristics and the pathogenesis were studied.

MATERIALS AND METHODS

The model was established according to the method of Paronetto's[1]. Forty Wistar female rats weighing about 100g and fed with common stuff and water were randomly divided into 5 groups. In each group, 5 rats were injected with 0.5ml porcine serum intraperitoneally twice a week for 10 weeks, and 3 rats with sterile physiological saline in stead. Three groups of rats were killed at the end of the 3rd, 8th and 10th week, and the other two groups at the end of the 15th and 20th week respectively. The liver tissue was regularly fixed, embedded and sliced for light or electron microscopy, and serial paraffin sections were stained with H.E. , von Gieson and toluidine blue. IgG and complement C_3 were detected by immunofluorescence in the frozen sections. Rabbit antibody against human C_3 was purchased from Dako Co. Rabbit antibody against rat IgG and FITC labeled goat antibody against rabbit IgG were prepared in our department. Eosinophils and mast cells in the liver tissue were counted and statistically analyzed with rank-sum test.

RESULTS

Morphological changes

During the whole period of the experiment no rats died and all the experimental rats advanced into liver fibrosis after injection of porcine serum for 8 weeks. Observed with the naked eye, the liver surface appeared normal until the end of the 8th week, and presented tiny particle-like changes, the tissue became hard afterwords, and the hardness increased progressively.

Microscopically, at the end of the 3rd week of the injection, one rat remained almost normal. The portal tracts enlarged mildly with extracellular matrix (ECM) and proliferated mesenchymal cells and small bile ducts without canal were visible in 4/5 rats although there existed the structure of the liver lobules. Most of the interstitial cells were enlarged and spindled in shape (Figure 1). The increased ECM and cells were also observed around the hepatic veins and central veins. In some areas, the early cellular septa consisting of the increased interstitial cells were found and inserted into the parenchyma. In one of the rats, the lobules were almost completely separated by the septa. At this stage, the liver cells had no obvious damage except the apoptosis of individual cells near the septa. Under the electron microscope, the sorts of mesenchymal cells in septa were different, some of which were typical fibroblasts, and some appeared as primitive mesenchymal cells (PMCs) with a high ratio of nucleus to plasm and a large elliptic nucleus containing 2.4 nucleolus and a few of cell organels (Figure 2). Hepatic stellate cells (HSCs) of perisinusoid close to the portal tracts or septa were elongated with less or none lipid droplets and increased and dilated endoplasmic reticula, which was often near the mesenchymal cells (Figure 3).

At the end of the 8th week, the structure of liver lobules was undiseriminated in all of 5 experiment rats, and markedly enlarged portal tracts with connective tissues were distinctly exhibited in VG stain. The septa containing many mesenchymal cells and collagen fibrils (so-called cellular fibrious septa) were extended into parenchyma, connected with adjacent portal tracts or hepatic veins and separated the lobules. The number of mesenchymal cells increased apparently in the portal tracts and septa, and PMCs were relatively less in these areas. Hepatic cells were swollen with vacuoles in cytoplasm, and some of which trapped in septa. Elcotronmicroscopically, among the mesenchymal cells in or around the portal tracts or septa, PMCs were less in number while HSCs increased as compared with those at the end of the 3rd week. The transitional cells between PMCs and fibroblasts were also seen with increased and dilated endoplasmic reticula and slightly leaner nucleus with small wrinkled?nuclear membrane (Figure 4). However, myocyte-like structure as macula densa or dense body was not seen in these mesenchymal cells. At the end of the 10th week, the amount of ECMs in portal tracts and septa increased obviously, but the number of mesenchymal cells decreased. As a result, the fibrous septamainly composed of ECMs were formed and revealed strong VG stain (Figure 5). The cells in the fibrous septa were fibroblasts and fibrocytes with leggy and deeply colored nucleus. At the end of the 15th week, i.e. 5 weeks after the serum injection, the liver structure was similar to that in the 10th week, but the number of mesenchymal cells declined progressively, and some of fibrous septa were thin or even diminished, and faded in VG stain. Under the EM, lipid droplets in HSCs increased again, although a large amount of bunched and intersected collagen in septa remained the same. In addition, some blood vessel walls thickened and became homogeneous in portal tracts and septa, but necrosis and infiltration of neutrophils were never discerned throughout the experiment.

Changes of eosinophils and mast cells

Dramatic changes were found in the number of eosinophils and mast cells in portal tracts and septa. The average of their counts in the experimental groups was higher than that of the control groups (Table 1). Infiltration of eosinophils was also shown in the portal tracts and some of early septa at the end of the 3rd week (Figure 1), and peaked at the end of the 8th week. However,it gradually decreased from the end of the 10th week, and was seldom seen after the intermission of the injection. Mast cells stained with toluidine blue were seen around blood vessels in the larger portal tracts in the normal rats, but were scarce in the smaller portal tracts. After injection of porcine serum, the number of mast cells in the smaller portal tracts and septa also increased in different stages of the experiment with the same trend of count changes as that of eosinophils although there was no significant difference between various stages.

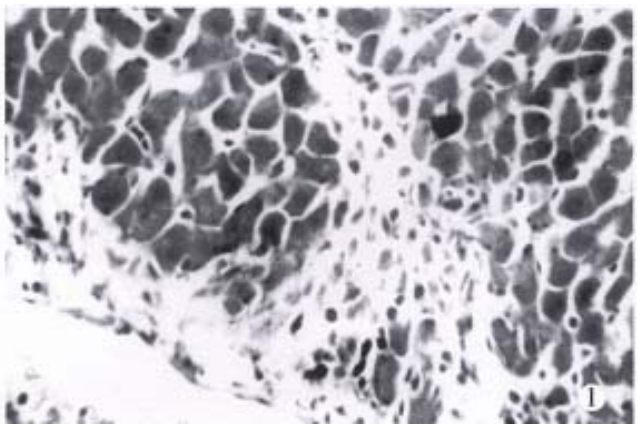

Figure 1 At the end of the 3rd week, the structure of liver lobules was defined well, the portal tracts were enlarged mildly with increased ECM and proliferated mesenchymal cells. The infiltration of eosinophils was visible in these areas. HE×200

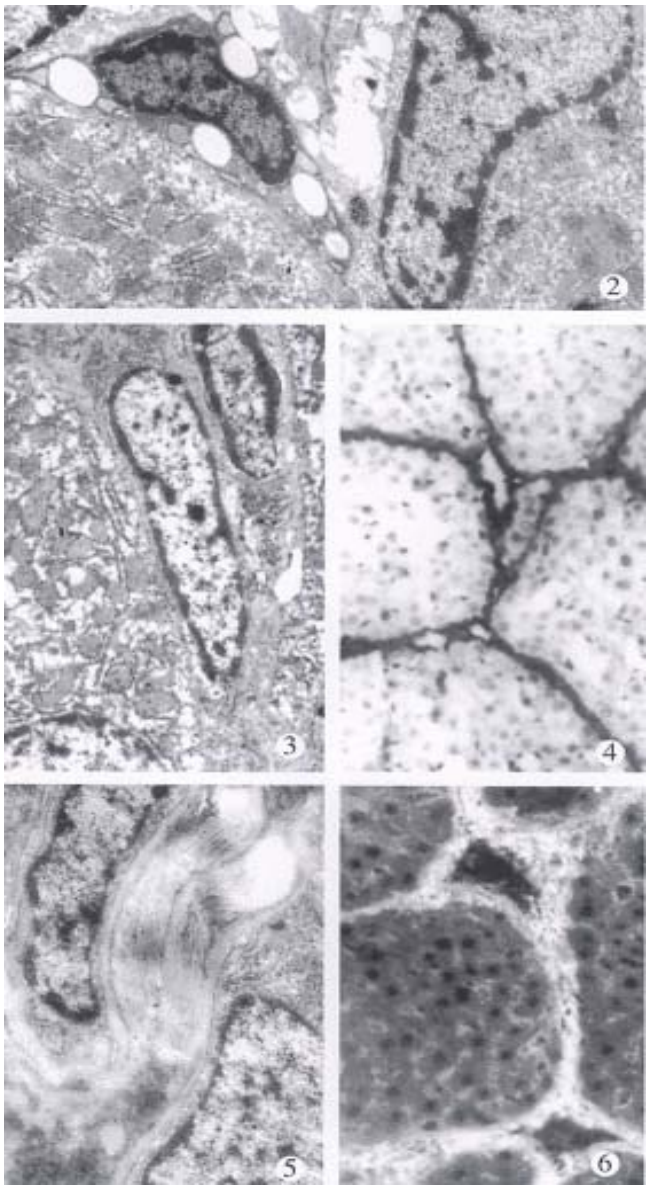

Figure 2 PMC with larger clliptic nucleus and HSC nearby at the end of the 3rd week. EM×5000

Figure 3 The activated HSC enlarged with organels and less lipid droplets at the end of the 3rd week. EM×4000

Figure 4 A large quantity of collagen fibrils around the PMC and the fibroblast. EM×8000

Figure 5 The fibrous septa inserted into and circled the pasenchyma at the end of the 10th week. VG×40

Figure 6 IgG was diffusedly deposited in the septa and portal tracts at the end of the 15th week. Immunofluoresence×100

Table 1 Average count of eosinophils and mast cells in different groups

Groups	Eosinophil	Mast cell
Control	1.17±0.80	1.24±0.31
3rd week	18.35±7.74[a]	2.82±0.72[a]
8th week	22.72±11.76[b]	7.30±2.72[b]
10th week	8.10±2.16[a]	6.20±1.05[a]
15th week	6.60±3.96[b]	2.94±0.71[a]
20th week	3.30±1.18[b]	1.85±0.52[a]

[a]$P<0.01$, [b]$P<0.05$, *vs* control group.

Detection of IgG and complement C3 in liver tissue

IgG and complement C3 in the normal liver tissue detected with immunofluoresence was lightly distributed along the sinusoids and blood vessels. At the end of the 3rd week, besides the deposition as that in the control rats, linear or spotty positive reaction of IgG and C3 were also detected in the portal tracts and early formed septa. At the end of the 8th week the degree of their positive reaction was enhanced and the reaction looked like threads and strands in the same area, and was also strongly positive in the wall of sinusoid and blood vessels. At the end of the 10th and 15th week, the distribution of IgG and C3 was diffused in the septa and portal tracts (Figure 6), and weakened obviously at the end of the 20th week.

DISCUSSION

The different modes of immune rat liver fibrotic model induced with human or bovine albumin intravenously have been reported[2,3]. After a large dose of injection, focal necrosis and fibrosis were found, leading to allergic shock and a high mortality of about 50%. if a small dose was administered for 16 weeks, different degrees of fibrosis formed in 80% with a mortality of 20%-30%, although the mortality could be reduced when the mixture of albumin and prostaglandin E2 were added. Therefore, those models were not ideal for their complicated procedures, severe damage of liver tissue and high motality of animal. In our experiment, liver fibrosis formed in all the rats after continuous injection of poreine serum intraperitoneally for 8 weeks, and no rat died during the experiment. In addition, morphology of liver tissue was distinct without severe injury of hepatic cells, therefore, it famitates in situ study and is superior to the the CCl4-induced fibrosis model with severe distortion of liver structure. As a result, our model is more suitable for research on liver fibrogenesis with the advantages of less expenses, short duration and higher success rate and simplicity of pathological changes. Our model can reveal clearly the three stages in the process of the experiment: the cellular septa formation, cellular-fibrous septa and fibrous septa. As for the source of ECM-producing cells, it has been considered that HSCs are the most important cells. This was further confirmed in our model by the appearance of proliferation and activation of HSCs with abundant collagen fibrils around. At the same time, PMS, the immature mesen chymal cells mostly located in the portal tracts and early septa, were considered as another source of ECM-producing cells, increased and developed into fibroblasts. It is suggested that in porcine serum induced liver fibrosis model, ECM-producing cells may both originate from PMCs and HSCs, and synthesize and excrete ECM,

sequentially accumulate and finally result in liver fibrosis. However, in this observation the myofibroblast, the another sort of ECM-related cells characterized with the myocyte-like structure such as macula densa or dense body in cytoplasm, was not found, which differed from the CCl4-induced model but was similar to that of Bhunchet[4].

Pathogenesis of heteroserum-induced immune liver fibrosis has not been clarified. Wang BN and Zhu QG and their coworkers[2,3] reported that IgG and complement C3 were detected in the liver tissue with obvious fall of C3 in serum, and they considered the mechanism of their model as type III allergic reaction due to the immune complex deposition. In our experiment, there was no typical type III allergic reactive pathological changes such as fibrinoid necrosis and infiltration of neutrophils in connective tissues or blood vessels although the deposition of IgG and C3 was seen in the portal tracts and septa and the walls of blood vessels were thickened. The role of immune complex in this model was still needed to be confirmed in the future. It was noticed that the appearance of the large number of eosinophils infiltrated in the portal tracts in the early stage was exactly the same as what happened in the late phase reaction (LPR) in type I allergic response. Eosinophils infiltration was considered to be intimately associated with chronic inflammations with fibrosis such as sclerotic mediastinitis, sclerotic cholangitis, idiopathic pulmonary fibrosis and so on[5]. It was reported that a number of eosinophils existed in bleomycin-induced pulmonary fibrosis and the high level of TGF-β_1 was expressed in the tissue with in situ hybridization and immunohistochemical techniques[6]. Upregulation of expression of TGF-β_1 was proved to be closely related with tissue repair and fibrosis[7,8]. All these phenomena suggest the hypothesis of this experimental liver fibrogenesis that LPR is initiated by heteroserum and mediated by mast cells to attract a number of eosinophils, which release active mediators such as TGF-β_1 to activate and proliferate PMCs and HSCs, and to increase the synthesis of ECM and eventually result in excessive accumulation of ECM in the tissue.

Acknowledgments We wish to thank Mr. Chao HK for animal feeding and Miss Zhuang L and Gu YH for their technical work. We are also grateful to Prof. Liang ZL for polishing the English language in this paper.

REFERENCES

1 Paronetto F, Popper H. Chronic liver injury induced by immunologic reaction: cirrhosis following immunization with heterologous sera. *Am J Pathol,* 1966; 49(6):1087-1101
2 Wang BE, Wang ZF, Yin WY, Huang AF, Li JJ. Study of experimental model of immune liver fibrosis. *Natl Med J China,* 1989;69(9):503-505
3 Zhu QG, Fang BW, Hu QG, Li JN, Feng QL. Investigation of bovine albumin-induced liver fibrosis model with immune damage. *Chin J Pathol,* 1993;22 (2):121-122
4 Bhunchet E, Wake K. Role of mesenchymal cell populations in porcine serum-induced rat liver fibrosis. *Hepatology,* 1992;16(6):1452-1473
5 Noguchi H *et al*. Tissue eosinophilia and eosinophil degranulation in syndromes associated with fibrosis. *Am J Pathol,* 1992;140(2):521-528
6 Zhang K, Flanders KC, Phan SH. Cellular localization of transformation growth factor β expression in Blcomycin-induced pulmonary fibrosis. *Am J Pathol,* 1995;147(2):352-361
7 Nakatsukasa H, Nagy P, Evarto RP, Hsia CC, Marsden E, Thorgeirsson SS. Cellular distribution of transforming growth factor-β_1 and procollagen types I, III and IV transcripts in carbon tetrachloride-induced rat liver fibrosis. *J Clin Invest*,1990;85(6):1833-1842
8 Yoshioka K, Takemoza T, Muzakami K, Okada M, Hino S, Miyamoto H *et al.* Transforming growth factor β protein and mRNA in glomeruli in normal and diseased human kidneys. *Lab Invest,* 1993;68(2):154-163

 ISSN 1007-9327 CN 14-1219/R WJG, 1998;4(3):210-213

Transduction of human hepatocellular carcinoma cells with human γ-interferon gene via retroviral vector *

QIAN Shu-Bing and CHEN Shi-Shu

Subject headings Carcinoma,hepatocellular/therapy; interferon II/genetics;retroviridae;immunotherapy,adoptive

Abstract

AIM To investigate the therapeutic potential of gamma interferon (IFN-γ) genemodified human hepatocellular carcinoma (HCC) cells.

METHODS The IFN-γ gene was introduced retrovirally into four HCC cell lines. Secreted IFN-γ activity was assessed using bioassay. The expression of MHC molecules was detected by FACS. Tumorigenicity was analysed by tumor formation in nude mice.

RESULTS Four IFN-γ gene transduced HCC cell lines secreted different amounts of IFN-γ, as in the same case of five clones derived from one HCC cell line. Transduction with IFN-γ caused significant increase in the expression of major histocompatibility complex (MHC) antigens on HCC cells. The expression of HLA class I was increased by 2-3 times in terms of mean fluorescence intensities, while for class II expression, the percentage of positive cells augmented from <10% to >50%. When equal amount of tumor cells were injected into nude mice, the tumor igenicity some transduced cells decreased dramantically.

CONCLUSION IFN-γ gene transduction can convert weakly imunogenic HCC cells to activate antitumor immune response, and further pave the way for the future use of such gene modified tumor cells as a modality for the cancer immunotherapy.

Department of Biochemistry and Molecular Biology, Research Center for Human Gene Therapy, Shanghai Second Medical University, Shanghai 200025 China

Dr. QIAN Shu Bing, male, born on 1970-04-03 in Zhejiang province, Han nationality, graduated from Shanghai Second Medical University as a postgraduate in 1997, lecturer of biochemistry, majoring cancer molecular biology and gene therapy, having 6 papers published.

Presented at the First International Symposium on Gene Therapy, Beijing, July 7-10, 1997

***Supported by the National "863" High Tech Project Foundation No.863-102-16-05 and the National Natural Science Foundation of China, No.39470792.**

Correspondence to: Dr. CHEN Shi Shu, Research Center for Human Gene Chongqing Rd, Shanghai 200025, China

Tel. +86 • 21 • 63846590 ext 400 Fax. +86 • 21 • 6384961, E-mail. zpwu@fudan.ac.cn

Received 1997-10-28

INTRODUCTION

The past several years have seen an explosive growth in cancer immunotherapy using cytokine genetransduced tumor cell vaccines. This strategy seeks to locally alter the immunological environment of the tumor cell so as to enhance either antigen presentation of tumor-specific antigens to the immune system or both the activation of tumor-specific lymphocytes and nonspicific immunity. Many cytokine genes have been introduced into tumor cells with varying effects on both tumorigenicity and immunogenicity [1,2]. The success of cytokinesecreting tumor vaccines in murine models of cancer has led to the initiation of clinical trials in patients[3]. IFN-γ is a pleiotropic cytokine produced by activated T-lymphocytes, which can influence the outcome of an immune response in several distinct ways[4]. An important property of IFN-γ is the ability to up-regulate the expression of major histocompatibility complex (MHC) molecules, which play a central role in immune response. An increase in immunogenicity after MHC class I up-regulation by IFN-γ is thought to be due to improved presentation of tumor-specific antigens to CD8+ CTLs[5]. We successfully transduced IFN-γ into four HCC cell lines with retroviral vector results showed a significant up-regulation of surface MHC molecules. Moreover, transduced HCC cells decreased in tumor growth. The increased immunogenicity and decreased tumorigenicity might reflect the immunotherapeutic potential of such IFN-γ gene transduced HCC vaccines.

MATERIALS AND METHODS

Cell lines

The following human hepatocellular carcinoma cell line were used: QGY7701, SMMC7721, BEL7404 and HHCL. All the cell lines were purchased from Bank of Cell, Institute of Cell Biology, Chinese Academy of Sciences (Shanghai). HCC cells were maintained in RPMI 1640 (GIBCO) supplemented with 10% heat-inactivated fetal bovine serum (FBS), penicillin (100U/mL), streptomycin (100 μg/mL) and 2mML-glutamine. The monolayer was propagated by trypsinization as required.

Construct of retroviruses and IFN-γ transduction

Human full-length IFN-γ cDNA encoding a leading peptide and IFN-γ was cloned into pLXSN retroviral vector (provided by Dr. AD Miller), generating recombinant construct pL (IFN-γ)SN. The inserted IFN-γ gene was driven by the long terminal repeat (LTR), of moloney murine leukemia virus (MLV) while the neomycin phosphotransferas gene (Neo-R) was driven by both the LTR and the simian virus early promoter (SV40). The vector was introduced into amphotropic packaging cell line PA317. Transfected cells were selected in 0.4mg/mL G418 (Gibco) and resistant colonies were isolated and amplified. Viral titers of the retroviral supernatant ranged from 5×104 to 2×106 colony forming units (CFU)/mL, when assayed for their ability to transfer neomycin-resistance to NIH3T3 cells.

HCC cells (0.5-1×106) were cultured overnight in T80 flasks (Nunc). Retroviral supernatants supplemented with 8mg/L polybrene (Sigma) were added to each flask to obtain a ratio of about 1MOI/cell. The following day, cells were fully selected by the neomycin analogue, geneticin G418. The concentration of G418 used for the selection ranged from 0.5 to 1g/L (active dose), depending on the sensitivity of each cell to the toxic effects of G418. Approximately, cells were maintained in selecting medium for 2 weeks. Colonies that survived the G418 selection were isolated and expanded.

IFN-γ assay

The amount of IFN-γ produced by transduced cells was determined by the standard cytopathic inhibition assay. Briefly, 5×105 cells were incubated for 24 hours, then supernatants were harvested, centrifuged and aliquoted as test asmples. Human fibroblasts were clutured with serial dilutions of test samples or standard IFN-γ (Boehringer Mannheim). The cells were challenged with vesicular stmatitis virus (VSV) and cultured overnight. The IFN-γ titer was calculated as the reciprocal of the dilution that protected 50% of the monalayer cells from the cytopathic effect of the virus.

Flow cytometric analysis

Flow cytometry was performed for quantitative analysis of surface MHC class I and II expression. One million cells were harvested by trypsinization, washed twice in phosphate balance solution (PBS) containing 2% FCS and 0.1% sodium azide (Sigma), and incubated for 30min at 4℃ with saturating amounts of monoclonal antibodies (anti-HLA class I and anti-HLA class II, Dept. Immunology, Beijing Medical University). After twice washing, cells were incubated with a 1×50 dilution of fluorescence isothiocyanatic-conjugated goat anti[a2]mouse IgG (Huamei Co., Shanghai) for 30min at 4℃ in the dark. The cells were washed twice, fixed with PBS containing 0.2% formaldehyde and examined by an FACScan flow cytometer (Becton Dickinson) for the percentage of positive cells and mean fluorescence intensities.

Tumor formation in nude mice

Female athymic nude BALB/c mice of 4-5 weeks (purchased from Animal Center, Chinese Academy of Sciences, Shanghai) were housed under pathogen free conditions. Six to eight animal in a group were used. Cells (3×106 in 200μL) were injected into the right flank of the mice. The tumors were measured by a caliper in two dimensions and the volume were calculated using the formula (width2×length/2). At the end of 45 days, the tumors were removed and weighed.

RESULTS

Production of IFN-γ from transduced clones

The tumor cell lines were successfully infected with recombinant retrovirus containing IFN-γ cDNA. G418-resistant colonies were isolated and expanded to cell lines for further analysis. According to the number of selected clone, each transduced cell line was designated as QGY7701. 3A, SMMC7721.2C, BEL7404.6A and HHCL.5D, respectively. Five different clones derived from the transduced HHCL were designated following the same rule. Southern blot analysis was made and showed that the intact gene of interest was present in the transduced cell lines in the form of provirus. Northern blot analysis further indicated that the correct mRNA species were transcribed (data not shown). Secretion of IFN-γ by HCC cells transduced with the retroviral vectors was determined by an appropriate bioassay. As shown in Table 1, transduced cell lines derived from different HCC cell lines produced different amounts of IFN-γ, as the same case of five clones derived from one parental HHCL.

Enhancement of the MHC molecule expression after IFN-γ gene transduction

All the four HCC cell lines used in this study were screened for cell surface expression of HLA molecules by flow cytometry as described above. As shown in Table 1, all the cell lines expressed HLA class I molecules, however the expression? of HLA. DR, a HLA class II molecules was very low. Transduction with the IFN-γ gene resulted in significant increases in the expression of HLA molecules. The expression of HLA class I molecules was increased 2-3 times in terms of

fluorescence intensities, while for class II molecules, the percentage of positive cells was augmented from <10% to >50%. There was nocorrelation between the degree of increase in HLA expression and the amounts of IFN-γ production, even when five transudced clones derived from one parental cell line HHCL were compared. But it is fairly clear that the cells with lower expression of HLA class I molecules, such as QGY7701 and BEL7404, have stronger response to IFN-γ transduction in inducing the expression of HLA molecules, and thus resulting in more increase in the intensities of such molecules (Table 1).

Tumor growth in nude mice

Live parental 3×106 or transduced HCC cells were injected s.c. into the thigh region of nude mice, and tumor growth was measured weekly. The tumorigenicity was different in each parental HCC cell. The tumor growth of QGY7701 was more rapid than HHCL. Injection of the former cells resulted in palpable tumor within 7 days, while the latter formed discernible tumor after 14 days. However, the tumor formation of respective IFN-γ transduced HCC cells was also different. Transduced QGY7701.3A showed no distinguishable decrease in its tumor growth as compared with that of parental cell line, whereas transduced HHCl.5D reduced its tumorigenicity dramatically (Table 2). In addition to the much lower tumor incidence (1/7), there was a significant decrease in both the size and the weight of the tumor (P<0.01). The other two transduced HCC cells also inhibited the tumor growth, although in different degrees. It is notable that the reduction in tumor growth following IFN-γ transduction was related to the original tumor formation potential of its parental HCC cell line.

Table 1 Secretion of IFN-γ and expression of HLA antigens by transduced hepatocellular carcinoma cells in culture

Cell lines	IFN-γ Production (U/5×105 cells/24h)	Control* MCN(% positive)△△	HLA class I * * MCN (% positive)	HLA class II△ MCN (% positive)
QGY7701	0	18(6)	159(99)	26(11)
QGY7701.3A	75	21(5)	306(100)	28(77)
SMMC7721	0	9(2)	200(100)	13(12)
SMMC7721.2C	150	21(3)	348(100)	14(58)
BEL7704	0	20(7)	34(93)	21(8)
BEL7404.6A	75	22(5)	117(100)	29(47)
HHCL	0	10(3)	232(100)	12(10)
HHCL.2C	100	22(6)	340(100)	37(56)
HHCL.2D	25	14(6)	440(100)	12(68)
HHCL.5C	100	11(4)	401(100)	19(83)
HHCL.6C	75	15(3)	550(100)	10(44)
HHCL.5D	200	10(3)	341(100)	10(40)

*Cells were stained with fluorescence isothiocyanatic-conjugated goat anti-mouse IgG (FITC-IgG) as a control.
**Cells were stained with anti-HLA class I McAb following with FITC-IgG.
△Cells were stained with anti-HLA class II McAb following with FITC-IgG.
△△Mean fluorescence channel number (MCN) and percentages of positive cells (in parenthese).

Table 2 Formation of tumors by parental and transduced hepatocellular carcinoma cells in nude mice

Cell	Incidence	Volume (cm3)	Weight (g)
QGY7701	8 / 8	5.58±0.90	1.62±0.36
QGY7701.3A	8 / 8	5.16±16	1.60±0.72
SMMC7721	7 / 7	3.87±0.24	0.55±0.12S
MMC7721.2C	5 / 6	1.26±0.32[a]	0.28±0.08[a]
BEL7404	8 / 8	4.32±0.28	0.78±0.14
BEL7404.6A	8 / 8	3.35±0.21	0.50±0.12
HHCL	8 / 8	2.04±0.32	0.35±0.18
HHCL.5D	1 / 7	0.15[b]	0.02[b]

All the values are measured at 6 weks after injection with equal amounts of cells (3×10^6 each), and presented as the average value ± the standard error of the mean
[a]P<0.05, compared with SMMC7721 value by Student's t test
[b]P<0.01, compared with HHCL value by Student's t test

DISCUSSION

In this study human hepatocellular carcinoma cell line were the genes for human IFN-γ were transduced successfully. Four different HCC cells transduced with the IFN-γ gene produced varying levels of IFN-γ, and such difference is also existed among the five clones derived from one parental HCC cell line (HHCL). Since the distinguished feature of retroviral vector is its integration into the host genomic DNA in the form of provirus[5], the expression difference might be due to the random integration resulting in varying efficiency of gene expression derived by interior promoter.

It has been repeatedly demonstrated that IFN-γ

can exert significant antitumor effects via either direct antiproliferative effects on the tumor or indirectly through the host immune system, including enhancement of MHC class I and II expression, activation of macrophage and natural killer cells, generation of cytotoxic T-lymphocytes and induction of tumor associated antigen[4]. MHC class I and II molecules play a central role in cellular immunity and tumor survillance. Recent studies have demonstrated that the loss of MHC class I expression was associated with tumor progression or metastasis[7]. Enhancing MHC class I expression by tumor cells may promote antitumor response against them. Our results in MHC as consistent with most others in melanoma and RCC [8-10]. The cell surface expression of both HLA class I and II molecules was increased in HCC cells transduced with the IFN-γ gene. Considering the original display of HLA class I, but not class II in parental HCC cells, it is not surprising that following IFN-γ transduction, HLA class I expression was significantly in creased in terms of mean fluorescence intensities, while for class II, in terms of percentage of positive cells. There was no definite correlation between the magnitude of the increase in the expression of HLA molecules and the amount of the IFN-γ secreted by tranduced HCC cells. However, the magnitude of the increase in the expression of HLA class I in mean fluorescence intensities appeared to be greater in transduced HCC cells with lower expression of such molecules in its parental cells. This suggests that the augmentation of MHC expression is associated with both the effects of IFN-γ and the potential of expression of such molecules.

Most animal studies have showed that IFN-γ secretion by tumor cells results in reduced tumorigenicity. However, when the tumorigenicity of human tumor cells was examined in nude mice, several element must be considered. Nude mice is a T cell deficient strain, but other components of the immune system may still exist. In addition, human IFN-γ secreted by transduced HCC cells have little effect on mouse immune system. Our results obtained from nude mice injected with parental or transduced HCC cells were different. That the tumor growth of the transduced QGY7701.3A in nude mice was not significantly different from that of the parental untransduced cell lines was surprising. But it should be noted that QGY7701 was of the highest tumorigenicity among the four HCC cell lines. In contrast to QGY7701, HHCL, which was of the lowest tumorigenicity, showed dramatic decrease in tumor growth in nude mice following transduction with IFN-γ gene. The observation of such difference might reflect either the heterogeneity of the cells with which we worked or the limited effects of IFN-γ for tumor cells of high tumorigenicity.

In summary, the data obtained in this study indicated that IFN-γ gene modified HCC cells might be useful in the treatment of human cancers, especially in inducing specific immune responses. However, the heterogeneity of tumor cells should be considered in establishing effective tumor vaccine, thus a more potential tumor vaccine can be selected and an increased antitumor immunity induced *in vivo* can be obtained. This study has laid ground for the future use of cytokine gene modified tumor cells as a modality for the cancer immunotherapy.

REFERENCES

1 Gansbacher B, Zier K, Daniels B, Cronin K, Mannerji R, Gilboa E. Interleukin-2 gene transfer into tumor cells abrogates tumorigenicity and induces protevtive immunity. *J Exp Med,* 1990;172(5):1227-1224

2 Giboa E, Lyerly HK, Vieweg J, Satio S. Cytokine gene therapy in tumor. *Semin Cancer Biol,* 1994;5(3):409-417

3 Special report. Human gene marker / therapy clinical protocols. *Hum Gene Ther,* 1996;7(4):567-588

4 Sigel JP. Effects of interferon-gamma on the activation of human T-lymphocytes. *Cell Immunol,* 1988;111(3):461-472

5 Restifo NP, Spiess PJ, Karp SE, Mule JJ, Rosenberg SA. A nonimmunogenic sarcoma transduced with the cDNA for inteferon γ elicits CD8+T cells against the wild type tmor: correlation with antigen presentation capability. *J Exp Med,* 1992;175(6):1423-1431

6 Crystal RG. Transfer of genes to humans: early lessons and obstacles to success. *Science,* 1995;270(4):404-414

7 Ferrone S, Marincola FM. Loss of HLA class I antigens by melanoma cells: molecular mechanisms, functional significance and clinical revelance. *Immunol Today,* 1995;16(7):487-497

8 Nayak SK, MeCallister T, Han LJ, Gangavalli R, Barber S, Dilloman RO. Transduction of human renal carcinoma cells with human γ-interferon gene via retroviral vector. *Cancer Gene Ther,* 1996;3(3):143-150

9 Gansbucher B, Bannerji R, Dannids B, Zier K, Cronin K, Gilboa E. Retroviral vector mediated γ interferon gene transfer into tumor cells generates potent and long lasting antitumor immunity. *Cancer Res,* 1990;50(14):7820-7825

10 Ogasawara M, Rosenberg SA. Enhanced HLA molecules and stimulation of autologous human tumor infiltrating lymphocytes following transduction of melanoma cells with γ-interferon genes. *Cancer Res,*1993;53(7):3561-3568

 ISSN 1007-9327 CN 14-1219/R WJG, 1998;4(3):214-218

Animal experiments and clinical application of CT during percutaneous splenoportography

ZHANG Xue-Lin, QIU Shi-Jun, CHANG Ren-Min, and ZOU Chang-Jing

Subject headings portography; tomography,X-ray computed;animals,laboratory;liver neoplasms/ radiography

Abstract

AIM To introduce computed tomography during percutaneous splenoportography (CTSP), a new method for determining hepatic diseases.

METHODS Ten hybrid dogs and 20 patients with primary hepatic cancer (PHC) were included in the study. Each dog was examined by CT, CTAP (computed tomography during arterial portography) and CTSP to compare the enhanced degrees of the liver. The 20 PHC patients were examined by CTSP and the appearance of PHC was compared with their pathological results to evaluate the diagnostic significance of CTSP.

RESULTS The animal experiments showed that both CTAP and CTSP could obviously enhance the liver ($P<0.01$), but there was no significant difference in the enhanced results between the two methods ($P>0.05$). On the CTSP images in the 20 patients, the density of the livers was increased to 168-192Hu, whereas the density of the cancers remained as low as that on the images of CT scans (<58Hu). The CTSP findings were consistent with the surgical ones from spaceoccupying lesions. Its diagnostic value was obviously superior to that of general enhanced CT and ultrasonic examination. However, it was difficult for CTSP to show nodules less than 1cm in size located on the surface of the liver or the hepatic portal zone.

CONCLUSIONS Like CTAP, CTSP is also a sensitive method for showing occupants in the liver. But the equipments and the procedures for CTSP are simpler than for CTAP. Therefore, it is an alternative procedure in clinical practice.

Department of Imaging Diagostics, Nanfang Hospital, the First Military Medical University, Guangzhou 510515, Guangdong Province, China
ZHANG Xue Lin, male, born on 1954-06-18 in Changsha City, Hunan Province, Han nationality, professor and director of department of imaging diagnostics, having over 80 papers and 5 books published.
Correspondence to: Dr. ZHANG Xue Lin, Department of Imaging Diagostics, Nanfang Hospital, First Military Medical University, Guangzhou 510515, Guangdong Province, China
Tel. +86 • 20 • 87705577 ext 3223
Received 1998-01-31

INTRODUCTION

Computed tomography during arterial portography (CTAP) established by Hisa in 1980 is the most sensitive method for showing occupantis in the liver[1-3]. Unfortunately, CTAP is not convinient for arterial catherization, which is necessary before CT examination. Based on CTAP, we used CT during splenoportography (CTSP) to show occupants in the liver. CTSP does not require complicated instruments and is easy to operate. And it has been proved to be sensitive and safe for clinical application[4-5].

MATERIALS AND METHODS

Animal experiments

Animals and instruments Ten hybrid dogs were supplied by the Animal Experimental Unit of Nanfang Hospital. The instruments used in this experiment were: 800mA remote controlled gastrointestinal machine (Daojin, Japan), 5F Cobna catheters, somaton plus whole body CT machine (Simens Corporation, German), syringes of MCT310-2 model (Medrad Corporation, USA), and 20G trocar (Terumo Corporation, Italy).

Procedures Firstly, plain CT scaning was performed in all of the dogs from the top of the diaphragm to the inferior margin of the liver. Each layer was and distance between two neighbouring layers was 10mm. Then, the animals were examined by CTAP. Using Seldinger technology, a catheter was inserted from the left femoral artery to the anterior mesenteric artery (Figure 1). Four hours later, 76% compound meglumine diatrizoate (1. 5ml/kg body weight) was injected through the catheter at a rate of 1.5ml/sec and the animals were examined by continous dynamic scanning. Seven days after CTAP, CASP was performed. In this procedure, the point of a 20G trocar was inserted into the relatively larger veins or the splenic paronchyma (Figure 2). The same quantity of compound meglumine diatrizoate was injected at the same rate as CTAP. The animals were examined as in the second step.

Clinical application

General data Seventeen men and three women with PHC were examined by CTSP. Nine of the 20 patients were operated on after CTSP to remove the tumors who were proved pathologically to have primary hepatocellular carcinomas. Seven patients

had postoperative recurrence of hepatocellular carcinomas. Diagnosis of PHC in 4 patients was made according to the criteria formulated in the National Consonsus Conference on Prevention and Therapy of Hepatic Carcinoma in 1977.

Instruments The same trocar, syringes and CT scan machine were used as for the animal experiments.

Examination methods The position for insertion of a 20G trocar was determined by CT. The puncture point for CT was generally on the middle or posterior axillary line of the 8th to 11th intercostal space. The depth of the needle was determined by CT image. When the needle was inserted, the patients were scanned once again. When proper position, depth and direction of the needle were achieved (Figure 3), a total volume of 60ml-80ml 60% angiografin (SCHRING Corporation, Germany) was injected at a rate of 1ml/sec. Twenty seconds later, continuous dynamic scanning was started. When the scanning was finished, the trocar was quickly pulled out and the puncture point was pressed for 4-5 minutes and covered with gauze. If necessary, the puncture site should be scanned to get 1-3 images to observe whether bleeding happens.

RESULTS

Animal experiments

The CT values of the dog livers in plain CT scan, CTAP and CTSP were 70.5Hu ± 8.7Hu, 209Hu ± 23. 9Hu and 212Hu ± 28.2Hu, respectively. CTAP and CTSP could markedly enhance the liver ($P<0.01$), with no significant difference ($P>0.05$) (Figures 4). To observe the liver, kidney and spleen, two of the ten dogs were killed each time immediately, 3, 5, 7 or 10 days after CTSP examination. No abnormality was seen in the livers and kidneys of all the dogs. The surface of the spleens was smooth, without haematoma.?In the spleens, dotted bleeding sites about 2mm×2mm appeared where the needle was inserted. Those bleeding sites were substituted by connective tissues later (Figures 5-7).

Clinical application

The apearance of PHC in CTSP. In the 20 patients with PHC, 58 foci with low density were found by CTSP. After the contrast medium was injected, the CT values of normal livers could reach 168Hu-192Hu, whereas the values of hepatic cancers were no more than 58Hu. The carcinomas showed similar density in CTSP and plain CT scan. The neoplasms showed clear borders (Figures 8a-c, 9a-c and 10a-d).

The density of the spleen was not high after injection of the contrast medium, because most of the contrast medium was quickly excreted. Sometimes, block-shaped contrast medium could be seen remaining in the spleen (Figure 11). In three patients, image of high density could be observed beneath the capsule of the spleen, which may be resulted from reflux of the contrast medium there.

The postoperative reaction of the patients. The patients did not feel obviously uncomfortable when the contrast medium was injected at a rate of 1ml/sec. They felt slight local swelling and pain at the beginning when the injection was rapid (2ml/sec-3ml/sec). The pain was alleviated 10-20 minutes later. Three patients felt more severe pain because the drug was injected into the pleural cavity. The contrast medium was spontaneously absorbed one week later. No bleeding occurred.

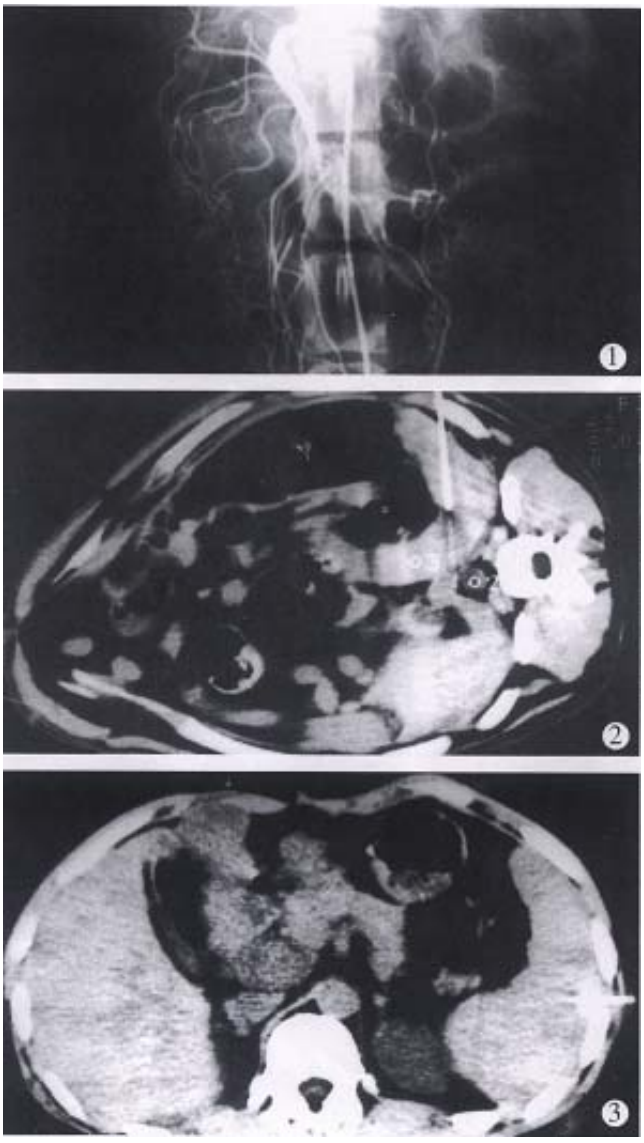

Figure 1 Anterior mesenteric arteriography in a dog. The point of the catheter is in the stem of the anterior mesenteric artery.
Figure 2 The point entered the right place of the dog's spleen.
Figure 3 The point entered the right place of the patient's spleen.

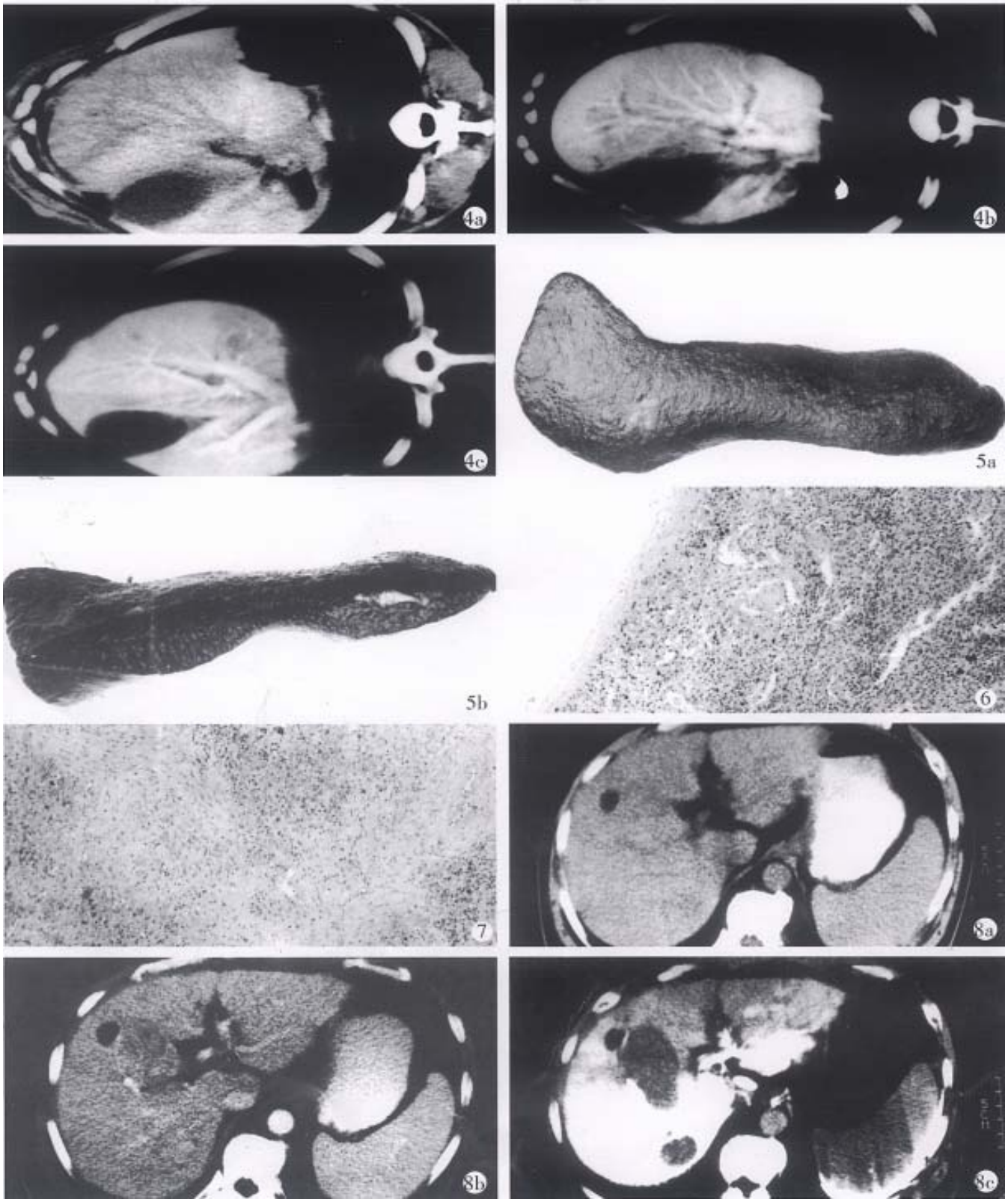

Figure 4a-c The CT images of the same dog's liver. a. plain CT scan; b. CTAP; c. CTSP.
Figure 5 The spleens of the dogs eviscerated 5 days after CTSP. a. The surface of the spleen is smooth and b. there is nobleeding foci in the longitudinally dissected spleen.
Figure 6 The splenic tissue of one dog killed immediately after CTSP. HE stain 3.3×10.
Figure 7 The spleen of a dog killed 10 days after CTSP. A little proliferation of connecuive tissue could be seen at the point where the catheter entered the spleen. HE stain 3.3×10.
Figures 8 PHC of a 59-year-old male patient. a. plain CT scan: only a small cyst was seen in the anterior part of the right lobe of the liver. b. enhanced CT: except the cyst, the carcinoma could not be shown clearly. c. CTSP: two carcinomas were clearly shown behind the cyst, and proved to be primary hepatocyte carcinoma.

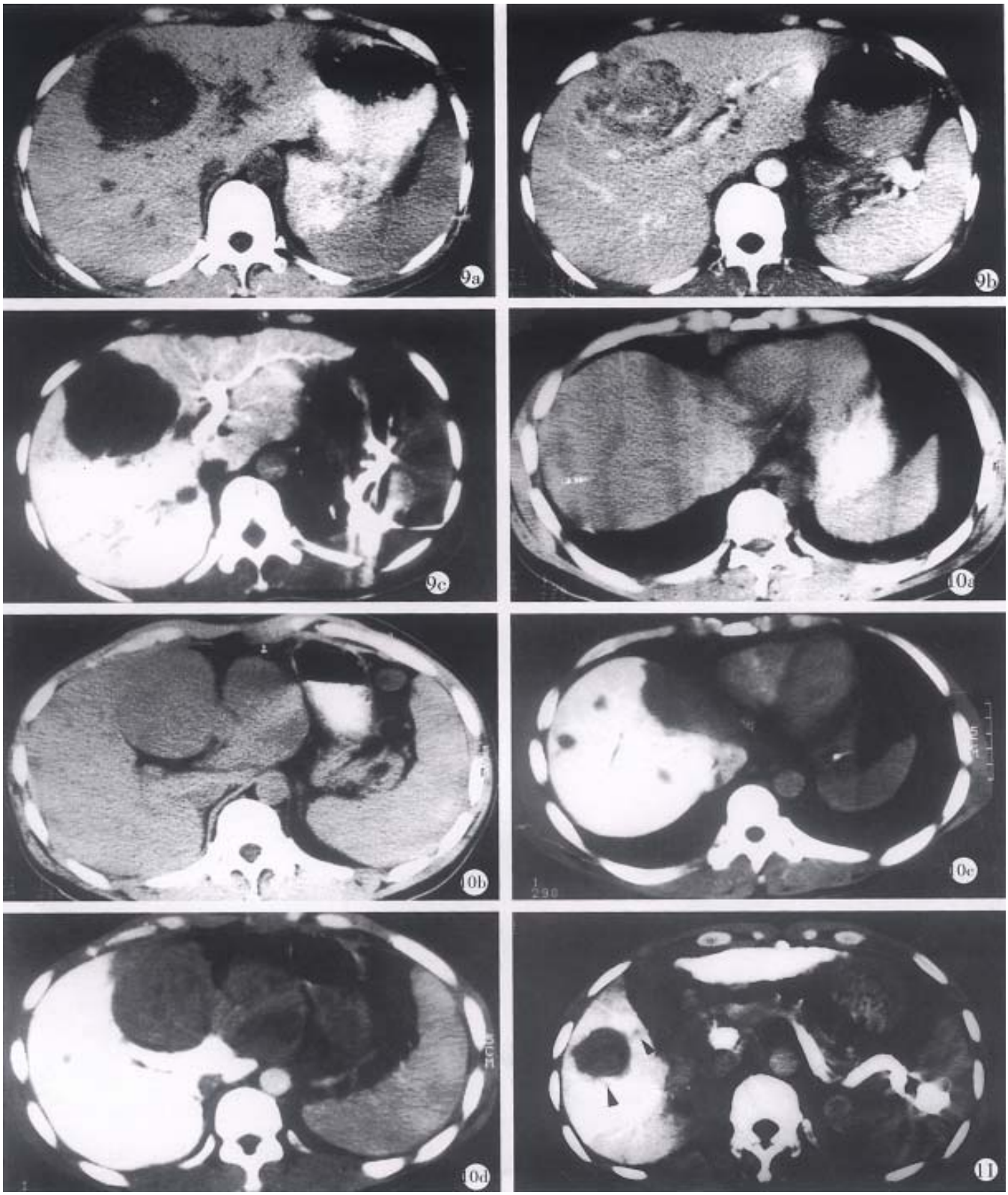

Figure 9 Primary hepatocyte carcinoma of a 30- year-old female patient. a. plain CT scan; b. enhanced CT; c. CTSP. Though they all could show carcinoma, CTSP not only could show it more clearly than the other two, but also show metastases to the right of the inferior vena cava.

Figure 10 Postoperative recurrence and hepatic metastases of primary hepatocyte carcinoma of a 44-year-old female patient. a, b, plain CT scans; c, d, CTSP.

Figure 11 The contrast medium remained in the spleen after CTSP. The splenic veins show high density. The recurrent cancer in the liver and the child focus in the portal vein (the left posterior arrow) are both shown clearly.

DISCUSSION

The liver was supplied with blood by the portal vein and the hepatic arteries, but by the portal vein, whereas the hepatic carcinoma was mainly supplied by the hepatic arteries. In CTSP, the contrast medium injected into the spleen reached the liver through the portal vein, therefore, the density of the normal liver tissue obviously increased and that of the hepatic carcinoma tissue remained unchanged. Animal experiments showed that CTSP could have the same enhancement effects as CTAP did, which provided a good radiological basis for CTSP to show occupants in the liver.

CTSP has been shown to be a very sensitive method for showing both primary and metastatic foci of PHC. In 9 patients, CTSP was as sensitive as operative exploration in finding the foci of 1cm in size in the liver. In the other three patients, CTSP could not find nodules <1cm on the surface of the liver or metastatic foci <1cm in the hepatic portal zone that were found during operation. Compared with ultrasonic examination, CTSP could find more foci. Ultrasonic examination could find only 5 of 15 foci $\leqslant$1.5cm found by CTSP in 12 patients. CTSP was even superior to ultrasonic examination in showing nenoplasms located on the diaphragmatic surface of the liver. In four patients examined by enhanced CT and CTSP, CTSP showed seven foci $\leqslant$ 1.5cm, whereas enhanced CT found only three foci unclearly. In general, according to our limited experiences, CTSP could show PHC with high sensitivity. Further work is necessary for qualitative diagnosis of PHC by CTSP.

CTSP is sensitive in showing occupants of as small as 5mm in size in the liver. Therefore, CTSP should be done when primary or metastatic occupants were suspected in the liver that could not be shown clearly by other examinations. For patients with occluded portal veins, CTSP is not acceptable, because the contrast medium is difficult to pass through the portal veins.

CTSP is a microtraumatic examination. Though early observation in animal experiments could find bleeding foci at the splenic puncture sites, their diameters were less than 2 mm and substituted by connective tissues later, without spleen rupture. No bleeding in the abdominal cavity and spleen rupture occurred either in our clinical application. The vein intima remained smooth and no portal veins were obstructed, no injuries were seen in the livers and the kidneys. Therefore, CTSP could be safely used in clinical practice.

REFERENCES

1 Matsui O, Takahima T, Kadoya M. Dynamic computed tomography during arterial portography: the most sensitive examination for small hepatocellular carcinoma. *J Comp Assist Tomography*, 1985;9(1):19-24
2 Matsui O, Takashima T, Kadoya M. Liver metastases from colorectal concers detection with CT during arterial portography. *Radiology*, 1987;165(1):65-70
3 Takayasu K, Moriyama N, Muramatsu Y. The diagnosis of small hepatocellular carcinoma: efficacy of various imaging procedures in 100 patients. *AJR*, 1990;155(1):49-54
4 Zhang XL, Chang RM, Cheng GX. Discussion of primary hepatic carcinoma by CT during percutaneous splenoportography. *J Image Intervent Radiol*, 1996; 5(6):339-341
5 Zhang XL, Chang RM, Zou CJ. Early diagnosis of primary hepatic carcinoma by liver enhancing CT during percutaneous splenoportography. *J Med Coll PLA*, 1996;11(4):309-313

Relationship between expression of laminin and pathological features in human colorectal carcinoma *

FENG Shu[1], WANG Yu-Ying[1] SONG Jin-Dan[2]

Subject headings rectal neoplasms/pathology; colonic neoplasms/pathology;laminin/metabolism; immunohistochemistry

Abstract

AIM To study the expression and significance of laminin in human colorectal carcinoma.

METHODS Using the monoclonal antibody to laminin and streptavidin-peroxidase immunohistochemical method, the expression of laminin in 63 cases of human colorectal carcinoma tissues was determined.

RESULTS In normal marge intestinal mucosa adjacent to carcinoma, laminin was largely restricted to basement membrane in continuous linear pattern. In contrast, human colorectal carcinomas exhibited a progressive loss of an intact basement membrane that was correlated with decreasing differentiation degree. Well and moderately differentiated tumors exhibited a thin basement membrane with intermittent disruptions, and poorly differentiated tumors exhibited no areas of intact basement membrane. An association was found between lack of basement membrane laminin immunohistochemical staining in colorectal carcinoma and poorly differentiated tumor ($P<0.01$).

CONCLUSION Immunohistochemical staining for laminin could provide a very useful indexfor the determination of the differentiation degree of colorectal carcinoma.

[1]Microbial Engineering Department, Institute of Applied Ecology, Academia Sinica, Shenyang 110015, Liaoning Province, China
[2]Key Laboratory of Cell Biology, Ministry of Public Health of China, China Medical University, Shenyang 110001, Liaoning Province, China
Dr FENG Shu, female, born on 1965-02-09, graduated from Jiamusi Medical College in 1986, got a master degree in 1989 and doctorate degree in 1996 in China Medical University, and now working as a postdoctorate in the Institute of Applied Ecology, Academic Sinica, having had 13 papers published.

***Project supported by the National Natural Science Foundation of China, No. 3904005.**

Correspondence to: Dr. FENG Shu, Microbial Engineering Department, Institute of Applied Ecology, Academia Sinica, Shenyang 110015, Liaoning Province, China
Tel. +86 • 24 • 3916243

Received 1997-11-26 **Revised** 1998-01-10

INTRODUCTION

Normal epithelial tissues secretes, assembles, and adhere to well-defined basement membranes. Loss of a well-defined basement membrane is one of the features of neoplastic proliferation for epithelial-derived tumors[1]. Laminin, a major glycoprotein of basement membrane which has been shown to regulate a variety of biological phenomena including cell attachment, growth, morphology and cell migration by specific high affinity receptors, plays an important role in the interaction of tumor cells with the basement membrane, the differentiation, invasion and metastasis of tumors[2,3]. Immunohistological studies, by using antibodies specific for laminin and other basement membrane components, such ast type-IV collagen, have revealed disruption or loss of basement membrane staining in a number of malignant tumors, including breast, pancreatic, bladder, prostatic and colorectal carcinomas[4]. In this study, basement membrane protein laminin was assessed by streptavidin-peroxidase immunohistochemical method to facilitate the understanding of the relationship between laminin expression in human colorectal carcinoma and the pathological features of tumor

MATERIALS AND METHODS

Materials

Sixty-three cases of human colorectal carcinoma specimens were obtained from the Department of Pathology, China Medical University. Thirty-three were male and 30 were female with ages ranging from 26 to 72 years. The tissues were fixed in 10% nautral buffered formalin and embedded in paraffin wax. Five μm paraffin sections were cut and used for HE staining and immunohistochemistry.

Methods

Laminin expression was determined by using streptavidin-peroxidase (SP) immunohistochemical method with anti-laminin monoclonal antibody (SIGMA, 1:1000; SP kit ZYMED). Both negative and positive controls were set. The staining was scored according to both intensity and continuity of the basement membrane. they were scored as negative(-), fragment pattern (+), interrupted linear pattern(++), and continuous linear pattern (+++). Negative and fragment patterns were

classified as discontinuity and the other two patterns as continuity. Statistical analyses were conducted by χ^2 test. Results were considered significantly different when *P* value was less than 0.05.

RESULTS

Tumor grading and laminin expression

Normal large intestinal mucosa adjacent to carcinoma exhibited an organized glandular epithelium overlying a well-defined continuous linear basement membrane that stained for laminin (+++), (Figure 1). Well and moderately differentiated colorectal carcinomas differed from normal colon in which periglandular basement membrane staining was thin and intermittently discontinuous (++ to+++), (Figure 2). Poorly differentiated tumors consisted of solid nonglandular islets of cells. Patches of laminin staining was scatered throughout the tumor. Nonpolarized cytoplasmic laminin staining without a surrounding basement membrane (- to +) (Figure 3) was found sometimes in the nests of cells in these tumors.

Relationship between tumor grade and basement membrane laminin staining pattern in the tumors is shown in Table 1. Of the well and moderately differentiated cases, 80% and 57.1% showed continuous basement membrane laminin staining respectively, compared with 14.6% of poorly differentiated ones. When the staining patterns for poorly differentiated tumors were compared statistically with well and moderately differentiated tumors, a significant difference was found (χ^2: $P<0.01$). Hence, discontinuous basement membrane laminin staining is associated with poor differentiation of tumors.

Table 1 Tumor grading and laminin staining patterns

Tumor grade	*n*	Laminin staining pattern	
		++ to +++	- to +
Well differenciated	20	16(80.0%)	4(20.0%)[a]
Moderately differenticated	21	12(47.1%)	9(42.9%)[a]
Poorly differenticted	22	3(13.6%)	19(86.4%)

[a]$P<0.01$ *vs* poorly differentiated tumor.

Tumor stage and laminin expression

Comparison between basement membrane laminin staining pattern in tumor and tumor stage is given in Table 2. When regional lymph nodes were involved (Dukes's stage C), there was no linear staining of basement membrane laminin in 13/21 (61%) cases of primary tumors, whereas the majority (23/42) of stages A and B tumors showed continuous basement membrane laminin staining. However, there was no statistical significance (χ^2: $P>0.05$).

Table 2 Tumor stage and laminin staining pattern

Tumor grade	*n*	Laminin staining pattern	
		++ to +++	- to +
Dukes's stage A	36	20(45[a]±6%)	16(44.4%)
Dukes's stage B	6	3(50.0%)	3(50.0%)[a]
Dukes's stage C	21	8(38.1%)	13(61.9%)

[a]$P>0.05$ *vs* Dukes's stage A tumor.

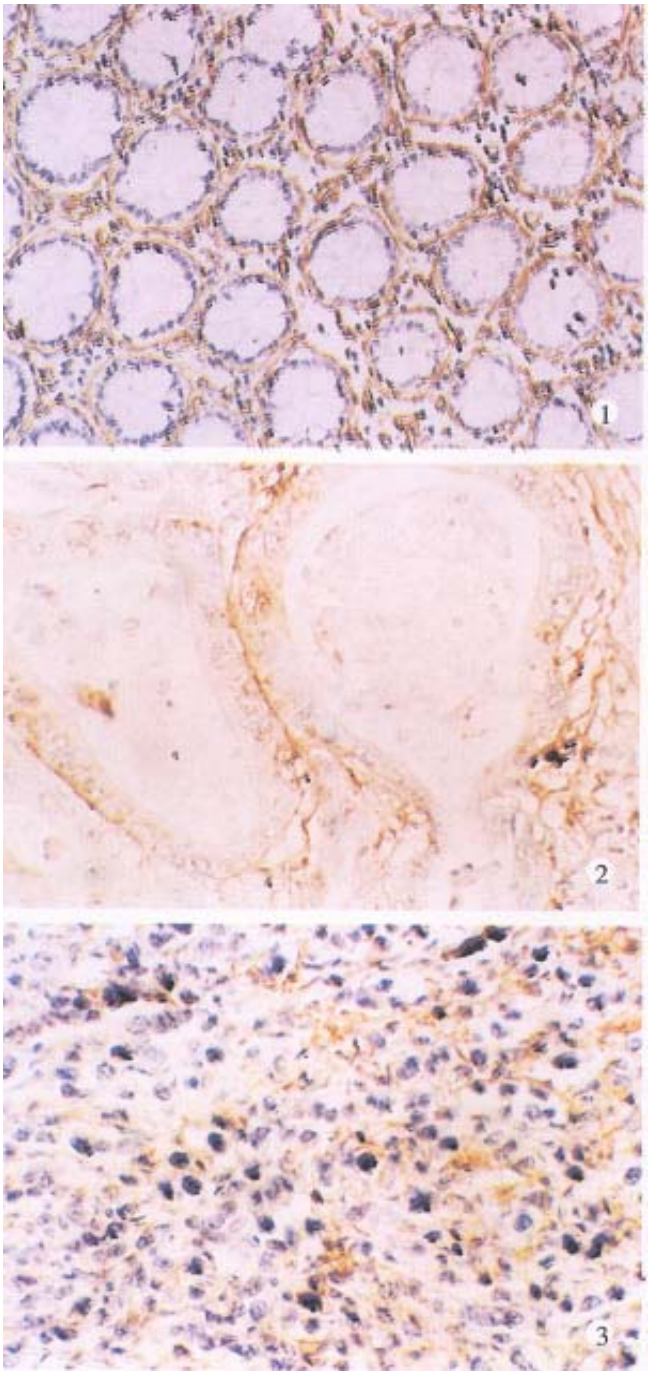

Figure 1 Expression of laminin in normal large intestinal mucosa. SP×100

Figure 2 Expression of laminin in well differentiated colorectal carcinoma. SP×200

Figure 3 Expression of laminin in poorly differentiated colorectal carcinoma. SP×200

Tumor invasion depth and laminin expression

With the increasing maximum depth of tumor invasion, discontinuous basement membrane laminin staining became more prominent in tumors (Table 3), but without statistical significance (χ^2: P>0.05).

Table 3 Tumor invasion depth and laminin staining pattern

Depth of invasion	*n*	Laminin staining pattern	
		++ to +++	- to +
Mucosa and submucosa	4	3(75.0%)	1(25.0%)
Muscularis	32	17(53.1%)	15(46.9%)[a]
Serosa and subserosa	27	11(40.7%)	16(59.3%)[a]

[a]P>0.05 *vs* tumor not extended beyond the submucosa.

DISCUSSION

Human colorectal carcinomas are comprised, in part, of malignant cells of varying degrees of differentiation from well to poorly differentiated. At present, tumor histology is the primary criterion used to determine the degree of differentiation of a given tumor. It is becoming increasingly apparent, however that the morphological characteristics of tumors that relate to their degree of differentiation result from alterations in the biological properties of the cells[5]. Moreover, these biological properties probably contribute to the clinical be havior associated with tumors of a particular differentiation state. For example, poorly differentiated colorectal carcinomas are considered, in general, to be more aggressive and to offer a worse progress than well and moderately differentiated tumors[6].

Laminin, the major basement membrane component, was determined by using immunohistochemical method. We demonstrated a defined, continuous basement membrane underlying normal colonic epithelium. In contrast, human colorectal carcinomas exhibited a progressive loss of an intact basement membrane that was correlated with decreasing differentiation degree. Well and moderately differentiated tumors showed a thin basement membrane with intermittent disruptions, and poorly differentiated tumors exhibited no areas of intact basement membrane. An association was found between lack of basement membrane laminin immunohistochemical staining in colorectal carcinoma and poorly differentiated (P<0.01).

We also found an association between discontinuous basement membrane laminin immunostaining in colorectal carcinomas and more advanced tumor stage; and with increasing depth of invasion, tumors more frequently show discontinous basement membrane laminin staining. An important underlying factor may be the basement membrane laminin discontinuity in tumor is associated with poor tumor differentiation, which itself is linked with a more invasive phenotype.

There is an evidence for a number of mechanisms explaining basement membrane discontinuity in malignant tumors. Daneker *et al*[7] reported that in poorly differentiated colon carcinoma cells, newly synthesized laminin was secreted more slowly than in well differentiated cells. Basement membrane degradation by tumor-derived proteinases may also be important. Proteinase specific for the basement membrane component type-IV collagen has been identified in invasive tumors. Increased amount of the degradative enzymes cathepsin B, urokinas-type plasmignogen activator and β-glucuronidase has been demonstrated in colorectal carcinomas[4,8-9].

Up to now, the genetic and biochemical factors that under the tumore differentiation and other biological properties are poorly understood. Studies aimed at defining these factors would not only contribute to an understanding of differentiation at molecular and cellular level but also would provide new reagents and criteria for a more precise determination of the degree of tumor differentiation, thus faciliate the understanding of the biological behaviors of tumors. The results of this study confirmed that immunohistochemical staining of laminin could provide a very useful index for the determination of the differentiation degree of human colorectal carcinoma.

REFERENCES

1 Grover A, Andrews G, Adamson ED. Role of laminin in epithelium formation by F9 aggregates. *J Cell Biol,* 1983;97(1):137-144
2 Terranova VP, Hujanen ES, Martin GR. Basement membrane and the invasive activity of metastatic tumor cells. *J Natl Cancer Inst*, 1986;77(2):311-316
3 Liotta LA. Tumor invasion and metastasis'role of the extracellular matrix: Rhoads memorial award lecture. *Cancer Res,* 1980;46(1):1-7
4 Liotta LA. Cancer cell invasion and metastasis. *Scientific Am,* 1992;266(2): 34-41
5 Wewer UM, Taraboletti G, Sobel ME, Albrechtsen R, Litta LA. Role of laminin receptor in tumor cell migration. *Cancer Res,* 1987;47(21):5691-5698
6 Klimplifinger M, Beham A, Denk H. Pathologic findings in colorectal cancers and discussion of their significance for tumor therapy according to stage. *Wien Klin Wochenschr,* 1987;99(2):488-493
7 Daneker Jr GW, Mercurio AM, Wolf LGB, Salem RR, Bagli DJ, Steele Jr GD. Laminin expression in colorectal carcinomas varying in degree of differentiation. *Arch Surg,* 1987;122(12):1470-1474
8 Boyd D, Florent G, Kim P, Brattain M. Determination of the levels of urokinase and its receptor in human colon carcinoma cell lines. *Cancer Res,* 1988; 48(11):3112-3116
9 Feng Shu, Song Jindan. Study on the relationship between invasiveness and β-glucuronidase secreted by human colorectal carcinoma cell line. *Chin J Cell Biol,* 1996;18(4):138-140

 ISSN 1007-9327 CN 14-1219/R WJG, 1998;4(3):222-224

Peripheral mechanism of inhibitory effect of centrally administrated histamine on gastric acid secretion

ZHANG Zhi-Fang, WANG Zhu-Li, and LU Guang-Qi

Subject headings gastric acid/secretion; histamine; stomach/physiology; somatostatin; acetylcholine M ceceptor; rats

Abstract

AIM To study the peripheral mechanism of the inhibitory effect of intra-third ventricular administration (icv) of histamine (HA) on gastric acid secretion in rats.

METHODS Gastric acid was continuously washed with 37℃ saline by a perfusion pump in male adrenalectomized SD rats. Drugs were injected intravenously (iv) by a syringe pump and their effect on pentagastrin-induced (10 μg • kg • h, iv) gastric acid secretion was observed.

RESULTS The inhibitory effect of HA (1 μg, icv) on gastric acid secretion was blocked by subdiaphragmatic vagotomy, and pretreatment with atropine (0.005 mg • kg • h, iv). Pretreatment with somatostatin antagonist, cyclo-[7-aminoheptanoyl-Phe-D-Trp-Lys-Thr(Bzl)], (2 μg-4 μg • kg • 100 min, iv) could also block the inhibitory effect of HA on gastric acid secretion in a dose dependent manner.

CONCLUSION The inhibitory effect of centrally administrated HA on gastric acid secretion may be mediated by vagi, acetylcholine M receptor and somatostatin.

Department of Physiology, Sun Yat-Sen University of Medical Sciences, Guangzhou 510089, Guangdong Province, China

ZHANG Zhi Fang, male, born on 1964-10-14 in Pingdingshan City, Henan Province, graduated from Henan Medical University as a postgraduate in 1991, now a lecturer of physiology majoring gastrointestinal physiology, having 5 papers published.

***Supported by the Doctoral Program Fund for Institutions of Higher Education. This subject was awarded the first prize of outstanding thesis by the Guangdong Association of Physiological Sciences.**

Correspondence to: ZHANG Zhi Fang, Department of Physiology, Sun Yat-Sen University of Medical Sciences, Guangzhou 510089, Guangdong Province, China

Tel. +86 • 20 • 87778223 ext 3274, Fax. +86 • 20 • 87765679

Received 1998-01-31

INTRODUCTION

It has been reported by our laboratory that intra-third-ventricular administration (icv) of histamine (HA) or 2-pyridylethylamine (PEA), a H1-receptor agonist, inhibits gastric acid secretion induced by intravenous (iv) pentagastrin (G-5) in rats. The inhibitory effect of HA or PEA on gastric acid secretion was mediated in turn by corticotropin-releasing factor (CRF) and β-endorphin in central nervous system and abolished by subdiaphragmatic vagotomy (SV)[1-3]. The aim of the present study was designed to determine the peripheral mechanism of inhibitory effect of centrally administrated histamine on gastric acid secretion.

MATERIALS AND METHODS

Animals

Male Sprague-Dawley (SD) rats weighing between 200g-300g were used. The animals were deprived of food for 24 hours, but were allowed free access to water prior to anesthesia.

Animal models

The rats were anesthetized with a single intraperitoneal injection of pentobarbital (50mg/kg). Intra-third-ventricular implantation and acute gastric lumen perfusion were carried out as described previously by our laboratory[1]. Gastric perfusion samples were collected every 10 minutes and were titrated by 0. 01mol/L NaOH to neuter. Total acid output per 10 minute was calculated. The anus temperature of rats was kept at 37℃ by electric light during the experiment. Sufficient pentobarbital was given subcutaneously before G-5 was injected.

In has been reported by our laboratory[2] that adrenal gland was associated with stimulating effect of icv PEA on gastric acid secretion in SV rats. To remove this effect, the following experiments were done in adrenalectomized rats.

After gastric acid secretion was kept at base level (0.8-3.5 μmol/10min) for 20 minutes, G-5 was injected iv by a syringe pump to increase gastric acid secretion. After the gastric acid secretion was increased and kept stable for 30 minutes, other experimental drugs were given. HA was administered by a syringe pump in a silicon tube, which was equally long and connected with the

implanted cannula. The injected volume of HA solution or vehicle was 5 μl. The acute SV was performed as described previously[4].

G-5 and HA were purchased from Shanghai Dongfeng Biochemistry Reagent Factory, Chinese Academy of Sciences. Cyclo-[7-aminoheptanoyl-Phe-D-Trp-Lys-Thr (Bzl)] (c-PTLT), from Sigma Company, U.S.A. and atropine sulfate, from Guangzhou Qiaoguang Pharmaceutical Factory.

Data analysis

Experimental data was expressed in % change of total acid output, which was calculated as follows: % change of total acid output=(E2-E1)/E1×100%, in which E1 represents total acid output per 10 minutes before experimental drugs were given (it is the mean of total acid output of 30 minutes before experimental drugs were given); E2, the total acid output (TAO) per 10 minutes after experimental drugs were given; "+", the TAO increase and "-', TAO decrease. Significance was assessed by Student's paired *t* test. The results were expressed in $x \pm s_x$.

RESULTS

All the experiments were done on the basis of iv injection of G-5 in a dosage of 10 μg • kg • h. HA, injected icv in the dosage of 1 μg/5 μl (n=9), decreased significantly the TAO (the maximum reached 44%). When HA group was compared with NS group (5 μl, n=9), P values were less than 0.05, 0.01 or 0.001 at 10min, 20min, 30min, 40min, 50min and 60min (Figure 1). In SV rats (n=8), icv injection of HA in the same dosage had no significant effect on the TAO (Figure 1).

HA (icv 1 μg/5 μl, n=8) was injected 40 minutes after the atropine (iv, 0.05mg • kg • 100min) was administered, the total acid output, had no significant change (Figure 2) compared with that before HA. If HA (icv, 1 μg/5 μl, n=9) was injected 40 minutes after iv NS was given, the total acid output, decreased significantly (the maximum to -44%) compared with that before HA. Compared with NS group, atropine group had significant changes at 50min, 60min, 70min, 80min, 90min and 100min (P<0.05, 0.01 or 0.001), (Figure 2).

There were no significant changes (P>0.05) in the total acid output at 10min, 20min, 30min, 40min, 50min, 60min, 70min, 80min, 90min, and 100min with pretreatment of c-PTLT (4 μg • kg • 100min, iv). These results suggest c-PTLT in the dosage of 4 μg • kg • 100min had no significant effect on gastric acid secretion induced by iv G-5. The following experiments were divided into three groups according to the difference of c-PTLT dosage: group 1, 4 μg • kg • 100min; group 2, 3 μg • kg • 100min; and group 3, 2 μg • kg • 100min. In group 1 (n=9), 40 minutes after c-PTLT was given HA (icv, 1 μg/5 μl), had no significant effect on the TAO(Figure 3), suggesting the inhibitory effect of HA (icv) on gastric acid secretion was blocked. In the control group (iv NS), HA (icv, 1 μg/5 μl), injected 40 minutes after NS was injected, could still inhibit gastric acid secretion. Compared between the two groups, P values were less than 0.01 or 0.001 at 60min,70min, 80min, 90min and 100min.

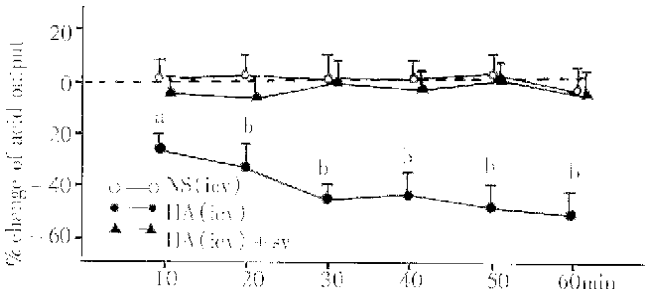

Figure 1 Effects of intra-third-ventricular injection of histamine (HA) on gastric acid output induced by G-5 in adrenalectomized and subdiaphragmatic vagotomized (SV) rats.

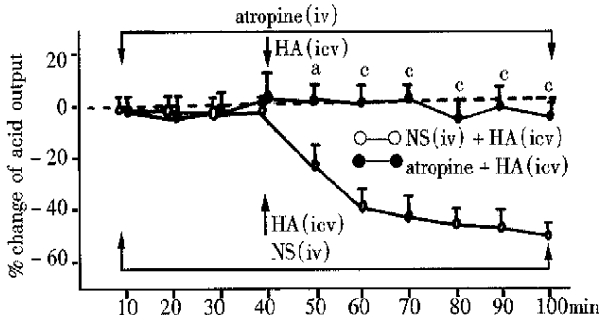

Figure 2 Effects of iv administration of atropine sulfate on icv histamine-induced inhibition of gastric acid output in adrenalectomized rats.

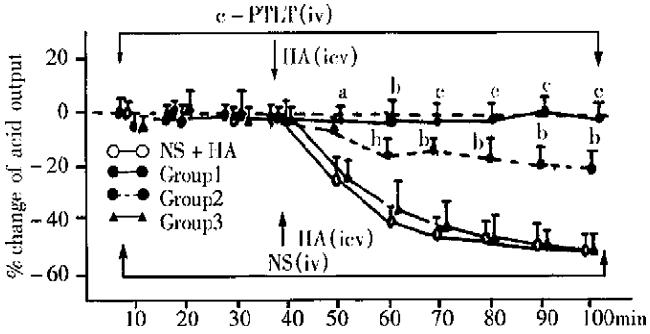

Figure 3 Effects of iv administration of c-PTLT on icv histamine-induced inhibition of gastric acid output in adrenalectomized rats. [a]P<0.05 compared with NS group; [b]P<0.01; [c]P<0.001.

In group 2(n=9), the inhibitory effect of HA (icv,1 μg/5 μl) on gastric acid secretion was partly blocked (Figure 3). Compared with the control group, *P* values were less than 0.05, 0.01 or 0.001 at 50min, 60min, 70min, 80min, 90min and 100min.

In group 3 (n=8), the inhibitory effect of HA (icv, 1 μg/5 μl) on gastric acid secretion was not changed. Compared with the control group, *P* values were more than 0.05.

DISCUSSION

The present study demonstrated that HA has central inhibitory effect on gastric acid secretion in adrenalectomized rats. This result is consistent with the results reported by Wang, Sun and Li[1-3]. The central inhibitory effect of HA on gastric acid secretion could be blocked by pretreatment with either SV, or atropine and c-PTLT, an antagonist of somatostatin, suggesting that the central inhibitory effect of HA on gastric acid secretion may be mediated by vagi, acetylcholine M receptor and somatostatin.

It is D cell that synthetises and secrets somatostatin in mammals. D cell is located near G cell in gastric antrum, and along gastric gland, particularly near the parietal cell in oxyntic mucosa. Somatostatin, mediated by its receptor in the membrane of parietal cells, inhibits gastric acid secretion induced by gastrin and acetylcholine. In addition, somatostatin inhibits the gastrin secretion in the basal condition or the gastrin secretion induced by feeding, acetylcholine and bombesin. In stomach, somatostatin inhibits the histamine secretion in the basal condition or induced by gastrin. The c-PTLT, as an artificial antagonist of somatostatin, completely blocked the inhibitory effects of exogenous somatostatin on growth hormone, insulin, and glucagon release. The efficiency of c-PTLT was demonstrated by the almost complete and sustained reversal of acid inhibition after exogenous infusion of somatostatin. Therefore, c-PTLT should have effectively reversed inhibition by endogenously released somatostatin throughout the period of the intraduodenal fat perfusion[5]. In the present study, c-PTLT, dose-dependently inhibited central inhibitory effect of HA on gastric acid secretion, which might be mediated by somatostatin in the periphery. The blocked central inhibitory effect of HA on gastric acid secretion by SV suggests that this effect was accomplished by the vagi. That vagi was involved in the control of somatostatin secretion was proved by some early studies. Vagotomy reduced the somatostatin responses to feeding during the first 30-min period following the ingestion of the meal. Atropine sulfate in the dosage of 0.02 mg • kg • h, iv decreased the somatostatin responses to the meal, while the dosage of 0.05mg • kg • h blocked such responses[6]. This suggests that vagus and cholinergic mechanisms play important roles in the control of somatostatin secretion responses to the meal. After vagotomy, atropine sulfate still decreased the somatostatin secretion[6], indicating that local factors are involved in the control of somatostatin secretion. CRF, injected icv, increased blood level of somatostatin. This effect was blocked by vagotomy or pretreatment with atropine[7]. Li *et al*[3] in our laboratory reported that the central inhibitory effect of PEA on gastric acid secretion was blocked by antiserum of CRF, suggesting that the effect of PEA is mediated by CRF in the central nervous system. According to this report and the present study, vagi or cholinergic mechanisms are involved in the control of somatostatin secretion. Holst[8] reported that vagus stimulation or atropine mediated by GRP (gastrin-releasing polypeptide)-containing fibers stimulated somatostatin secretion in the isolated perfused porcine antrum. Schubert[9] reported that methacholine exerted dual inhibitory and stimulatory effects on somatostatin cells of mucosal segments from the fundus and antrum of rat or the isolated luminally perfused mouse stomach. There are some contradictory reports about somatostatin secretion of vagal control. For example, somatostatin secretion was deoreased by vagus stimulation and this effect was abolished by atropine 10-9M[10]. As there are lots of fibers in vagi, the above contradictory reports may be related with too much fibers stimulation when vagi was stimulated electrically. In summary, the mechanism that somatostatin secretion is controlled by vagi still remains unclear and more studies are needed.

REFERENCES

1 Wang ZL, Lu GQ. Effect of intra ventricular administration of histamine and its receptor agonists on pentagastrin-induced gastric acid secretion. *Acta Physiologica Sinica,* 1992;44(3):261-268
2 Sun CG, Wang ZL, Wang TZ, Lu GQ. Mechanism of effect of intra ventricular administration of histamine H-1-receptor agonists on gastric acid secretion in rats. *Acta Physiologica Sinica,* 1993;45(6):581-586
3 Li MY, Wang ZL, Lu GQ. Central mechanism of inhibitory effect of histamine H-1-receptor agonists PEA on gastric acid secretion. *Acta Physiologica Sinica,* 1995;47(3):259-263
4 Tache Y, Goto Y, Gunion MW, Rivier J, Debas H. Inhibition of gastric acid secretion in rats and in dogs by corticotropin-releasing factor. *Gastroenterol Jpn,* 1984;86:281-286
5 Fung L, Pokol-Daniel S, Greenberg GR. Cholecystokinin type A receptors mediate intestinal fat-induced inhibition of acid secretion through somatostatin-14 in dogs. *Endocrinology,* 1994;134(6):2376-2382
6 Woussen-Colle MC, Lalieu C, Simoens C, De-Graef J. Effect of vagotomy and atropine on plasma somatostatin responses to a meal in conscious dogs. *Regul Pept,* 1988;21(1,2):29-36
7 Smedh U, Uvnas-moberg K. Intracerebroventricularly administered corticotropinreleasing factor releases somatostatin through a cholinergic, vagal pathway in freely fed rats. *Acta Physiol Scand,* 1994;151(2):241-248
8 Holst JJ, Skak-Nielsen T, Orskov C, Seier-Pousen S. Vagal Control of the release of somatostatin, vasoactive intestinal polypeptide, gastrin-releasing peptide, and HCl from porcine non-antral stomach. *Scand J Gastroenterol,* 1992;27(8):677-685
9 Schubert ML, Hightower J. Functionally distinct muscarinic receptors on gastric somatostatin cells. *Am J Physiol,* 1990;258(Gastrointest. Liver Physiol,21):G982-987
10 Madaus S, Bender H, Schusdziarra V, Kehe K, Munzert G, Weber G *et al.* Vagally induced release of gastrin, somatostatin and bombesin-like immunoreactivity from perfused rat stomach. Effect of stimulation frequency and cholinergic mechanisms. *Regul Pept,* 1990;30(3):179-192

A clinical evaluation of serum concentrations of intercellular adhesion molecule-1 in patients with gastric cancer

LIU Yong-Zhong, CHEN Bin and SHE Xi-Dian

Subject headings stomach neoplasms/immunology; intercellular adhesion molecule-1/blood; lymphatic metastasis; intercellular adhesion molecule-1/analysis; enzyme-linked immunosorbent assay

Abstract

AIM To investigate the correlation between the serum soluble intercellular adhesion molecule-1 (sICAM-1) and the clinicopathologic features and to evaluate the possible prognostic significance of sICAM-1 concentration in gastric cancer.

METHODS Thirty-four patients with gastric cancer were prospectively included and evaluated. Venous blood samples were collected before the surgery. Sera were obtained by centrifugation, and store at -30℃ until assay. The control group consisted of 20 healthy volunteers. Serum concentrations of ICAM-1 were measured with the quantitative sandwich enzyme immunoassay technic. Differences between the two groups were analyzed by Student's t test. $\bar{x}$+2s of normal control sICAM-1 was taken as upper limit to calculate the positive rates.

RESULTS The mean value of serum ICAM-1 in patients with gastric cancer was 367.7 μg/L±104.7 μg/L and that of control group was 236.9 μg/L±74.3 μg/L, and the difference was significant (P<0.001). The patients with tumor size of ⩾ 5cm had significantly higher serum concentrations of sICAM-1 than those with smaller ones (406.7 μg/L±90.2 μg/L *vs* 319.9 μg/L±105.3 μg/L, P <0.01). Compared with stages I-II gastric cancer patients, patients with more advanced clinical stage (III-IV) had higher levels of sICAM-1 (397.1 μg/L±102.4 μg/L *vs* 306.0 μg/L±82.3 μg/L, P<0.05). Difference was significant statistically in sICAM-1 levels between patients with positive lymph node status and those without lymph node involvement (403.6 μg/L±99.7 μg/L *vs* 302.7 μg/L±81.4 μg/L, P<0.01). No relation was observed between the level of sICAM-1 and grade of histological differentiation in the patients with gastric cancer.

CONCLUSION Serum sICAM-1 concentration may be a valuable parameter for predicting the prognosis and degree of the gastric cancer.

INTRODUCTION

Cell adhesion is essential for establishing and maintaining a normal immune defense system. Intercellular adhesion molecule-1 (ICAM-1; CD54), a 80-110KD cell surface glycoprotein and a member of the immunoglobulin supergene family, functions as a ligand for the leucocyte integrin adhesion receptors CD11a/CD18 (LFA-1) and CD11b/CD18 (mac-1). ICAM-1 expresses in various cell types and plays an important role in immunemediated mechanisms, especially in the process of antigen presentation and recognition, lymphocyte cytotoxicity, lymphocyte recruitment and targeting. It has been reported that the upregulated expression of ICAM-1 on cell surfaces occurred in a variety of diseases, including autoimmune diseases, endocrine diseases, and some cancers[1,2]. A soluble form of ICAM-1 (sICAM-1) lacking cytoplasmic tail and transmembrane region has also been found [2]. sICAM-1 can compete with membranous ICAM-1 to bind LFA-1, so that it can block leukocyte LFA-1 and prevent effective recognition and lysis of target cells by effector leukocyte. This phenomenon represents an important mechanism for tumor escaped from immune surveillance[3,4]. The sICAM-1 levels and its prognostic significance for various malignant diseases have been evaluated[5-8]. In this study, we determined the concentrations of sICAM-1 antigen in the sera of patients with gastric cancer to reveal the possible relationship between sICAM-1 and clinical pathological parameters such as histologic type, size of tumors and so on.

Institute of Clinical Medical Sciences, Affiliated Yijishan Hospital, Wannan Medical College, Wuhu 241001, Anhui Province, China
LIU Yong Zhong, male, born in 1968 in Anhui Province, graduated from Shandong Academy of Medical Sciences as a postgraduate in 1996, having 4 papers published.
Correspondence to: LIU Yong Zhong, Institute of Clinical Medical Sciences, Affiliated Yijishan Hospital, Wannan Medical College, Wuhu 241001, Anhui Province, China
Tel. +86 • 553 • 5855956-2328
Received 1997-11-10 **Revised** 1998-01-04

MATERIAL AND METHODS

Patients and specimens

A group of 34 patients (24 men and 10 women) with gastric cancer were investigated. Their ages ranged from 35 to 74 years with a mean of 54. Eleven patients were in stages I and II, and 23 in stages III and IV. Blood samples were obtained from patients before the initial treatment. Samples collected from 20 healthy volunteers served as controls. All blood samples were processed immediately for centrifugation, and the sera were stored at -30℃ until the sICAM-1 assay.

Measurement of sICAM-1

Serum sICAM-1 concentrations were determined with sICAM-1 ELISA (Biosource International, USA). Briefly, serum samples were diluted at 1: 100 and applied to prepared polysteyrene microcells precoated with mouse monoclonal antibody to human ICAM-1, a horseradish peroxidase conjugated anti-ICAM-1 was then added. Test wells are incubated to allow any ICAM-1 to be bound by antibodies on the microtiter plate. The walls were then washed and stabilized chromogen was added to the walls producing a blue color in the presence of peroxidase enzyme. The color reaction was then stopped by the addition of 1mol/L H2SO4 and changed from blue to yellow. Absorbances for samples and sICAM-1 standards were determined on a spectrophotometer using 450nm. Average absorbance values for each set of duplicate samples or standards were within 15% of the mean. sICAM-1 concentrations in serum sample were determined by comparing the mean absorbance of duplicate samples with the standard curve for each assay.

Statistical analysis

The Student's *t* test was used for statistical significance of differences between groups. $P<0.05$ was considered to be significant.

RESULT

The mean serum sICAM-1 levels in healthy volunteers and patients with gastric cancer were 236.9 μg/L±74.3 μg/L, 367.7 μg/L±104.7 μg/L, respectively; and serum sICAM-1 levels in 58. 8% of patients exceeded 385.5 μg/L ($\bar{x}$+2s of normal controls), the difference being significant between patients with gastric cancer and healthy controls.

The relationship between serum sICAM-1 levels and clinicopathological features of gastric cancer patients was also observed. Patients with tumor size ⩾5cm showed remarkable elevated levels of sICAM-1 than those with tumor size <5cm ($P<0.01$). Patients with advanced gastric cancer (stage III-IV) had higher serum levels of sICAM-1 ($P<0.05$) than early-stage gastric cancer patients (stage I-II). sICAM-1 levels in patients with lymph node matastasis were significantly higher than in those without lymph node invasion ($P<0.01$). No correlation was found between sICAM-1 levels and grade of differentiation in the observed gastric cancer patients. The positive rates of each group were calculated with $\bar{x}$+2s of normal control sICAM-1 as a limit. The results are shown in Table 1.

Table 1 Correlation between soluble ICAM-1 concentrations and clinical histopathology in gastric cancer

Factors	*n*	ICAM-1 ($\bar{x}$±s, μg/L)	Positive rate %(*n*)
Tumor size			
⩾5cm	19	406.7±90.2[a]	73.3 (14/19)
<5cm	15	319.9±105.3	40.0 (6/15)
Lymph node invasion			
Positive	21	403.6±99.7[a]	71.4 (15/21)
Negative	13	302.7±81.4	38.5 (5/13)
Grade of differentiation			
Differentiated	12	320.5±93.2	33.3 (4/12)
Poorly differentiated	22	393.9±103.1	72.7 (16/22)
Clinical staging			
I-II	11	306.0±82.3	36.4 (4/11)
III-IV	23	397.1±102.4[b]	69.6 (16/23)

[a]$P<0.01$, [b]$P<0.05$, *vs* the control.

DISCUSSION

A previous studies indicated that ICAM-1 was expressed on tumor cells in 12 of 28 cases of gastric carcinoma[9]. Expression of ICAM-1 by tumor cells facilitated immune recognition and cytotoxicity[10,11]. However, ICAM-1 also represents an escape mechanism in certain cancers. sICAM-1, after shedding from tumor cells or originating from other cells especially mononuclear cells, may block the attachment of cytotoxic T lymphocyte (CTL) cells and/ or NK cells to tumor cells, since LFA-1 on immune cells could be blocked with sICAM-1[3]. Recently, Becker *et al* found that cytolysis of melanoma cells mediated by CTL in an MHC-restricted manner, could be completely blocked in the presence of sICAM-1, the concentration of sICAM-1 for blocking cytotoxicity was 950 μg/L[4]. Because the serum sICAM-1 concentration may reflect the level of sICAM-1 in tumor microenviroment in vivo, an increase in the circulating level of ICAM-1 may reflect unfavourable prognosis. It has been found that patients with malignant melanoma, having high levels of sICAM-1, had a statistically significantly shorter time to first relapse and lower overall survival[7]. In this study, we have found that serum

sICAM-1 levels were significantly increased in patients with gastric cancer, which were above the normal range in 20 of 34 gastric cancer patients. It is entirely possible that concentration of sICAM-1 in gastric tumor microenviroment may be high enough to block the cytotoxicity mediated by immune effector cells. To further confirm this hypothesis, we will establish a method to assess the sICAM-1 level in gastric carcinoma tissues.

In this study, we observed the correlation between the level of sICAM-1 and the clinical parameters in patients with gastric carcinoma. Patients with tumor size of $\geqslant$5cm had higher level of sICAM-1 than those with small ones. This results indicated that tumor load may be correlated with the level of sICAM-1. In other words, the gastric tumor cells were probably the major source of sICAM-1. This was confirmed by the study of Hyodo *et al*. They found that the elevated serum levels of sICAM-1 in a patient with hepatocellular carcinoma decreased after treatment with tracatheter arterical embolization (TAE) in a same pattern of change with the AFP levels. As AFP is produced and shed by hepatocellular carcinoma cells, it could be interpreted that sICAM-1 in HCC patients is released from tumor cells[8]. Our study also showed that sICAM-1 levels were correlated with both clinical staging and lymph node involvement. Patients with lymph node invasion and advanced clinical stage of tumors had significantly higher serum concentrations of sICAM-1. Lymph node status, tumor size and clinical stage are significant prognostic indicators, therefore, sICAM-1 may be a valuable predictor for gastric cancer clinically.

In summary, elevated levels of sICAM-1 exist in gastric cancer as in some other types of tumors. Though serum level of sICAM-1 can not be served as a specific parameter for gastric cancer, it is no doubt that the measurement of the ICAM-1 level may provide a convenient means to obtain a general indication of gastric cancer.

REFERENCES

1 Springer TA. Adhesion receptors of the immune system. *Nature,* 1990;346 (6283):425-434
2 Rothlein R, Mainolfi EA, Czajkowski M, Marlin SD. A form of circulating ICAM-1 in human serum. *J Immunol,* 1991; 147(11):3788-3793
3 Becker JC, Dummer R, Hartmann AA, Burg G, Schmidt RE. Shedding of ICAM-1 from human melanoma cell lines induced by IFN-γ and tumor necrosis factor-α: functional consequences on cell-mediated cytotoxicity. *J Immunol,* 1991;147(12):4398-4401
4 Beker JC, Christian T, Schmidt RE, Brocker EB. Soluble intercellular adhesion molecule-1 inhibits MHC-restricted specific T cell / tumor interaction. *J Immunol,* 1993;151(12):7224-7232
5 Nasu K, Narahara H, Etoh Y, Kawano Y, Hirota Y, Miyakawal. Serum levels of soluble intercellular adhesion molecule-1 (ICAM-1) and the expression of ICAM-1 mRNA in uterine cervical cancer. *Gynecol Oncol,* 1997;65(2):304-308
6 Tsujisaki M, Imai K, Hirata H, Hanzawa Y, Masuya J, Nakano T *et al*. Detection of circulating intercellular adhesion molecule-1 antigen in malignant diseases. *Clin Exp Immunol,* 1991;85(1):3-8
7 Harning R, Mainolfi E, Bystryn JC, Henn M, Merluzzi VJ, Rothlein R. Serum levels of circulating intercellular adhesion molecule 1 in human malignant melanoma.*Cancer Res,* 1991;51(18):5003-5005
8 Hyodo I, Jinno K, Tanimizu M, Hosokawa Y, Nishikawa Y, Akiyama M *et al*. Detection of circulating intercellular adhesion molecule-1 in hepatocellular carcinoma. *Int J Cancer,* 1993;55(5):775-779[a¤]
9 Nasu R, Mizuno M, Kiso T. Immunohistochemical analysis of intercellular adhesion molecule 1 expression in human gastric adenoma and adenocarcinoma. *Virchows Arch,* 1997;430(4):279-283
10 Anichini A, Mortarini R, Alberti S, Mantovani A, Parmiani G. Enhanced lysis of melanoma clones by autologous tumor infiltrating lymphocyte clones after tumor ICAM-1 up regulation: correlation with T cell receptor engagement. *Int J Cancer,* 1993;53(6):994-999
11 Liu YZ, Zhang L, Yu YS, Wan Y, Guo M. Cytokine regulations on expression of intercellular adhesion molecule-1 (ICAM-1) in human hepatoma cell line and ins susceptibility to lysis by anti-CD3 monoclonal antibody-activated (CD3AK) cells. *Shanghai J Immunol,* 1997;17(2):74-77

ISSN 1007-9327 CN 14-1219/R WJG, 1998;4(3):228-230

Expression of bcl-2 protein in gastric carcinoma and its significance *

LIU Hai-Feng, LIU Wei-Wen, FANG Dian-Chun and MEN Rong-Pu

Subject headings stomach neoplasms/pathology; bcl-2 protein; gene expression; immunohistochemical; lymphatic metastasis

Abstract

AIM To further study the role of bcl-2 protein expression in gastric carcinogenesis and tumor progression.

METHODS Using immunohistochemical staining, the bcl-2 protein expression in 50 cases of gastric carcinoma and its relation to clinical status and pathomorphological parameters were observed.

RESULTS Forty-one (82%) cases were positive for bcl-2 protein staining which was located in the cytoplasm and nuclear membrane of tumor cells. The rate of bcl-2 protein expression was not correlated with the patient, sex, tumor size, lymph node status or clinical stages ($P>0.05$). It was strongly associated with intestinal-type tumors and poorly differentiated tumors ($P<0.05$ and $P<0.01$).

CONCLUSION Aberrant bcl-2 protein expression appears to be specifically associated with development of intestinal-type gastric carcinoma, bcl-2 protein expression might play an important role in the early development/promotion and phenotypic differentiation of gastric carcinomas, but not in tumor progression.

Department of Gastroenterology, Southwest Hospital, Third Military Medical University, Chongqing 400038, China

Dr. LIU Hai Feng, physician-in-charge, having 16 papers published.

***Key project of the 9th 5-year plan for Medicine and Heath of Army, No.96Z047.**

Correspondence to: Dr. LIU Hai Feng, Department of Gastroenterology, Southwest Hospital, Third Military Medical University, Chongqing 400038, China

Tel. +86 • 23 • 65318301 ext 73049

Received 1998-01-20

INTRODUCTION

Recently, emphasis has been placed on the role of apoptosis and its regulation in tissue homeostasis and carcinogenesis. To determine whether bcl-2 plays a role in the gastric carcinogenic sequence, an immunohistochemical study of bcl-2 expression in gastric carcinoma and its relation to clinical status, pathomorphological parameters was carried out.

MATERIALS AND METHODS

Histological specimens

Fifty cases of surgically resected gastric carcinomas (male 34, female 16; mean age 56.3 years) were extracted from the files of the Department of Pathology, Southwest Hospital, Third Military Medical University. All blocks were fixed in 10% formalin and embedded in paraffin. Serial sections were cut from each block in 4 μm, stained with hematoxylin and eosin and confirmed pathologically.

Immunohistochemical methods

Immunohistochemical staining for bcl-2 protein was performed using SP technique with the following procedure: ① slides were diparaffinized in two changes of xylene for 10 minutes each and then were hydrated in decreasing concentrations of ethanol and rinsed in phosphate-buffered saline. Endogenous peroxidase was blocked by 3% H2O2 in methanol for 5 minutes, and then incubated for 10 minutes at room temperature in normal goat serum (1:20). ② slides were incubated with a 1:50 dilution of the primary rabbit antihuman bcl-2 monoclonal antibody (Santa Cruz, USA) for 30 minutes at 37℃. A biotin-streptavidin detection system was employed with diaminobenzidine as the chromogen. ③ slides were washed twice with phosphate-buffered saline and incubated with the linking reagent (biotinylated anti-immunoglobulin) for 10 minutes at 37℃. After rinsing in phosphate-buffered saline, the slides were incubated with the peroxidase-conjugated streptavidin label for 10 minutes at 37℃, and incubated with diaminobenzidine and H2O2 for 10 minutes in the dark, the sections were then counterstained with hematoxylin. With each batch of test samples, a positive control consisting of a tissue section from tonsil was evaluated. In addition, a negative control was prepared for each

sample using an irrelevant antibody of the same isotype as the primary antibody.

The immunostaining of bcl-2 was visually classified into four groups by observing 1 000 tumor cells in areas of the sections: no staining present in any of tumor cells (-); slight staining in most of the tumor cells or less than 25% tumor cells with strong staining (+); 26%-50% tumor cells with strong staining (++); and strong staining in more than 51% tumor cells (+++). The classification was done by two senior pathologists who did not know the clinicopathological data.

Statistics

Analysis of data was accomplished using Chi square test. *P* values less than 0.05 were considered to be statistically significant.

RESULTS

Expression of bcl-2 protein in gastric carcinoma

Forty-one (82%) of the fifty gastric carcinomas showed immunoreactivity for bcl protein in gastric carcinoma cells. Expression of varied: + in bcl-2 protein, 6(12%), ++ in 20(40%) and +++ in 15 (30%). The bcl-2 protein immunoreactivity appeared brown or dark brown, which was localted on the cytoplasm and nuclear membrane of tumor cells (Figure 1). Some of the mature lymphocytes infiltrating in the stroma of gastric carcinomas had bcl-2 protein expression with a strong staining intensity.

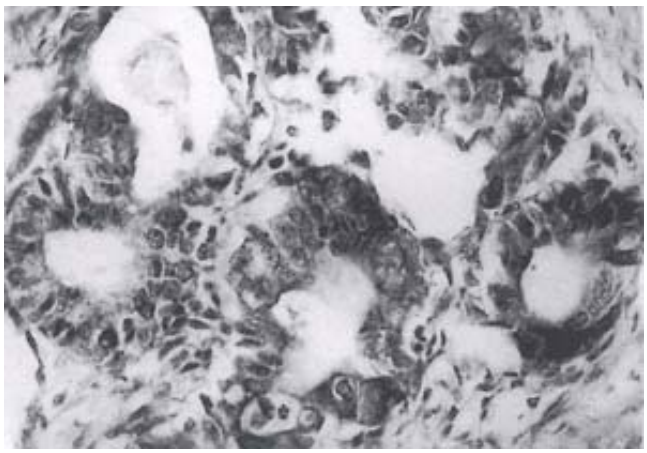

Figure 1 Immunoreactivity of bcl-2 was detected in the cytoplasm of gastric carcinoma cells. SP ×200

Correlation between bcl-2 protein expression and clinicopathological parameters of gastric carcinomas

Correlations between bcl-2 protein expression and clinical pathological data of gastric carcinoma are illustrated in Table 1. The rate of bcl-2 protein expression was not correlated with patient age, sex, tumor size, lymph node status and clinical stages ($P>0.05$). The immunoreactivity of bcl-2 was significantly associated with morphologic phenotype and grades of differentiation of gastric carcinoma. Twenty-six (92.86%) of 28 gastric carcinomas of intestinal morphologic phenotype were immunoreactive versus 15 (68.16%) of 22 diffuse tumors ($P<0.05$). Twenty-one (95.45%) of 22 poorly differentiated gastric carcinomas were immunoreactive versus 11 (61.11%) of 18 well and moderately differentiated carcinomas ($P<0.01$).

Table 1 Correlation between bcl-2 protein expression and clinicopathological parameters of gastric carcinomas

	n	bcl-2 protein expression				Positive rate (%)
		-	+	++	+++	
Age (a)						
≤59	36	7	4	15	10	80.56
≥60	14	2	2	5	5	85.71
Sex						
M	34	7	2	13	12	79.41
F	16	2	4	7	3	87.50
Type						
Intestinal	28	2	3	13	10	92.86[a]
Diffuse	22	7	3	7	5	68.18
Grade of differentiation						
Well/moderate	18	7	1	5	5	61.11
Poor	22	1	4	12	5	95.45[b]
Mucoid	10	1	1	3	5	90.00
Tumor size						
<5cm	31	8	4	11	8	74.19
≥5cm	19	1	2	9	7	94.74
Lymph-node metastasis						
Negative	21	4	2	9	6	80.95
Positive	29	5	4	11	9	82.76
Serosal invasion						
Absent	25	7	3	9	6	72.00
Present	25	2	3	11	9	92.00
Clinical stages						
I and II	32	6	5	12	9	81.25
III and IV	18	3	1	8	6	83.33

[a]$\chi^2=5.082$, $P<0.05$, *vs* diffuse-type gastric carcinoma; [b]$\chi^2=7.298$, $P<0.01$, *vs* well/moderately differentiated gastric carcinoma.

DISCUSSION

The bcl-2 proto-oncogene is initially identified in human follicular and diffuse B-cell lymphomas characterized by the reciprocal translocation[1]. The product of the proto-oncogene bcl-2 is a 26-kDa protein that blocks apoptosis. bcl-2 protein is localized in the mitochondria, endoplasmic reticulum and nuclear envelope membranes. More recently, several normal and malignant tissues other than hematolymphoid cells have been shown to express bcl-2, including the lung, breast, prostate, stomach, small bowel and colon[2-5].

The relation of bcl-2 protein expression to clinicopathological parameters of tumors was still unclear. Joensuu *et al*[6] demonstrated that bcl-2 expression was correlated with the age of patients, which was more common in aged than in young patients. Silviastrini *et al*[7] found that bcl-2 protein expression was related to the tumor size. A significantly higher fraction of bcl-2 positive cells was observed in small tumors than in large tumors. Sierra *et al*[8] found that bcl-2 protein was more frequently expressed in tumors with early metastasis than in lymph-node negative tumors. Our study showed that bcl-2 protein expression was associated with morphologic phenotype and grades of differentiation of gastric carcinomas. The difference in the bcl-2 protein expression in the intestinal and diffuse types demonstrated that aberrant bcl-2 protein expression was preferentially associated with development of intestinal-type gastric carcinoma, indicating again the different biologic mechanisms involved in the development of these two histologic subtypes. The difference in the bcl-2 protein expression between poorly differentiated and well/moderately-differentiated gastric carcinomas demonstrated that aberrant bcl-2 protein expression was associated with differentiation or growth speed of gastric carcinomas. There was no significant relationship between bcl-2 protein expression and tumor size, lymph-node metastasis, serosal invasion or clinical stages. Therefore, bcl-2 protein expression might play an important role?in the early development and phenotypic differentiation of gastric carcinomas, but not so in tumor progression.

REFERENCES

1 Korsmeyer SJ. Bcl-2 initiates a new category of oncogenes: regulators of cell death. *Blood,* 1992;80(4):879-886
2 Higashiyama M, Doi O, Kodama K, Yokouchi H, Tateishi R. High prevalence of bcl-2 oncoprotein expression in small cell lung cancer. *Anticancer Res,* 1995;15(2):503-505
3 Lauwers GY, Scott GV, Karpeh MS. Immunohistochemical evalution of bcl-2 protein expression in gastric adenocarcinomas. *Cancer,* 1995;75(9):2209-2213
4 Alderson LM, Castleberg RL, Harsh IV GR, Louis DN, Henson JW. Human gliomas with wild-type p53 express bcl-2. *Cancer Res,* 1995;55(5):999-1001
5 Qi-Long LU, Richard Poulsom, Leslie Wong, Couliamos AD. Bcl-2 expression in adult and embryonic non-haematopoietic tissues. *J Pathol,* 1993;169 (4):431-438
6 Joensun H, Pylkkanen L, Toikkanen S. bcl-2 protein expression and long-term survival in breast cancer. *Am J Pathol,* 1994;145(5):1191-1198
7 Silviastrini R, Veneroni S, Daidone MG, Benini E, Boracchi P, Mezzetti M *et al*. The bcl-2 protein: a prognostic indicator strongly related to p53 protein in lymph-node negative breats cancer patients. *J Natl Cancer Inst,* 1994;86(7): 499-504
8 Sierra A, Lloveras B, Castellsague X, Moreno L, Ramirez MG, Fabra A. Bcl-2 expression is associated with lymph node metastasis in human ductal breast carcinoma. *Int J Cancer,* 1995;60(1):54-60

Telomeric associations of chromosomes in patients with esophageal squamous cell carcinomas

XIAO Lin[1], ZHOU Hong-Yuan[1], LUO Zhong-Cheng[2], LIU Jun[1]

Subject headings esophageal neoplasms; carcinoms, squamous cell; chromosome; lymphocytes; telomeric DNA

Abstract

AIM To investigate the role of telomeric association in the development of esophageal cancer.

METHODS Using chromosome R banding technique,telomeric association of chromosome in peripheral blood lymphocytes from 16 untreated patients with esophageal squamous cell carcinoma were observed and 16 healthy adults served as controls.

RESULTS The teloemeric association frequencies of cell and chromosomes were significantly higher than those of controls (χ^2=9.56, P<0.01), but its distribution on the chromosome showed no significant difference (χ^2=1.01, P>0.05) between the two groups.

CONCLUSION Chromosomal instability can be initiated by telomeric associations, and sequential chromosome analysis can aid the understanding of the tumor occurrence and progression.

[1]Institute of Oncology, West China University of Medical Sciences, Chendu 610041, Sichuan Province, China

[2]Department of Paediatrics, Queen Mary Hospital, the University of Hong Kong, Hong Kong

XIAO Lin, female, was born on Dec. 30, 1962, Chendu, Sichuan Province. Master of Medical Sciences, graduated from Institute of Oncology, West China University of Medical Sciences, having 10 papers published.

***Project supported by the National Natural Science Foundation of China, No.39570392.**

Correspondence to: XIAO Lin, Institute of Oncology, West China University of Medical Sciences, Chendu 610041, Sichuan Province, China

Tel. +86 • 28 • 5501282

Received 1997-11-25

INTRODUCTION

Telomeres are genetic elements located at the end of all eukaryotic chromosomes and are essential for normal cell viability. One or their basic functions is to pretect themselves. DNA at the terminal end of all chromosomes has a special structure to avoid binding to the end of DNA from other chromosmes, thus preventing end-to-end fusion or telomeric association (TAs). Telomeric DNA consists of terminal repeat arrays in the 3' strand $(TTAGGG)_n$ and has been isolated from telomeres in human. Recent studies have suggested that abnormal telomeric behavior plays a key role in cancer development. Fitzgeral[1] reported a case of B-cell leukemia and found chromosomal translocation resulting from Tas. The phenomenon has also been observed in tumor cells from a malignant hishocytoma[2] and a case of pre-T-cell acute lymphoblastic leukemia[3], three cases of cardiac myxoma[4], and two cases of renal tumor[5]. In the present report, we observed the telomeres in the peripheral blood lymphocytes from 16 untreated patients with esophageal cancer and 16 controls. So as to explore the relationship between abnormal telomeric behavior and chromosomal instability.

MATERIALS AND METHODS

Samples

Sixteen patients (12 men, 4 women) with esophageal squamous cell carcinoma admitted to the Institute of Oncology, Yanling County, Sichuan Province, aged 42 to 60 years were selected before the start of any kind of therapy. Sixteen healthy adults (12 men and 4 women) with no history of cancer; genetic diseases aged 35-65 years and radiation exposure served as controls.

Methods

Whole blood lymphocytes from all individuls were cultured in 199 medium (pH 7.5) containing 5% fetal calf serum, phytohemaggutinin and antibiotics. The cells were grown in the dark at 37℃ for 96 hours. At 94 hours, colcemid was added to a final concentration of 0.1ng/L. After hypotonic treatment with KCl and fixation in methenol: acetic (3:1), the slides were prepared by air drying. R banding of chromosomes were obtained according to the technique of GAO Chung-

Sheng[7] with slight modification. For each individual, 50 metaphases were studied under a same microscope to record the frequency of TAs and the distribution on chromosomes.

RESULTS

Data on the frequency of TAs per cell in esophageal cancer patients and normal control are shown in Table 1.

Table 1 Cellular telomeric association frequencies in patients with esophageal cancer and controls

	Cells observed	Telomeric associations	
		No. of cells	Frequencies(%)
Patients	800	115	14.38
Controls	800	75	9.38

The patients had a TAs frequency of 14.38%, which was significantly higher than that observed in normal controls (9.38%) (χ^2=9.56, P<0.01).

Comparison of distribution of TAs on chromosomes between the patients and controls is shown in Table 2. The frequency of TAs per chromosome was increased as compared with the controls (P<0.01). Statiscal analysis showed that the distribution of TAs in two groups was nonrandom. In the patients, there was a high frequency in groups E and B, and a low frequency in groups D and G+Y (P<0.01).

Proportion analysis of telomeric associations indicated that TAs distribution on chromosome was not different between the two groups (P>0.05).

Table 2 Distribution of TAs on each chromosome in peripheral blood lymphocyte from patients and controls

Chrom osome groups	Chrom osomes observed	Patients			Control		
		No. of Tas	Frequencies (%)	Percent (%)	No. of TAs	Frequencies (%)	Percent (%)
A	4 800	42	0.88	16.2	23	0.48	15.3
B	3 200	50	1.56	19.3	30	0.94	20.0
C+X	12 200	72	0.59	27.8	57	0.47	38.0
D	4 800	16	0.33	6.2	6	0.13	4.0
E	4 800	51	1.06	19.7	18	0.38	12.0
F	3 200	14	0.44	5.4	9	0.28	16.0
G+Y	3 800	14	0.37	5.4	7	0.18	4.7
Total	36 800	259	0.70	100	150	0.41	100

DISCUSSION

Recently, the study on the relationship between abnormal telomeric behavior and machanism of canceration has become a 'hot spot' in the field of molecular genetics. TAs of human chromosome is a rare phenomenon, which has been observed mostly in metephase cell of a pathologic nature. Since the 1990s, it has been found that telomeric lengths are evidently shortened in human colorectal carcinoma, Wilms' tumor; giant cell tumor of bone, breast cancer, lung cancer, etc. while loss of telomeric sequences would lead to chromosomal instability. Because telomere integrity is critical for the normal replication of chromosomes in mitosis, telomeric reduction may lead to chromosomal dysfunction and manifest cytogenetically as TAs. Sawyer[8] reported TAs evolving to ring chromosomes in a Pleomorphic xanthoastrocytoma. TAs between chromosomes 15pter and 20qter, and between chromosome 1q and 22qter, evolved in a stepwise fasion to ring chromosome 20 and 22. Thus, TAs is one of the mechanisms that can initiate chromosomal instability by generating subclones with unstable chromosome intermediates and result in ring chromosomes and subsequent chromosome loss. Adamson[9] postulated that absent telomere sequence causes chromosome loss and instability, and that it may cause bridge break-fusion cycles, leading to partial chromosome deletion/ duplication. In the early tumorgenesis, the telomore repeat sequence $(TTAGGG)_n$ is often shortened in tumor cells, which may trigger the activation of telomerase to elongate telomere sequence. The shortened telomeric sequence was often shown to be TAs. TAs not only causes nondisjunction but also trigger further structural changes, which may contribute to the complexity of karyotypes of solid tumors and could be one of mechanisms of oncogene activation and/or tumor-suppressor gene disruption.

We had reported genetic instability in patients with esophageal cancer. However, it is necessary to prove whether there is a relationship between chromosomal unstablility and TAs. In our experiment cellular TAs rate was 14.38% in patients and 9.3% in controls, compared with the report in literature[10], the frequency of TAs was decreased slightly, which may be the difference of susceptibility of tumor and chromosome banding techniques.

To our knowledge, this is the first report on TAs in esophageal cancer. It is not known whether the biologic changes resulting in TAs have any causal role in the carcingogenic process, or are of any importance in tumor cell progression. Molecular studies should increase our understanding of mechanisms involved in telomeric rearrangements and the relationship between chromosome change and pathogenesis and disease course in esophageal cancer.

REFERENCES

1 Fitzgerald PH, Morris CM. Telomeric association in B-cell lymphoid leukemia, *Hum Genet*, 1984;67(4):385-390
2 Mandahl N, Heim S, Kristoffersson U, Mitelman F, Rooser B, Rydholm A *et*

al. Telomeric association in a malignant fibrous histiocytoma. *Hum Genet*, 1985;71(4):321-324
3 Morgan R, Jarzhabek V, Jaffe J. Telomeric fusion in pre-T-cell acute lymphoblastic leukemia. *Hum Genet*,1986;73(3):260-263
4 Dewlap GW, Dahl RJ, Spurbeck JL, Carney JA, Cordon H. Chromosomally abnormal clones and nonnandom telomeric translocation in cardiac myxomas. *Mayo Clin Proc*,1987;62(7):558-567
5 Kovacs G, Muller-Brechlin R, Szucs S. Telomeric association in two human renal tumors. *Cancer Genet Cytogenet*, 1987;28(2):363-366
6 Gao CS, Qiu HC, Cheng ZY. A simple, stable method for chromosome R banding. *Heredity and Disease,* 1991;8(2):98
7 Herbert S, Sehwartz, George A, Schwartz HS, Dahir GA, Butler MG. Telomere reduction in giant cell tumor of bone and with aging. *Cancer Genet Cytogenet*, 1993;71(2):132-138
8 Sawyer JR, Thomas EL, Roloson GJ, Chadduck WM, Boop FA. Telomeric association evolving to ring chromosomes in a recurrent pleomorphic xanthoastrocytoma. *Cancer Genet Cytogenet*, 1992;60(2):152-157
9 Adamson DJA, King DJ, Haites NE. Significant telomere shortening in childhood leukemia. Cancer Genet Cytogenet, 191(2):204-206
10 C. Fusrer,R Miro, L Barrions, J. Egozcue. Telomere association of chromosomes induced by aphidicolin in a normal individual. *Hum Genet*, 1990;84 (5):424-426

ISSN 1007-9327 CN 14-1219/R WJG, 1998;4(3):234-237

Detection of bacterial DNA from cholesterol gallstones by nested primers polymerase chain reaction

WU Xiao-Ting[1], XIAO Lu-Jia[2], LI Xing-Quan[3] and LI Jie-Shou[1]

Subject headings cholelithiasis/microbiology; propionibacterium acnes; staphylococcus aureus; DNA, bacterial; polymerase chain reaction

Abstract

AIM To search for bacterial DNA sequences in cholesterol gallstones with negative bacterial culture.

METHODS DNA was extracted from cholesterol gallstones in gallbladders and nested primers polymerase chain reaction (NP-PCR) was used to amplify bacterial gene fragments for identifying the existence of bacteria. The samples of bacterial DNA extracted from potentially causative or unrelated living bacteria were amplified in vitro as the standard markers and comparative 16S ribosomal RNA sequence analysis was made for bacterial identification.

RESULTS The gallbladder gallstones of 30 patients were analyzed and bacterial DNA was found in 26 patients. Among them, gallstones with cholesterol content between 30%-69% were seen in 5 (5/5) patients, 70%-90% in 11(11/14) patients, and more than 90% in 10(10/11) patients. There was no difference either in cholesterol and water content of gallstones or in harboring bacterial DNA of gallstones. *E. coli*-related DNA fragments appeared in the stones of 8 (26.67%) patients; propionibacteria type DNA in 7 (23.33%); and harbored bacterial gene fragments in 2 patients, similar to Streptococcus pyogenes. A more heterogenous sequence collection was found in 7 (23.33%) patients, which could belong to multiple bacterial infections. Two (6.67%) patients had bacterial DNA with low molecular weight which might be related to some unidentified bacteria.

CONCLUSION Most cholesterol gallstones harbor bacterial DNA. It is important to determine whether these microorganisms are innocent bystanders or active participants in cholesterol gallstone formation.

[1]Research Institute of General Surgery, Nanjing General Hospital of PLA, Clinical School of Medical College, Nanjing University, Nanjing 210002, Jiangsu Province, China

[2]Department of Hepatobiliary Surgery, First Clinical School of Medicine, West China University of Medical Sciences, Chengdu 610041, Sichuan Province, China

[3]Department of Hemotology, Affiliated Hospiotal, Chinese Academy of Military Medical Sciences, Beijing 100039, China

Dr. WU Xiao Ting, male, born on January 31, 1957 in Chengdu, Sichuan Province, graduated from West China University of Medical Sciences as M.D. in 1996, post-doctorate of clinical medicine, associate professor of surgery specializing in hepatobiliary surgery, having 16 papers published.

Presented at the 11th Biennial Congress, Asian Surgical Association, 2-5 March, 1997, Hong Kong and the 7th Chinese Biliary Surgery Congress, Xi'an, 10-13 April, 1997.

***Supported by the State Education Commission Research Foundation for Scientists Returning from Abroad (1997)436.**

Correspondence to: Dr. WU Xiao Ting, Research Institute of General Surgery, Nanjing General Hospital of PLA, Clinical School of Medical College, Nanjing University, Nanjing 210002, Jiangsu Province, China
Tel. +86 • 25 • 4826808 ext 58064, Fax. +86 • 25 • 4803956

Received 1998-03-01

INTRODUCTION

Although several factors are known to trigger nucleation and/or growth of cholesterol crystals, the pathogenesis of cholesterol gallstones so far is still unclear. Most studies suggested that cholesterol gallstones may originate mainly from the disturbances of cholesterol metabolism, especially involving the balance between biliary pronucleating and antinucleating proteins[1]. Unfortunately, the role of bacterial etiology was usually neglected. We searched for bacterial DNA sequence in cholesteral gallbladder gallstones with negative bacterial culture by highly sensitive and specific nested primers polymerase chain reaction (NP-PCR) as the molecular genetic evidence of bacterial colonization of cholesterol gallstones.

MATERIALS AND METHODS

Subjects

The gallbladder gallstones were consecutively collected from October to December 1995. Patients with positive aerobic or anaerobic bile cultures were excluded. The group for analysis consisted of 5 men and 25 women with a mean age of 54.5 years, ranging from 27-73 years. All of them had symptomatic gallstone disease and underwent selective surgery. Fresh gallbladder bile samples were obtained by needle puncture aspiration during surgery. All stones had diameters of more than 5mm and stored at -20℃.

Methods

DNA extraction. DNA (3.1 μg-26.2 μg) was obtained from stone samples by the special purification methods using an UV-240 spectrophotometer (Shimadzu Corporation, Japan). Stone samples of about 300mg were crushed in a 5ml Eppendorf tube with a glass rod and incubated with 600 μl 1% sodium dodecyl sulfate rotating overnight at 20℃. Lithium chloride solution (7mol/L) was added to a final concentration of 1.5mol/L for precipitating the interfering substances in gallstones. Bacterial DNA was extracted from potentially causative or unrelated living bacteria including *E. coli*, Propionibacterium acnes, *Streptococcus pyogenes*, *Pseudomonas aeruginosa*, *Staphylococcus aureus* and *Serratia odorifera*. All of them were ATCC strains. The DNA was then extracted by the conventional purification methods, resuspended in 50 μl TE buffer (Tris/EDTA), and stored at -4℃.

NP-PCR amplification According to the literature[2], primers sequences were designed for amplifying bacterial 16S ribosomal RNA gene in vitro, including a generic 5'primer set p1: 5'-AGAGTTTGAT (c/t)(c/a) TGGCTCAG-3', P2: 5'- ACTAC (c/t) (a/c/g) GGGTATCTAA(g/t) CC-3' and a new nested 3'primer P3: 5'-ACCGC(g/t) (a/g)CTGCTGGCAC (Institute of Cellular Biology, Chinese academy of Sciences, Shanghai).

The PCR was done in 0.5ml polyproylene microcentrifuge tube with a PTC-100TM Programmable Thermal Controller (MJ Research, INC., USA). The total incubation volume was 25 μl, containing 100mmol/L "tris"-hydrochloric acid, pH 8.3, 500mmol/L potassium chloride, 15mmol/L magnesium chloride, 100 μmol/L of each dNTP, 0.2 μg-1.0 μg template DNA and 1 unit of Taq DNA polymerase (Sino-American Biotec Engineering, China). The reaction mixture was covered with 1 drop of mineral oil. In the first round of amplification, 0.2pmols each of the outer primers (P1, P2), was used then the reaction tubes were supplemented with 0.2pmols each of the inner primers (P1, P3), and 1 μl amplified DNA and 1 unit of Taq DNA polymerase were used in the second round. The PCR cycle took place at 94℃ for 30s, 56℃ for 1min, and 72℃ for 1min 40s. During the last cycle, the 72℃ step was extended to 8min. Thirty-five cycles were carried out for each reaction.

NP-RCR product comparative analysis The sequence of 16S ribosomal RNA gene fragments amplified by NP-PCR was approximately 500-base pairs. Lambda DNA/EcoR I+ Hind III (Promega Corporation, USA) was used as molecular standard. Five μg reamplified DNA was applied to a 1.4% agarose gel containing 0.8g/L ethidium bromide and after electrophoresis 4.0V/cm, 40min was visualised with an ultraviolet light source. The reamplified DNA of ATCC bacteria was included in every run. The agarose gels from the NP-PCR procedure were then subjected to computer image system for further bands comparative analysis. If the NP-PCR of the first gallstone (chosen at random) was positive, the rest of the stones of a given patient were usually not analyzed. Otherwise, all gallstones or at least five stones would be analyzed.

Cholesterol and water content analysis DNA isolated from a part of a same gallstone was used for NP-PCR amplification and another part for cholesterol and water content analysis. Accurate 100mg of nativeg allstone material was dried at 105℃ for 3 hours to a constant weight. The cholesterol was extracted by a modified chemical method and underwent photometric test using a 722 Spectrophotometer (Shanghai Third Analysis Instrument Factory). The cholesterol and water content was analyzed according to the manufacturer's instructions.

Statistical analysis All values were expressed as $\bar{x}\pm s$. The relationship between cholesterol or water content and NP-PCR results were analyzed with Wilcoxon rank sum test.

RESULTS

The gallstones of 30 patients were analyzed. Bacterial 16S ribosomal RNA gene fragments were amplified in the stones of 26 patients. Amplification was not possible in the remaining 4 patients whose stones had no detectable bacterial DNA (Figure 1). In the 26 patients, the positive gallstones contained cholesterol content between 30%-69% in 5 (5/5) patients, 70%-90% in 11 (11/14) patients, and more than 90% in 10 (10/11) patients. The water content of gallstones changed from 10.3% to 52%. The group with bacterial DNA in the gallstones had water content of 26.5%±10.39% while the group without bacterial DNA had water content of 19.18%±4.88%. There was no difference either in cholesterol and water content or in harboring bacterial DNA of gallstones ($P>0.05$) (Tables 1, 2).E.coli related DNA fragments were found in the stones of 8 (26.67%) patients. Propionibacteria-type DNA was obtained in 7 (23.33%) patients. Stones of 2 (6.67%) patients harbored bacterial gene fragments similar to Streptococcus pyogenes. Simultaneously, multiple heterogenous sequence collections were found in 7 (23.33%) patients, which could belong to the mixed infections including *E.coli*,

Propionibacterum acnes and *Streptococcus pyogenes* or some other unidentified bacteria such as *Clostridium difficile*. The stones of the other 2 (6.67%) patients had bacterial DNA with lower molecular weight and could be related to some unidentified bacteria.

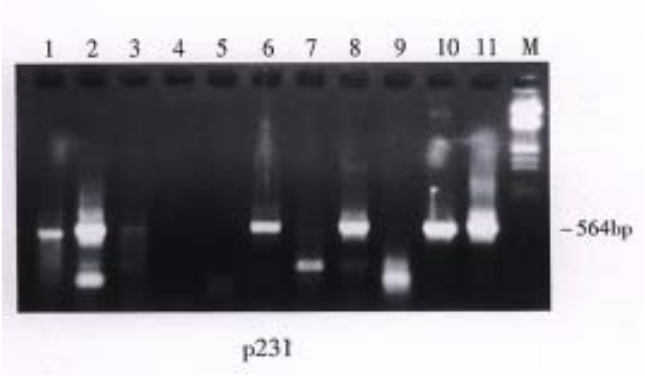

Figure 1 Agarose gel electrophoresis comparative analysis of NP-PCR products of bacterial DNA fragments from gallstones. M: Molecular standard, Lambda DNA/EcoR I+ Hind III. Lanes 1, 2, 3, 6, 8 and 10: NP-PCR positive products similar to the amplified products of 11 *P.acnes* 16S rRNA gene; 11: amplified product of *P.acnes* 16S rRNA gene; 7, 9: NP-PCR positive products, molecular weight less than 300bp; 4: negative control; 5: NP-PCR negative product.

Table 1 The relationship between cholesterol content of gallstones and the rate of gallstones harbor bacterial DNA

Cholesterol content (%)	Harbor bacterial DNA		No harbor bacterial DNA		Total	
	Case	%	Case	%	Case	%
30-69	5	16.67	0	0	5	16.67
70-90	11	36.66	3	10.0	14	46.67
>90	10	33.33	1	33.33	11	36.66

Table 2 The relationship between water content of gallstones and gallstones harbor bacterial DNA

Group	Case	Water content (%)
Harbor bacterial DNA	26	26.57±10.39
No harbor bacterial DNA	4	19.18±4.88

DISCUSSION

Few previous studies considered the role of bacteria in the pathogenesis of cholesterol gallstone as there was no direct evidence of bacterial existence, because of the failure in the bacteria culture from cholesterol stones. However, the process in gallbladder gallstone formation may take a longer time, and the embedded bacteria may be destroyed or killed. PCR technique has a high sensitivity and specificity as compared with the bacterial routine culture. Theoretically, PCR can detect a copy gene of a bacterium or cell. The nested primer approach increases the specificity as well as sensitivity of PCR[3]. To prevent artifacts resulting from contamination, gallbladder stones were collected and prepared with stern sterilization, control experiments omitting template DNA were made in parallel, and pre and post-PCR procedures were performed in different rooms. Furthermore, primers were designed according to bacterial genes coding for 16S ribosomal RNA. The structure of these ribosomal RNA genes is highly specific for different bacteria.

Bacteria can invade the biliary tract by ascending from the duodenum and via the hematogenous route from the hepatic portal venous blood[4]. Many aerobe, facultative aerobe and anaerobe species such as *E.coli*, *P.vulgaris*, B.fragilis, Clostridium perfringens, can produce β-glucaronidase that catalyzes the hydrolysis of bilirubin conjugates in bile, leading to increased amounts of unconjugated bilirubin, which precipitates as calcium bilirubinate stones. Bacteria could also disturb gallbladder wall secretion and cause acute or chronic inflammation with resultant precipitation of bile. Bacteria have adhesive properties and can produce glycocalyx or other matrices within which the pigment or cholesterol coalesces. In fact, most of cholesterol gallstones have a pigment nucleus or section. It seems likely that bacterial infection serves as an initiating factor or plays other important roles in the development of gallstones. Besides most bacteria that cause biliary infection can produce palmitate via a phospholipase, and result in precipitation of calcium palmitate. Meanwhile, the reduction of lecithin in bile leads to a lower solubility of bilirubin and promotes banding of bilirubin and calcium. Bacterial phospholipase, on the other hand, degrades lecithin which will reduce the solubility of cholesterol and promote cholesterol nucleation in bile.

Propionibacterium acnes is a gram-positive anaerobic rod bacterium which is a normal bacterial colony usually located on the skin and mucosa. The role of *Propionibacterium acnes* in gallstone formation has not been clarified. Up to the present, the possible pathogenic mechanisms are[5]: ①This bacterium produces a nonspecific extracellular lipase that catalyses the total hydrolysis of triacylglycerols to free fatty acids and glycerol and that is able to use lecithin as a substrate. ② *Propionibacterium acens*- also produces a phospholipase C, which is a promoter of cholesterol procipitation[6]. ③ *Propionibacterium* can bind to lipids[7], and the binding is increased as lipid hydrophobicity increases. This ability may permit *Propionibacterium acnes* to bind biliary lipid vesicles and degrade them with the extracellular lipolytic enzymes. The nonspecific lipase is a chemotactic

agent for neutrophils, and activation of neutrophils would result in the release of oxygen radicals capable of causing phospholipid perioxidation, which reduces the stability of mixed micellar systems containing cholesterol, lecithin, and cholate. ④ *Propionibacterium acnes* has specific affinity for the calcium containing regions of gallstones and can promote calcium salt procipitation. Once the calcium bilirubinate salt and calcium palmitate salt were formed, the bacterial colony would secrete sufficient lipolytic enzymes to promote cholesterol nucleation.

We found that most cholesterol gallstones harbor bacterial DNA with the highly sensitive, specific and reproducible NP-PCR technique. Bacteria and their metabolites might play an important role in the formation of cholesterol gallstones with different mechanisms. Obviously, the study searching for molecular genetic evidence of bacterial conolization of cholesterol gallstones is only at the initial stage. A lot of work remains to be done before it can be decided whether these microorganisms have a cause and effect relationship in cholesterol gallstone formation and an infectious etiology can be established. We are now determining heterologous sequence collections with the dideoxy chain termination technique.

REFERENCES

1 Holzbach RT, Busch N. Nucleation and growth of cholesterol crystals. Kinetic determinants in supersaturated native bile. *Gastroenterol Clin North Am*,1991;20(1):67-84
2 Swidsinski A, Ludwig N, Pahlig H *et al*.Molecular genetic evidence of bacterial colonizations of cholesterol gallstones. *Gastroenterology*, 1995;108(3): 860-864
3 Aurelius E, Johansson B, Skoldenberg B *et al*. Rapid diagnosis of herpes simplex encephalitis by nested polymerase chain reaction assay of cerebrospinal fluid. *Lancet*,1991;337(8735):189-192
4 Wu XT, Xiao LJ. The progress of studies on the role of bacteria in the formation of gallstone. *Foreign Medicine (Surgery)*, 1996;23(5):277-279
5 Soloway RD, Growther RS. Bacteria and cholesterol gallstones: molecular biology comes to gallstones pathogenesis. *Gastroenterology*, 1995;108(3):934-936
6 Pattinson NR, Willis KE. Effect of phospholipase C on cholesterol solubilization in model bile. *Gastroenterology*, 1991;101(5):1339-1344
7 Gribbon EM, Cuniffe WJ, Holland KT. Interaction of propionibacterium acnes with skin lipid in vitro. *J Gen Microbiol*, 1993;139(8):1745-1751

 ISSN 1007-9327 CN 14-1219/R WJG, 1998;4(3):238-241

Effects of octreotide on gallbladder pressure and myoelectric activity of Oddi sphincter in rabbits

ZHOU Jian-Hua, LIU Chuan-Yong, ZHANG Ru-Hua, WANG Han-Ru and LIU Ke-Jing

Subject headings octreotide/pharmacology; gallbladder/drug effects; oddi sphincter/drug effects; electrophysiology; rabbits; somatostatin; electric stimulation

Abstract

AIM To observe the effect of octreotide (OT) and somatostatin (SS) on gallbladder pressure and myoelectric activity of SO in rabbits.

METHODS Male rabbits fasted for 15h-18h and anesthetized with urethane. The mean gallbladder pressure (GP) and myoelectric activity of SO were simutaneously measured with a frog bladder connected to a transducer and a pair of copper electrodes.

RESULTS After injection of OT (10 μg/kg, iv), the GP decreased in 2min and reached the lowest value in about 60min ($P<0.01$, $n=19$), and completely or partially returned to the normal level in 120min. The frequency of myoelectric activty of SO was reduced, even disappeared in 2min ($P<0.01$, $n=19$) and returned to normal in about 20min. Injection of SS (10 μg/kg, iv) also decreased GP and myoelectric activity of SO ($P<0.01$, $n=7$); Before and after injection of OT or SS, injection of CCK-8 (100ng or 200ng) caused similar increase in myoelectric activity of SO and GP ($P>0.05$). Before and after injection of OT, there were no significant differences in increases of myoelectric activity of SO and GP caused by electric stimulation of dorsal motor nucleus of vagus ($P>0.05$).

CONCLUSION OT and SS decreased GP and myoelectric activity of SO, demonstrating that effects of OT were similar to those of SS. Intravenous injection of OT did not affect the increase of myoelectric activity of SO and GP caused by CCK-8 or electric stimulation of dorsal motor nucleus of vagus.

Department of Physiology, Shangdong Medical University, Jinan 250012, Shandong Province, China.

Zhou Jian Hua, female, born on 1935-09-04 in Ruichang City, Jiangxi Province, graduated from Shandong Medical College as a postgraduate in 1960, now a professor of physiology working in Shandong Medical University, having 27 papers published.[a]*Project supported by the Naturual Science Foundation of Shandong Province, No.91C0428.

Correspondence to Zhou Jian Hua, Department of Physiology, Shandong Medical University, Jinan 250012, Shandong Province, China.[a]

Tel. +86¡¤531¡¤2941907[a]

Received 1998-01-12

INTRODUCTION

Octreotide (OT) is an 8 amino acids synthetic analog of somatostatin (SS). Treatment with OT in acromegaly is effective but leads to gallstone formation. OT injections inhibit gallbladder contraction in acromegalic patients[1,2] and normal subjects[3], stimulating human sphincter of Oddi (SO) activity[4], which may impair bile evacuation. However, studies of SS, especially effect of OT on motor function of biliary system in animals are scarce and controversial. The aim of this study was to observe the effects of OT and SS on gallbladder pressure (GP) and myoelectric activity of SO in rabbits.

MATERIALS AND METHODS

Preparation of animals

Thirty-eight male rabbits, weighing 2kg-2.5kg were used. They were fasted for 15h-18h with free intake of water and then anesthetized with urethane (1.0g/kg, iv). A cannula was inserted into trachea and the unilateral femoral artery was cathered for the blood pressure measurement.

Measurement of GP and myoelectric activity of SO

A frog bladder perfused with saline was placed into the gallbladder and connected to a transducer (TP-200T). A pair of copper electrodes was inserted into subsera of SO. Blood pressure, GP and myoelectric signals of SO were simutaneously measured by a polygrapher (RM-6000, NIHON KHODEN).

Administration of drugs

OT, cholecystokinin octapeptide (CCK-8) and SS were injected through ear vein. SS and CCK-8 were products of Sigma Chemical Company (St. Louis, U.S.A.) and Pennisula Laboratories (Belmont, U.S.A.) respectively. OT was produced by the Sandoz Pharm Ltd (Besel, Switzerland).

Electric stimulation of dorsal motor nucleus of vagus (DMV)

The animal's head was fixed in a sterotaxic instrument (I-C model, Jiang Wan, China) A wire electrode was inserted into DMV for stimulation (0.2mA, 10Hz, 0.5ms duration, 1min) according to Messen's method. An indifferent electrode was placed on the skin tissure of skull.

Statistical analysis

The constant mean GP of each animal was taken as control level (i.e., basic GP served as 0kPa in place of the real value) and the frequency of myoelectric activity of SO was considered as normal value. The percentage of frequency changes=(effect value-normal value) ÷ normal value×100%. All values were expressed as $\bar{x}\pm s_{\bar{x}}$. Experimental data were treated statistically by Student's *t* test.

RESULTS

Effect of intravenous injection of OT on GP

Intravenous injection of OT caused dose-dependent decrease of GP. After injection of OT (10 μg/kg, iv), the GP decreased in 2min (-0.142kPa±0.029kPa, $P<0.01$) and reached the lowest value in 60min (-0.257kPa±0.065kPa, $P<0.01$), and completely or partially returned to the normal level in 120min. Small dose of OT (5 μg/kg, iv), also decreased GP ($P<0.01$) but the effect was slight. No change in GP was found after injection of 1ml of 0.9% saline ($P>0.05$). The differences were significant ($P<0.01$) (Figure 1, Table 1) between the two groups of OT.

Effect of intravenous injection of OT on myoelectric activity of SO

After injection of OT (10 μg/kg, iv), the frequency of myoelectric activity of SO was reduced, even disappeared in 2min (-83.1%±8.0%, $P<0.01$) and returned to normal in about 20min. At the dose of 5 μg/kg of OT, frequency of myoelectric activity of SO also decreased (-54%±6.1%, $P<0.01$). In contrast to OT 10 μg/kg group, the effect is weak ($P<0.05$). Injection of the same volume of 0.9% saline influenced neither GP nor myoelectric activity of SO (Figures 1, 2, Table 2).

Effect of iv injection of SS on GP and myoelectric activity of SO

After injection of SS (10 μg/kg, iv) in 7 rabbits, GP and myoelectric activity of SO were decreased. These changes were similar to those in OT ($P>0.05$) (Figure 3, Tables 1, 2).

Effect of iv OT and SS on changes in GP and myoelectric activity of SO caused by CCK-8

Ten minutes before and 15 minutes after injection of OT (10 μg/kg, iv), and CCK-8 (100ng) there was a marked increase in GP and myoelectric activity of SO. Before and after injection of SS (10 μg/kg), and CCK-8 (200ng) greatly increased GP and myoelectric activity of SO. These responses to CCK-8 showed no significant differences between pre- and post-injection of OT or SS ($P>0.05$), (Figure 4, Table 3).

Table 1 Effect of OT and SS on gallbladder pressure

Groups	*n*	Changes in gallbladder pressure (basic pressure=0kPa)							
		2	10	20	40	60	80	100	120min
NS	5	-0.024	-0.000	-0.013	-0.013	-0.010	-0.010	-0.012	-0.020
		±0.020	±0.024	±0.024	±0.032	±0.024	±0.024	±0.024	±0.040
OT	6	-0.074[a]	-0.097[b]	-0.068	-0.135	-0.101	-0.120	-0.068	-0.052
(5 μg/kg)		±0.012	±0.023	±0.024	±0.050	±0.062	±0.052	±0.038	±0.031
OT2	19	-0.142[bc]	-0.196[bd]	-0.184[a]	-0.154[a]	-0.257[a]	-0.145	-0.104	-0.040
(10 μg/kg)		±0.020	±0.052	±0.034	±0.052	±0.065	±0.048	±0.036	±0.042
SS(10 μg/kg)	7	-0.143[b]	-0.122[a]	-0.071	-0.021	0.029			
		±0.034	±0.037	±0.021	±0.036	±0.028			

[a]$P<0.05$, [b]$P<0.01$ *vs* NS group; [c]$P<0.05$, [d]$P<0.01$, *vs* group 1 OT.

Table 2 Effect of OT and SS on frequency of myoelectric activity of SO

Groups	*n*	Changes in frequency of myoelectric activity of SO (%)							
		2	10	20	40	60	80	100	120min
NS	5	-8.0	-4.0	-2.0	0.0	4.0	-3.0	-1.0	-2.0
		±8.2	±6.5	±5.0	±11.0	±6.0	±6.0	±8.2	±5.0
OT1	6	-51.4[b]	-42.3[a]	-18.5	-5.0	-4.0	5.0	-2.0	4.0
(5 μg/kg)		±6.1	±11.9	±9.0	±10.0	±6.0	±6.5	±4.5	±5.3
OT2	19	-83.1[bd]	-65.0[a]	-21.5	5.0	3.5	-4.0	-4.0	-3.5
(10 μg/kg)		±8.0	±11.3	±9.3	±6.2	±9.1	±7.0	±5.0	±8.5
SS	7	-86.7[b]	-78.5[a]	-48.9	-10.0	7.0			
(10 μg/kg)		±11.0	±14.0	±14.0	±18.8	±9.0			

[a]$P<0.05$, [b]$P<0.01$ *vs* NS group; [c]$P<0.05$, [d]$P<0.01$, *vs* OT 1 group.

Table 3 Comparision of effects of iv CCK-8 and electric stimulation of DMV on gallbladder pressure and myoelectric activity of SO after

Group	*n*	Changes of frequency of myoelectric activity of SO (%)		Changes in gallbladder pressure (basic pressure = 0kPa)	
		Before	After	Before	After
DMV OT	10	283.8±69.6	285.8±75.8	0.128±0.046	0.123±0.031
CCK-8 (100ng) OT	12	346.8±79.2	275.8±37.7	0.363±0.113	0.321±0.112
CCK-8(200ng) SS	4	485.8±78.9	426.4±59.0	1.795±0.468	1.955±0.340

Before, before injection of TO or SS; After, after injection of OT or SS.

Effects of iv OT on changes of GP and myoelectric activity of SO caused by electric stimulation of DMV

Ten minutes before and after injection of OT (10 μg/kg, iv), electric stimulation of DMV increased GP, frequency and amplitude of myoelectric activity of SO, the effects being similar (P>0.05), (Table 3).

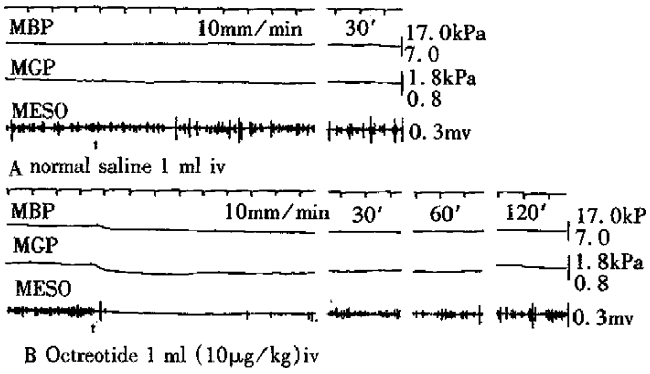

Figure 1 Effect of iv octreotide on gallbladder pressure and myoelectric activity of SO. A, injection of normal saline; B, injection of OT; MBP, mean blood pressure; MGP, mean gallbladder pressure; MESO, myoelectric activity of SO. ↑, intravenous injection mark.

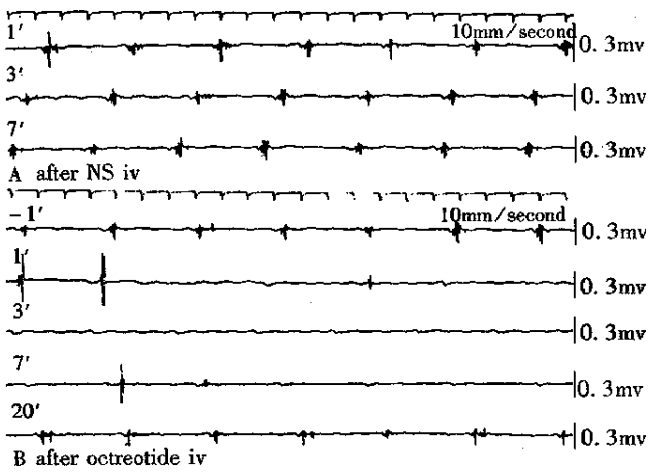

Figure 2 Effect of octreotide on myoelectric activity of SO. A, injection of normal saline; B, injection of OT (10 μg/kg, iv)

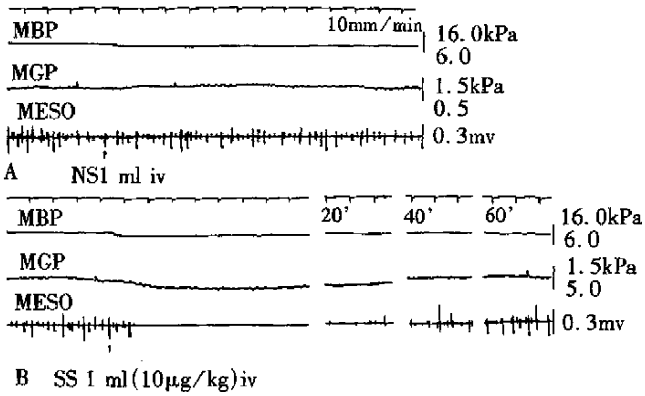

Figure 3 Effect of iv SS on gallbladder pressure and myoelectric activity of SO. A, injection of normal saline; B, injection of SS; MBP, mean blood pressure; MGP, mean gallbladder pressure; MESO, myoelectric activity of SO; ↑, iv injection mark.

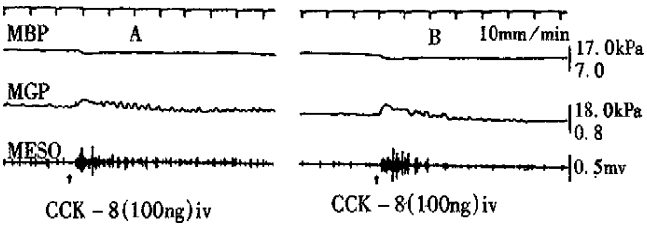

Figure 4 Effect of iv CCK-8 on gallbladder pressure and myoelectric activity of SO after injection of octreotide. A, before injection of OT; B, After injection of OT.

DISCUSSION

Several studies of SS effect on biliary motility have been reported but the results are different. SS has no effect on contraction of gallbladder smooth muscle strips in guinea pigs, dogs[5] and rabbits[6], but inhibits gallbladder motility in human[7] and

dogs[5] in vivo. SS has been reported to either stimulate or inhibit the SO of dogs[8,9]. In the present study, SS decreased both GP and myoelectric activity of SO. The latter response was similar to the inhibitory SS effect on SO in rabbits reported before[10]. OT, a long-acting analog of SS, has been found to inhibit human gallbladder motility and to stimulate SO contraction which may impair bile evacuation with a risk of gallstone formation[1,2,4]. The animal experiment of OT effect was only conducted on prairie dogs in which OT decreased the motility index of SO, but did not affect the gallbladder pressure[11]. In the present study, OT decreased GP and myoelectric activity of SO in rabbits. These results were consistent with those of SS, demonstrating that inhibitory effect of OT is similar to that of SS. The diverse effects of SS and OT on motility of SO and gallbladder may be explained by the species difference.

The motility of gallbladder and SO is regulated by both autonomic nervous system and intestinal hormones. CCK is an important hormone for mediating motility of biliary tract. In the experiments on dogs, SS inhibits contraction of gallbladder strips induced by electric stimulation and decreased GP by CCK-8 in vivo probably through suppressing Ach release by the intrinsic cholinergic neurons, but does not affect contraction of gallblader strips intiated by Ach or CCK[5]. Intravenous injection of SS inhibits contraction of human gallblader in response to CCK[7]. In our study, injection of CCK-8 markedly raised GP and increased myoelelctric activity of SO in rabbits. After injection of OT or SS, and CCK-8 resulted in increases of GP and myoelectric activity of SO, indicating that SS and OT do not affect the stimulatory effect of CCK-8 on gallbladder and SO. It is reported that electric stimulation of DMV raises GP and increases myoelectric activity of SO through a cholinergic mechanism of vagal nerve. In this study, before and after injection of OT, electric stimulation of DMV caused similar increases in GP and myoelectric activity of SO. These results imply that OT did not inhibit the increase in motility of gallbladder and SO caused by DMV stimulation. The mechanisms of OT effect on motor function of biliary tract require further investigations.

In conclusion, OT and SS decrease GP and myoelectric activity of SO, demonstrating that the inhibitory effect of OT is similar to that of SS in rabbits. Before and after injection of OT and SS, and CCK-8 injection or electric stimulation of DMV similar increases are caused in GP and myoelectric activity of SO, suggesting that OT and SS do not affect the increases in motility of gallbladder and SO caused by CCK-8 and electric stimulation of DMV.

REFERENCES

1 Zhu XF, Shi YF, Zhang JX, Dai Q, Harris AG. Prospective study of long-term therapeutic and wide effects on gallbladder function in Chinese acromegalic patients. *Chin J Int Med*, 1991;30(7):405-408

2 Stolk MFJ, Van Erpecun KJ, Lopposchaar HPF, de Bruin WI, Jansen JBMJ, Lamers CBHW *et al*. Postprandial gallbladder motility and hormone release during intermittent and continuous substaneous octreotide treatment in aeromegaly. *Gut*, 1993;34(6):808-813

3 Grimaldi C, Darcout J, Harris AG, Lebot E, Lapalus F, Delmont, J. Cholescintigraphic study of effect of somatostatin analog, octreotide, on bile secretion and gallbladder emptying in normal subject. *Dig Dis Sci*, 1993;38 (9):1718-1721

4 Binmoller KF, Dumas R, Harris AG, Dilmont JP. Effect of somatostatin analog octreotide on human sphincter of Oddi. *Dig Dis Sci*,1992;37(5):775-777

5 Milenov K, Rakovska A, Kalfin R, Mantovani P. Effect of somatostatin of canine gallbladder motility. *Neuropeptide*, 1990;17(1):75-80

6 Johnson AG, Marshall CE, Wilson IAI. Effect of some drugs and peptide hormones on the responsiveness of rabbits isolated gallbladder to cholecystokinin. *J Physiol*, 1982;332(2):415-425

7 Gullo L, Bolondi L, Scarpignato C, Priori P, Casanova P, Labo G. Effect of somatostatin and thyrotropin releasing hormone on cholecystokinin-induced gallbladder emptying. *Dig Dis Sci*,1986;31(12):1345-1350

8 Sievert CE, Potter TJ, Levine AS, Morley JE, Silvis SE, Vennes JA. Effect of bombesin and gastrin-releasing peptide on canine sphincter of Oddi. *Am J Physiol*, 1988;254(3):361-365

9 Lin TM, Tust RH. Action of somatostatin on choledochal sphincter, gallbladder and bile flow in rabbits. *Federation Proc*, 1997;36(3):557-558

10 Adami GF, Leandri R, Sarles JC. Effect of somatostatin on rabbit Oddi's sphincter in vivo. interrelation of somatostotin and cholecystokinin. *Gastroenterol Clin Biol*, 1986;10(2):108-112

11 Ahrendt SA, Ahrendt GH, Lillemore KD, Pitt HA. Effect of octreotide on sphincter of Oddi and gallbladder motility in prairie dogs. *Am J Physiol*, 1992;262(25):G909-G914

 ISSN 1007-9327 CN 14-1219/R WJG, 1998;4(3):242-245

Relationship between enteric microecologic dysbiosis and bacterial translocation in acute necrotizing pancreatitis *

WU Cheng-Tang, LI Zhan-Liang and XIONG De-Xin

Subject headings pancreatitis; bacterial translocation; intestines; lipopolysaccharide/blood; amylase/blood; bifidobacterium; lactobacillus

Abstract

AIM To investigate the potential role of intestinal microflora barrier in the pathogenesis of pancreatic infection.

METHODS Fifteen dogs were colonized with a strain of *E.coli* JM109 bearing ampicillin resistance plasmid PUC18. The animals were divided into two groups. In experimental group (n=8), acute necrotizing pancreatitis (ANP) was induced by injection of 0.5 ml/kg of sodium tarocholate with 3000U/kg trypsin into the pancreatic duct. The control group (n=7) underwent laparotomy only. All animals were sacrificed 7 days later. Mucosal and luminal microflora of intestine were analyzed quantitatively, and various organs were harvested for culturing, blood samples were obtained for determination of serum amylase activities and plasma lipopolysaccharide (LPS) concentrations.

RESULTS In the experimental group, the number of *E.coli* in the intestine was much higher than those of the controls, while bifidobacterium and lactobacillus were decreased significantly (Jejunum, 1.75±0.95 *vs* 2.35±0.79, P<0.05; 1.13±0.8 *vs* 1.83±0.64, P<0.05; ileum, 2.89±0.86 *vs* 3.87±1.05, P<0.05; 1.78±0.79 *vs* 3.79±1.11, P<0.01;cecum, 2.70±0.88 *vs* 4.89±0.87, P<001; 2.81±0.73 *vs* 3.24±0.84, P<0.05. Content of Cecum, 3.06±0.87 *vs* 5.15±1.44, P<0.01; 2.67±0.61 *vs* 4.25±0.81, P<M0.01), resulting in reversal of bifido-bacterium/*E.coli* ratio as compared with the control group (jejunum,0.51±0.76 *vs* 1.23±0.53, P<0.05; ileum, 0.62±0.68 *vs* 1.16±0.32, P<0.05; cecum,0.46±0.44 *vs* 1.03±0.64, P<0.05). In addition, intestinal bacteria were isolated from organs of all animals in the experimental group, and JM109 was also detected in most cases. Positive blood culture was 75.0% and 62.5% on day 1 and 2 after induction of ANP, respectively, but no bacterium was found in the controls. As compared with the control group, blood LPS levels and serum amylase activities increased 1-3 times and 3-8 times respectively.

CONCLUSION Microecological disturbance could occur in ANP, and overgrowth of intestinal gram-negative bacteria may lead to translocation to the pancreas and other organs, becoming the source of pancreatic and peripancreatic infection.

INTRODUCTION

Secondary pancreatic and peripancreatic infection is a common severe complication in acute necrotizing pancreatitis (ANP) and responsible for 80% of death due to this disease. The pathogenesis of pancreatic infection has not been clear completely. Pathogens isolated from infected pancreas were similar with common intestinal flora, providing indirect evidence of gut origin of pancreatic infection.

The microecological disturbances of intestine might play an important role in the development of pancreatic infection following ANP. The purpose of this study was to determine if indigenous enteric flora were a primary source of pancreatic infection, and to reveal the relationship between enteric microecologic dysbiosis and bacterial translocation in ANP in dogs.

MATERIALS AND METHODS

Adult mongrel dogs weighing 13kg to 18kg were observed for at least 1 week, prior to the experiment, stools were cultured with eosin methylene blue agar containing ampicillin (100ng/L). Animals without resistant bacteria in stool culture entered the experiment and received

Trauma Center, The 304th Hospital of Chinese PLA, Beijing 100037, China

Dr. WU Cheng-Tang, male, born on 1967-08-10 in Beihai City, Guangxi Autonomous Region, Han nationality, graduated from the Beijing PLA Medical College as a postgraduate in 1996. Now he is working in Nanfang Hospital as an attending surgeon, First Military Medical University, having 10 papers published.

***Supported by a grant from the foundation for specialized key scientific projects of the People¡äs Liberation Army.**

Correspondence to: Dr. WU Cheng Tang, Department of General Surgery, Nanfang Hospital, First Millitary Medical University, Guangzhou 510515, China

Tel. +86 • 20 • 87705577 ext 3124

Received 1997-12-06

20 000IU gentamicin orally for 2 days to suppress the indigenous enteric flora. *E.coli* JM109 bearing ampicillin-resistance plasmid PUC18 (approximately 109 colony-forming units) administered with food. For the rest of the experiment, drinking water was supplemented with 100ng/L ampicillin. Stool samples were cultured with eosin methylene blue agar (supplemented with 100ng/L ampicillin), Colonization was considered established when culture was positive for 3 successive days. Fifteen dogs were then randomly divided into two groups: ANP group (n=8) and control group (n=7), and laparotomy was performed under general anesthesia (i.v. thiopentalsodium). In ANP group, pancreatitis was induced by injection of 0.5 ml/kg sodium taurocholate with 3 000IU/kg trypsin into the pancreatic duct under pressure of 7.8kPa. The dogs in the control group received laparotomy only.

Before the operation and on days 1, 2, 4 and 7 postoperatively, blood samples were obtained for determination of serum amylase activities (iodium-starch method) and plasma LPS concentrations (LAL test), and blood was cultured for aerobic and anaerobic bacteria on each postoperative day. All dogs were killed on the 7th day after operation. Under strict aseptic conditions, specimens of tissues from mesenteric lymph nodes (MLN), liver, pancreas, spleen, kidney and lung were harvested, weighed, and homogenized. Ten μl of each homogenate was cultured for aerobic and anaerobic bacteria. All bacteria isolated from organs were cultured in luria-bertani (LB) supplemented with 100ng/L ampicillin for 24 hours. Positive germs were initially identified as resistant bacteria. Final identification of those strains was accomplished by confirming the presence of plasmid PUC18. Plasmid DNA was purified by an alkaline lysis method and subjected to restriction digestion with endonuclease EcoR1 (Sigma Corp.) in 37℃ water for 1 hour. Ten μl DNA fragments were separated by electrophoresis through horizontal 0.8% agarose gel, stained with ethidum bromide and photographed under ultraviolet lamp in 590nm.

Jejunum, cecum, ileum and content of cecum were harvested, weighed and homogenized in 5ml physiological saline. Homogenate (0.5ml) was serially diluted (10 times), and 10 μl dilution was plated on selective media for *E.coli*, enterococci, bacteroids, bifidobacteria and lactobacilli, respectively, and incubated at 37℃ for 24-48 hours, aerobically or anaerobically for 48 hours, positive specimens were subcultured and the bacteria identified by standard procedures.

Sections of cecum and pancreas were stained with hematoxylin and eosin and examined under light microscopy.

Data were analyed by Student's t test, and results were expressed as $\bar{x}\pm s$. Differences were considered significant when $P<0.05$).

RESULTS

Acute necrotizing pancreatitis

Laboratory tests showed significant hyperamylasemia on days 1, 2, 4 and 7 after operation in dogs with pancreatitis (Table 1). The pancreas in ANP group appeared enlarged and swollen with visible grey or black areas. Histologic examination revealed severe hemorrhagic necrotizing pancreatitis (Figure 1).?In the control group, no abnormalities were found both macroscopically and histologically (Figure 2).

Intestinal morphology

Cecal mucosa were severely damaged in dogs with pancreatitis. The surface epithelium was denuded on the top of the villi, and there was an extensive neutrophilic granulocyte infiltration of the lamina propria. No pathologic changes were noticed in the controls.

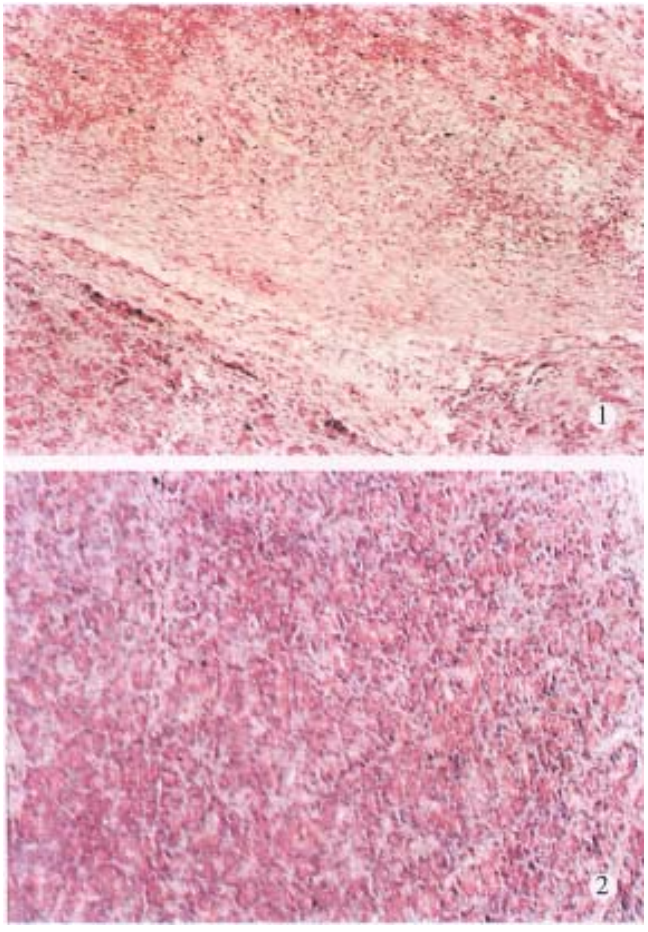

Figure 1 Light micrography showing severe hemorrhage in pancreas of ANP. HE×100

Figure 2 Light micrography of a normal pancreas. HE×100

Intestinal microflora

The population levels of *E.coli* in the mucosa of jejunum, ileum, cecum and in the cecal content were increased significantly in ANP dogs on day 7 postoperatively ($P<0.05$ or $P<0.01$, Table 2), while bifidobacteria and lactobacilli were decreased obviously. The ratio of bifidobacterium/*E.coli* (B/E) was reversed ($P<0.05$, Table 3).

Bacterial translocation

Blood and tissue cultures were negative except for 2 episodes of bacterial translocation to MLN in the control group and were positive in the ANP group, bacterial translocation was found in MLN (100%), pancreas (87.5%), liver (87.5%), lung (75%), kidney (75%) and spleen (50%). The isolation rate of *E.coli* JM109 was 75% in pancreas, 50% in the liver and lung. Blood positive cultures were seen mainly on the first (75%) and second (62.5%) postoperative day, and JM109 was found in more than 60% of cases.

LPS concentration

The LPS concentrations in ANP group were elevated significantly as compared with those of the control group in each postoperative day ($P<0.05$ or $P<0.01$, Table 4).

Table 1 Activity of plasma amylase (U/L)

Group	Preoperation	d1	d2	d4	d7
Control	796.61±82.41	816.56±57.82	787.26±78.66	807.68±89.56	778.59±80.95
ANP	825.50±82.94	7363.25±1383.26[b]	7060.75±1135.65[b]	4590.25±1312.44[b]	2783.75±893.42[b]

[b]$P<0.01$, compared with the control group.

Table 2 Population levels of mucosal and luminal flora (CFUlogn/g, $\bar{x}\pm s$)

Content	Group	*E.coli*	Enterococcus	Bacteroid	Bifidobacterium	Lactobacillus
Jejunum	Control	1.91±0.49	1.69±0.79	2.23±0.92	2.35±0.79	1.83±0.64
	ANP	3.42±0.93[b]	0[b]	3.75±0.77[a]	1.75±0.95[a]	1.13±0.80
Ileum	Control	3.51±0.84	2.05±0.44	3.61±1.06	3.87±1.05	3.79±1.11
	ANP	5.80±1.27[b]	1.17±0.95[a]	4.35±0.98[a]	2.89±0.86[a]	1.78±0.79b
Cecum	Control	4.74±0.93	2.61±0.77	3.54±0.99	4.89±0.87	3.24±0.84
	ANP	5.88±1.18[a]	1.27±1.04[a]	4.01±1.10	2.70±0.88[b]	2.81±0.73a
Content	Control	4.86±0.64	3.50±0.85	4.81±0.95	5.15±1.44	4.25±0.81
of cecum	ANP	7.43±1.19[b]	2.27±1.49[a]	4.72±1.13	3.06±0.89[b]	2.67±0.61b

[a]$P<0.05$, [b]$P<0.01$ compared with the control group.

Table 3 Ratio of bifidobacterium/*E.coli* (B/E)

Group	Jejunum	Ileum	Cerum
Control	1.23±0.53	1.16±0.82	1.03±0.64
ANP	0.51±0.76[a]	0.62±0.68[a]	0.16±0.44[a]

[a]$P<0.05$ compared with the control group.

Table 4 Changes of plasma LPS (Eu/ml)

Group	d1	d2	d4	d7
Control	0.068±0.005	0.074±0.008	0.064±0.009	0.066±0.007
ANP	0.217±0.085[b]	0.346±0.127[b]	0.268±0.054[b]	0.107±0.064[a]

[a]$P<0.05$, [b]$P<0.01$, compared with the control group.

Plasmid DNA analysis

The strain of ampicillin-resistant *E.coli* was isolated in all dogs with pancreatitis. All ampicillin-resistant *E.coli* isolated from different organs had identical antibiograms and contained plasmid DNA that appeared identical as shown by plasmid electrophoresis profile, indcating that they were the same strains.

DISCUSSION

Numerous studies have revealed that intestinal microecologic dystiosis may lead to decreased colonization resistance of the gut, which plays an important role in the pathogenesis of enterogenous infection. Runkel found that gram-negative germs overgrew in cecal mucosa 24-48 hours after onset of pancreatitis, suggesting that microecological disturbance of intestine was an important factor for sepsis following pancreatitis [3]. Kazantsev used plasmid labeled *E.coli* (kanamycin-resistant) to confirm that intestinal bacteria could translocate to pancreas in pancreatitis, but he could not explain the relationship between bacterial translocation and enteric microecologic dysbiosis[4].

The present study showed that the enteric microecologic disturbance did take place following pancreatitis. The population levels of *E.coli* were

increased significantly, while the bifidobacteria and lactobacilli were decreased obviously. So the main manifestation of the disturbance of enteric flora were overgrowth of opportunistic pathogens including aerobic bacteria and facultative anaerobes, and reduction of anaerobic bacteria such as bifidobacteria and lactobacilli, as reported earlier by Gianotti[5] *et al*. Blood and organ culture further showed that bacteria translocated to organs and blood in all animals with pancreatitis, and to pancreas in 87.5% of cases, 75% of them were *E.coli* JM109 colonized previously in the gut. These results provided substantial evidence that the gut was the primary source of pancreatic infection, and the translocation of the enteric overgrowing gramnegative germs in the gut, were the main pathogens of pancreatic infection.

The enteric microecologic dysbiosis following ANP might be explained by the overgrowth of gramnegative germs (mainly *E.coli*) and their inhibitory effect on the growth of dominant bacteria in gut such as bifidobacteria, resulting in the decreased colonization resistance and the immunity of host. This disturbance might lead to colonization of potential opportunistic pathogens and increase the chance of bacterial translocation. The intestinal epithelium was also injured by enteric ischemia and ischemia-reperfusion in ANP. In such circumstances, enteric bacteria which attached to and colonized on the surface of intestinal epithelium, could penetrate the mucosal barrier and translocate to MLN, other organs and blood, and caused infection in the pancreas which was seriously damaged by inflamation, hemorrhage and necrosis. The overgrowth of *E.coli* may also produce a large amount of LPS, becoming the source of endotoxemia following pancreatitis.

In conclusion, our data demonstrated that the enteric microecologic dysbiosis played an important role in the pathogenesis of infection complicating ANP. Taking effective measures to reduce the microecological disturbance and to protect the gut barrier function should be an important principle to prevent infection secondary to acute necrotizing pancreatitis.

REFERENCES

1 Bjornson HS. Pancreatic "abscess": diagnosis and management. *Pancreas*, 1991;6(s1):s31-s36
2 Frey CF, Bradley III EL, Beger HG, Rodriguez LF, Larocco MT, Miller TA. Progress in acute pancreatitis. *Surg Gynecol Obstet*, 1988;167(4):282-286
3 Runkel NSF, Moody FG, Smith GS. The role of the gut in the development of sepsis in acute pancreatitis. *J Surg Res*, 1991;51(1):18-23
4 Kazantsev GB, Hecht DW, Rao R, Fedorak IJ, Gattuso P, Thompson K. Plasmid labeling confirms bacterial translocation in acute pancreatitis. *Am J Surg*, 1994;167(1):201-207
5 Gianotti L, Munda R, Alexander JW, Tchervenkov JI, Babcock GF. Bacterial translocation: a potenial source for infection in acute pancreatitis. *Pancreas*, 1993;8(1):551-556

 ISSN 1007-9327 CN 14-1219/R WJG, 1998;4(3):246-248

Effect of Helicobacter pylori infection on gastric epithelial proliferation in progression from normal mucosa to gastriccarcinoma

LIU Wen-Zhong, ZHENG Xiong, SHI Yao, DONG Quan-Jiang and XIAO Shu-Dong

Subject headings helicobacter infections;gastric mucosa/microbiology; stomach neoplasms/microbiology; gastric mucosa/pathology

Abstract

AIM To study the effect of Helicobacter pylori (H. pylori) infection on gastric epithelial proliferation in the progression from normal mucosa to gastric carcinoma.

METHODS Gastric biopsy specimens from normal controls (*n*=11), superficial gastritis (*n*=32), atrophic gastritis with intestinal metaplasia (*n*=83), dysplasia (*n*=25) and gastric carcinoma (*n*=10) were studied by immunohistochemical stianing of proliferating cell nuclear antigen (PCNA).

RESULTS The gastric epithelial proliferation, expressed as PCNA labeling index (LI)%, was progressively increased in successive stages from normal mucosa to gastric carcinoma regardless of H. pylori status. There was significant difference in PCNA LI% among all groups ($P<0.01$). The analysis pursuing the effect of *H. pylori* infection on gastric epithelial proliferation in the progression from normal mucosa to gastriccarcinoma showed that in superficial gastritis and mild atrophic gastritis groups, PCNA LI% in *H. pylori* positive patients were 13.14±1.6 and 19.68±2.22 respectively, significantly higher than 6.95±0.78 and 11.34±1. 89 in *H. pylori* negative patients ($P<0.01$); but there was no such difference in other groups ($P>0.05$).

CONCLUSION *H. pylori* infection causes increased gastric epithelial proliferation in the stages of superficial and mild atrophic gastritis and may play a part in triggering gastric carcinogenesis.

Shanghai Second Medical University, Ren Ji Hospital, Shanghai Institute of Digestive Diseases, Shanghai 200001, China

LIU Wen Zhong, professor of internal medicine, gastroenterologist, having 30 papers published.

***Supported by the Shanghai Municipal Commission of Science and Technolog, No.954119023.**

Correspondence to: Dr. LIU Wen-Zhong, Shanghai Second Medical University, Ren Ji Hospital, Shanghai Institute of Digestive Diseases, Shanghai 200001, China

Tel. +86 • 21 • 63200874, Fax.+86 • 21 • 63730455

Received 1997-12-18

INTRODUCTION

Gastric carcinoma is one of the leading causes of malignancy-related death in China, and its etiology has not been fully elucidated. The epidemiological and histopathological studies have shown that *Helicobacter pylori* (*H. pylori*) infection is closely associated with gastric carcinogenesis[1-5]. However, the mechanism and the stages in which *H. pylori* participates in the process of gastric carcinogenesis are largely unknown. An increase in epithelial cell proliferation is one of the earliest mucosa changes in the development of gastric cancer, and may serve as a risk indicator for it[6,7]. The proliferation nuclear cell antigen (PCNA) expression is a reliable marker for evaluation of cell proliferation[8,9]. In this study, we used PCNA as a marker to investigate the effect of *H. pylori* infection on gastric epithelial proliferation in the progression from normal mucosa to gastric carcinoma.

MATERIALS AND METHODS

Subjects

Archival gastric biopsy specimens used in this study were randomly selected from those kept in the pathological department of Shanghai Institute of Digestive Diseases between January and December 1996. The specimens were taken from 161 subjects, and the diagnosis was made based on the endoscopic and histological findings. Subjects were assigned to one of the following five study groups according to the histological diagnosis: Group 1, normal gastric mucosa, *H. pylori* negative; group 2, chronic superficial gastritis; group 3, chronic atrophic gastrits with intestinal metaplasia; group 4, dysplasia; and group 5, gastric carcinoma (intestinal type). The atrophy and intestinal metaplasia in gastric mucosa were graded as mild, moderate and severe respectively according to the criteria proposed in Sydney system, and scored 1, 2 and 3. Atrophic gastritis was usually accompanied by intestinal metaplasia, so the scores of atrophy and intestinal metaplasia in each patient were added up, and then further classified as mild for total score equal or less than 2, moderate for scores 3-4, and severe for scores more than 4. The patients with chronic gastritis accompanied by dysplasia all belonged to group 4.

PCNA staining

PCNA staining of antral biopsy specimens was performed using immunohistochemial ABC method. Briefly, PCNA staining was proceeded, after deparaffinizing in xylene, clearing in ethanol, rehydrating through graded ethanol and washing in PBS. Endogenous peroxidase was blocked by 0.3% H2O2, and then washed slightly in PBS. The sections were preincubated with diluted normal goat serum, and then incubated with anti-PCNA antibody (PC10, mouse anti-human, DAKO Company) diluted 1:80 at 4℃ overnight. After draining, the sections were incubated with a biotinylated anti-mouse IgG diluted 1:50 for 60min, then incubated with ABC working solution for 30min according to manufaturer's instruction (Sino-American Biotechnology Company). After another washing, the sections were incubated with 3-3'diaminobenzidine tetrahydrochloride (DAB) solution under microscopic monitoring, and then counterstained with hematoxylin. The stained PCNA positive tissue (gastric polyp) sections served as positive controls. A negative control, where primary antibody was replaced by PBS, was also stained parallelly.

Analysis of gastric epithelial proliferative activity

PCNA positive cells were counted only in well oriented sections with visible entrire gastric pits. A mean number of 10 pits were examined for each specimen, and greater than 500 cells were analysed. Labeling index per cent (LI%) was measured by counting the percentage of the number of PCNA positive cells of the total number of cells.

Identification of H. pylori infection

H. pylori was detected under microscopy on the histological sections stained with a modified Giemsa staining method.

Statistical analysis

LI% was compare among groups, and the significance was analysed using Student' *t* test for unpaired data, *P* values less than 0.05 were considered statistically significant.

RESULTS

Table 1 shows the demographic profileand *H. pylori* status in 161 subjects. Figure 1 shows PCNA LI% in the study groups regardless of *H. pylori* status. PCNA LI% in normal gastric mucosa, superficial gatritis, atrophic gastritis, dysplasia and gastric carcinoma group was 6.31±1.67 ($\bar{x}$±*s*), 10.04±1.32, 17.11±2.55, 32.46±4.16 and 46.05±4.63, respectively. PCNA LI% was progressively increased from normal mucosa to gastric carcinoma, and there was significant difference between the groups (P<0.01).

Table 1 The demographic profile and *H. pylori* status in 161 subjects

Study groups	No. of patients	Femal/ male	Average ages(yrs)	No. of Hp positive	No. of Hp negative
Normal gastric mucosa	11	2/9	44.5	0	11
Superficial gastritis	32	10/22	43.6	16	16
Atrophic gastritis					
Mild	32	11/21	42.1	16	16
Moderate	26	11/15	51.0	15	11
Severe	25	8/17	56.1	10	15
Dysplasia	25	7/18	53.2	13	12
Gastric Carcinoma	10	3/7	66.2	5	5

Figure 2 shows the PCNA LI% in the groups associated with *H. pylori* status. Atrophic gastritis group was further classified into mild, moderate and severe subgroups based on the scores of atrophy and intestinal metaplasia. In superficial gastritis and mild atrophic gastritis groups, PCNA LI% in *H. pylori* positive patients was 13.14±1.6 and 19.68±2.22 respectively, significantly higher than 6.95±0.78 and 11.34±1.89 in *H. pylori* negative patients (P<0.01); but there was no such difference in other groups (P>0.05).

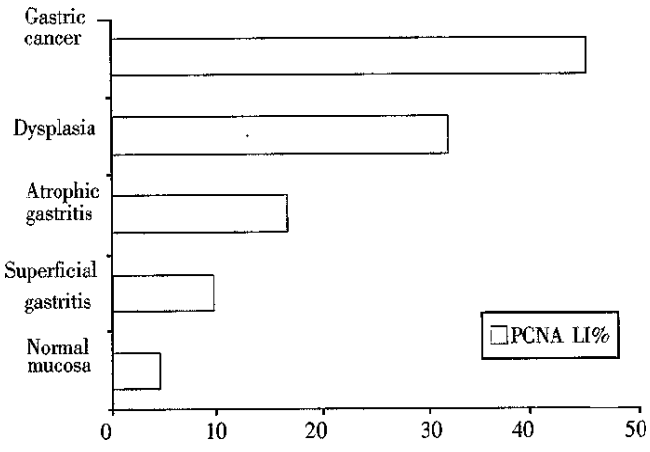

Figure 1 PCNA LI% in thestudy groups from normal gastric mucosa to gastric carcinoma regardless of *H. pylori status.*

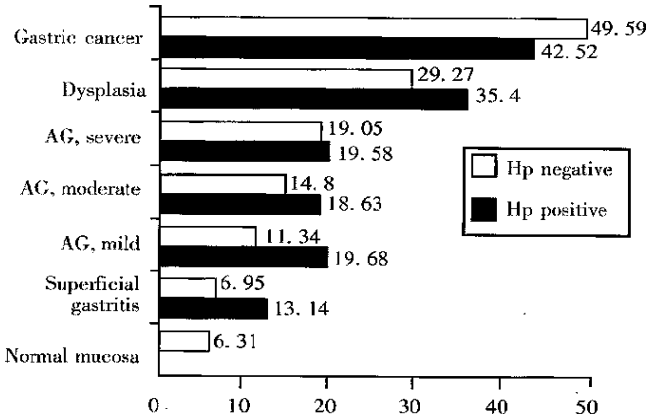

Figure 2 PCNA LI% in study groups associated with *H. pylori* status from normal mucosa to gastric carcinoma. AG=atrophic gastritis.

DISCUSSION

The etiology of gastric carcinoma has not been fully elucidated. In 1988, Correa[10] proposed a human model of gastric carcinogenesis based on the epidemiological, pathological and clinical findings. He postulated that gastric cancer develops through a complex sequence of events from normal to superficial gastritis, atrophic gastritis, intestinal metaplasia, dysplasia and finally to intestinal type gastric carcinoma, and that the chronic gastritis in the first step in the progression to malignancy. This postulation was proved correct later by several studies[11,12].

H. pylori is the primary etiological cause of chronic gastritis[13,14], and is associated with a sixfold increased risk of gastric carcinoma[2]. Long-term studies of *H. pylori* infection have provided evidence of a progression from *H. pylori* gastritis to atrophic gastritis, intestinal metaplasia, and dysplasia. *H. pylori* has been listed by the WHO as class 1 carcinogen for gastric cancer. But the exact mechanisms that *H. pylori* participates in gastric carcinogenesis are not clear.

Excessive cell proliferation increases the chance of spontaneous error of DNA replication, and potentiates the action of any carcinogen targetting DNA, and therby enhences the risk of neoplastic transformation of cells[15]. The assessment of epithelial cell proliferation as an indicator of risk has been validated in gastric carcinoma, even before *H. pylori* was found to be associated with chronic gastritis[6]. Several recent studies have shown that *H. pylori* infection can promote gastric epithelial proliferation[16,17] so that *H. pylori* infection links to increased risks of gastric carcinogenesis. But few studies have pursued the effect of *H. pylori* infection on gastric epithelial proliferation in the progression from normal mucosa to gastric carcinoma[18].

Our results showed that gastric epithelial proliferative activity expressed as PCNA LI% increased progressively from normal mucosa to superficial gastritis, atrophic gastritis, dysplasia and gastric carcinoma, suggesting that increased gastric epithelial proliferation is associated with gastric precancerous changes and gastric cancer, and can be used as an indicator for evaluating the risk of gastric carcinogenesis.

The analysis of the effect of *H. pylori* infection on gastric epithelial proliferation in progression from normal mucosa to gastric carcinoma indicated that the increase in gastric epithelial proliferation associated with *H. pylori* infection was only seen in superficial gastritis and mild atrophic gastritis, and in other groups, there was no significant difference in PCNA LI% between *H. pylori* positive and negative patients. The results suggested that *H. pylori* infection causes increased gastric epithelial proliferation primarily in the stages of superficial and mild atrophic gastritis, and it may not have so strong influence in the late stages of gastric carcinogenesis. There, *H. pylori* infection may be the precipitating factor in triggering gastric carcinogenesis.

Once *H. pylori* gastritis develops to the stage of gastric atrophy, the gastric acid secretion will decrease markedly, leading to changes in gastric bacterial flora, and subsequently promoted the endogenous formation of carcinogenic N-nitrosocompounds[19,20], and gastric epithelial proliferation. This may explain why *H. pylori* infection has less effect on gastric epithelial proliferation in late stages of gastric carcinogenesis.

REFERENCES

1 Forman D, Newell, DG, Fullerton F, Yarnell JWG, Stacey AR, Wald N *et al.* Association between infection with Helicobacter pylori and risk of gastric cancer: evidence from a prospective investigation. *BMJ,* 1991;302(6788):1302-1305
2 Eurogast Study Group. An international association between Helicobacter pylori infection and gastric cancer. *Lancet,* 1993;341(8857):1359-1362
3 Parsonnett J, Friedman GD, Vandersteen DP, Chang Y, Vogelman JH, Orentreich N *et al.* Helicobacter pylori infection and risk of gastric cancer. *N Engl J Med,* 1991;325(16):1127-1131
4 Craanen ME, Blok P, Dekker W, Tytgat GNJ. Helicobacter pylori and early gastric cancer. *Gut,*1994;35(10):1372-1374
5 Aska M, Kimura T, Kato M, Kudo M, Miki K, Ogoshi K *et al.* Possible role of Helicobacter pylori infection in early gastric cancer development. *Cancer,* 1994;73(11):2691-2694
6 Xu YL, Zheng ZT. Cell proliferation kinetics in chronic gastritis and gastric cancer. *Chin Med J,* 1984; 97(8): 526-532
7 Lipkin M. Biomarkers of increased susceptibility to gastrointestinal cancer: new application to studies of cancer prevention in human subjects subjects. *Cancer Res,*1988; 48(2):235-245
8 Hall PA, leivison Da, Woods AL, Yu CC, Kellock DB, Watkins JA *et al.* Proliferating cell nuclear antigen (PCNA) immunolocalization in some neoplasia. *J Pathol,* 1990;162(4):285-294
9 Yamada K, Yoshitaka K, Sato M and Ahnen DJ *et al.* Proliferating cell nuclear antigen in normal, and colonic epithelium in the rat. *Gastroenterology,* 1992; 103(1):160-167
10 Correa P. A human model of gastric carcinogenesis. *Cancer Res,* 1988;48(13): 3554-3560
11 Correa P. A human model of gastric carcinogenesis. *Cancer Res,* 1988;48(13): 3554-350
12 Correa P, Haenszel W, Cuello C, Zavala D, Fonthanm E, Zarama G *et al.* Gastric precancerous process in a high risk population: Cohort follow-up. *Cancer Res,* 1990;50(15):4737-4740
13 Jiang SJ, Liu WZ, Zhang DZ, Shi Y, Xiao SD, Zhang ZH. Campylobacter-like organisms in chronic gastritis, peptic ulcer and gastric carcinoma. *Scand J Gastroenterol,* 1987;22(6):553-555
14 Wyatt JI. Histopathology of gastroduodenal inflammation: The impact of Helicobacter pylori. *Histopathology,* 1995;26(1):1-15
15 Ames BN, Gold LS. Too many rodent carcinogens: Mitogenesis increases mutagenesis. *Science,* 1990;249(4970):970-971
16 Fan XG, Kelleher D, Fan XJ, Xia HX, Keeling PWN. Helicobacter pylori increases proliferation of gastric epithelial cells. *Gut,* 1996;38(1):19-22
17 Lynch DAF, Mapstone NP, Clarke AMT, Sobala GM, Jackson P, Morrison L et al. Cell proliferation in Helicobacter pylori associated gastritis and the effect of eradication therapy. *Gut,* 1995;36(3):346-350
18 Cahill RJ, Kilgallen C, Beattie S, Hamilton H, O'Morain C *et al.* Gastricepithelial cell kinetics in the progression from normal mucosa to gastric carcinoma. *Gut,* 1996;(2)28:177-181
19 Correa P. Helicobacter pylori and gastric carcinogenesis. *Am J Surg Pathol,* 1995;19(suppl 1):S37-43
20 Sobala GM, Pignatelli B, Schorah CJ, BartschH, Sanderson M, Dixon MF *et al.* Levels of nitrite, nitrate, nitroso compound, asocrbic and total bile acids in gastric juice of patients with and without precancerous conditions of the stomach. *Carcinogenesis,* 1991;12(2):193-198

Serum IgG response to differentiated antigens of Helicobacter pylori

HUA Jie-Song[1], KHIN Mar Mar[1], ZHENG Peng-Yuan[1], YEOH Khay-Guan[2], Ng Han Chong[1] and HO Bow[1]

Subject headings Helicobacter pylori; spiral form;coccoid form; ELISA; helicobacter pylori infection;helicobacter pylori;antigens, bacterial; IgG; antigens,differentiation; antigen-antibody reactions; stomach ulcer; sotamach neoplasms; gastritis

Abstract

AIM To detect antibodies against Helicobacter pylori spiral and coccoid antigens in human sera.

METHODS Blood samples were collected from 278 patients with gastric diseases. A 3-day-old culture of H. pylori on chocolate blood agar was used to providespiral form. 'Synchronous' coccoids were cultured in (BHY) (brain heart infusion supplemented with 10% horse serum and 0.4% yeast extract) medium in a chemostat. Antigens from spiral and coccoid form were prepared using acid glycine extraction. Enzyme-linked immunosorbent assay (ELISA) was performed to detect serum IgG antibodies against spiral and coccoid forms of *H. pylori*.

RESULTS Seroprevalence of *H. pylori* infection was higher in patients with gastric ulcer (79%) and gastric cancer (83%) than those with non-ulcer dyspepsia (NUD)(44%) and other diseases (45%) ($P<0.05$). IgG antibodies against spiral and coccoid antigens were detected in 50.7% (141/278) and 49.6% (138/278), respectively.

CONCLUSION The spiral and coccoid forms of *H. pylori* coexist in patients infected with the bacterium.

Department of Microbiology1, Department of Medicine2, National University of Singapore, Lower Kent Ridge Road, Singapore 119074, Republic of Singapore

Dr. HUA Jie Song, male, born on 1961-11-16, in Shanghai, graduated from Shanghai Medical University as bachelor in 1985 and master in 1991. Having 20 papers published.

Correspondence to: Dr. HUA Jie Song, Department of Microbiology, National University of Singapore, Singapore 119074, Republic of Singapore.

Tel. +65 • 8743285, E-mail:michob@nus.edu.sg

Received 1998-04-25

INTRODUCTION

It was reported that *Helicobacter pylori* can convert to coccoid form from spiral form *in vitro* after prolonged incubation[1] or under antibiotic stress [2]. By histological examination, Chan *et al*[3] and Janas *et al*[4] observed two morphological forms of the bacteria in *H. pylori*-positive gastric specimens. The dimorphism of *H. pylori* has stimulated researchers to investigate whether coccoid form of *H. pylori* is viable and pathogenic[1,5,6]. Coccoid form like its spiral form has similar proteins except that a high-molecular-mass antigenic fraction (>94kDa), absent in spiral forms, was detected during coccoid conversion[6] and that a smaller number of immunoreactive bands were recognized in the coccoid antigens compared with the spiral antigens [5]. In this study, we used ELISA technique to detect immune response of IgG to spiral and coccoid antigens.

MATERIALS AND METHODS

Serum specimens

Blood samples were collected from 278 patients with gastric disorders at the National University Hospital, Singapore. Informed consent was obtained from all the patients. After collection, blood specimens were allowed to clot at room temperature for 36mins-60mins. The sera were removed from the clot and any remaining insoluble material removed by centrifugation at 2 000×g for 10min at 4℃. Sera were stored at -20℃ until use.

Antigen preparation

A local *H. pylori* strain V2 isolated from a patient with non-ulcer dyspepsia was used. A 3-day-old culture of *H. pylori* on chocolate blood agar was used to provide spiral form. 'Synchronous' coccoids were cultured in BHY (brain heart infusion supplemented with 10% horse serum and 0.4% yeast extract) medium in a chemostat. Antigens from spiral and coccoid form were prepared according to a modified method of Goodwin *et al*[7] as described by Vijayakumari *et al*[5].

Enzyme-linked immunosorbent assay (ELISA)

ELISA was performed according to the method described previously[8]. Briefly, flat-bottomed microtitre plates (Nunc) were coated with acid

glycine extract antigens of *H. pylori*. The sera tested were diluted at 1:100. Each diluted serum was examined in triplicate. Positive control serum was diluted at 1:100, 1:200, 1:400, 1:800, 1:1 600 and 1:3 200 and negative control serum at 1:100. Horse radish peroxidase-labelled rabbit anti-human IgG (Dako) was used as conjugates. The substrate used was ophenylenediamine dihydrochloride (OPD, Sigma). The optical density at wavelength 490 and 620nm reference filter was read immediately using an ELISA reader (Ceres 900 Bio-Tek Instruments, Inc). The cut-off value for the ELISA was derived according to Khin and Ho[8].

RESULTS

Seroprevalence of *H. pylori* infection was higher in patients with gastric ulcer (79%) and gastric cancer (83%) than those with non-ulcer dyspepsia (NUD) (44%) and other diseases (45%) ($P<0.05$). Furthermore, of the 278 sera, IgG antibodies against NCTC 11637 spiral and coccoid antigens were detected in 141 (50.7%) cases and 138 (49.6%) cases.

In 191 NUD patients, 84 (43.9%) and 86 (45.0%) were detected with IgG antibodies to spiral and coccoid antigens, respectively. There was no significant difference in seroreactivity to spiral and coccoid antigens in patients with NUD ($P>0.05$) (Figure 1).

Of the 47 peptic ulcer patients, 37 (78.7% and 33 (70.2%) showed antibodies IgG against spiral and coccoid antigens ($P>0.05$). Among the peptic ulcer patients, 69.2% (9/13) and 76. 9% (10/13) of the gastric ulcer patients while 82.1% (23/28) and 67.9% (19/28) were positive for spiral and coccoid antigens, respectively. Serum IgG antibodies against spiral antigens were detected in 83.3% (5/ 6) patients with both gastric and duodenal ulcer, while 66.7% (4/6) of these were seropositive for IgG antibodies against coccoid antigens (Figure 1).

Of the 6 cases of gastric cancer antibodies IgG 5 (83.3%) cases were positive with IgG antibodies to spiral antigens and 2 (33%) cases were positive with IgG antibodies to coccoid antigens. No statistical difference was found in IgG antibodies against spiral and coccoid for antigens in this group ($P>0.05$) (Figure 1).

Of the 34 cases of other diseases, there was 45. 4% (15/33) and 51.5% (17/33) had positive seroreactivity against *H. pylori spiral* and coccoid antigens respectively. There was no significant difference ($P>0.05$) (Figure 1).

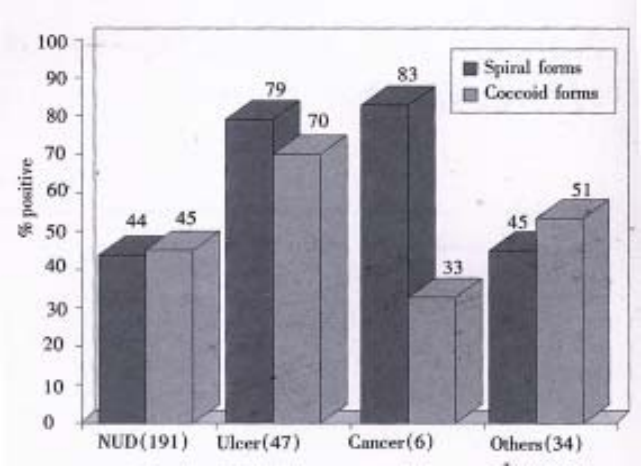

Figure 1 Prevalence of antibodies against *H. pylori* spiral and coccoid antigens in patients with different gastric diseases.

DISCUSSION

Most adult patients colonized with *H. pylori* elicit a measurable systemic antibody response which comprises predominantly IgG. In this study, the systemic immune response of 278 sera was examined by ELISA. IgG to *H. pylori* spiral and coccoid antigens was found to be 50.7% and 49.6%, respectively. The serological response to both spiral and coccoid antigens indicates the possibility of coexistence of two forms of *H. pylori* in these patients which leads to the production of similar IgG responses in patients. It has been shown earlier that there were differences in protein profiles of spiral and coccoid antigens[6]. *in vitro,* coccoid form could be detected 6 hours after exposure to 10ng/L of amoxycillin[2]. Janas *et al*[4] reported the presence of two different morphological forms of *H. pylori* in gastric antrum specimens. Could these two morphological forms of spiral and coccoid of *H. pylori* be the complete cell cycle *in vivo* The morphological changes could have been triggered under physical or chemical stress which is unfavourable to *H. pylori*. Spiral form may then convert into coccoid form. When the environment becomes favourable, the bacteria may revert from coccoid form to spiral form *in vivo*. However, what could have led to the revision is still unknown. Some *in vitro* studies indicated that coccoid form of *H. pylori* might be viable[1,9-11]. Furthermore, Vijayakumari *et al*[5] showed that the adherence patterns of coccoid form of *H. pylori* on kato III *in vitro* were similar to those observed with spiral form in gastric biopsy specimens *in vivo*. It was reported that the vital cytotoxic proteins of spiral forms were also conserved in the coccoids[6]. Therefore, like its counterpart, coccoid form could be an infective, transmissible, immunogenic and pathogenic form of *H. pylori* which participates in

the pathogenesis of gastroduodenal diseases.

The coccoid form was present above damaged epithelial cells[4] and is not easy to be detected by the techniques now being used. Patients with morphological conversion of *H. pylori* from spiral to coccoid form after treatment may be neglected and considered as eradication of *H. pylori*. The possible cell cycle of *H. pylori* may have clinical relevance. Xia *et al*[12] reported that recurrence of *H. pylori* infection was probably caused by recrudescence in the patients studied. One possible reason of relapse could be morphological reversion of *H. pylori* form coccoid from to spiral form after treatment.

This study demonstrated the presence of antibodies to different antigens of *H. pylori* in patients. Coccoid form like its counterpart spiral form may have clinical relevance in the outcome of gastric diseases.

REFERENCES

1 Hua J, Ho B. Is the coccoid form of *Helicobacter pylori viable Microbioscience,* 1996;87:103-112

2 Berry V, Jennings K, Woodnutt G. Bactericidal and morphological effects of Amoxicillin on Helicobacter pylori. *Antimicrob Agents Chemother,* 1995;39: 1859-1861

3 Chan W. Y., Hui P. K., Leung K. M. and Thomas T. M. M. Modes of Helicobacter colonization and gastric epithelial damage. *Histopathology,* 1992;21:521-528

4 Jans B, Czkwianianc E, Bak Romaniszyn L, Bartel H, Tosik D, Ptaneta-Malecka I. Electro microscopic study of association between coccoid forms of Helicobacter pylori and gastric epithelial cells. *Am J Gastroenterol,* 1995; 90:1829-1833

5 Vijayakumari S, Khin MM, Jiang B, Ho B. The pathogenic role of the coccoid form of Helicobacter pylori. *Cytobioscience,* 1995;82:251-260

6 Benaissa M, Babin P, Quellard N, Pezennec L, Cenatiempo Y, Fauchere JL. Changes in Helicobacter pylori ultrastructure and antigens during conversion from the bacillary to the coccoid form. *Infect Immun,* 1996;64:2331-2335

7 Goodwin CS, Blincow E, Peterson G, Sanderson C, Cheng W, Marshall BJ, Warren JR, McCulloch R. Enzyme-liked immunosorbant assay for Campylobacter pyloridis: correlation with presence of C. pyloridis in the gastric mucosa. *J Infect Dis,* 1987;155:488-494

8 Khin MM, Ho B. Immunological detection of Helicobacter pylori pregnant woman. *Biomedical Letters*, 1994;52:71-78

9 Mai U, Geis G, Leying H, Ruhl G, Opferkuch S. Dimorphism of Campylobacter pylori. In: Megraud F, Lamouliatee H, eds. Gastroduodenal pathology and *Campylobacter pylori*. Amsterdam: *Elsevier Science,* 1989:29-33

10 Bode G, Mauch F, Malfertheiner P. The coccoid forms of Helicobacter pylori. Criteria for their viability. *Epidemiol Infect,* 1993;111:483-490

11 Sorber M, Nilsson M, Hanberger H, Nilsson LE. Morphologic conversion of Helicobacter pylori from bacillary to coccoid form. *Eur J Clin Microbiol Infect Dis,* 1996;15:216-221

12 Xia HX, Windle HJ, Marshall DG, Smyth CJ, Keane CT, O'Morain CA. Recrudescence of Helicobacter pylori after apparently successful eradication:novel application of randomly amplified polymorphic DNA fingerprinting. *Gut,* 1995;37:30-34

 ISSN 1007-9327 CN 14-1219/R WJG, 1998;4(3):252-255

In vitro production of TNFα, IL-6 and sIL-2R in Chinese patients with ulcerative colitis *

XIA Bing[1], GUO Hai-Jian[1], JBA Crusius[2], DENG Chang-Sheng[1], SGM Meuwissen and AS Pena[2]

Subject headings tumor necrosis factor alpha; interleukin 6; interleukin 2, receptor; colitis, ulcerative

Abstract

AIM To determine the tumor necrosis factor alpha (TNFα), interleukin 6 (IL-6) and soluble interleukin 2 receptor (sIL-2r) from peripheral blood mononuclear cells (PBMC) in 25 Chinese patients with ulcerative colitis and 20 healthy controls.

METHODS PBMC were isolated by density gradient centrifugation of heparinized blood and cultures for 24 or 48 hours by stimulation with LPS or PHA. TNFα and sIL-2r were measured by ELISA method and IL-6 measured by biossay.

RESULTS TNFα production stimulated by LPS and sIL-2r production by PHA in ulcerative colitis were significantly lower than in healthy controls (TNFα 509(46-7244)ng/L vs 1995(117-18 950)ng/L, $P<0.05$; sIL-2r 320U/ml±165U/ml *vs* 451U/ml±247U/ml, $P<0.05$). Spontaneous TNFα and sIL-2r production were not significantly different between ulcerative colitis and controls (TNFα 304(46-7044) ng/L *vs* 215(46-4009)ng/L, $P>0.05$; sIL-2r 264U/ml±115U/ml *vs* 236U/ml±139U/ml, $P>0.05$). IL-6 production by spontaneous release from PBMC in ulcerative colitis group was 109U/ml±94U/ml *vs* 44U/ml±39U/ml for those in healthy controls, $P<0.01$. IL-6 stimulated by LPS in ulcerative colitis group was (261U/ml±80U/ml) higher than in healthy controls (102U/ml±54U/ml, $P<0.01$). No correlation of TNFα, IL-6, sIL-2r production was found to disease activity, disease location and medication.

CONCLUSION Cytokine production from PBMC was also disturbed in Chinese patients with ulcerative colitis.

1Department of Gastroenterology, The Second Hospital of Hubei Medical University, Wuhan 430071, China

2Department of Gastroenterology, Free University Hospital, Amsterdam, The Netherlands XIA Bing, MD, graduated from Department of Medicine in Hubei Medical University, associate professor of internal medicine, having 56 papers published.

***Project supported by IBD cooperative study between the Second Affiliated Hospital of Hubei Medical University and Free University Hospital of Amsterdam.**

Correspondence to: Dr. XIA Bing, Department of Gastroenterology, The Second Hospital of Hubei Medical University, Wuhan 430071, China

Tel. +86 • 27 • 7824243-3045, Fax. +86 • 27 • 7307622

Received 1997-04-18 **Revised** 1997-05-05

INTRODUCTION

Ulcerative colitis (UC) is a chronic inflammatory bowel disease (IBD). Its etiology is still unknown so far. Immunological abnormality demonstrated in IBD patients and imbalance between proinflammatory cytokines and anti-inflammatory cytokines play an important role in the initiation and regulation of the immune responses[1,2]. Tumor necrosis factor alpha (TNFα) produced by activated mononuclear cells is a potent proinflammatory and immunoregulatory cytokine[3]. It was named TNF at beginning because of its cytotoxic and anti-tumor activities[4]. Now it is known to have a wide spectrum of importance in IBD, e.g., TNF antibodies have been successfully used for treatment of Crohn's disease[5].

IL-6 is produced by a variety of cells, such as monocytes, macrophages, T lymphocytes, B lymphocytes, fibroblasts, endothelial cells, etc. It may affect the proliferation of epithelial cells and act as an autocrine growth factor for enterocytes[6,7]. It has been shown to stimulate T cell and B cell activation and proliferation[8-10], and to increase immunoglobulin synthesis from epithelium of human intestine[11,12]. It is interesting to know that IL-6 has been proposed as a marker of inflammation in IBD and its concentration was elevated in serum, peripheral blood mononuclear cells (PBMC), mucosa biopsy and lamine propria mononuclear cells (LPMC) in IBD patients[13-16]. Some papers also show that IL-6 is increased in the systemic circulation in Crohn's disease and is not elevated in UC patients[17].

Soluble interleukin-2 receptor (sIL-2r) is one form of IL-2 receptor secreted by activated T cells and other monocytes[18]. It corresponds to the "Tac" antigen (alpha chain) and could bind IL-2, and then participate in the regulation of IL-2 mediated lymphocyte activation[19,20]. Recent studies reported that sIL-2r was increased in vivo and in vitro in active IBD patients and may be an index for IBD activity[21-23]. The present study was to determine in vitro production of TNFα, IL-6 and sIL-2r in PBMC in Chinese UC patients and analyze the relation of these three cytokine production from PBMC to disease activity, location and medication.

MATERIALS AND METHODS

Patients

Twenty-five patients with UC were studied (13 male,

12 females; mean age 43 and range 23-67 years). Diagnosis of UC was based on the conventional clinical, radiological, endoscopical and pathological criteria designed by Lennard-Jones[24]. Assessment of its activity followed Sutherland's score criteria [25]. Of 25 patients, 7 patients had Sutherland's scores 1-4, 12 had scores 5-8, and 6 patients 9-12; 3 patients had proctitis, 14 left-sided colitis, 8 total colitis; 16 patients were on oral sulphasalazine (SASP) treatment (2 patients were being treated with corticosteroid), 8 patients were on Chinese medicine and one patient was treated with metronidazole.

Twenty healthy volunteers served as controls (9 male, 11 females; mean age 37 and range 21-66 years). There is no statistical difference in age and sex between these two groups.

Laboratory methods

From each patient, five ml of heparinized blood were collected. Vials were coated and PBMC isolated within two hours after blood collection.

Stimulation of PBMC PBMC were isolated by density gradient centrifugation of heparinized blood and washed three times with Hank's balanced salt solution (without Ca^{++} and Mg^{++}). After washing, cells were suspended in RPMI 1640(GIBCO) with 15% fetal calf serum (GIBCO), 2mM L-glutamine, 100U/ml penicillin and 100 μg/ml streptomycin. The isolated cells were cultured for 24 hours (for TNFα and IL-6 determination) or 48 hours (for sIL-2r determination) at 37℃ under 5% CO2 and 100% humidified air in small sterile culture flasks in 2ml culture medium at a concentration of 1×10^6/ml. The cells were cultured in the presence of 100mg/L of LPS (SIGMA) for TNFα and IL-6 stimulation production, and in the presence of 200mg/L PHA (SIGMA) for sIL-2r stimulation production. For spontaneous production of these cytokines, no stimulators were added in cell culture medians. After culturing, cell culture supernatant was harvested, added 1mmol/ml PMSF, aliquoted and stored at -30℃ until assay. Viability was determined using 3% trypan blue. Only more than 95% viable cells were used in this study.

TNFα measurement TNFα was determined using specific TNFα ELISA kit (Beijing Biotin Biomedicine Co.). In brief, 100μl/well TNFα standard markers and supernatant samples (in duplicate) were added into immunoplates and incubated for 2 hours at 20℃ and washed three times with 0.01M PBS (pH 7.4) and 0.05% Tween 20. The plates were subsequently incubated with 100 μl/well horseradish labelled polyclonal rabbit-anti-TNFα (1:1 000) for 1 hour and washed three times with 0.01M PBS (pH 7.4) and 0.05% Tween 20. Then 100 μl/well substrate Ophenylenediamine added. Incubation was allowed for 15 minutes in the dark at room temperature. The reaction was stopped by 50 μl/well 2 M H2SO4 solution. Absorption was read at 492nm on ELISA reader. A standard curve was drawn according to OD values of TNFα markers. TNFα concentration of each sample was read to its OD value within standard curve and expressed as ng/L.

IL-6 bioassay The IL-6 bioassay was performed using the IL-6 dependent cell line B9 according to Hou[26]. Briefly, each 100 μl of different samples and standard recombinant human IL-6 was added into 96 well microtitration plate (CORNING). Meanwhile, the IL-6 dependent cell line B9 cells were suspended in RPMI 1640 containing 10% fetal calf serum (GIBCO) and regulated at a concentration of 5×10^4 cells/ml. Each 100 μl/ml of the cells were added into the plate and cultured at 37℃ in 5% CO2 for 68 hours. Ten μl/well of 5g/L methyl thiazolyl tetrazolium blue (MTT, FLUKA) was added. The culture was continued for another 4 hours. Absorption value was read at 570nm on an automatic ELISA Reader and represented B9 cell proliferation. The concentration of IL-6 in a supernatant sample was calculated as follows: IL-6(U/ml)=the diluted concentration of supernatant of giving rise to half maximal proliferation of B9 cells × standard IL-6 activity (100U/ml) ÷ the diluted concentration of standard IL-6 giving rise to half maximal proliferation of B9 cells.

sIL-2r measurement sIL-2r concentration in supernatants from 48-hour culture of PBMC with or without PHA stimulation was determined using specific sIL-2r ELISA kit (Beijing Biotin Biomedicine Co.). In brief, 48-well plate was coated with monoclonal anti-IL-2r alpha antibody and blocked with 1% BSA in PBS. IL-2r markers and samples (in duplicate) were added, and incubated for 2 hours at 37℃. After washing three times with 0.01M PBS (pH 7.4) and Tween 20, 100 μl/well horseradish labelled polyclonal rabbit-anti-IL-2r alpha antibody (1:40) was added and incubated at 37℃ for one hour and a half, then washed three times, and added substrate Ophenylenediamine for 30 minutes at room temperature. The reaction stopped with 50 μl of 2M H2SO4. The absorption was read at 490nm on a ELISA reader. sIL-2r concentration was expressed as U/ml.

Statistical analysis

All values were transformed by log transformation.

Then *t* test was used for comparison of TNFα, IL-6 and sIL-2r between UC and healthy control groups. Relations of TNFα, IL-6 and sIL-2r production to disease activity, disease location and medication were analyzed by linear correlation. *P* value less than 0.05 was considered statistically significant.

RESULTS

TNFα, IL-6 and sIL-2r production The spontaneous and stimulated TNFα, IL-6 and sIL-2r production are shown in Table 1. TNFα production stimulated with LPS and sIL-2r production by PHA in UC group was significantly lower than that in healthy control group. Spontaneous TNFα and spontaneous sIL-2r production were not different significantly between UC and control groups. Large inter individual differences were observed in TNFα production. However, both spontaneous and stimulated IL-6 production in UC group were significantly higher than those in healthy controls.

Linear correlation of TNFα, Il-6 and sIL-2r production from PBMC to disease activity, location and medication No significant correlation was found between TNFα, IL-6 and sIL-2r production and disease activity, disease location and medication, but a tendency of correlation was shown between spontaneous IL-6 production and disease activity (r = 0.37) and medication (r = 0.38).

Table 1 Spontaneous and stimulated production of TNFα, IL-6 and sIL-2r from PBMC

	UC (*n* = 25)	HC (*n* = 20)
TNFα (spontaneous) ng/L	304(46-7044)	215(46-4009)
TNFα (stimulated) ng/L	509(46-7244)*	1995(117-18950)
IL-6 (spontaneous) U/ml	109±94*	44±39
IL-6 (stimulated) U/ml	261±80*	102±54s
IL-2r (spontaneous) U/ml	264±115	236±139
sIL-2r (stimulated) U/ml	320±165*	451±247*

P<0.05. Median values shown in TNFα, range in brackets; Mean values with standard diviation shown in IL-6 and sIL-2r; HC: heathy controls.

DISCUSSION

In this study there was a marked decrease in LPS stimulated release of TNFα and a significant decrease in PHA stimulated release of sIL-2r by PBMC from patients with UC as compared with healthy controls. No significant difference was found in spontaneous release of TNFα or sIL-2r by PBMC between these two groups. Our study also showed that both spontaneous and stimulated IL-6 production was increased from PBMC as compared to healthy controls. These implied that the release of TNFα, IL-6 and sIL-2r by activated PBMC may not always be paralleled.

IL-1β, TNFα and IL-6 are three important proinflammatory cytokines which respond to the initial stimulation. Many studies on TNFα production in UC have been reported with a different results[27-31]. Our previous study in Dutch population showed a tendency towards lower TNFα production in PBMC from UC patients[32]. The present study in Chinese UC patients confirmed this result. A large inter-difference was observed in TNFα production in Chinese UC patients.

Several studies have shown that IL-6 concentration is increased in active IBD and may be an index of disease activity[13-16]. Our study confirmed these observations, but only a tendency of correlation between spontaneous IL-6 concentration and disease activity was found in UC patients. The explanation may be that, the patients with mild inflammation often take maintenance dose of SASP or no medicine, only the patients with severe diseases were administered with high dose of SASP and corticosteroid. The latter medicine may have an inhibiting effect on immune reaction of the body. Our data also showed that IL-6 had norelation to the disease location. These results suggested that IL-6 from PBMC may reflect the active stage of the disease.

sIL-2r concentrations were increased in serum, tissue homogenates and PBMC from IBD patients, especially in Crohn's disease[20-22]. However, Schreiber *et al* reported a moderately increased spontaneous release of sIL-2r and significantly less sIL-2r secretion stimulated by pokeweed mitogen in 14 days culture of colonic LPMC from UC patients[33]. Our study had a similar result that wIL-2r concentration was silightly higher in spontaneous release from PBMC in UC patients than in healthy controls. When PBMC were cultured with PHA only for 48 hours, less release of sIL-2r was observed in UC group than in healthy controls.

PBMC is a very heterogeneous cell population. Macrophages and T cells may be mostly responsible for release of these three cytokines. The circulatary changes of proinflammatory cytokines may reflect the original status for cytokine secretion. For this reason, studies on local tissue production of cytokines are more accurate and more exact than studies on circulation. The changes of the proinflammatory cytokines may also reflect different genetic background. Our previous study showed in Dutch population TNF gene polymorphisms are present in five combinations[34] and TNFα production is associated with TNF haplotypes. These data strongly supported the concept that a different immunogenetic background may determine the degree of the immune response in IBD.

Our findings showed that TNFα, sIL-2r in vitro production were reduced and IL-6 was increased

from PBMC activation in Chinese UC patients. Further study is necessary to confirm these in vitro findings to in vivo conditions. Studies at local intestinal level should be undertaken in order to assess the significance of the cytokine dysregulation in the inflammatory response.

REFERENCES

1 McCabe RP, Dean P, Elson CO. Immunology of inflammatory bowel disease. *Curr Opin Gastroenterol,* 1996;12(4):340-344
2 Sartor RB. pathogenesis and immune mechanism of chronic inflammatory bowel disease. *Am J Gastroenterol,* 1997;92(Suppl 12):5S-11S[a¤]
3 Ruddle NH. Tumor necrosis factor (TNF-A) and lymphotoxin (TNF-A). *Curr Opin Immunol*,1992;4(3):327-332
4 Carswell EA, Old LJ, Kassel RL, Green S, Fiore N, Williamson B. An endotoxin-induced serum factor that causes necrosis of tumors. *Proc Natl Acad Sci USA,* 1975;72(9):3666-3670
5 Derkx B, Taminiau J, Radema S, Stronkhorst A, Wortel C, Tytgat G *et al*. Tumour necrosis-factor antibody treatment in Crohn's disease. *Lancet,* 1993; 342(8864):173-174
6 Krueger J, Ray A, Tamm I, Sehgal PB. Expression and function of interleukin-6 in epithelial cells. *J Cell Biochem,* 1991;45(4):327-334
7 Jones SC, Trejdosiewicz LK, Banks RE, Howdle PD, Axon AT, Dixon MF *et al*. Expression of interleukin-6 by intestinal enterocytes. *J Clin Pathol,* 1993; 46(12):1097-1100
8 Van Seventer GA, Shimizu Y, Horgan KJ, Luce GE, Webb D, Shaw S. Remote T cell co-stimulation via LFA-1 / ICAM-1 and CD2 / LFA-3: demonstration with immobilized ligand / mAb and implication in monocyte mediated co-stimulation. *Eur J Immunol,* 1991;21(7):1711-1718
9 Hilbert DM, Cancro MP, Scherle PA, Nordan RP, Van Snick J, Gerhard W *et al*. Tcell derived IL-6 is differentially required for antigen-specific antibody secretion by primary and secondary B cells. *J Immunol,* 1989;143(12):4019-4024
10 Okada M, Kitahara M, Kishimoto S, Matsuda T, Hirano T, Kishimoto T. IL-6 / BSF-2 function as a killer helper factor in the in vitro induction of cytotoxic T cells. *J Immunol,* 1988;141(5):1543-1549
11 Roldan E, Brieva JA. Terminal differentiation of human bone marrow cells capable of spontaneous and high rate immunoglobulin secretion: role of bone marrow stromal cells and interleukin 6. *Eur J Immunol,* 1991;21(11):2671-2677
12 McGhee JR, Fujihashi K, Beagley KW, Kiyono H. Role of interleukin 6 in human and mouse mucosal IgA plasma cell responses. *Immunol Res,* 1991;10 (3-4):418-422
13 Holtkamp W, Stollberg T, Reis HE. Serum interleukin-6 is related to disease activity but not disease specificity in inflammatory bowel disease. *J Clin Gastroenterol,* 1995;20(2):123-126
14 Susiki Y, Saito H, Kasanuki J, Kishimoto T, Tamura Y, Yoshida S. Significant increase of interleukin 6 production in blood mononuclear leukocytes obtained from patients with active inflammatory bowel disease. *Life Sci,* 1990; 47(24):2193-2197
15 Reinecker HC, Steffen M, Witthoeft T, Pflueger I, Schreiber S, MacDermott RP. Enhanced secretion of tumour necrosis factor-alpha, IL-6, and IL-1β by isolated lamina propria mononuclear cells from patients with ulcerative colitis and Crohn's disease. *Clin Exp Immunol,* 1993;94(1):174-181
16 Hyams JS, Fitzgerald JE, Treem WR, Wyzga N, Kreutzer DL. Relationship of functional and antigenic interleukin 6 to disease activity in inflammatory bowel disease. *Gastroenterology,* 1993;104(5):1285-1292
17 Gross V, Andus T, Caesar I, Roth M, Sch-lmerich J. Evidence for continuous stimulation of interleukin 6 production in Crohn's disease. *Gastroenterology,* 1992;102(2):514-519
18 Rubin LA, Kurman CC, Fritz ME, Biddison WE, Boutin B,Yarchoan R *et al*. Soluble interleukin 2 receptors are released from activated human lymphoid cells in vitro. *J Immunol,* 1985;135(5):3172-3177
19 Rubin LA, Jay G, Nelson DL. The released interleukin 2 receptor binds interluekin 2 efficiently. *J Immunol,* 1986;137(12):3841-3844
20 Jacques Y, Le-Mauff B, Boeffard F, Godard A, Soulillou JP. A soluble interleukin 2 receptor produced by a normal alloreactive human T cell clone binds interleukin 2 with low affinity. *J Immunol,* 1987;139(7):2308-2316
21 Brynskov J, Tvede N. Plasma interleukin-2 and a soluble shed interleukin-2 receptor in serum of patients with Crohn's disease. Effect of cyclosporin. *Gut,* 1990;31(7):795-799
22 Mahida YR, Gallagher A, Kurlak L, Nawkey CJ. Plasma and tissue interleukin 2 receptor levels in inflammatory bowel disease. *Clin Exp Immunol,* 1990;82 (1):75-80
23 Mueller C, Knoflach P, Zielinski CC. T-cell activation in Crohn's disease. Increased levels of soluble interleukin 2 receptor in serum and in supernatants of stimulated peripheral blood mononuclear cells. *Gastroenterology,* 1990;98(3):639-646
24 Lennard-Jones JE. Classification of inflammatory bowel disease. *Scand J Gastroenterol.* 1989;24(Suppl 170):2-6
25 Sutherland LR, Martin F, Greer S. 5-Aminosalicylic acid enema in the treatment of distal ulcerative colitis, proctosigmoiditis, and proctitis. *Gastroenterology,* 1987;92(6):1894-1898
26 Hou J, Kong XT. Interleukin 6 bioassay by MTT colorimetry. *Chin J Med Lab Technol*,1993;16:208-210
27 Maeda M, Watanabe N, Neda H, Yamauchi N, Okamoto T, Sasaki H *et al*. Serum tumor necrosis factor activity in inflammatory lowel disease. *Immunopharmacol Immunotoxical,* 1992;14(3):451-461
28 Murch SH, Lamkin VA, Savage MO, Walker-Smith JA, MacDonald TT. Serum concentrations of tumour necrosis factor alpha in childhood chronic inflammatory bowel disease. *Gut,* 1991;32(8):913-917
29 Mahmud N, O'Connell MA, Stinson J, Goggins MG, Weir DG, Kelleher D. Tumor necrosis factor-alpha and microalbuminuria in patients with inflammatory bowel disease. *Eur J Gastroenterol Hepatol*,1995;7(3):215-219
30 Mazlam MZ, Hodgson H. Peripheral blood monocyte cytokine production and acute phase response in inflammatory bowel disease. *Gut,* 1992;36(6): 773-778
31 Nielsen OH, Brynskov J, Bendtzen K. Circulating and mucosal concentrations of tumour necrosis factor and inhibitor(s) in chronic inflammatory bowel disease. *Dan Med Bull,*1993;40(2):247-249
32 Bouma G, Oudkerk Pool M, Scharenberg JGM, Kolkman JJ, von Blomberg BME, Scheper RJ *et al*. Differences in the intrinsic capacity of T-cells to produce the cytokines tumor necrosis factor alpha and beta in patients with inflammatory bowel disease and healthy controls. *Scand J Gastroenterol,* 1995;30(11):1095-1100
33 Schreiber S, Raedler A, Conn AR, Rombeau JL, MacDermott RP. Increased in vitro release of soluble interleukin 2 receptor by colonic lamina propria mononuclear cells in inflammatory bowel disease. *Gut,* 1992;33(2):236-241
34 Bouma G, Xia B, Crusius JBA, Bioque G, Koutroubakis I, von Blomberg BME *et al*. Distribution of four polymorphisms in the tumour necrosis factor (TNF) genes in patients with inflammatory bowel disease (IBD). *Clin Exp Immunol,* 1996;103(3):391-396

ISSN 1007-9327 CN 14-1219/R WJG, 1998;4(3):256-259

Protective effect of YHI and HHI-I against experimental acute pancreatitis in rabbits

ZHAO Lian-Gen, WU Xiao-Xian, HAN En-Kun, CHEN Yu-Ling, CHEN Chi and XU Dong-Qin

Subject headings pancreatitis/pathology; pancreatitis/therapy; Yuanhu; Huoxuehuayu; amylase/blood; interleukin-6/blood; microcirculation; rabbits

Abstract

AIM To observe the protective effect of combined i.v. administraction of Yuanhu injection (YHI) and Huoxuehuayu injection-I (HHI-I) against acute pancreatitis (AP) in rabbits.

METHODS Sever acute pancreatitis (SAP) was induced by retrograde infusion of artificial bile juice into biliary-pancreatic duct, and treated with YHI and HHI-I intravenously. The protective effect was judged by the survival time and rate, serum amylase, serum interleukin-6, pancreatic microcirculation and pathological alteration.

RESULTS Combined use of YHI and HHI-I could markedly increase the rabbits' 5-day survival rate after AP (83.3% in the treatment group and 33.3% in control). The serum amylase value ($\bar{x}\pm s$) decreased to 1596.6U/L±760.50U/L in the 5th day from the high level (6320.83U/L±2614.12U/L) in the 1st day after AP in the treatment group, while in the control group the amylase activity in the 5th day was 2095.0U/L±1081.87U/L, being significantly different from that before AP (837.17U/L±189.12U/L). YHI and HHI-I also obviously improved the pancreatic microcirculation and lowered the serum interleukin-6 level, one of the indices of severe pancreatitis. Pathological examination indicated all the changes typical for AP in YHI and HHI-I treatment group were milder than those in the control.

CONCLUSION YHI and HHI-I used in combination might have protective effect against acute pancreatitis in rabbits.

Research Laboratory of Pathophysiology, Institute of Acute Abdominal Diseases of Integrated Traditional Chinese and Western Medicine, Tianjin 300100, China

Dr. ZHAO Lian Gen, male, born on 1938-07-02 in Tangshan, Hebei Province, graduated from Pathophysiology Department, Beijing Medical College, research fellow, Director of Pathophysiology Research Laboratory, majoring experimental research of acute pancreatitis and TCM Huoxuehuayu therapeutic principle, having 44 papers published.

Correspondence to: Dr. Zhao Lian Gen, Research Laboratory of Pathophysiology, Institute of Acute Abdominal Diseases of Integrated Traditional Chinese and Western Medicine, Tianjin 300100, China

Tel. +86 • 22 • 27370021

Received 1997-12-30

INTRODUCTION

Autodigestion of pancreatic enzymes in pancreatic tissues and pancreatic ischemia are two most important pathogenic factors in acute pancreatitis (AP). In order to lower the morbidity and mortality of AP, inhibition of pancreatic digestive enzymes and prevention and treatment of pancreatic ischemia are the two necessary therapies. Recently, many experimental researches and clinical trials are being addressed to these fields. Yuanhu (Rhizoma Corydalis) injection (YHI) is the most effective inhibitory Chinese medicine screened from the decoction used in our institute for AP. Huoxue Huayu Injection I (HHI-I) is one of best Huoxue Huayu (promoting blood circulation to remove blood stasis) decoctions. It has been demonstrated that YHI can inhibit the activity of typsin and elastase and HHI-I can improve the pancreatic blood flow and oxygen supply[1]. In this experiment, we have observed the protective effect of YHI and HHI-I against AP in rabbits.

MATERIAL AND METHOD

Animal model of AP

The AP model in rabbit was produced according to Klar's method with slight modefication[2]. Male white healthy rabbits weighing 2.5kg±0.4kg were used. After overnight fasting, the animals were anesthetized with intravenous 6% pentobarbital (20mg/kg) and intramuscular ketamine (25mg/kg). Under sterile condition, the abdoman was opened and biliary pancratic duct at duodenum wall was found and inserted with a polyethylene catheter. A mixture of 5% sodtaurocholate, trypsin (24U/ml) and homologous blood (30 μl/ml), incubated at 37 ℃ for 60min was infused at 0.8ml/kg body weight into the duct under 5.3kPa, at an interval of about 10min.

Reagent

Sod taurocholate (Sigma Co, USA); Trypsin (Boehringer Mannheim CO), Activity was determined by the Biological Department, Nankai University; and Kit of amylase (Zhongsheng Co, Peijing).

Instrument and assay method

Dynamic analyzer of Doppler laser microcirculation (JM-200, Jinke Co, Tianjin). Serum amylae activity was determined with UNIFAST analyzer. Serum interlukin-6 was assayed by the MTT method.

Experimental design

Twelve rabbits were divided into treatment and control groups 6 each. During experiment, the abdomen was opened, the state of pancreatic microcirculation was determined and AP was then induced. Immediately, 30, 60, 90 and 120min after the AP was induced, microcirculation was evaluated once more. The abdoman was then closed and the survival time and rate were observed. Before AP and 1 and 2 days after the operation blood samples were obtained from auricle vein to measure the serum amylase and interleukin-6 levels. Normal saline was infused intravenously in control animals immediately after AP and 1 and 2 days after that. The treatment group was administered with YHI and HHI-I simultaneously at lg/kg desolued in 10ml normal saline. When the animals died, sample of pancreas was harvested for pathological examination.

RESULTS

Survial time and survival rate

Two of 6 animals in the control group died 12 and 24 hours after AP was produced respectively. Another two died at 96 hours and the remaining survived till the end of experiment, with a 5-day survival rate of 33.3%. In treatment group, one rabbit died at 72 hours after AP and all the others survived, with a 5-day survival rate of 83.3%. An increased trend of survival rate was observed in treatment group but was not different significantly from the control group ($P<0.05$).

Serum amylase

Serum amylase activity increased obviously in the control group at the 1st and 3rd day. At the 5th day it began to decrease, but still remained markedly higher than before AP. In treatment group, higher levels of amylase activity could be seen at first day after AP. At the 3rd day, however, it decreased significantly and almost reached to the normal level at the end of experiment (Table 1).

Changes of pancreatic microcirculation

Immediately after AP, the microcirculation of pancreatic tissue became obviously deteriorated. In treatment group pancreatic blood flow was improved somewhat at 30, 60, 90 and 120min after AP was induced, but in the control group it was getting worse and worse (Figures 1 and 2).

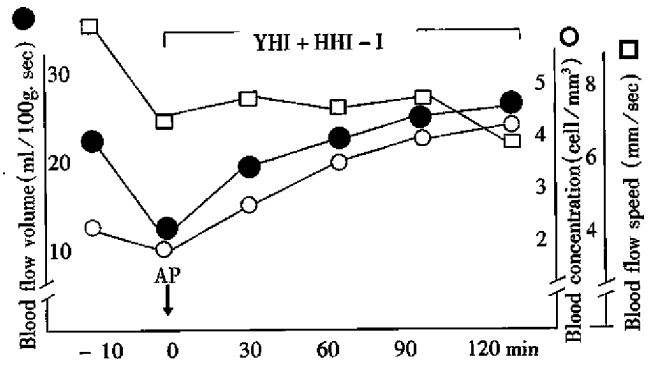

Figure 1 Effect of YHI and HHI-I on pancreatic blood flow, blood concentration, flow speed in rabbits with SAP.

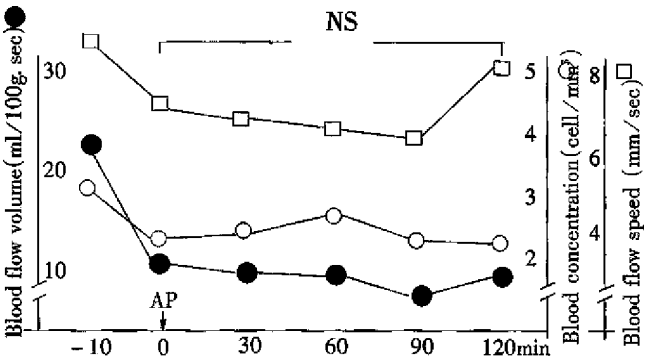

Figure 2 Effect of normal saline on pancreatic blood flow, blood concentration and flow speed in rabbits with SAP.

Serum interleukin-6

All animals after AP had increased level of serum interleukin, which remained high in the control group at the 3rd and 5th day while in treatment group it decreased more significantly than the control group (Table 2).

Pathologic examination

Most parts of pancreatic and fat tissue in control group had necrosis and large areas of hemorrhage. In the necrotic tissues there were many foci of PMN infiltrations and abscesses. The necrosis dimension and the number or size of hemarrhage in the treatment group were obviously lower than in the control. The extent of PMN leukocyte infiltration and the size or number of abscesses were also milder, with some more intact pancreatic bolules. Even though some lobules were dystroyed severely, the was still intact (Table 3).

Table 1 The effect of YHI and HHI-I on serum amylase of rabbit with SAP ($x \pm s$)

Group	Before AP	After AP (d)		
		1	3	5
Treatment(U/L)	867.67±374.62	6320.83±2614.12(6)[b]	4774.0±1859.36(5)[b]	1596.6±760.50(5)
Control(U/L)	838.17±189.12	7586.67±3745.03(5)[b]	7380.0±3687.41(4)[b]	2095.0±1081.87(2)[a]

( ) number of survived, [a]$P<0.05$ and [b]$P<0.01$ compared with before AP.

Table 2 The effect of YHI and HHI-I on serum interleukin-6 in AP rabbits ($\bar{x} \pm s$)

Group	Before AP	After AP (d)		
		1	3	5
Control(U/L)	32.37±9.11(6)	69.75±19.18(5)	72.35±10.14(4)	70.25±10.34(2)
Treatment(U/L)	30.0±16.40(6)	59.50±17.59(6)	50.33±16.57(5)[a]	46.50±14.94(5)[a]

( ): animal number, [a]$P<0.05$ compared with control.

Table 3 Effect of YHI and HHI-I on pathologic changes of pancreas in rabbits with SAP

	Control group	Treatment group
Lobule structure	Destroyed totally	Relatively intact
Acinus	Destroyed	Atrophied
Intralobular duct	Destroyed seriously	Existed, expanded
Interlobular duct	Residually existed	Existed
Fatty tissue	Destroyed totally	Mild-moderately destroyed
Inflammatory cell	Abscess formed	A few abscesses and WBC
Focal hemorrhage	Large size	Small size and a few number
Interstitial hyperplasia of fibrous tissue	A few around abscess and necrosis	Much more around abscess and necrosis
Island	No	Existed

DISCUSSION

Aprotinin was an antiprotease used firstly in clinical practice. However, the therapeutic effect for SAP was not satisfactory possibly because its molecular weight was too heavy to enter into acinar cells, and the half-life was short in blood circulation. Subsequently, some other antiproteases with low molecular weight were found such as Gabexate Mesilate (GM, *Mr* 417.5) and Camostate (FOY-305, *Mr* 494.5). Several experiment studies showed that GM was a very valuable medicine for prevention and treatment of AP, especially when it was before the disease was induced. The results of the first mult-center clinical research was also encouraging. A report of a case-control clinical trial indicated that GM (900mg/d) could decrease the number of operations associasted with AP. Owing to the relative low dosage used, Büchler and his co-workers increased the dose of GM to 4000mg/d in 223 patients with moderate to severe pancreatitis (average Ranson score at 3.7) for 7 days, and found there was no difference in the mortality, pancreatitis-associated operation, hospitalized days, complication score and some parameters of biochemical assays as compared with those in the control group. Their conclusion was that GM was not effective in prevention of complications and deeth[3]. According to the result of the recent retrospective reviews GM could obviously decrease the incidence of complications in operations. Being expensive in price could only be used in those patients at high risk to create a better cost-effect ratio[4].

Possessing wider enzyme-inhibitory spectrum, FOY-305 could markedly increase the survival rate in experimental SAP animals[4]. The beneficial effect of FOY-305 could be obtained by FOY-305 and its metabolites which could be absorbed from intestine into blood circulation; by stimulating the endogenetic secretion of secretin and CCK to increase the exocrine pancreas; and decreasing the intra-acinar vacuolization. Recently, it was demonstrated that oral administration of FOY-305 could also decrease the extent of pancreatic edema and vacuolization of acinar cells in AP rats induced by cerulein. FOY-305 could decrease the level of trypsin in pancreatic tissues as well. By means of above actions, FOY-305 might be beneficial to cerulein-induced AP rats[6]. To date no information was found on clinical application of FOY-305.

Antiprotease was not satisfactory for treating AP clinically made the researchers suspect the cerrectness of the concept of enzyme-inhibition in treatment AP. It was important to recognize that

the patients could not be admitted to hospital 12 to 24 hours after the occurrence of inflammation, during which the patients' kinin and complement system were already activated, capillary endothelium cells injuried, some enzymes released from activated leukocytes. All these were related to the poor therapeutic effect of trypsin antagonist used after that period.

It was demonstrated that Chinese medicines, such as Banxia (Penellia ternata), Dahuang (Rheum palmatum), Huangqin (Scutellaria baicalensis), Hulian (Rhizoma picrorhizae) and Baishao (Radix paeoniae alba), that had enzyme inhibitory actions. The results from our institute indicated that among the 9 medicines investigeted, Yuanhu (Rhizoma corydalis) was the most potent inhibitor for trypsin activity.

Pancreatic ischemia was the etiologic and deteriorating factor for AP, and played an important role in necrosis of pancreas in the early period of AP[7,8]. Pancreatic ischemia imposed on pancreatic edema could induce necrotic AP. After AP was induced by ligation of pancreatic duct and overstimulation to exocrine pancreas, blockade of pancreatic artery for only 5 minutes could induce parenchymal necrosis of pancreas. Temporary ischemia of pancreas made the acinar cells more sensitive to the degradation effect of enzyme and more easy to form necrosis. Mithofer used bleeding method to induce blood hypotension (30mmHg, 30min) in rats, resulting in pancreatic ischemia, and found the serum amylaseincreased in 1 hour after ischemia and rose at the 4th hour. Trypsinogen activative peptide (TAP) of pancreatic tissue was also increased at the first hour, and further increase occurred at 24 hour. Pancreatic edema and necrosis were observed as well. In our opinion, besides deteriorated action, pancreatic ischemia itself, if serious, could also initiate AP[9]. On the other hand, changes of pancreatic blood circulation could be found in the course of AP. That reported that 5min after AP was induced, segmental spasma of arteriole and venule of acinus could be observed, and there was blood stasis at 15min. Using vital microscopy technique, Klar observed that perfusion of pancreatic capillaries of rabbit diminished gradually 30min after AP and stopped completely at 3 hours[2]. Klar also found that isovolemic hemodilution with dextran 60 could maintain pancreatic capillary perfusion, and the relative number of vacuolization in acinar cells and parenchymal edema were both obviously lower than in the control group. Clinicaly, Klar carried out a trial treatment in 13 patients with SAP (mean Ranson score 4.6). The time interval between appearance of symptoms of AP to the beginning of hemodilution was 38 (19-90) hours. The hematocrit (HCT) decreased to 34%±6% at the first hour and 31%±4% at the second hour. The mean exchanging time was 45.70 minutes and the exchanging volume was 750ml-170ml. The ultimate results showed a mortality of only 7.7%. Therefore, we think that the isovolemic hemodilution had no harmful side-effect and could be used in further clinical trial[11].

In vitro screening test in our research indicated that YHI was the most potent inhibitor for pancreatic digestive enzymes among the nine screened Chinese herbs. Optimized selection experiment showed that HHI-I was the most beneficial herb for both intestinal and pancreatic blood flow and oxygen consumption. In this experiment satisfactory results were obtained in treatment of AP in rabbits with YHI and HHI-I in combination. These were related with their enzyme-inhibitory action and improvement of pancreatic blood circulation.

However, this is a preliminary experiment only, further investigation on toxity, side-effect, effective dosage, and pharmacodynamics etc. are needed.

REFERENCES

1 Zhao LG, Wu XX, Zhu ZM, Chen YL, Liu FS, Chen JT. Screening and pharmacologic study of new Chinese medicine treating severe acute pancreatitis. *China Natl J New Gastroenterol*,1996;2(3):136-138

2 Klar E, Herfarth C, Messemer K. Therapeutic effect of isovolemic hemodilution with dextran 60 on the impairment of pancreatic microcirculation in acute biliary pancreatitis. *Ann Surg*, 1990;211(7):346-353

3 Büchler M, Malfertheiner P, Waldemar UHL, Jurgen S, Fritz S, Guido A *et al*. Gabexate mesilate in human acute pancreatitis. *Gastroenterology*, 1993;104 (4):1165-1170

4 Messiru A, Rampazzo R, Scroccaro G, Olivato R, Bassi C Falconi M *et al*. Effectiveness of gabexate mesilate in acute pancreatitis. *Dig Dis Sci*, 1995;40 (4):734-738

5 Leonhared V, Seidensticker F, Fussek M, Stockmann F, Creutzfeldt W. Camostate (FOY-305) improves the therapeutic effect of peritoneal lavage on taurocholate induced pancreatitis. *Gut*,1990;31(8):934-937

6 Kisfalvi K, Papp M, Friess H, Büchler M, Goracz UG. Beneficial effects of preventive oral administration of camostate on cerulein-induced pancreatitis in rats. *Dig Dis Sci*,1995;40(3):546-547

7 Klar E, Messmer K, Warshaw AL, Herfarth C.Pancreatic ischemia in experimental acute pancreatitis: mechanism, significance and therapy. *Br J Surg*, 1990;77(11):1205-1210

8 Kyogoku T, Manabe T, Tobe T.Role of ischemia in acute pancreatitis.Hemorrhagic shock converts edematous pancreatitis to hemorrhagic pancreatitis in rats. *Dig Dis Sci*, 1992;37(9):1409-1417

9 Mithofer K, Castillo CF, Frick TW, Foitzikt T, Bassi DG, Lewandrowski KB *et al*. Increased intrapancreatic trypsinogen activation in ischemia-induced experimental pancreatitis. *Ann Surg*, 1995;221(4):364-371

10 Klar E, Mall G, messemer K, Herfarth C, Rattner DW, Wasrchaw AL. Improvement of impaired pancreatic microcirculation by isovolemic hemodilution protects pancretic morphology in acute biliary pancreatitis. *SGO*, 1993; 176(2):144-150

11 Klar E, Foitzik T, Buhr H, Messmer K, Herfarth C. Isovolemic hemodilution with dextran 60 as treatment of pancreatic ischemia in acute pancreatitis. *Ann Surg*, 1993;217(4):369-374

 ISSN 1007-9327 CN 14-1219/R WJG, 1998;4(3):260-263

Therapeutic effect of Zijin capsule in liver fibrosis in rats

CAI Da-Yong, ZHAO Gang, CHEN Jia-Chun, YE Gan-Mei, BING Fei-Hong and FAN Bu-Wu

Subject headings liver cirrhosis/therapy; Zijin capsule; integrated TCM-WM; diseases models, animal; rats

Abstract

AIM To confirm the therapeutic effect of Zijin capsule on liver fibrosis in rat model.

METHODS Model group: Bovine serum albumin (BSA) Freund's incomplete adjuvant 0.5ml was injected subdermally at d1 d15 d22 d29 and d36 for primary sensitization. Seven days after the fifth injection, BSA antibody in the serum was detected by double agar diffusion method. Normal saline of 0.4ml was injected through cauda vein to BSA antibody-positive rat twice a week for fifteen times. Traditional Chinese medicine (TCM) decoction group and Zijin capsule group: In the attack injection period, Chinese medicinal decoction or Zijin capsule was given ig, the others were the same as in the model group. NS was used in the control group. The collagen content of rat liver was determined by Bergman's method and expressed as $\bar{x}\pm s$. The liver pathological changes were divided into four grades and expressed as the avarage of the total rank sum.

RESULTS The collagen content (mg/g) of the liver in the control group (7.2±1.9) was significantly lower than that in the other groups; it was higher in the model group (31.7±16.6) than that in the two therapeutic groups; and lower in Zijin capsule group (9.7±2.8) than that in the TCM decoction group (11.5±5.3). The pathological changes were more aggravated in the model group (37.4) than those in the two therapeutic groups; and more severe in the TCM decoction group (30.2) than in the Zijin capsule group (22.9).

CONCLUSION The therapeutic effect of Zijin capsule on the model was confirmed.

Department of Basic Medical Sciences, Hubei College of Traditional Chinese Medicine, Wuhan City 430061, Hubei Province, China

CAI Da-Yong, male, born in 1962 in Hubei Province, graduated from Hubei Medical University as a postgraduate in 1989, now a lecturer of pathology majoring the research of combined TCM and western medicine, having 18 papers published.

***Supported by the key Project Fund of Scientific Committee of Hubei Province.**

Correspondence to: Dr. Cai Da Yong, Department of Basic Medical Sciences, Hubei College of Traditional Chinese Medicine, Wuhan City 430061, Hubei Province, China

Tel. +86 • 27 • 8863607, E-mail:CZ971010@public.wh.hb.CN

Received 1998.02-25

INTRODUCTION

The pathological changes of the rat liver fibrosis induced by bovine serum albumin (BSA) injections are similar to those in human portal cirrhosis. Compared with the TCM decoction proved effective in clinic the therapeutic effect of Zijin capsule in rat liver fibrosis was observed.

MATERIALS AND METHODS

Materials

Wistar rats (female 30, male 30, 150g-210g) were purchased from Hubei Medical Institute. BSA was product of Shanghai Medical Testing Agent Plant, prepared as 18g/L in normal saline, clean from bacteria through filtration, and stored at 4℃. Freund's incomplete adjuvant: One gm lipid from sheep hair (CP Third Lipid Company in Shanghai) was mixed with 2 gm liquid paraffin (Fushan Chemical Industry), sterilized in a steam autoclave and stored at 4℃. L-hydroxyproline, standard sample, was from Biochemistry Institute of the Chinese Academy of Sciences. Zijin capsule. prepared mainly from *herba swertiae puniceae* and *endothelium corneum gigeriae galli* in Hubei College of Traditional Chinese Medicine. The concentration of crude drugs was
5g/1ml. The TCM decoction provided by the Department of Infectious Diseases, the Afficiated Hospital of Hubei TCM College, containing mainly *Radix astragali, Radix condonopsis pilosulae, Rhizoma atractylodis macrocephalae, Rhizoma polygoniti, fructus lycii, fructus corni, radix rehmanniae* and *Radix rehmanniae preparata.*

Method

Wistar rats with free access to water were randomly divided into four groups.

Control group (n = 12). Normal saline was used for immunological primary (sensilization) and second (attack) injection instead of BSA, the others were the same as those in the model group.

Model group (n=12). BSA Freund' incomplete adjuvant 0.5ml was injected subdermally at d_1 d_{15} d_{22} d_{29} and d_{36} for primary sensitization. Seven days after the fifth injection, BSA antibody in rats' serum was detected by double agar diffusion method. BSA of 0.4ml in normal saline was administered once through cauda vein for attack injection in BSA antibody-positive rats, twice a week for fifteen times, the concentration of BSA

was 5.00, 5.25, 5.50, 5.75, 6.00, 6.25, 6.50, 6.75, 7.00, 7.25, 7.50, 8.50, 9.00, 9.50 and 10.00g/L. The rats were given 10ml • kg • d N.S. ig at the same period. All animals were killed with decollation nine days after the last injection. The livers were taken for biochemistry detection and morphological observation. The whole period was 95 days.

TCM decoction group (n = 18). In the attack injection period, the Chinese medicinal decoction equivalent to 36g crude drugs/kg • d was given ig, the others were the same as those in the model group.

Zijin capsule group (n = 18). In the attack injection period, Zijin capsule, equivalent to 12.8g crude drugs kg • d, was given ig, the others were the same as those in the model group.

The collagen content in rat liver was determined by Bergman's method[1], and expressed as $\bar{x}\pm s$ and analyzed by t test. Value of $P<0.05$ was considered at a significant level. The rat livers were embedded with paraffin and stained with HE. The pathological changes were classified into four grades according to the quality and quantity of the liver histological features, expressed as the avarage of the total rank sum in each group and analyzed by *H- test*. Value of $P<0.05$ was considered at a significant level.

RESULTS

Collagen content in rat liver

The indexes are shown in Table 1. The collagen content was significantly lower in the control group than that in the model group ($P<0.01$), the TCM decoction group ($P<0.05$) and Zijin capsule group ($P<0.05$); it was higher in the model group than that in the TCM decoction group ($P<0.01$) or Zijin capsule group ($P<0.01$); and not significantly lower in Zijin capsule group than that in the TCM decoction group ($P>0.05$).

Table 1 The collagen content in rat liver ($\bar{x}\pm s$)

Groups	Dosage	n	Content (mg/g)
Control	10.0ml/(kg • d)	10	7.2±1.9
Model	10.0ml/(kg • d)	6	31.7±16.6[b]
TCM decoction	36.0g/(kg • d)	12	11.5±5.3[ad]
Zijin capsule	12.8g/(kg • d)	9	9.7±2.8[ad]

[a]$P<0.05$, [b]$P<0.01$, *vs* control group; [d]$P<0.01$, *vs* model group.

The pathologic change grade in rat livers

After a comprehensive observation on the pathologic changes, a distinct grading standard was defined as follows:

Grade 0 (normal rat liver) Liver capsula was a thin connective tissue. The parenchyma consisted of hepatic lobules and portal areas. The hepatic lobules were similar to round balls, their central veins, laminae of hepatocytes (radiated arrange) and siunsoids were normal and clear. The hepatic lobule boards were hepatic cell layers as limiting laminae. There was hepatic sinusoid between the hepatic laminae, their endothelia were distributed regularly, Kupffer's cells can be seen obviously. The ratio of the hepatic laminae to the hepatic sinusoids was 3 to 2. The hepatocytes are polygonal cells, cytoplasm was normal acidophil, the hepatic nuclears in round shape, the chromatin distributed rarefactionally along the nuclear membrane with nucleole. The portal area was mainly connective tissues, including the interlobular hepatic artery, the portal vein branches and interlobular bile ducts. Some lymphocytes and plasma cells had infiltrated into the portal areas. The necrosis within a few hepatocytes and their lymphocyte or plasma cell infiltration (spotty necrosis) were occasionally observed in one hepatic lobule or two. There were many red-dyed microgranules (slight cloudy swelling) in some hepatocytes.

Grade 1 (liver injury change). Serious and extensive changes were present as the degeneration and necrosis of hepatocytes and the congestion or bleeding in the hepatic sinusoid. Cloudy swelling of hepatocytes: enlarged volume, round shape, many small red-dyed granules in hepatic cytoplasm were observed; hepatic laminae became wider, and hepatic sinusoid were pressed to ischemia. Thin hepatic cytoplasm: the hepatocyte volume became larger, red-dyed cytoplasm thinner and less homogeneous; the nuclears stained dim; and the ratio of hepatic laminae to the hepatic sinusoids became higher. Ballooning degeneration of hepatocytes: the volume of hepatocytes became extremely large, round shaped; the cytoplasm appeared empty (light transparency) like a balloon; nuclear not located at the cell centre. Lytic necrosis of hepatocytes: the ballooning degeneration of hepatocytes further developed to karyopyknosis, karyorrhexis and karyolysis; the whole structure of the hepatocyte body even disappeared, only the network of the reticular fibers remained; however, the lymphocytes infiltration in necrotic focus was not obvious; and the necrosis of hepatocytes did not occur at the limiting laminae in the hepatic lobules. The congestion and bleeding in the hepatic sinusoid: the hepatic sinusoids were expanded and filled with blood. The bleeding in Disse's cavity was extensive. Two kinds of congestion and bleeding in hepatic lobules were observed in these cases, one

distribution was limited around central veins, which was seldomly observed, the other mainly appeared near the limiting laminae of hepatic lobules, which were predominant. At the same time, there were light hyperemia, edema and fibrous proliferation in the portal areas (Figure 1).

Grade 2 (liver prefibrosis). The necrosis within a few hepatocytes occurred at the limiting laminae (piecemeal necrosis); and the necrosis range may be expanded to a large region of hepatic necrosis which connected the central veins or portal areas (bridging necrosis). Serious congestion and bleeding near the limiting laminae in the hepatic lobules were common. The hepatic laminae became thinner in the same region accompanied by hepatocyte atrophy, cloudy swelling and fatty degeneration and the hepatocytes even disappear in the same region. The congestion may be connected with the central veins or portal areas (bridging congestion). In those cases, the Kupffer's cells in the hepatic sinusoid enlarged and proliferated obviously with more processes. In the portal areas, fibroblasts proliferated obviously and collagen increased, which made the boundary in the normal hepatic lobules more clear, but they were not streching into the hepatic lobules through the limiting laminae.

Grade 3 (liver fibrosis). The hepatocyte injury (degeneration and necrosis) at the limiting laminae has advanced obviously, while the proliferated collagen at portal areas has invaded into the hepatic lobules along with the injuried limiting laminae. It was called as liver fibrosis while the proliferated collagen has not been completely contacted each other and absolutely separated the hepatic lobules. It was the cirrhosis when the proliferated collagen has been contacted each other completely, and absolutely separated the hepatic lobules, leading to the formation of pseudolobules (many round islands of hepatocytes). Their hepatic laminae have not radiated regularly, the central vein dystopy (asymmetry, disappear or several veins), the structure of portal areas was located in the pseudolobules, there were some atrophy, fatty degeneration and necrosis of the hepatocytes in the pseudolobules; they were separated continuously with the proliferated collagen, the cholestatic bile capillaries appeared and their bile thrombus formed. Among the pseudolobules, the fibrous bands were continuous, homogeneous and delicate; and there are more infiltrated lymphocytes. The collagenous fibers were stained bright-red (Figure 2).

According to the grading, *H* test was used to analyse statistically the liver pathological changes among those groups. The pathological changes are more moderate in the control group than those in the other three groups ($P<0.01$, Table 2). They were more severe in the model group than those in the two therapeutic groups; and more aggravated in the TCM decoction group than those in the Zijin capsule group.

Table 2 The pathological change grades in rat liver

Groups	Dosage	*n*	Pathologic grade				Rang sum	$\bar{x}$-Rang sum
			1	2	3	4		
Control	10.0ml/kg • d	10	0	0	0	10	55.0	5.50
Model	10.0ml/kg • d	0	1	3	5	9	337.0	37.44[b]
TCM decoction	36.0g/kg • d	0	5	5	3	13	393.0	30.23[bc]
Zijin capsule	12.8g/kg • d	0	11	4	0	15	343.0	22.87[bde]

[b]$P<0.01$ *vs* control group; [c]$P<0.05$, [d]$P<0.01$, *vs* model group; [e]$P<0.05$ *vs* TCM decoction group (*H* test).

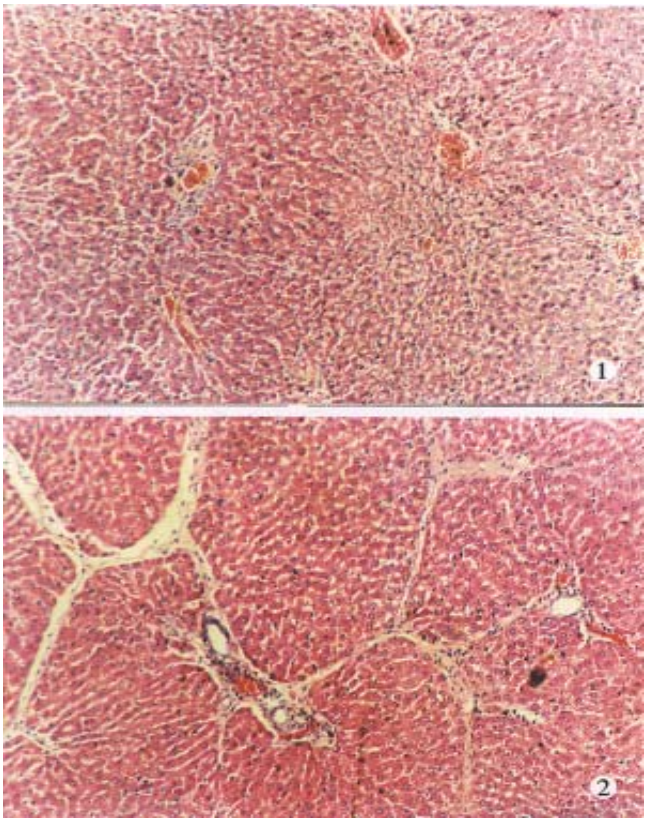

Figure 1 Grade 1 pathologic change (liver injury).HE×250
Figure 2 Grade 2 pathologic change (liver fibrosis).HE×250

DISCUSSION

Rat liver fibrosis induced by BSA injections After BSA sensitization injection (sc), the rats were intravenously injected with BSA as attack injection, the CIC (the circulating immune complex formed with BSA antigens and their antibodies) or the remained antigens (BSA) has deposited in some tissues of the rats, leading to classical type III or/and type II of the allergic reactions, subsequently local tissue injuries. The administration of antigen, including the route, time and dose of the injected antigen decides the location and features of injury lesions. Based on the references about the experimental methods, BSA injected with various

dosages, at different times and dates produced serious injuries (37/37) of livers and even obvious fibrosis or cirrhosis (8/37). The locations and features of the pathologic changes have suggested the pathogenesis of cirrhosis, i.e., the pathological changes were advanced near the limiting laminae in the hepatic lobules, because the CIC deposited earlier and more seriously at the location according to the circulative dynamics in the hepatic lobules. The features of the pseudolobules (such as shape, size, laminae arrange, cellular injuries) and the fibrous bands (delicate, homogeneous) were similar to the pathological changes in human poral cirrhosis. The hepatocytes did not regenerate to form pseudobobules obviously. However, the liver structures were normal ($P<0.01$) and the collagen content was low ($P<0.05$) in the control group. The results indicate that the rat cirrhosis models induced by BSA injections according to the immunological principles are succesful[1,2].

The therapeutic effect of Zijin capsule on rat liver fibrosis

In contrast to the model group, the collagen was low ($P<0.01$), and the pathologic changes were slight ($P<0.05$ or $P<0.01$) in Zijin capsule group as well as the TCM decoction group. It confirms the effect of Zijin capsule to treat the rat liver fibrosis. Compared with that in the TCM decoction?group with confirmed therapeutic effect in human liver fibrosis[3], the collagen content remained the same level ($P>0.05$) in Zijin capsule group. The main active components[4] of Zijin capsule can increase the permeability of capillary, lead to the CIC depositing in different locations, enhance the ability of the mononuclear phagocyte system (it may promote the elimination of the CIC from the circulating blood), activate the hepatocyte metabolism to normalize their biology, and protect the hepatocytes from injuries. All these may be associated with the therapeutic effect of Zijin capsule in the rat liver fibrosis induced by BSA injections.

REFERENCES

1 Zhu QG,Fang BW, Wu HS, Lan SL, Fu QL. The study of the immunity liver fibrosis animal model induced by bovine serum albumin. *Chin J Pathol*, 1993; 22(2):121-122
2 Wang BE. The study of the experimental model in immunity liver fibrosis. *Chin Med J*, 1989;69(9):503-506
3 Fang BW, Zhu QG, Zhu JE, Wu HS, Lan SL, Fu QL. The experimental study of the drugs for supplementing Qi and activating blood circulation in the liver fibrosis animal model by bovine serum albumin. *J Chin Traditio West Med*, 1992;12(12):738-739
4 Chen JC, Huang XS. The chemical component analysis of Swertia Punicea Plant in Hubei Province. *Chin Materia Med*, 1990;13(2):29-31

 ISSN 1007-9327 CN 14-1219/R WJG, 1998;4(3):264-265

A new method of extensive resection for gastric carcinoma: selective type III operation

LIN Chao-Hong

Subject headings stomach neoplasms/surgery; lymphatic metastasis; lymph node excision/method; life quality; survival rate; prognosis

INTRODUCTION

One of the most important factors related to the prognosis of progressive gastric carcinoma is the metastasis to lymph nodes. Since 1968, we have made researches on the lymphatic metastasis and the proper scope of resection of lymph node in progressive gastric carcinoma. On the basis of this research, we designed a new method of extensive radical operation with special reference to the resection of lymph nodes.

MATERIALS AND METHODS

Theoretical basis of selective D3 operation

Since 1968, we have studied comprehensively the lymphatic metastasis in gastric carcinoma in 181 patients and reviewed 1317 cases reported in literature[1,2]. There were 784 cases of carcinoma in gastric antrum, and the overall rate of lymphatic metastasis in stations 1 and 2 were 16.5%-58.1%. The rate of lymphatic metastasis in station 3 was group 12, 20.7%; group 14, 13.4%; group 10, 13. 2%, group 15, 12.8%; group 13, 11.6%; group 11, 9.0%, group 2, 4.1%; and in station 4: group 16, 3. 7%. There were 481 cases of carcinoma in the gastric body, the overall rate of lymphatic metastasis were 13.5%-60.4% in stations 1 and 2. The rate of lymphatic metastasis in station 3 was: group 12, 12%; group 13, 4.9%; group 14, 4. 3%; group 15, 2.4%; and in station 4: group 16, 3.8%. There were 162 cases of carcinoma in gastric cardia, the overall rate of lymphatic metastasis in stations 1 and 2 were 8.1%-60.2%. The rate of lymphatic metastasis in station 3 was group 12, 7%; group 111, 5%; group 13, 2.5%; group 14, 15 and in station 4: group 16, 1%. There were 71 cases of carcinoma in the whole stomach, and the overall rate of lymphatic metastasis in stations 1, 2, 3 were 8.6%-80.3%.

According to the above results, in cases of progressive gastric carcinoma, the resection of only station 2 lymph nodes will result in incomplete resection of lymph node metastases, and if routine resection of station 3 lymph nodes is performed, the operational injury and postoperative complications will be increased, leading to unnecessary total gastrectomy. All these may influence the quality of post-operational life. On the basis of our study and with reference to the Japanese Clinical Pathological Standard for Gastric Carcinoma, we designed selective D_3 operation.

The scope of lymph node resection in selective D3 operation

This operation is characterized by the routine resection of lymph nodes in stations 1 and 2, and high lymph nodes metastasis rate in station 3.

In the cases of carcinoma of gastric antrum, the lymph nodes in groups 3, 4, 5 and 6 in station 1 and groups 1, 7, 8 and 9 in station 2, and the groups 11, 12, 13, 14, 15 in station 3 should be resected. The groups 2 and 10 lymph nodes in station 3 and group 16 in station 4 should not be routinely resected, unless they are suspected of having metastasis. In the cases of carcinoma of gastric body, the lymph nodes in groups 3, 4, 5 and 6 of station 1 and groups 2, 7, 8, 9, 10 and 11 of station 2 and groups 12 and 13 of station 3 should be resected. The lymph nodes in groups 14 and 15 in station 3 and group 16 in station 4 are not routinely resected, unless they are suspected to have metastasis. In the cases of carcinoma of gastric cardia, the lymph nodes in groups 1, 2, 3 and 4 of station 1 and groups 5, 6, 7, 8, 9, 10, 11 and 110 of station 2, and groups 12 of station 3 should be resected. The lymph nodes in groups 13, 14, 15 and 111 of station 3 and group 16 of station 4 are not routinely resected, unless they are suspected to have metastasis.

Department of Surgery, Shanghai Second Medical University, Siliu Medical College, Shanghai Sixth People's Hospital, Shanghai 200233, China

Dr. LIN Chao-Hong, male, born on 1933-09-21, in Xianyou City, Fujian Province, author of 69 papers, professor and post-graduate tutor of Shanghai Second Medical University, Director of the Department of Surgery, Shanghai Sixth People's Hospital.

Presented at the 8th Sino-Japanese Conference of Gastroenterological Surgery, 1996

Correspondence to: Dr. LIN Chao Hong, Department of Surgery, Shanghai Second Medical University, Siliu Medical College, Shanghai Sixth People¡äs Hospital, Shanghai 200233, China

Tel. +86 • 21 • 64369181 ext 401, **Fax.** +86 • 21 • 64367041

Received 1997-06-10 **Revised** 1997-07-26

RESULTS

Complications and mortality

In the 834 cases of gastric carcinoma treated from 1960 to 1982 in our hospital, the rates of complication treated with different operational modalities were D_1 2.4% and D_2 4.7%; and selective D_3 6.7% and D_3 6.7%, with no significant statistical difference (P>0.05). The mortality rates were D1 0.7% and D_2 2.3%; and selective D_3 2. 1% and D_3 6.7%, with no significant statistical difference (P>0.05)[3]. No complications and death occurred. In the 216 cases of stage III carcinoma of gastric antrum and body treated from 1972 to 1989 with D_2 or selective D_3 in our hospital.

Survival time

In the 834 cases of gastric carcinoma from 1960 to 1982, no significant statistical difference was observed in the 243 stage I and II cases, whether treated with D_1, D_2 or selective D_3. The 5-year survival rate were 2.8%, 49.2%, 68.3% and 83.8%, respectively in the stage III gastric carcinoma treated with D1 in 139 cases, D_2 in 181 cases, selective D_3 in 88 cases and D_3 in 6 cases. The 5-year survival rate in cases treated with D_3 and selective D_3 were significantly higher than that of cases treated with D_1 and D_2 (P<0.01), but no significant difference was noted between cases treated with D_3 and selective D_3 (P>0.05). Among 216 cases of stage III gastric antrum and body carcinoma managed from 1975 to 1989 in our hospital. The 5-year survival rate was 35.7% in 114 cases treated with D_2, and 56.3% in 102 cases treated with selective D_3, difference was significant statistically (P<0.01).

DISCUSSION

Surgical resection is the treatment of choice for gastric carcinoma and the resection of lymph nodes is a very important part of the operation. To reduce the residual lymphatic metastasis as much as possible, we conducted a research into the lymph node metastasis of gastric carcinoma, and found that there was a close relationship between the site of tumor, the depth of invasion, the size of tumor and the biological behavior of the tumor. And there was a definite role of lymph node metastasis, except for the carcinoma involving the whole stomach.

Based on the research, we designed the selective D_3 operation. This operation includes mainly: a. The complete resection of lymph nodes in stations 1 and 2, and those of higher rate of metastasis in station 3. b. As to the low lymph node metastasis rate of stations 3 and 4, whether they should be resected or not may be judged by if any metastasis was found during the operation in combination with the clinical pathological factors. No statistical difference of complication and mortality rate was noted between selective D_3 and D_1 and D_2 modality. Long-term clinical practice showed that the selective D_3 operation can significantly prolong the survival of stage III cases and part of the stage IV cases, with significant statistical difference from D1 and D_2. No significant statistical difference in survival time was noted in comparison with D_3, but the operational injury was less severe and unnecessary resection of whole stomach can be avoided in part of the selective D_3 cases with better quality of post-operational life.

Through more than 20 years of practice, we consider the indications for selective D_3 operation are: a. carcinoma with invasion to the serosa without involvement of liver and peritoneum; b. direct invasion to neighboring tissues and organs, which can be radically resected by combined resection; and c. minor metastasis to peritoneum close to the primary lesion and isolated metastasis to liver, which can be completely resected. Contraindications: a. carcinoma with invasion to mucosa and submucosa only. In case except there was metastasis to lymph nodes in station 3, D_2 was used routinely; b. carcinoma involving whole stomach (>2 regions). If these lesions can be completely resected, D_3 was used; and c. extensive metastases to liver and peritoneal cavity.

REFERENCES

1 Lin CH, Wang RS, Ma XZ, Qian YQ, Chen QS, Zhang YT *et al.* Gastric carcinoma study of lymphatic metastasis. *Chin Med J,* 1984;97(10):741-746
2 Lin CH. Gastric carcinoma study of lymphatic metastasis. *J Abdom Surg,* 1992;5(1):43-44
3 Lin CH. Clinical experience in the surgical treatment of 1399 cases of gastric carcinoma. *Chin Med J,* 1987;100(4):273-280

 ISSN 1007-9327 CN 14-1219/R WJG, 1998;4(3):266-267

Expression of nm23 gene in hepatocellular carcinoma tissue and its relation with metastasis

HUANG Bei, WU Zhong-Bi and RUAN You-Bing

Subject headings liver neoplasms; carcinoma, hepatocellular; nm23 gene; gene expression; neoplasm metastasis; immunohistochemistry

INTRODUCTION

Among the mostly expressed 23 genes in nonmetastatic tumors, *nm23* had the highest frequency. Steeg *et al*[1] first identified and cloned its complementary DNA and confirmed that its lower expression was related to the high metastatic activity of melanoma cell lines. Many studies found afterwards that the expression of *nm23* at the RNA or protein level was inversely correlated with the development of metastasis or poor clinical course in cohorts of several human tumor types, including breast, colorectal and gastric carcinomas. But the effects of *nm23* on metastasis of hepatocellular carcinoma (HCC) is still unclear. In this study we have investigated *nm23* expression in HCC with immunohistochemical techniques and the correlation between its expression level and metastatic progression.

MATERIALS AND METHODS

Subjects

Specimens of 24 cases of human HCC were obtained from surgical resections in Tongji Hospital. Observations were carried out on tissues from tumor areas, nonneoplastic areas and their boundary areas when available. Ten of them showed cancer cell emboli in portal vein or metastasis in portal lymph nodes or in distant organs, e.g. in the lung. Fourteen cases without metastasis were characterized by no findings of tumor invasion into the surrounding tissues at operation or no metastasis outside the liver by X-ray and sonography. The samples were fixed with 4% paraformaldehyde and embedded with paraffin. Successive sections were stained with HE, as well as immunohistochemically with the SP method. The staining was considered negative (-) when no cells were stained on the section, and weakly (+), moderately (++) and strong (+++) positive, when a few, more and a lot of cancer cells were darkly stained, respectively.

RESULTS

The positive signal revealed brown grains in cytoplasm of tumor cells. *nm23* protein expressed highly in HCC, but was not obviously related to the degree of malignancy histologically. The positive rate was 67% (16/24). The expression of *nm23* was heterogeneitic in different cancer cell nodules and in the same nodule. The positive cells presented focal distribution or scattered through the cancer nodules. *nm23* protein also expressed in the normal liver tissues around the carcinoma. The positive rate of *nm23* was 86% in the group without metastasis, and 40% in the group with metastasis. The *nm23* expression level in metastatic HCC was significantly lower than that in nonmetastatic HCC ($P<0.05$, Table 1).

Table 1 Relationship between [a]«nm23[a]« expression and metastasis of HCC

Groups	*n*	*nm23* expression				Positive rate(%)
		-	+	++	+++	
Nonmetastatic	14	2	3	3	6	85
Metastatic	10	6	2	1	1	40[a]

[a]$P<0.05$ compared with metastatic group.

DISCUSSION

nm23 is a suppressor gene for tumor metastasis that encodes nucleoside diphosphokinase (NDPK). NDPK causes activation of a G protein pathway involved in the signal transduction of many growth factors and hormones. Expression of *nm23* at the RNA or protein level was shown to be inversely correlated with the staging and differentiation of human breast cancer. In later period of poorly differentiated tumors, *nm23* showed in general a lower expression and their recidive rate was higher, and survival rate was low[2]. Similar results were obtained by prostate and thyroid carcinoma[3]. Our data showed that the expression level of *nm23* was

Department of Ultrastructural Pathology, Research Center of Experimental Medicine, Tongji Medical University, Wuhan 430030, Hubei Province, China

Dr. HUANG Bei, female, was born on Feb. 13, 1964 and graduated from Tongji Medical University in 1987.

***Project supported by the National Natural Science Foundation of China, No. 39070376**

Correspondence to: Dr. HUANG Bei, Department of Ultrastructural Pathology, Research Center of Experimental Medicine, Tongji Medical University, Wuhan 430030, Hubei Province, China

Tel. +86 • 27 • 3692639

Received 1997-09-10

significantly lower in cases of HCC with metastasis than that without metastasis, suggesting that *nm23* had some effects of inhibiting metastasis of HCC. However, no relation between expression of *nm23* and lymph node metastasis was reported by Haut *et al*[4]. However, Cohn *et al*[5] found that nm23 was associated with distant metastasis after operation in colorectal carcinoma. Moreover, *nm23* was reported to be related with lymph node metastasis in pulmonary squamous cell carcinoma, but not in pulmonary adenocarcinoma[6]. Our preliminary study also showed that there was no nm23 expression in 2 nonmetastatic HCC tissues, but stronger expression in 1 metastatic HCC. These suggested that some other regulatory factors may exist evidently in the process of metastasis of HCC.

REFERENCES

1 Steeg PS,Bevilacqua G, Kopper L, Thorgeirsson UP, Talmadge JE, Liotta LA *et al*. Evidence for a novel gene associated with low tumor metastatic potential. *J Natl Cancer Inst,* 1988;80(3):200-204

2 Hennessy C, Henry JA, May FEB, Westley BR, Angus B, Lennard TWJ. Expression of the antimetastatic gene nm23 in human breast cancer and associated with good prognosis. *J Natl Cancer Inst,* 1991;83(4):281-285

3 Konishi N, Nakaoda S, Tsuzuki T, Matsumoto K, Kitahori Y, Hiasa Y *et al*. Expression of nm23-H1 and nm23-H2 proteins in prostate carcinorma. *Jpn J Cancer Res,* 1993;84(10):1050-1054

4 Haut M, Steeg PS, Willson JKV, Markowitz SD. Induction of nm23 gene expression in human colonic neoplasms and equal expression in colon tumors of high and low metastatic potential. *J Natl Cancer Inst,* 1991;83(10):712-716

5 Cohn KH, Wang F, Desoto-Lapaix F, Solomon WB, Patterson LG, Arnold MR *et al.* Association of nm23-H, allelic deletions with distant metastasis in colorectal carcinoma. *Lancet,* 1991;21.Sep,338(8769):722-724

 ISSN 1007-9327 CN 14-1219/R WJG, 1998;4(3):268-270

Detection of blood AFPmRNA in nude mice bearing human HCC using nested RT-PCR and its significance

LIU Yang, ZHANG Bai-He, QIAN Guang-Xiang, CHEN Han and WU Meng-Chao

Subject headings carcinoma,hepatocellular/pathology; lung neoplasms/secondary;kidney neoplasms/secondary; alpha-fetoproteins/analysis; RNA, messenger; polymerase chain reaction

Prognosis of patients with HCC is estimated by several factors, such as histological differentiation of tumor cells, tumor size, and extent of lymhatic or hemotogenous spread. In this study, we detected the AFPmRNA in the blood of nude mice bearing human hepatocellular cacinoma (HCC) using nested reverse transcriptase polymerase chain reaction (nested RT-PCR) and study its significance and role in blood spread and distant metastasis.

MATERIALS AND METHODS

Animal SMMC-LINM cell lines which can secrete AFP (provided by the pathology department of our university[1]) were inoculated into the neck and back of nude mice (BALB/C/NU, 4 weeks after birth), (107 HCC cells to each mouse). After 6 weeks, 20 nude mice (15g-20g in weight) with tumors growing to 2cm-4cm were used in the experiment.

Collection of samples Both eyes of the nude mice bearing HCC were scooped out and blood (about 1ml) was collected and placed into a 12ml centrifuge tube. The subcutaneous tumors were resected, and their integrity and relationship with the surrounding tissues were observed. The liver, lung, kidneys and other oragans of the mice were cut and examined pathologically.

Methods One ml whole blood was collected from the peripheralvein of each subject into a centrifuge tube. AFPmRNA was detected with nested RT-PCR. The detailed procedures were as follows.

The East Institute & Hospital of Hepatobiliary Surgery, Second Military Medical University, Shanghai 200438, China

*Supported by the Fund for Key Laboratories of PLA.[a¤]

Correspondence to Dr. Liu Yang, The East Institute & Hospital of Hepatobiliary Surgery, Second Military Medical University, Shanghai 200438, China[a¤]

Tel. +86¡¤21¡¤65564166 ext 75417

Received 1998-04-01

Detection of AFPmRNA Heparinized whole blood was centrifuged and the plasma fraction was removed. The cellular fraction was enriched for mononuclear cells or possible tumor cells according to the method by Komeda[2]. Total cellular RNA was extracted by a single-step method of RNA isolation[3]. The reverse transcription reaction was carried out in 20 μl reaction mixture using a first-strand cDNA synthesis kit (Promega USA) according to the manufacturer's instructions. Nested PCR was conducted by addition of 5 μl solution of cDNA to 100 μl reaction mixture containing 10mM Tris HCl (pH 9.0), 50mM potassium chloride,4.5mM magnesium chloride, 250nM dNTP 15pmol of each outer primer (EX-sense and EX-antisense) and 2.5 units of Taq DNA polymerase (Promega, USA). The reaction mixtures were subjected to 35 cycles of amplification in a programmable thermal cycler (Perking-Elmer Cetus, USA) using the following sequence: 94℃ for 1.5min, 57℃ for 1.5min and 72℃ for 2.5min, and a final extension step at 72℃ for 10min. A sample of 10 μl of the first amplification product was further amplified using an inner pair of primers (IN-sense and IN-antisense). To verify the amplified AFP DNA fragment, the samples were digested with the restriction enzyme Pst I and analysed by electrophoresis on a 2% agrose gel and stained with ethidium bromide for the specific bands of 174 base pairs (first amplification product) and 101 base pairs (second amplification product). Nested PCR was performed two or three times for samples with conflicting results. The external and inner pair of primers were designed as follows:

EX-sense 5'-ACTGAATCCACAACACTGCATAG-3'

EX-antisense 5'-TGCAGTCAATGCATCTTCACCA-3'

IN-sense 5'-TGGAATAGCTTCCATATTGGATTC-3'

IN-antisense 5'-AAGTGGCTTCTTGAACAAACTGG-3'

According to this design, the PCR products of 176 and 101 base pairs were amplified from AFPcDNA by external (EX-sense and EX-antisense) and internal (IN-sense and IN-antisense) primer pairs, respectively. EX-sense was located in exon 1 (AFPmRNA nucleotides 90-112), EX-antisense in exon 2 (AFPmRNA nucleotides 241-263), IN-sense over exon 1 and exon 2 (AFPmRNA nucleotides 122-145) and IN-antisense in exon 3

(AFPmRNA nucleotides 200-222). cDNA sequences followed the method reported previously[4].

Statistical analysis The relationship between the AFPmRNA in peripheral blood and various clinical parameters was examined by Chi-square test.

RESULTS

AFP mRNA was detected in the blood of 6 (30. 0%) mice bearing HCC, 4 (66.67%) of 6 nude mice had distant metastasis in lungs, liver or kidneys (Figures 1-3).

Table 1 The relationship between detectable rate of AFPmRNA and distant metastasis

Types	Cases	Cases of metastasis	Metastasis rate
AFPmRNA (+)	6	4	66.67[b]
AFPmRNA (-)	14	0	0.00

[b]$P<0.01$, *vs* AFPmRNA (-).

The diameters of HCC in 6 mice with positive AFP mRNA in blood were more than 3cm, no distant metastasis occurred in tumors below 3cm in diameter (Table 2).

Table 2 The relationship between tumor diameters and distant metastasis

Diameter	Cases	Cases of AFPmRNA (+)	Positive rate
>3cm	9	6	66.67[b]
<3cm	11	0	0.00

[b]$P<0.01$, *vs* tumors below 3cm in diameter.

AFPmRNA was detected among 12 (50%) nude mice bearing HCC with serum AFP levels beyond 4 000 μg/L while no AFPmRNA was found in 8 nude mice with serum AFP levels below 4 000 μg/L (Table 3).

Table 3 The relationship between AFP levels in serum and detectable AFPmRNA

AFP levels(μg/L)	Cases	AFPmRNA (+)	Positive rate
>4000	12	6	50.0[b]
<4000	8	0	0.0

[b]$P<0.01$, vs nude mice with serum AFP levels below 4 000 μg/L.

The first-cycle PCR products, 174 base pairs, can be cut into two pieces of 102 and 72 base pairs by restriction enzyme Pst I. The second-cycle PCR product, 101 base pairs, can be cut into two pieces of 60 and 41 base pairs (Figure 4).

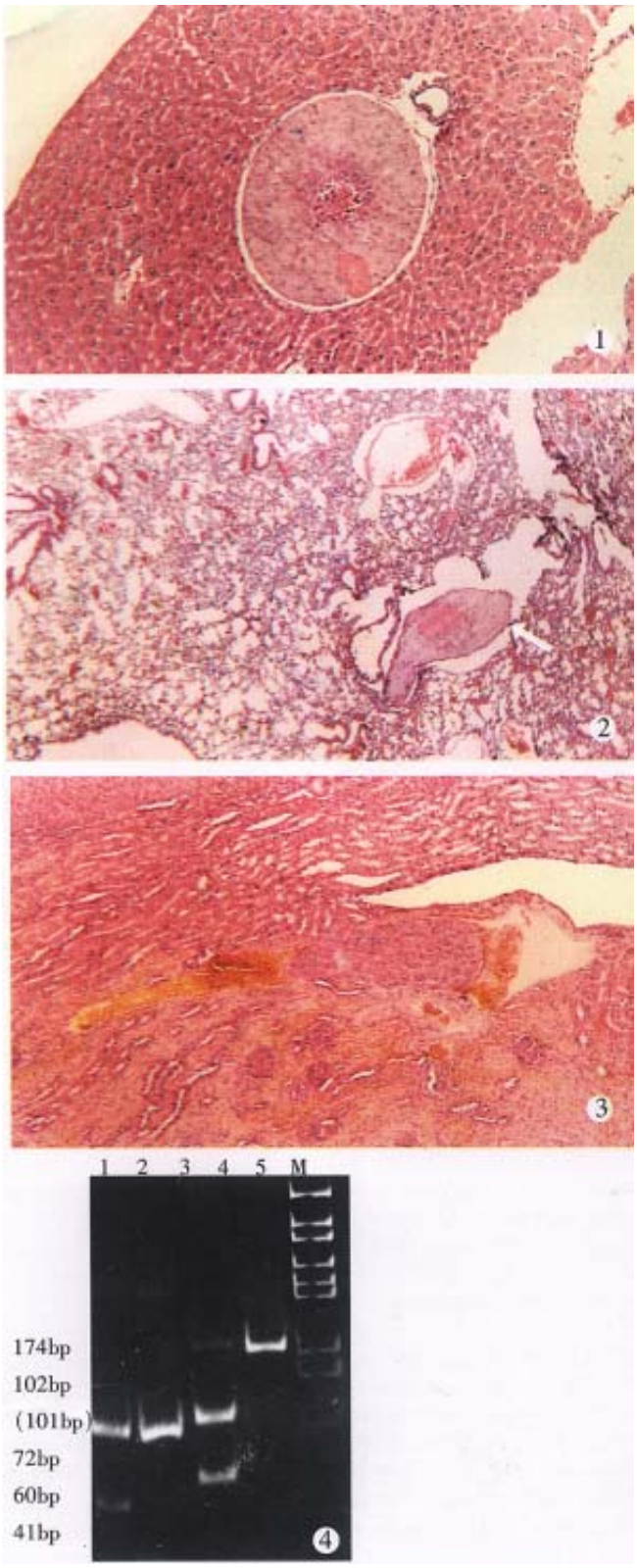

Figure 1 Metastasis in liver. (×30)
Figure 2 Metastasis in lungs. (×30)
Figure 3 Metastasis in kidney. (×30)
Figure 4 The first-cycle PCR products was cut into two pieces of 102 bp and 72 bp by restriction enzyme Pst I; and the final PCR products was cut into two pieces of 60 bp and 41 bp.

DISCUSSION

Recently, there have been some reports about the employment of the reverse transcriptase-polymerse chain reaction (RT-PCR) technique to detect tumor cells spreading into the peripheral blood, bone marrow, and lymph nodes [5-7]. There trials have aimed to amplify tumor-specific gene transcripts which can not be detected in these tissues under normal conditions. Free mRNA is so fragile under conditions of abundant RNAse activity that the specific mRNA in blood can indicate the presence of intact cells producing such proteins just before the extraction of RNA.

This study showed that AFPmRNA was detected in 6 (30.0%) of 20 nude mice bearing human HCC 4 (66.67%) of them had distant metastasis. None of 14 nude mice with negative AFPmRNA in blood had distant metastasis ($P<0.01$), suggesting that the distant metastasis occurred via blood circulation. The detectable rates of AFPmRNA was significantly related with AFP levels, tumor size and distant metastasis ($P<0.01$). In other words, AFPmRNA in blood may be a prerequisite for distant metastasis of HCC.

In conclution, AFPmRNA may be an effective and sensitive marker for HCC matestasis in blood and distant metastasis as well.

REFERENCES

1 Ji YY, Liu YF, Chen ZN. Radioimmuno-detection and autoradiographic localization of monoclonal antibody against human hepatocellular cancinoma in xenografts. *Cancer*, 1992;69:2055-2059
2 Komeda T, Fukuda Y, Sando T, Kita R, Furukawa M, Nishida N *et al*. Sensitive detection of circulating hepatocellular cacinoma cells in peripheral venous blood. *Cancer*, 1995;75(9):2214-2219
3 Chomzynski P, Sacchi N. Single-step method of RNA isolation by acid guanidinium thiocyanate-phenol-chloroform extraction. *Anal Biochem*, 1987;162:156-159
4 Morinaga T, Sakai M, Wegmann TG, Tamaoki T. Primary structures of human α-fetoprotein and its mRNA. *Proc Natl Acad Sci USA*,1980;80:4604-4608
5 Schoenfeld A, Luqmani Y, Smith D, Reilly SO, Shousha S, Sinnett HD *et al*. Detection of breast cancer micrometastasis in axillary lymph nodes by using polymerase chain reaction. *Cancer Res*,1994;54:2986-2990
6 Ghossein RA, Scher HI, Gerald WL, Kelly WK, Curley T, Amsterdam A *et al*. Detection of circulating tumor cells in patients with localized and metastatic prostatic cacinoma: clinical implications. *J Clin Oncol*, 1995;13(5):1195-1200
7 Pfleiderer C, Zoubek A, Gruber B, Kronberger M, Ambros PF, Lion T *et al*. Detection of tumor cells in peripheral blood and bone marrow from ewing tumor patients by RT-PCR. *Int J Cancer*, 1995;64:135-139

Biological effects of hepatoma cells irradiated by 25MeV/u$^{40}Ar^{14+}$

ZHOU Guang-Ming[1], CHEN Wei-Qiang[1], GAO Qing-Xiang[2], LI Wen-Jian[1], LI Qiang[1] and WEI Zeng-Quan[1]

Subject headings carcinoma,hepatocellular/radiotherapy; liver neoplasms/radiotherapy;argon/therapeutic use

INTRODUCTION

Radiotherapy was initiated when Grubbe treated tumor with X-rays in 1896[1]. Afterwards, radioisotopes such as Ra and Rn, were used for clinical?diagnosis and treatment. Basic researches on the biological effects of X-rays, γ-rays, fast neutron, and so on discovered that damages to mammalian cells induced by high-LET irradiation were more serious than that by low-LET[2].

Because of their low oxygen enhancement ratio (OER) and high relative biological effectiveness (RBE), heavy ions can kill carcinoma cells efficiently[3], among which about 5%-20% was hypoxia. There was a Bragg peak along the energy deposition of heavy ions, so that more dose could reach to the tumor while less to the normal tissues[4]. Therefore, heavy ion beam is believed to play an important role in the future in the radiotherapy for tumors.

The treatment with heavy ion beam has been studied and put into clinical practice since the 1970s in America and since 1994 in Japan. But in our country, this research is still in its initial stage. This is our preliminary report on the dose--response and fractionated irradiation with 25MeV/u^{40} Ar^{14+} in human hepatoma SMMC-7721 cells.

MATERIALS AND METHODS

Cell culture

The human hepatoma SMMC-7721 cell line was obtained from the Second Military Medical University[5]. The cells were cultured in RPMI-1640 medium (Gibco Inc.) supplemented with 10% calf, 100u penicillin and 100 μg/ml streptomycin. The medium was placed at 37℃ in humidified atmosphere with 5% CO2. The cells were inoculated in the glass flasks with a diameter of 35mm and density of 5×104cells/ml 2 days before irradiation.

Irradiation

25MeV/u $^{40}Ar^{14+}$ was accelerated by HIRFL. The intensity of the beam was 2.1×106 ions/s.

Before irradiation, the medium was removed and the cells were washed twice with D-Hank's buffer. The flasks were enveloped with 4 μm mylar membrane. A part of cells were irradiated at the dose of 0.68 Gy, 6.8 Gy, 68 Gy, 680 Gy and 6800 Gy, respectively. The others were irradiated with tractionated dose of 68 Gy for 1, 2, 3 and 4 times, respectively, at an interval of 2 hours. After irradiation, each flask was added 2ml medium and kept in 37℃ incubator for 24 hours.

Analysis of samples

After washed with D-Hank's buffer, the cells were fixed for 4 hours and then stained with acridine orange (0.01mg/L, pH 6.8) for 10min and differentiated with stilled water for about 5min. Cells with micronuclei were counted under the fluorescence microscope to obtain frequency of micronuclei (FM). Afterwards, cells were washed once with PBS (pH 6.8) and stained with Giemsa (1:20, pH 6.8) for 8 min to gain number of cells per mm^2 (NC).

RESULTS

Observation of cellular configuration

Under the florescence microscope, the null were bright yellow while cytoplasm and nucleolus were red. After irradiation, many types of aberration were observed, such as micronuclei, small nuclei, free chromosomes, chromosome bridge, and so on (Figure 1).

Cells treated with 680 Gy and 6 800 Gy were dead, but the remnants appeared different. The remnants induce by 680 Gy were far smaller than controls and the nuclei were bright yellow and the cytoplasm was light yellow, while those induced by 6 800 Gy change little in size, but the nucleus and the cytoplasm could not be distinguished. The death of the former may be caused by the change of the permenace ability of cellular membrane caused by

[1]Institute of Modern Physics, Chinese Academy of Sciences, Lanzhou 730000, Gansu Province, China
[2]Biological Department of Lanzhou University, Lanzhou, 730000, Gansu Province, China
Dr. ZHOU Guang Ming, male, born on 1970-07-01 in Zhijiang City, Hubei Province graduated from Biological Department of Lanzhou University in 1990, research intern majoring nuclear biology, having 6 papers published.
Presented at the 4th Symposium on Radiation Research and Radiation Technology, Changchun, 24-27 June, 1996.
***Supported by the Top Project of National Fundamental Research, No. 01-3.**
Correspondence to: GAO Qing Xiang, Institute of Modern Physics, Chinese Academy of Sciences, Lanzhou 730000, Gansu Province, China
Tel. +86 • 931 • 8854897
Received 1997-11-26 **Revised** 1998-01-04

the high dose, and shrinking of the cells. When fixed, the nuclei were smaller than controls but not disperse. The dose for the latter one was even higher, and cells died quickly after irradiation. So, the nuclear membrane was broken, and the nuclei entered the cytoplasm when fixed.

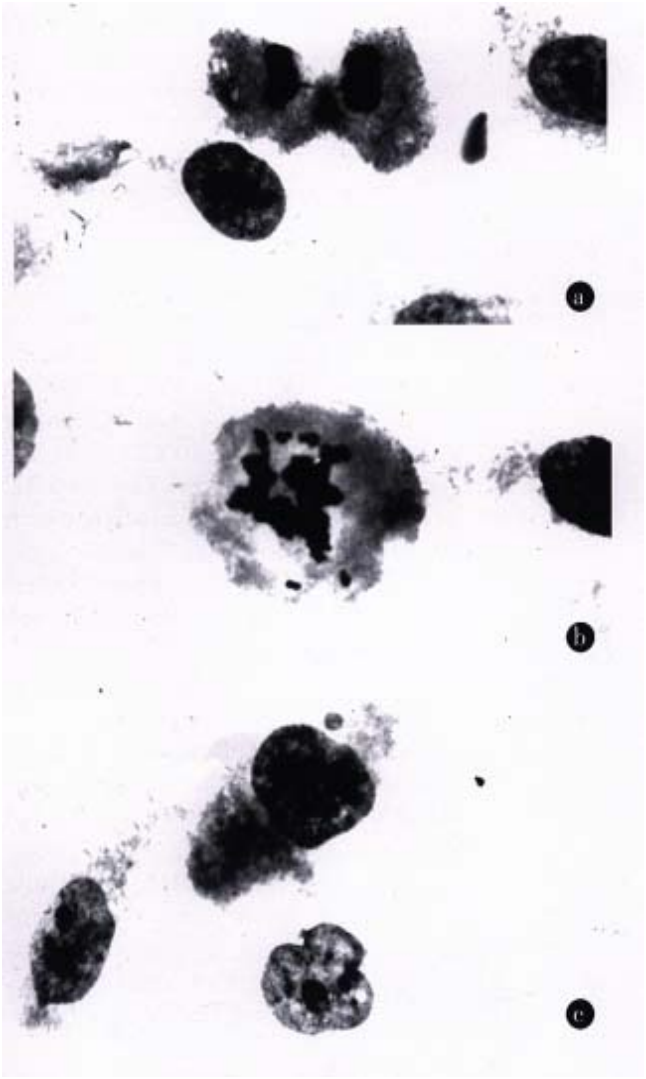

Figure 1 Abnormal nuclei and chromosome aberration induced by 25MeV / u$^{40}Ar^{14+}$
a. micronuclei, b. free chromosome, c. chromosome bridge.

Dose-response

As shown in Table 1, FM of the samples was higher than the control, which was correlated positively with the dosage (r = 0.9952) while NC was negatively correlated with dosage (r = -0.9279). This is consistent with other approaches[6].

Response of fractionated irradiation

As shown in Table 2, with the increase of irradiation times FM decreased and NC increased. The correlation coefficient was r = -0.9590 and r = 0. 9681, respectively.

Table 1 Dose-response of single irradiation with heavy ions

Dose (Gy)	Number of cells	FM (%)	NC
0	861	2.56	380
0.68	1952	4.27	391
6.8	2008	4.83	235
68	1960	5.62	207

Table 2 Biological effects of fractionation irradiation

Times of irradiation	Number of cells	FM (%)	NC
1	1960	5.62	207
2	971	5.13	213
3	974	2.47	250
4	1000	1.80	281

DISCUSSION

The damages induced by heavy ions were intensified with the increasing dose, but NC induced by 0.68 Gy was higher than that of the control, possibly because very low dose can stimulate cell propagation.

When the times of irradiation were increased, the repair mechanism is activeted and the efficiency of repair was enhanced. FM induced with four divided doses was less than that of control. This may be due to the high repair efficiency.

MF peaked when cells underwent one division cycle after irradiation[6]. The time of a division cycle was about 24 hours because of the delayed division induced by irradiation. According to our approach, FM was not the highest one (the data are not shown), but there was significant correlation between MF and dosage, MF and the times of irradiation. Micronucleus was one kind of nuclear structure, less than 1/5 of the normal nucleus, forming fragments induced by irradiation during the cell division. Therefore, FM after one division cycle represented the direct effects of irradiation with heavy ion beam.

NC was closely correlated with FM, but NC represented by the lethal effect more directly that FM. The correlation efficient was -0.8870 for single one. Both as the endpoints of radiosensitivity, they reflected the same results.

REFERENCES

1 Manuel Lederman MB, FRCR. The early history of radiotherapy: 1895-1939. *Int J Radiat Oncol Biol Phys*, 1981;7(5):639-648
2 Ritter MA, Cleaver JE, Tobias CA. High-LET radiations induce a large proportion of non-rejoining DNA breaks. *Nature*, 1977;266(5603):653-655
3 Zhu RB, Liu Y, Luo ZY. *Radiobiology*.1st ed, *Beijing: Science Press*, 1987: 572-592
4 Lu ZL.Application of accelerator in medicine. *Trends Nucl Phys*, 1989;6(1): 38-42
5 Dong RC, Zhou RH, Lu FD. The establishment and biological study of human hepatoma SMMC-7721 cells. *Second Military Med Univ*, 1980;1(1):5-9
6 Midander J, Revesz L. The frequency of micronuclei as a measure of cell survival in irradiated cell populations. *Int J Radiat Biol*, 1980;38(2):237-242

Effects of Yibei multi-active elements on mesenteric microcirculation in rats

SHAO Bo-Qin[1], SHI Yi-Ju[2], LIU Sai[1], ZHANG Jian[1], GUO Jin-Tai[1]

Subject headings **microcirculation; mesentery; Yibei multi-active elements (YBMAE); blood flow velocity**

Mytilus edulis linnaeus (Yibei) belongs to mytilide, gill lamella, and mollusc. There are rich resources in Bohai and Huanghai of China. Yibei multi-active elements (YBMAE)[1] come from mytilus edulis linnaeus containing taurine, EPA, Zn, Ci, Ferris, etc. Its preparation and composition were described previously[2]. This paper aims at studying the effect of YBMAE on the mesenteric microcirculation in rats.

MATERIALS AND METHODS

Materials

YBMAE was provided by the Department of Pharmacology, Medical College of Qingdao University. Sterile amniotic fluid and Panax Notoginsenosidum (PNS) were obtained from Taishan Medical College. Wistar rats were purchased from the Animal Center of Shandong Medical University. The microcirculation monitoring system was product of Xuzhou Optic Instrument Factory, China.

Methods

Thirty Wistar rats (male or female, weighing 300g±50g) were divided into 5 groups: YBMAE group I (1.2g/kg), group II (3g/kg), group III (6g/kg), PNS group (40mg/kg) and control group (with saline). Each group consisted of 6 rats. The drugs were givenig qd for 28 days[3-5]. Thirty minutes after the last administration of drugs, the rats were anaesthetized with vinbarbitol 50mg/kg ip. A 2-cm incision was made on the abdominal wall. The blood color, flow velocity and vessel wall clarity of tertiary blood vessels were observed, meanwhile blood flow and flow velocity were monitored with microcirculation monitoring system. Sterile amniotic fluid (1ml/kg) was given intravenously. The above-mentioned indexes were monitored and video recorded immediately 10 and 30min after amniotic fluid injection.

Statistical analysis Student's *t* test was used for the statistical study.

RESULTS

Effect of YBMAE on blood flow of Wistar rat mesenteric microcirculation

Immediately, 10min and 30min after amniotic fluid injection, blood flow of the control group was decreased significantly ($P<0.05$, $P<0.01$, $P<0.01$), while the blood flow of YBMAE groups I and II showed no obvious changes compared with that before amniotic fluid injection, but more significant changes than that of the control groups ($P<0.05$, $P<0.01$). In YBMAE group III, the blood flow at 10min was lower than that before amniotic fluid injection ($P<0.05$), significantly higher at 30min than the control group ($P<0.01$). In PNS group, the blood flow had no obvious changes immediately and 10min after amniotic fluid injection, and increased at 30min ($P<0.01$), being significantly different compared with the control group ($P<0.05$, $P<0.01$) (Table 1).

Effect of YBMAE on blood flow velocity of rat mesenteric microcirculation

The blood flow velocity was greatly decreased immediately, 10min and 30min after amniotic fluid injection in the control group ($P<0.05$, $P<0.01$), while in the YBMAE group I, there was little change in the blood flow velocity, but greater than that of the control group ($P<0.05$, $P<0.01$). In YBMAE group II, right after amniotic injection, the velocity was significantly decreased ($P<0.05$), but still faster than that of the control group. At 10min, 30min, the velocity was increased, but not faster than that before amniotic injection. In YBMAE group III, the velocity was decreased

[1]Department of Pharmacology, Medical College of Qingdao University, Qingdao 266021, Shandong Province, China
[2]Research Laboratory of Microcirculation, Taishan Medical College, Taishan 271000, Shandong Province, China
Prof. SHAO Bo Qin, male, born on January 23, 1944, in Qingdao, Shandong Province, graduated from Qingdao Medical College in 1969, now associated professor of pharmacology, Vice Director of Clinical Pharmacological Institute, engaged in clinical pharmacology and antiaging drug studies, having 24 papers and 7 books published.
***One of the National "8.5" Key Projects of Scientific and Technical Researches, No.85-08-07-09.**
Correspondence to: Prof. SHAO Bo Qin, Department of Pharmacology, Medical College of Qingdao University, Qingdao 266021, Shandong Province, China
Tel. +86 • 532 • 2017880
Received 1997-11-26 **Revised** 1998-01-04

immediately and 10min after injection (P<0.05), and increased at 30min, which was significantly faster than that of the control group at any time (P<0.05, 0.01). In PNS group, the velocity had no obvious changes after injection, but significantly faster than the control group (P<0.05) (Table 2).

Effect of YBMAE on microcirculation status, blood color and vessel wall clarity of rat mesentery

The microcirculation condition of the control group changed from linear to linear granular flow after amniotic fluid injection. At 30min, 90% of the vessels turned to linear granular flow, the blood color was dark red, the vessel wall was not clear, and there was stasis in the venous blood. At 12 h, 50% of the animals died. In the three YBMAE groups and PNS group, 40%, 10%, 0% and 0% vessels had linear granular flow after amniotic fluid injection. The blood color changed from bright red to dark red in about 30%, 20%, 20%, 10% vessels respectively. Thirty minutes later, it returned to normal, and the vessel walls became clear. No animals died within 12 h.

Table 1 Effect of the drugs on blood flow (μm3 • s^{-1}) of mesenteric microcirculation in rats ($\bar{x}\pm s$)

Groups	Dosage (g/kg)	n	Before amniotic fluid injection	After amniotic fluid injection		
				Immediately	10min	30min
NS			6616±91.79	432±132.68[a]	358±64.32[b]	348±84.30[b]
YBMAE	1.2	6	576±67.41	545±105.47	593±70.63[d]	560±57.12[d]
	3.0	6	560±57.88	450±86.49	561±77.96[c]	588±50.75[d]
	6.0	6	733±100.76	602±99.26	578±93.03[ac]	665±73.12[d]
PNS	0.04	6	586±60.58	616±67.34[c]	638±55.11[d]	766±60.40[bd]

Compared with before amniotic fluid injection, [a]P<0.05, [b]P<0.01; compared with NS, [c]P<0.05, [d]P<0.01.

Table 2 Effect of the drugs on the blood flow velocity of rat mesenteric microcirculation ($\bar{x}\pm s$)

Groups	Dosage (g/kg)	n	Before amniotic fluid injection	After amniotic fluid injection		
				Immediately	10min	30min
NS			60.51±0.10	0.35±0.05[a]	0.32±0.10[a]	0.32±0.08[a]
YBMAE	1.2	6	0.56±0.05	0.52±0.07[c]	0.49±0.07[c]	0.55±0.05[d]
	3.0	6	0.54±0.05	0.45±0.07[a]	0.53±0.07[d]	0.55±0.04[d]
	6.0	6	0.64±0.06	0.48±0.08[a]	0.49±0.08[ac]	0.59±0.06[d]
PNS	0.0	6	0.50±0.07	0.45±0.06	0.49±0.06[c]	0.52±0.07[c]

Compared with before amniotic fluid injection, [a]P<0.05, [b]P<0.01; compared with NS, [c]P<0.05, [d]P<0.01.

DISCUSSION

Recent studies showed that the flow velocity, blood flow, flow status, the agglutination ability of platelet and red blood cell, the amount of opening capillary were important factors determining the functional status of the flow velocity, improve the blood flow status, the blood color, the vessel wall clarity, increased the amount of opening capillaries[6]. The results of this study demonstrated that YBMAE could increase the blood flow, and could improve the microcirculation status. The increment of flow velocity and blood flow were proportional to the amount of YBMAE before and 30min after amniotic fluid injection. According to the literature, taurine could regulate Ca^{++} metabolism and prevent arterial atherosclerosis[7]. EPA could inhibit the blood vessel constriction induced by norepinephrine, and vasoconstrictin A2 and increase elasticity of RBC, decrease the blood viscosity and synthesis of TXA2[8]. YBMAE contains plenty of taurine, EPA, amino acid and unsaturated lipid acid, therefore the effect of YBMAE in improving microcirculation may be related to its components.

REFERENCES

1 Health Department of Logistic Ministry of Navy, PLA, China. Pharmacological marine creature. 1st ed. Shanghai: *Shanghai People's Publication*, 1977: 68-69
2 Ming L, Shao BQ, Zhang Y, Li WP, Xu SY. The influence of YBMAE on quail experimental atherosclerosis. *Chin Pharmacol Bull*, 1996;12(6):554-556
3 Xu SY (editor). Pharmacological experimental methodology. 2nd ed. Beijing People's Health Publishing House, 1994:992-1003
4 Li YK (editor). Pharmacological experimental methodology. 1st ed. Shanghai: Shanghai Science and Technology Publishing House, 1991:141-147
5 Xu SK (editor). Antiaging material media. 1st ed. Beijing: China Medical and Pharmacentical Science and Technology Press, 1994:185-193
6 Pang DW, Liu MY, Tan JM, Li ZY, Shi SH. The influence of aspirin and reephedrine on the microcirculation of white mouse mesentery. *Chin Pharmacol Bull*, 1996;12(4):356
7 Wang SN, Zhang HL, Wu DC, Wang H. The pharmacological research advancement and clinical usage of taurine. *China Pharmacy*, 1993;4(4):33-34
8 Wu BJ (editor). Pharmacology of animal biochemical medicine. 1st ed. Beijing: China Commercial Press, 1993:54-63

Effects of erythromycin on pressure in pyloric antrum and plasma motilin and somatostain content in dogs

HUANG Yu-Xin[1], CHEN Yue-Xiang[1], HUI De-Sheng[3], LI Hua[4], LI Chun-An[5], SUN Tian-Mei[2], WANG Qing-Li[1]

Subject headings erythromycin/pharmacology; somatostatin/blood;motilin/blood;pyloric antrum/drug effects

INTRUDUCTION

Erythromicin (EM) is a potent agonist of motilin (MTL) receptors[1]. EM may enhance the gastroenteric motion by binding with MTL receptors[2]. However, effects of EM pyloric antrum and its mechanism are not clear. The purpose of this study was to investigate the relation between EM, plasma MTL and somatostatin in regulation of pyloric sphincter muscle function in dogs.

MATERIALS AND METHODS

A randomized study was performed using male or female dogs weighing between 11kg-19kg. Before operation, dogs was prohibited form eating food for 24h.

Animals were anaesthetised with i.v. injection of pentobarbital (2.5%, 1mg/kg). The upper medial incision of abdomen was performed. The anterior wall of gastric antrum was cut about 0.5cm, the tube of the gastric pressure meter (WYY-1 type, Sapceflight Medicine Engineer Research Institute) was inserted and fixed. The pressure graph was recorded by the pressure transducer.

Erythromycin lactate was dissolved in 5% glucose liquid, and transfused i.v. (5mg/kg per hour). Isoptin (1mg/kg) was injected i.v. at an interval of 60min. At 90min i.v. atropine sulfoacid (0.1mg/kg) was given. During 120min of pre- and post-infusion, pressure measure was done for 2min and 1ml blood sample was collected from dog femoral vein every 15min. Nine blood samples (1ml each) were collected from each dog. 3ml EDTA-Na2 and 200KIu aprotinin was added into the samples. Blood samples were immediately centrafuged at 3 500r/min for 15min at 4℃. The plasma was stored at -70℃. MTL and SS was assayed by radioimmune method. (MTL and SS radioimmune reagment box, East-Asia Immune Technique Research Institute). The concentration of MTL and SS in blood was counted with a FJ-2003-50G counter.

Statistical analysis

Statistical analysis was carried out using the Statistical analysis System. When a significant analysis of variance was found, Student's *t* test between two samples was performed.

RESULTS

The changes of plyoric pressure and the concentration of MTL and SS in plasma before and after i.v. transfusion (Table 1).

Our results showed that the dog pyloric antrum basic pressure, total pressure and wave amplitude significantly increased after administration of EM. The interval time of high pressure wave amplitude was reduced and the frequency increased. After i.v. injection of antagonists isoptin and atropine, the plyoric pressure was inhibited repidly. The level of MTL in plasma of dogs and the change of the plyoric pressue induced by EM was related significantly, and were also infuenced by atropine and soptin. The concentration of SS in plasma of dogs was increased after EM administration and not inhibited by atropine and isoptin.

DISCUSSION

EM is one of most common antibiotics. To investigate the gastroenteric side effects of EM, Pilot and Itol, *et al*[3], have found that the i.v. infusion of EM might mimick the migrating synthetical electric current of muscles (or contraction) during dog digestion induced by MTL. The effect of EM was similar with MTL in vivo or vitro, EM competitively inhibited the compination of receptors and MTL, therefore EM is considered one of the agonists on MTL receptors. Sarna, *et al*[4] have found that i.v. EM 1mg • kg^{-1}/h-3mg • kg^{-1}/h

[1]Department of Gastroenterology, [2]Department of Experimental Surgery Tangdu Hospital, Fourth Military Medical University, Xi'an 710038, Shaanxi Province, China
[3]Qingjian County Hospital of Shaanxi, China [4]Tianjin Armed Forces Hospital, China [5]Nanchang No.94 Hospital of PLA, China
Dr. HUANG Yu Xin, male, Born on 1954-02-28 in Qidong City Jiangsu Province, Han nationality graduated from the Fourth Military University as a postgraduate in 1979, professor and director of the department of gastroenterology majoring gastroenterology, having 90 papers published.
***Supported by the National Natural Science Foundation of China, No. 39570885**
Correspondence to: Dr. HUANG Yu Xin, Department of Gastroenterology, Tangdu Hospital, Fourth Military Medical University, Xi'an 710038, Shaanxi Province, China
Tel. +86 • 29 • 3510595 ext 77421
Received 1997-12-18

(far below the dose of antibiotics) might induce migrating synthetical electric current of III phase muscles, beginning at stomach and migrating downward, which was related to MTL release. The main physiological action of MTL is to enhance the gastroenteric motion and increase the gastric and plyoric pressure. By i.v. EM 5mg • kg^{-1}/h, the plyoric pressure increased immediately, suggesting that EM could increase the pressure in plyoric antrum and it was highly sensitive; and the effect of EM was related with MTL. We believe that EM might be used to treat the gastroduodenal reflux diseases in future.

It has been found that the effect of EM on dog stomach, duodenal and gall doct might be inhibited by atropine[5], indicating that EM act on preconjunctional receptors of cholinergic. Some studies have suggested that EM and MTL have a similar gastroenteral action and race specificity. EM could induce the contration of rabbit gastric smooth musles, and was not inhibited by atropine, but blocked by antagoists of calcium passway Nifedipine. This indicated EM effect was related with calcium passway. Our result is similar with other investigators'.

There have been a lot of investigations on the effect of gastroenteric hormone. Increase in plyoric pressure was increased by human or dog duodenal infusion of HCl or florence oil, suggesting that gastroenteric hormone could regulate pyloric motion. We observed for the first time the plasma SS changes, and found that the plasma SS level was not blocked by isoptin and atropine after i.v. EM, and the plasma SS was higher in late stage. This phenomenon may be related to be autoregulation in vivo in order to maintain the balance among gastroenteral hormones like MTL and normal plyoric pressure.

In summary, the study suggested EM may increase the pressure in plyoric antrum. The effect may be related to the plasma motilin and somatostatin level.

Table 1 Pyloric pressure and plasma MTL and SS content before and after infusion of erythromycin in dogs. (n = 10, $\bar{x}\pm s$)

Parameters	Before drug administration	Erythromycin	Verapamil	Atropine
Total pressure (kPa)	20.1±2.2	34.5±3.1[a]	10.3±0.4[a]	8.2±0.2[a]
Basic pressure (kPa)	4.1±2.5	6.9±0.9[a]	4.4±0.8	5.2±0.2
Wave amplitude pressure (kPa)	16.0±14.4	27.6±9.6[a]	5.9±0.4[a]	3.0±0.1[b]
Wave frequency (time/min)	9.8±4.5	5.4±0.5[a]	2.9±0.4[a]	2.0±1.0[b]
Wave interval (s)	3.0±1.1	6.7±0.6[a]	3.8±0.4	3.1±0.1
Plasma MTL (ng/L)	426.9±53.4	553.9±87.2[a]	447.9±67.6	378.3±8.2[a]
Plasma SS (ng/L)	64.6±13.7	75.2±4.7[a]	85.6±2.9[b]	105.6±0.2[b]

[a]P<0.05, [b]P<0.01 *vs* before used medicine.

REFERENCES

1 Peeters T, Itch Z. Erythromycin is a motilin receptor agonist. *Am J Physiol*, 1989;257(3):470-477
2 Weber FH, Richards RD, McCallam RM. Erythromycin: a motilin agonist and gastrointestinal prokinetic agent. *Gastrenterology*, 1993;104(3):485-493
3 Itoh Z, Peeters T. Erythromycin mimics exogenous motilin in gastrointestinal contractile activing in the dog. *Am J Physiol*,1984;247(6):688-694
4 Vantrappen G, Janssns J, Tack J. Erythromycin is a potent gastrokinetic in diabetic gastroparesis. *Gastroenterology*, 1989;96(5):525-529
5 Sarna SK, Ryan RP, Brandon A. Erythromycin acts on presynaptic neurons to stimulate gastrointestinal motor activity. *Gastroenterology*, 1991;100(5): 490-498